ISSN 0021-9673

VOL. 362 NO. 2 JULY 18, 1986

JOURNAL OF

CHROMATOGRAPHY

INTERNATIONAL JOURNAL ON CHROMATOGRAPHY, ELECTROPHORESIS AND RELATED METHODS

ELSEVIER

JOURNAL OF CHROMATOGRAPHY

Scope. The *Journal of Chromatography* publishes papers on all aspects of chromatography, electrophoresis and related methods. Contributions consist mainly of research papers dealing with chromatographic theory, instrumental development and their applications. The section *Biomedical Applications,* which is under separate editorship, deals with the following aspects: developments in and applications of chromatographic and electrophoretic techniques related to clinical diagnosis (including the publication of normal values); screening and profiling procedures with special reference to metabolic disorders; results from basic medical research with direct consequences in clinical practice; combinations of chromatographic and electrophoretic methods with other physicochemical techniques such as mass spectrometry. In *Chromatographic Reviews,* reviews on all aspects of chromatography, electrophoresis and related methods are published.

Submission of Papers. Papers in English, French and German may be submitted, in three copies. Manuscripts should be submitted to: The Editor of *Journal of Chromatography,* P.O. Box 681, 1000 AR Amsterdam, The Netherlands, or to: The Editor of *Journal of Chromatography, Biomedical Applications,* P.O. Box 681, 1000 AR Amsterdam, The Netherlands. Review articles are invited or proposed by letter to the Editors and will appear in *Chromatographic Reviews* or *Biomedical Applications.* An outline of the proposed review should first be forwarded to the Editors for preliminary discussion prior to preparation. Submission of an article is understood to imply that the article is original and unpublished and is not being considered for publication elsewhere. For copyright regulations, see below.

Subscription Orders. Subscription orders should be sent to: Elsevier Science Publishers B.V., P.O. Box 211, 1000 AE Amsterdam, The Netherlands. The *Journal of Chromatography* and the *Biomedical Applications* section can be subscribed to separately.

Publication. The *Journal of Chromatography* (incl. *Biomedical Applications, Chromatographic Reviews* and *Cumulative Author and Subject Indexes, Vols. 326–350*) has 38 volumes in 1986. The subscription prices for 1986 are:

J. Chromatogr. (incl. *Chromatogr. Rev.* and *Cum. Indexes, Vols. 326–350*) + *Biomed. Appl.* (Vols. 346–383): Dfl. 6080.00 plus Dfl. 912.00 (postage) (total *ca.* US$ 2742.00)

J. Chromatogr. (incl. *Chromatogr. Rev.* and *Cum. Indexes, Vols. 326–350*) only (Vols. 346–373): Dfl. 5040.00 plus Dfl. 672.00 (postage) (total *ca.* US$ 2240.00)

Biomed. Appl. only (Vols. 374–383): Dfl. 1850.00 plus Dfl. 240.00 (postage) (total *ca.* US$ 819.50).

Journals are automatically sent by airmail at no extra costs to Argentina, Australia, Brasil, Canada, China, Hong Kong, India, Israel, Japan, Malaysia, Mexico, New Zealand, Pakistan, Singapore, South Africa, South Korea, Taiwan, Thailand and the U.S.A. Back volumes of the *Journal of Chromatography* (Vols. 1 through 345) are available at Dfl. 219.00 (plus postage). Claims for issues not received should be made within three months of publication of the issue. If not, they cannot be honoured free of charge. Customers in the U.S.A. and Canada wishing information on this and other Elsevier journals, please contact Journal Information Center, Elsevier Science Publishing Co. Inc., 52 Vanderbilt Avenue, New York, NY 10017. Tel. (212) 916-1250.

Abstracts/Contents Lists published in Analytical Abstracts, ASCA, Biochemical Abstracts, Biological Abstracts, Chemical Abstracts, Chemical Titles, Current Contents/Physical, Chemical & Earth Sciences, Current Contents/Life Sciences, Deep-Sea Research/Part B: Oceanographic Literature Review, Excerpta Medica, Index Medicus, Mass Spectrometry Bulletin, PASCAL-CNRS, Referativnyi Zhurnal and Science Citation Index.

See page 3 of cover for Publication Schedule, Information for Authors and information on Advertisements.

0021-9673/86/$03.50

Printed in The Netherlands

Gilson Fraction Collectors

any quantity • any vessel • any mode

France : B.P. 45, F-95400 Villiers-le-Bel. Tél. : (1) 39.90.54.41. Télex : 696 682 F.
USA : Box 27, 3000 W. Beltline, Middleton, Wisc. 53562. Tel : (608) 836 1551. Telex : 26.5478 MTWI.

CLEOPATRA

Chemometrics Library: an Extendable Set of Programs as an Aid in Teaching, Research and Applications

Authors: G. Kateman, P.F.A. van der Wiel, T.A.H.M. Janse and **B.G.M. Vandeginste**

- a package of programs for
  - (post) graduate education
  - (industrial) training courses
- provides quick insight on how to solve your problems around:
  - sampling of lots
  - monitoring
  - reconstruction
  - autocorrelation
  - curve fitting
  - Fourier filtering
- highly interactive
- high quality graphics
- runs on IBM-PC and HP-9845
- clear, fully descriptive manual with tutorial
- easy to use
- no prior knowledge of any specific computer jargon necessary
- US $ 820.00 (IBM-PC), US $ 735.00 (HP-9845-B)
- CLEOPATRA, extension I
  Three New Modules: Modules Sequential Analysis, Kalman Filtering, Simplex Optimization
- US $ 375.00

AVAILABLE FROM:

Elsevier Scientific Software (JIC)
52 Vanderbilt Avenue
New York, NY 10017 USA
Phone: (212) 916 1250
Telex: 420643

or
Elsevier Scientific Software
P.O. Box 330
1000 AH Amsterdam
THE NETHERLANDS
Phone: (020) 5862 828
Telex: 18582

Write to us for further information on our other programs

No shipping charge if paid in advance

ELSEVIER SCIENTIFIC SOFTWARE

IBM-PC is a registered trademark of IBM

CONTENTS

(*Abstracts/Contents Lists published in Analytical Abstracts, ASCA, Biochemical Abstracts, Biological Abstracts, Chemical Abstracts, Chemical Titles, Current Contents/Physical, Chemical & Earth Sciences, Current Contents/Life Sciences, Deep-Sea Research/Part B: Oceanographic Literature Review, Excerpta Medica, Index Medicus, Mass Spectrometry Bulletin, PASCAL-CNRS, Referativnyi Zhurnal and Science Citation Index*)

(*Continued overleaf*)

Notes

In articles with more than one author, the name of the author to whom correspondence should be addressed is indicated in the article heading by a 6-pointed asterisk (*)

Journal of Chromatography, 362 (1986) 155–174
Elsevier Science Publishers B.V., Amsterdam — Printed in The Netherlands

CHROM. 18 671

ON-LINE GAS CHROMATOGRAPHIC ANALYSIS OF HYDROCARBON EFFLUENTS

CALIBRATION FACTORS AND THEIR CORRELATION

JAN L. DIERICKX, PATRICK M. PLEHIERS and GILBERT F. FROMENT*
Laboratorium voor Petrochemische Techniek, Rijksuniversiteit te Gent, Krijgslaan 281, B-9000 Ghent (Belgium)
(Received March 7th, 1986)

SUMMARY

A flexible gas chromatographic hydrocarbon analysis train has been calibrated for off-line analysis of petroleum fractions and for on-line analysis of a thermal cracking effluent. Special attention was paid to the calibration factors of hydrocarbons on flame ionization detectors. Correlations for these calibration factors that have been presented in the literature, together with those introduced in this paper, are tested against the experimental data for their adequacy and parameter significance.

INTRODUCTION

For the study of the thermal cracking of hydrocarbons ranging from ethane up to gas oil, the Laboratorium voor Petrochemische Techniek designed and built a flexible and highly automated pilot plant[1]. It is equipped with an analysis train that permits on-line analysis of the reactor effluent, ranging from hydrogen to C_{30} hydrocarbons[2]. Off-line analysis of petroleum fractions is also possible. The on-line analysis is entirely based on the internal standard technique. Nitrogen is injected into the reactor effluent and serves as an internal standard. A special hot-gas sampling device allows for the analysis of the complete reactor effluent without any previous condensation[2,3].

Calibration for C_4^- components has been current practice[2]. For most C_5^+ components, mass response factors on flame ionization detectors do not differ much, and it has been suggested that calibration is superfluous[4–7]. This approximation is no longer justified: to obtain the required precision in the characterization of the reactor effluent or feed, it was found necessary to perform a complete calibration of the gas chromatographs. In the present paper, calibration for C_5^+ components is discussed in detail. In particular, an experimental method for linking the C_5^+ calibration to the internal standard is presented.

Refining and petrochemical process feedstocks and effluents are often very

0021-9673/86/$03.50

complex hydrocarbon mixtures, containing a few hundreds of components. It is impossible to determine calibration factors for all of them. Therefore, it is important to devise correlations for the flame ionization detection (FID) calibration factors. A number of correlations that have been presented in literature are tested and a new type of correlation is introduced.

GAS CHROMATOGRAPHIC ANALYSIS

Sampling system

Fig. 1 shows a schematic view of the reactor outlet and of the sampling system. The reactor outlet pressure is controlled by means of a restriction valve (1). The nitrogen that is used as internal standard is injected into the effluent gas stream at the reactor outlet (2) to ensure efficient mixing. It also contributes to cooling and diluting the effluent. The nitrogen flow-rate is controlled by means of a thermal mass flow meter-controller with an accuracy exceeding 0.5%. A hot gas sample[2,3] of the full effluent is taken at 350–400°C, depending on flow-rates and reactor outlet temperature. The hot sampling device consists of two high temperature injection valves (3), kept at 300°C in an oven (4). Each sampling valve is preceded by a shut-off valve (5), kept at 350°C in a separate section of the oven. The temperature upstream of the shut-off valves is kept high to prevent condensation of high-molecular-weight products. The valves (5) are opened for only a short time just before injection to reduce fouling of the sampling valves (3). Between injections, the sampling valves can be

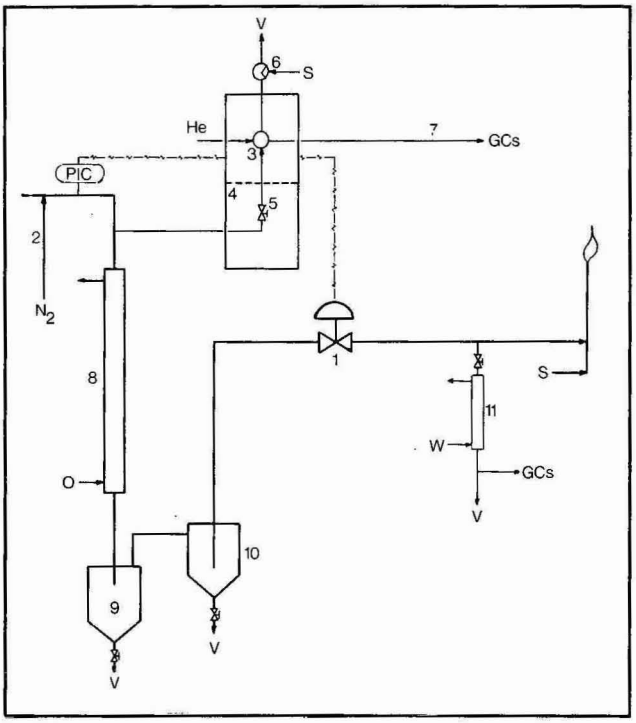

Fig. 1. Reactor outlet and sampling system. O = oil, S = steam, V = vent, W = water.

flushed with steam (6). From the sampling valves, the sample is led to the C_5^+ gas chromatographs for separation through stainless-steel capillary transfer lines (7). Internal coating with OV-1 prevents adsorption of the aromatic species on the stainless-steel piping. The temperature of these lines is limited to 275°C to prevent deterioration of the coating.

The reactor effluent is cooled to *ca.* 150°C in an oil cooler (8). Condensed hydrocarbons and coke particles are removed in a liquid separator (9) and a cyclone (10). The effluent then flows through traced piping to a flare, where it is burned. A fraction of the product stream is withdrawn for on-line analysis of the C_4^- fraction. The C_4^- fraction is analysed after removal of water and pyrolysis gasoline in a water cooler (11) at 45°C.

C_4^- Analysis

The C_4^- sample is analysed on two gas chromatographic (GC) systems simultaneously. Only hydrogen is not detected twice. The use of two different units for the same analysis improves the reliability of the results.

The first system is a set of three Packard 417 gas chromatographs, which perform an analysis designed at the Laboratorium voor Petrochemische Techniek[2]. The operating conditions for the three chromatographs are listed in Table I. All three instruments are equipped with precolumns to allow backflushing of higher boiling products. C_4^- chromatograms are shown in Fig. 2. The first chromatograph determines the nitrogen, carbon monoxide and methane contents of the product stream; C_2 and heavier components are backflushed. Methane is used as a secondary standard, because nitrogen cannot be detected by FID. The second chromatograph separates nitrogen and carbon monoxide, methane, carbon dioxide, ethene and ethane after backflush of C_3^+; all C_3 and C_4 saturates, mono-olefins, di-olefins and acetylenes are separated on the third chromatograph.

The second system consists of a Carle CGC 530 automated refinery gas analyser. This multicolumn instrument, equipped with eight columns and five switching valves, performs a similar analysis. The carrier gas is helium. Nitrogen, carbon monoxide, carbon dioxide and hydrocarbons up to C_2 are detected by thermal conductivity detection (TCD), C_3 and C_4 by FID. This chromatograph is also equipped

TABLE I

OPERATING CONDITIONS FOR THE PACKARD 417 CHROMATOGRAPHS

	Packard 417 GC1	*Packard 417 GC2*	*Packard 417 GC3*
Precolumn	Porapak N 1.0 m, 1/8 in.	Porapak N 1.0 m, 1/8 in.	Durapack *n*-octane 0.65 m, 1/4 in.
Analysis column	Carbosphere 1.8 m, 1/8 in.	Porapak N 6.0 m, 1/8 in.	17% Sebaconitrile on Chromosorb P-AW 10.0 m, 1/4 in.
Oven temp. (°C)	50	35	20
Carrier gas (ml/min)	H_2 (20)	H_2 (30)	N_2 (35)
Detection	TCD	TCD	FID

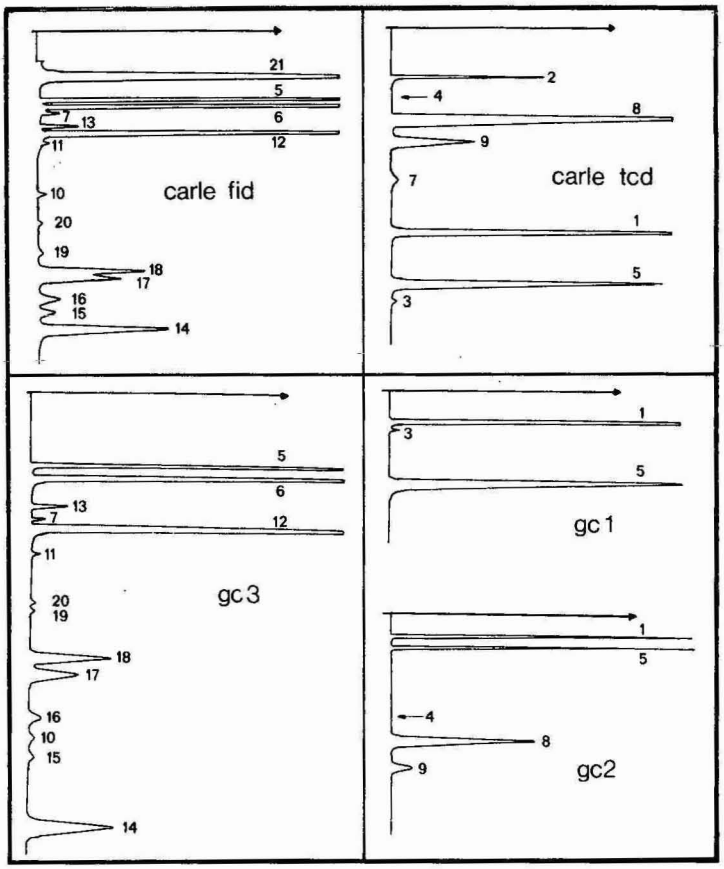

Fig. 2. C_4^- chromatograms. Peaks: 1 = N_2; 2 = H_2; 3 = CO; 4 = CO_2; 5 = CH_4; 6 = sumC_2; 7 = C_2H_2; 8 = C_2H_4; 9 = C_2H_6; 10 = C_3H_4(MA); 11 = C_3H_4(PD); 12 = C_3H_6; 13 = C_3H_8; 14 = 1,3-C_4H_6; 15 = *cis*-2-C_4H_8; 16 = *trans*-2-C_4H_8; 17 = *i*-C_4H_8; 18 = 1-C_4H_8; 19 = *n*-C_4H_{10}; 20 = *i*-C_4H_{10}; 21 = C_5^+ backflush.

with a hydrogen transfer system, a palladium tube that allows migration of hydrogen from helium into nitrogen carrier gas. In nitrogen, the hydrogen is easily detected by TCD.

C_5^+ Analysis

The C_4^- analysis takes 32 min on the Carle and 38 min on GC3. Since a C_5^+ analysis lasts more than 90 min, two C_5^+ chromatographs (Packard 428 and Packard 437A) are used in alternate operation. Each has two columns, inserted in the same injection port, and two flame ionization detectors. Both columns are fused-silica capillaries (30 m × 0.32 mm I.D.) and coated with DB1-30W (polymethylsiloxane). The only difference between them is the thickness of the coating: 0.25 μm for one and 5.0 μm for the other. The temperature is kept at −20°C for 1 min and is then programmed to 250°C at 3°C/min.

Fig. 3 shows chromatograms obtained from one of the two C_5^+ chromato-

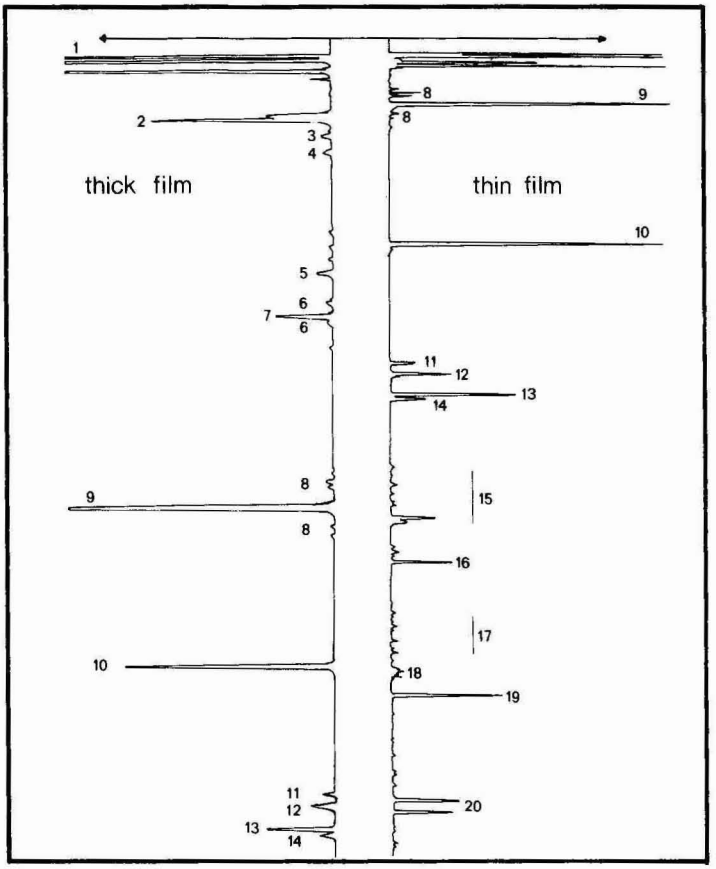

Fig. 3. C_5^+ chromatograms. Peaks: 1 = CH_4; 2 = 1,3-C_4H_6; 3 = *trans*-2-C_4H_8; 4 = *cis*-2-C_4H_8; 5 = isoprene; 6 = 1,3-pentadienes; 7 = 1,3-cyclopentadiene; 8 = methylcyclopentadienes and cyclohexadienes; 9 = benzene; 10 = toluene; 11 = ethylbenzene; 12 = *para*- and *meta*-xylene; 13 = styrene; 14 = *ortho*-xylene; 15 = C_9 aromatics and indane; 16 = indene; 17 = C_{10} aromatics; 18 = methylindenes; 19 = naphthalene; 20 = methylnaphthalenes.

graphs. On the thick-film column, methane is separated from ethene and ethane. It is used as a secondary standard for calculation of the yields of C_5 and C_6 components. This column, however, does not achieve a sufficient resolution in the higher boiling point range. Therefore, benzene is used as a tertiary standard for the analysis of C_6 to C_{30} hydrocarbons on the thin-film column.

Data treatment

A Data General S140 real-time process computer controls reactor temperatures and feed flow-rates, switches GC injection and backflush valves and acquires and digitizes GC outputs. Peak areas are computed by an integration and peak detection program. Both C_4^- and C_5^+ peaks are identified on-line, and a full report containing kinetic data and the product distribution is generated.

Calculations are based on the absolute flow-rates of the effluent components.

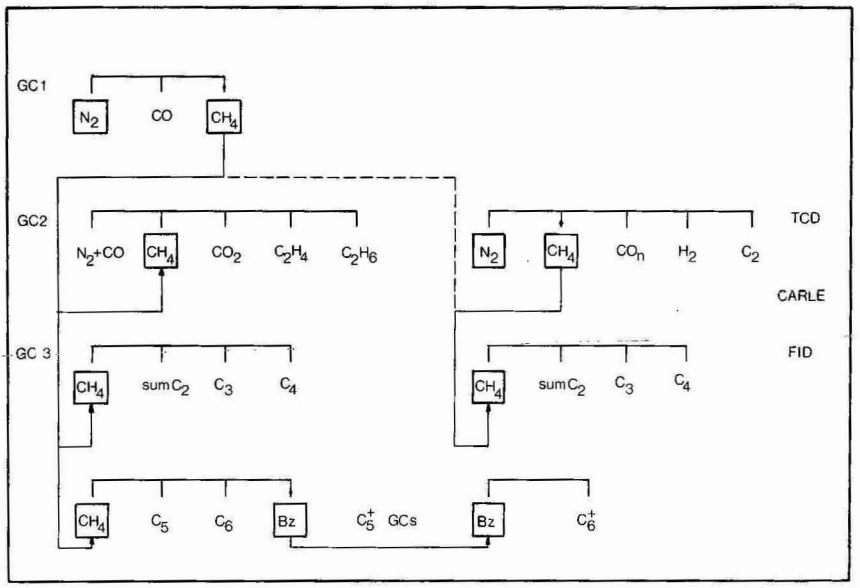

Fig. 4. Calculation procedure for the product yields.

This is made possible by the injection of a precisely known nitrogen flow at the reactor exit. The use of reference components is illustrated in Fig. 4. From the peak areas of the Packard GC1, the experimentally determined calibration factors on this instrument and the known amount of nitrogen, the flows of methane and carbon monoxide are calculated. Using the methane flow thus calculated, the flows of ethane, ethene and carbon dioxide are calculated from the data of GC2. The methane peak is used, because nitrogen and carbon monoxide are not always separated on GC2. The remaining C_4^- components are referred to methane on GC3, because nitrogen is not detected by FID. The results on the Carle can be calculated in two ways: by referring either to the known nitrogen flow or to the methane flow determined on GC1. The C_5^+ results of the thick film column are calculated in the same way as the results of GC3. Then benzene is used as a standard to calculate the flows of the components analysed on the thin-film column.

With these data, a product distribution in terms of weight percentages can be determined. As the feed flow-rate is known, yields (kilograms of product per kilogram of hydrocarbon fed) and a material balance can also be calculated. By way of example, the calibrated analysis of an effluent of the thermal cracking of an atmospheric gas oil is given in Table II. The total material balance and the agreement between the two C_4^- analyses are excellent.

RESULTS

Since the above calculations are based on mass flows, weight calibration factors are preferred to molar calibration or response factors. A calibration factor (CF) is the number by which the peak area (PA) has to be multiplied to obtain a measure

TABLE II

EFFLUENT ANALYSIS REPORT

Yields in weight percent.

Packard	N_2	10.417			
417	CO	0.124			
GC1	CH_4	11.472			
			0.623	H_2	Carle TCD
Packard	N_2 + CO	10.726	10.416	N_2	Carle TCD
417		–	0.103	CO	
GC2	CH_4	11.472	11.472	CH_4	
	CO_2	0.000	0.000	CO_2	
	C_2H_4	21.933	21.874	C_2H_4	
	C_2H_6	3.325	3.406	C_2H_6	
Packard	CH_4	11.472	11.472	CH_4	Carle FID
417	sumC_2	24.914	25.078	sumC_2	
GC3	C_3H_8	0.398	0.375	C_3H_8	
	C_2H_2	0.257	0.270	C_2H_2	
	C_3H_6	12.285	12.352	C_3H_6	
	i-C_4H_{10}	0.024	0.028	i-C_4H_{10}	
	n-C_4H_{10}	0.046	0.042	n-C_4H_{10}	
	C_3H_4(PD)	0.184	0.192	C_3H_4(PD)	
	1-C_4H_8	0.868	0.842	1-C_4H_8	
	i-C_4H_8	1.550	1.568	i-C_4H_8	
	t-2-C_4H_8	0.306	0.297	t-2-C_4H_8	
	C_3H_4(MA)	0.219	0.231	C_3H_4(MA)	
	c-2-C_4H_8	0.086	0.075	c-2-C_4H_8	
	C_4H_6	4.125	4.119	C_4H_6	
	C_4^-	57.624	57.869	C_4^-	
C_5^+ from thick-film column, up to benzene:				16.06	
of which: isoprene:				1.11	
1,3-cyclopentadiene:				2.13	
benzene:				9.63	
C_5^+ from thin-film column, up to naphthalene:				11.86	
of which: toluene:				4.84	
ethylbenzene:				0.31	
xylenes:				1.20	
styrene:				1.09	
C_5^+ higher than naphthalene, pyrolysis fuel oil:				14.02	
Total material balance		99.56	99.81		

for the weight flow or weight percentage (wt) of the component *i*:

$$\mathrm{wt}(i) = \frac{\mathrm{CF}(i) \cdot \mathrm{PA}(i)}{\mathrm{CF}(\mathrm{ref}) \cdot \mathrm{PA}(\mathrm{ref})} \cdot \mathrm{wt}(\mathrm{ref})$$

The CF of the reference component is chosen to be unity. Methane is the reference for the calibration factors on all detectors, except for the flame ionization detectors

of the thin-film columns, on which CFs are referred to benzene. Thus, the CF is:

$$CF(i) = \frac{PA(ref) \cdot wt(i)}{PA(i) \cdot wt(ref)} \quad (1)$$

This CF is the reciprocal of the relative weight response factor (RWR). Taking into account the molecular weights (MW) of i and (ref), the relative molar response factor (RMR) is easily derived:

$$RMR(i) = \frac{MW(i)}{MW(ref)} \cdot \frac{1}{CF(i)} \quad (2)$$

For on-line analyses, three sets of calibration factors are needed. The set of C_4^- calibration factors and the set of calibration factors for the thick-film columns are referred to methane. The C_5^+ calibration factors on the thin-film columns are referred to benzene. For off-line injections of hydrocarbon mixtures, such as naphtha or gas oil, internally consistent sets of C_5^+ calibration factors are also needed, in particular on the thin-film columns.

C_4^- Calibration

For C_4^- calibrations, certified standards containing up to nineteen components in concentrations as close as possible to the expected effluent composition, were pur-

TABLE III

C_4^- CALIBRATION FACTORS

Packard	N_2	1.460			
417	CO	1.520			
GC1	CH_4	1.000			
			0.295	H_2	Carle TCD
Packard	N_2 + CO	1.450	1.390	N_2	Carle TCD
417		–	1.400	CO	
GC2	CH_4	1.000	1.000	CH_4	
	CO_2	1.875	1.881	CO_2	
	C_2H_4	1.290	1.225	C_2H_4	
	C_2H_6	1.330	1.215	C_2H_6	
Packard	CH_4	1.000	1.000	CH_4	Carle FID
417	sumC_2	0.934	0.868	sumC_2	
GC3	C_3H_8	0.899	0.826	C_3H_8	
	C_2H_2	0.792	0.446	C_2H_2	
	C_3H_6	0.937	0.862	C_3H_6	
	i-C_4H_{10}	0.815	0.834	i-C_4H_{10}	
	n-C_4H_{10}	0.917	0.790	n-C_4H_{10}	
	C_3H_4(PD)	0.847	0.548	C_3H_4(PD)	
	1-C_4H_8	0.929	0.853	1-C_4H_8	
	i-C_4H_8	0.947	0.818	i-C_4H_8	
	t-2-C_4H_8	0.981	0.835	t-2-C_4H_8	
	C_3H_4(MA)	1.050	0.812	C_3H_4(MA)	
	c-2-C_4H_8	1.022	0.847	c-2-C_4H_8	
	C_4H_6	0.929	0.831	C_4H_6	

chased from Matheson. Consistence of CFs in time was checked. Standards with widely different compositions are available for flame ionization detector and electrometer linearity checks. CFs on a linear flame ionization detector are constant over a wide concentration range. Unfortunately, "linear" detectors are often linear only in a log–log plot of response *versus* concentration, with a slope that is not necessarily equal to one[8]. This results in variations of the CF with the concentration in the sample of the component concerned. This has been observed for some C_3 and C_4 hydrocarbons on the flame ionization detectors of the Packard GC3 and the Carle. It was noticed that the slope in the log–log diagram can be brought closer to unity by increasing the ratio of hydrogen to air in the detector flame. In Table III, a set of C_4^- calibration factors is listed. These results are compared with expected values derived from literature data and prediction methods as a test for GC tuning and accuracy of the standards. Correlations are less accurate for predicting the calibration factors for methane and highly unsaturated light hydrocarbons, such as ethyne[9,10] and propadiene.

C_5^+ Calibration

The C_5^+ calibration was performed in two steps. First, a set of C_5^+ CFs is determined for each detector by syringe injection of liquid calibration mixtures. They are referred to benzene. Then, the CF of benzene referred to methane on the thick-film columns was determined by means of on-line injection of methane–benzene mixtures. This method is preferred to the on-line determination of all C_5^+ calibration factors, because it is less sensitive to fractionation of the sample.

In order not to introduce uncertainties exceeding the GC reproducibility in the composition of the liquid calibration mixtures, extreme care is required in their preparation. Therefore, only products with a purity higher than 99% were used. All of them were analysed quantitatively (GC–FID) and qualitatively (GC–MS), to check for possible cross-contamination of components by impurities in other products. Some 25 hydrocarbons with widely varying molecular weights and structures were mixed on a digital balance, starting with the higher boiling products. The components of the calibration mixtures were also chosen in order to achieve a baseline-to-baseline separation of all peaks. Several mixtures with different compositions were prepared to check for detector non-linearity and for bias of the results by errors in the mixture composition. For syringe injection, some of the mixtures were diluted with a highly volatile solvent that does not disturb the analysis, such as pentane or acetone. The solvent is added to ensure a fast and complete evaporation of the mixture in the GC injector, to improve separation and to reduce inlet splitter influence to a minimum. The composition of one of the mixtures is given in Table IV.

For the determination of the calibration factors of C_5^+ referred to benzene, 0.1 μl of the calibration mixtures was injected with a Hamilton 1.0-μl syringe. When an internal standard is used, an exact reproduction of the injected amount is not required. In Table IV, experimental values of the CFs, averaged over five injections, are listed. No significant changes in CFs were noticed for the different calibration mixtures. The discussion below is based on the set of CFs given in Table IV, the conclusions being the same, whatever set, including C_4^-, is used. Typical values of CFs are 1.15 for paraffins and 1.12 for naphthenes. The CFs of aromatics range from 1.00 for benzene up to values that are typical of aliphatic compounds as the number

TABLE IV

CALIBRATION MIXTURE COMPOSITION AND C_5^+ CALIBRATION FACTORS

Component	*wt.%*	*CF*
n-Hexane	3.747	1.151
n-Heptane	4.154	1.151
n-Octane	4.402	1.130
n-Decane	3.798	1.148
n-Dodecane	3.980	1.145
n-Hexadecane	4.080	1.146
2,2-Dimethylbutane	3.956	1.182
2,3-Dimethylbutane	5.172	1.167
2,2,4-Trimethylpentane	2.687	1.131
1-Hexene	4.227	1.182
1-Octene	4.940	1.147
Cyclohexene	3.674	1.069
Methylcyclopentane	2.652	1.142
Cyclohexane	3.457	1.123
Methylcyclohexane	5.938	1.115
Decalin	4.026	1.127
Benzene	4.700	1.000
Toluene	3.697	1.019
Ethylbenzene	3.945	1.043
meta-Xylene	2.981	1.051
ortho-Xylene	4.460	1.045
ortho-Ethyltoluene	4.076	1.074
para-Diisopropylbenzene	4.874	1.146
Tetralin	3.372	1.078
Naphthalene	1.676	1.063
Biphenyl	1.309	1.021

of carbon atoms in the side-chains increases. Table IV clearly demonstrates that when CFs are not applied in the analysis of petroleum fractions, the aromatics content is overestimated. In naphtha analysis for instance, relative errors of 9–12% are typical, depending on the average molecular weight and composition. For mixtures with higher aromatics content, such as reformates or extracts, the relative error is smaller, but the absolute error on the aromatics content reaches a maximum of 2 to 3 percentage points for fractions containing 50% aromatics, as encountered in pyrolysis gasoline.

The on-line determination of the CF of benzene with respect to methane is much more complicated from the experimental point of view. The methane and benzene concentrations in the sample loop have to be reduced to an appropriate level, corresponding approximately to the expected effluent composition. Therefore, the sample is diluted with steam and hydrocarbon gases. The internal standard, nitrogen, is added as well to check the methane flow-rate on the C_4^- chromatographs. All gas flows are controlled by means of thermal mass flow controllers; liquids are fed from

balances and their flow-rates are controlled by the process computer. Water and benzene are evaporated separately in the furnace and are mixed with the hydrocarbon gases in the gas phase. To obtain reproducible results, the system is rigorously maintained at constant conditions. This means, in particular, that pulsations of the feed pumps for benzene and water should be absent or have a period that is at least one order smaller than the residence time of the products in the whole system. The reactor is kept at a temperature that is sufficiently high to prevent condensation, without causing thermal decomposition of the hydrocarbons, however. A temperature of 300–350°C at the reactor outlet was found to be appropriate. The CF of benzene with respect to methane differs significantly from one: 0.716 on the one instrument and 0.856 on the other. Along with the values listed in Tables III and IV, this illustrates the necessity of using CFs in quantitative FID analyses, even for hydrocarbons. CFs for C_2^+ components follow similar patterns on different, but decently operated flame ionization detectors. This rule does not apply to methane, as is clearly illustrated by the values in Table III.

Correlations

A number of correlations for RMRs or CFs on flame ionization detectors have been presented in the literature. In this paper, a new type of correlation is introduced. All of the correlations are then confronted with the experimental data of Table IV. Model discrimination, based on the statistical *F*- and *t*-tests, allows for the selection of the best correlation.

A first set of correlations is based on the observation that a flame ionization detector is essentially a carbon atom counter[9,11]. RMRs of hydrocarbons are approximately proportional to the number of carbon atoms in the component detected. In terms of calibration factors, this can be expressed as (*viz.* eqn. 2):

$$\frac{\mathrm{MW}(i)}{\mathrm{CF}(i)} = AN_{\mathrm{C}} \qquad \text{(correlation I)}$$

where N_{C} is the number of carbon atoms in the molecule i.

It was soon recognized that some dependence on the hydrocarbon structure has to be accounted for, and effective carbon number contributions were introduced[12]:

$$\frac{\mathrm{MW}(i)}{\mathrm{CF}(i)} = AN_{\mathrm{C,aliphatic}} + BN_{\mathrm{C,olefinic}} + CN_{\mathrm{C,aromatic}} \qquad \text{(correlation II)}$$

This method was further developed for oxygenated compounds[13,14]. For hydrocarbons, all contributions were found to be approximately equal[12]. From the present data, it is clear that this is not true. It has also been suggested that the relative weight response is proportional to the weight percent of carbon in the molecule[7]. This method is equivalent to correlation I, however:

$$\mathrm{RWR}(i) = [\mathrm{CF}(i)]^{-1} = A' \frac{12N_{\mathrm{C}}}{\mathrm{MW}(i)} = A \frac{N_{\mathrm{C}}}{\mathrm{MW}(i)}$$

It can also be investigated whether hydrogen atoms contribute to the RMR:

$$\frac{\mathrm{MW}(i)}{\mathrm{CF}(i)} = AN_{\mathrm{C}} + BN_{\mathrm{H}} \qquad \text{(correlation III)}$$

A different type of correlation was proposed by Bulewicz[10], who suggested that the RMR is proportional to the standard enthalpy change $(-\Delta H^0)_{\mathrm{ox}}(\mathrm{H_2})$ at 298 K of the hypothetical combustion reaction

$$\mathrm{C}_n\mathrm{H}_m + n\mathrm{O_2} \rightarrow n\mathrm{CO_2} + m/2\ \mathrm{H_2}$$

$$\frac{\mathrm{MW}(i)}{\mathrm{CF}(i)} = A(-\Delta H^0)_{\mathrm{ox}}(\mathrm{H_2}) \qquad \text{(correlation IV)}$$

The value of this model as an attempt to explain the mechanism of ion formation in the flame has been questioned[15–17]. Nevertheless, this kind of approach may be of some practical use.

Below, a new type of correlation, based on the standard Gibbs energy change $(-\Delta G^0)_{\mathrm{ox}}$[18] at 298 K of the complete oxidation reaction to carbon dioxide and water, is introduced. It is based on the observation that the molar FID responses of homologous series of organic compounds are straight lines when plotted against the carbon number, the slope being the response of a single methylene group[10,19]. In other words:

$$\mathrm{PA}(i) = (a + bN_{\mathrm{C}}) \cdot \mathrm{mol}(i) \qquad (3)$$

For hydrocarbons, the parameter a is a small number, since their responses are nearly proportional to N_{C}. For paraffins for instance, the parameter a is twice the difference in response between a methyl and a methylene group; for aromatics, it is six times the difference in response between an aromatic carbon atom and a methylene group. The contribution for a methylene group, b, is constant for all homologous series and depends solely on detector construction and operation.

In weight units, eqn. 3 becomes:

$$\mathrm{PA}(i) = (a + bN_{\mathrm{C}})/(c + dN_{\mathrm{C}}) \cdot \mathrm{wt}(i) \qquad (4)$$

with $(c + dN_{\mathrm{C}}) = \mathrm{MW}(i)$ and $d = 14$, the molecular weight of a methylene group. The parameter c depends on the type of hydrocarbon, but it is relatively small. From eqn. 4 and the definition of the calibration factor (eqn. 1):

$$\mathrm{CF}(i) = k(c + dN_{\mathrm{C}})/(a + bN_{\mathrm{C}}) \qquad (5)$$

For a homologous series, the standard Gibbs energy of formation[18] can be expressed as

$$\Delta G^0_{\mathrm{f,HC}} = u + vN_{\mathrm{C}}$$

with v again the constant contribution of a methylene group. Hence, the standard Gibbs energy change of the combustion reaction

$$C_nH_m + (n + m/4)O_2 \rightarrow nCO_2 + m/2\ H_2O$$

is

$$\begin{aligned}(-\Delta G^0)_{ox} &= -[N_C \Delta G^0_{f,CO2} + (2N_C + c)/2 \cdot \Delta G^0_{f,H_2O} - \Delta G^0_{f,HC}] \\ &= e + fN_C\end{aligned}$$

or

$$N_C = [(-\Delta G^0)_{ox} - e]/f \tag{6}$$

The parameter f is the contribution of a methylene group to the standard Gibbs energy change of the combustion reaction and is independent of the nature of the hydrocarbon. Substituting eqn. 6 into eqn. 5 yields

$$CF(i) = k \frac{(fc - de) + d(-\Delta G^0)_{ox}}{(fa - be) + b(-\Delta G^0)_{ox}} \tag{7}$$

$(-\Delta G^0)_{ox}$ covers a wide range of values (linear in N_C), while all CFs lie within a limited range. To estimate the parameters more conveniently, eqn. 7 is multiplied by the molecular weight of the component:

$$CF(i) \cdot MW(i) = k \frac{[(fc - de) + d(-\Delta G^0)_{ox}]^2}{(fa - be) + b(-\Delta G^0)_{ox}} \tag{8}$$

or

$$CF(i) \cdot MW(i) = A[B + (-\Delta G^0)_{ox}]^2/[C + (-\Delta G^0)_{ox}] \qquad \text{(correlation V)}$$

Simplification of eqn. 8 is possible, since both CFs and $(-\Delta G^0)_{ox}/MW(i)$ are approximately constant within a homologous series. Hence,

$$CF(i) = \frac{c + dN_C}{a + bN_C} = k_1 \qquad \text{and} \qquad \frac{(-\Delta G^0)_{ox}}{MW(i)} = \frac{e + fN_C}{c + dN_C} = k_2$$

for all N_C, and in particular for $N_C = 0$ and $N_C = \infty$:

$$c/a = d/b = k_1 \tag{9a}$$

and

$$e/c = f/d = k_2 \tag{9b}$$

From eqns. 9a and 9b, it follows that, with sufficient approximation

$$fa - be = 0 \tag{10a}$$

and

$$fc - de = 0 \tag{10b}$$

Using eqns. 10a and 10b, the dependence on the nature of the hydrocarbon, which appears in eqn. 8 through a, c and e, can be eliminated; eqn. 8 then becomes:

$$\mathrm{CF}(i) \cdot \mathrm{MW}(i) = kd^2/b(-\Delta G^0)_{ox} = A(-\Delta G^0)_{ox} \qquad \text{(correlation VI)}$$

From this basic correlation, two further ones are derived. First, it is investigated whether $(-\Delta G^0)_{ox}$ can be substituted by $(-\Delta H^0)_{ox}$, the lower heat of combustion, which may be more accessible than the standard Gibbs energy values, so that

$$\mathrm{CF}(i) \cdot \mathrm{MW}(i) = A(-\Delta H^0)_{ox} \qquad \text{(correlation VII)}$$

As a further simplification, $(-\Delta G^0)_{ox}$ is expanded into a linear combination of the number of carbon and hydrogen atoms in the molecule:

$$\mathrm{CF}(i) \cdot \mathrm{MW}(i) = AN_C + BN_H \qquad \text{(correlation VIII)}$$

Correlations II and VI can be expanded into group contribution methods, as is done for the estimation of thermodynamic properties[20]. In the present case, ten contributions are considered. They are listed in Table V. The following ways of calculating calibration factors by means of group contributions (a_j) are investigated:

$$\mathrm{CF}(i) = \sum_j n_{j,i} a_j \qquad \text{(correlation IX)}$$

TABLE V

GROUP CONTRIBUTIONS

1	CH_3	Methyl group in an aliphatic chain
2	CH_2	Methylene group in an aliphatic chain
3	CH	Tertiary carbon atom in an aliphatic chain
4	C	Quaternary carbon atom in an aliphatic chain
5	(5)	Additional contribution for a 5-membered naphthenic ring
6	(6)	Additional contribution for a 6-membered naphthenic ring
7	C_{aro}–H	Aromatic carbon atom, connected to a hydrogen atom
8	C_{aro}–C	Aromatic carbon atom, connected to another carbon atom
9	$C=H_2$	Olefinic carbon atom, connected to two hydrogen atoms
10	C=CH	Olefinic carbon atom, connected to a hydrogen and a carbon atom

TABLE VI

RELATIONS BETWEEN THE DIFFERENT CORRELATIONS

Correlation numbers are given in brackets.

	Basic correlation	*Derived correlations*			*Derived group contributions*
MW(i)/CF(i) as a function of contributions for types of carbon atom	N_C (I)	N_C, N_H (III)	*ECNC* (II)		$\sum_j n_{j,i}a_j$ (XI)
MW(i)/CF(i) as a function of the heat of reaction of a partial combustion	$(-\Delta H^0)_{ox}(H_2)$ (IV)				
CF(i) as a function of contributions for types of carbon atom					$\sum_j n_{j,i}a_j$ (IX)
CF(i) · MW(i) as a function of the Gibbs energy change of the complete combustion	$(-\Delta G^0)_{ox}$ (VI)	$(-\Delta H^0)_{ox}$ (VII)	N_C, N_H (VIII)	$(-\Delta G^0)_{ox}$ (V)	$\sum_j n_{j,i}a_j$ (X)

$$\mathrm{CF}(i) \cdot \mathrm{MW}(i) = \sum_j n_{j,i}a_j \qquad \text{(correlation X)}$$

$$\mathrm{MW}(i)/\mathrm{CF}(i) = \sum_j n_{j,i}a_j \qquad \text{(correlation XI)}$$

Correlation XI is nothing but an extended effective carbon number contribution method, while correlation X is an extension of correlation VI. The different correlations are interrelated as is shown in Table VI. The number of parameters and the amount of calibration effort required increase from left to right. The quality of the fit can be expected to follow the same trend. The preferred type of correlation, a group contribution method or one of the other correlations, depends on the specific requirements of each analysis problem. In the next section, the most appropriate correlations for calculating hydrocarbon calibration factors on a flame-ionization detector are selected on the basis of a detailed statistical check.

DISCUSSION

The parameters in the different correlations were estimated by minimizing the following sum of squares:

$$\sum_{i=1}^{k} \sum_{i=1}^{n_i} [\mathrm{CF}(i)_j - \hat{\mathrm{C}}\mathrm{F}(i)]^2$$

where k is the total number of components in the mixture and n_i the number of replicate experiments for component i. $\hat{C}F(i)$ is the predicted value of the calibration factor. For parameter estimation in the non-linear correlation V, a Marquardt minimization routine was used.

The discrimination between the different correlations (I–XI) is based on rigorous statistical testing.

First, model adequacy is tested by means of the lack-of-fit F-test[21]. This F-test can be used when replicate experiments are available. The total residual sum of squares is broken down into the pure-error sum of squares, which arises from experimental scatter, and the lack of fit sum of squares, which is caused by model inadequacy. The pure-error sum of squares is given by

$$\sum_{i=1}^{k} \sum_{j=1}^{n_i} [CF(i)_j - \overline{CF(i)}]^2$$

in which $\overline{CF(i)}$ is the average experimental value of the calibration factor for component i. This sum of squares has

$$\sum_{i=1}^{k} (n_i - 1) = \sum_{i=1}^{k} n_i - k$$

degrees of freedom. The lack-of-fit sum of squares is obtained from the total sum of squares by substraction of the pure-error sum of squares. The F-value is calculated from

$$F_{calc} = \frac{\text{lack-of-fit sum of squares}/[\text{total degrees of freedom} - (\Sigma n_i - k)]}{\text{pure error sum of squares}/(\Sigma n_i - k)}$$

The calculated F-value is compared with the tabulated 95% value of the F-distribution. If the calculated F-value is above the significance level, in other words, exceeds the tabulated one, there is a probability of 95% that the correlation is inadequate. It is then rejected because of lack of fit.

In a second step, the parameters are tested for significance. The actual parameter estimates are compared to zero, and the significance of the difference is tested on the t-distribution. Parameters that are not significantly different from zero at the 95% level are deleted. An inspection of the significance of the parameters is an additional tool in the discrimination between the rival correlations.

Among the resulting correlations, the one offering the best fit with the smallest number of significant parameters is finally selected. A distinction is made between group contribution methods (correlations IX to XI) and the other correlations (I to VIII), since they exhibit a different degree of complexity and may have different areas of application. Group contribution methods are more appropriate for high precision measurements, while the more simplified correlations, which are less demanding in calibration effort, can be used for automated routine analyses.

The results of the parameter estimation and of the statistical tests are given in Table VII.

TABLE VII

PARAMETER ESTIMATION AND RESULTS OF STATISTICAL TESTS

Correlation	*Parameter estimates 95% confidence limits*	*t-values*	*Lack-of-fit F-value*	*Average % error*
I	$A = 12.46 \pm 0.16$	155.0	0.5344	1.694
II	$A = 12.43 \pm 0.21$	121.6		
	$B = 11.97 \pm 1.31$	18.21	0.3642	1.234
	$C = 12.83 \pm 0.39$	65.32		
III	$A = 12.79 \pm 0.63$	40.75	0.5015	1.603
	$B = -0.180 \pm 0.324$	−1.112		
IV	$A = 7.272 \pm 0.106$	137.8	1.8399	3.402
V	$A = 0.1045 \pm 0.0169$	12.36		
	$B = 2.07 \pm 20540$	0.00	0.2628	1.134
	$C = -3.07 \pm 40700$	0.00		
VI	$A = 0.1052 \pm 0.0013$	161.9	0.2375	1.128
VII	$A = 0.1068 \pm 0.0016$	158.0	0.4479	1.482
VIII	$A = 11.01 \pm 0.70$	31.75	0.5108	1.614
	$B = 2.418 \pm 0.378$			
IX	$(CH_3) = 0.580 \pm 0.030$	38.84		
	$(CH_2) = -0.002 \pm 0.008$	−0.49		
	$(CH) = -0.583 \pm 0.062$	−19.01		
	$(C) = -1.163 \pm 0.111$	−21.06		
	$(5) = 1.151 \pm 0.186$	26.89	0.2955	0.888
	$(6) = 1.130 \pm 0.069$	32.76		
	$(C_{aro}–H) = 0.167 \pm 0.009$	38.38		
	$(C_{aro}–C) = -0.385 \pm 0.039$	−19.56		
	$(C=H_2) = 0.618 \pm 0.061$	20.36		
	$(C=CH) = -0.027 \pm 0.040$	−1.34		
X	$(CH_3) = 18.59 \pm 3.48$	10.66		
	$(CH_2) = 15.62 \pm 1.16$	26.92		
	$(CH) = 12.70 \pm 8.93$	3.66		
	$(C) = 10.23 \pm 12.55$	1.63		
	$(5) = 2.33 \pm 9.38$	0.50	0.1857	0.695
	$(6) = 0.52 \pm 8.65$	0.12		
	$(C_{aro}–H) = 12.99 \pm 0.71$	36.23		
	$(C_{aro}–C) = 11.31 \pm 4.19$	5.41		
	$(C=H_2) = 20.86 \pm 6.03$	6.93		
	$(C=CH) = 12.43 \pm 3.56$	6.98		
XI	$(CH_3) = 12.06 \pm 2.68$	8.98		
	$(CH_2) = 12.60 \pm 0.91$	27.74		
	$(CH) = 13.11 \pm 5.32$	4.92		
	$(C) = 13.26 \pm 9.58$	2.77		
	$(5) = -1.85 \pm 7.24$	−0.51	0.1838	0.697
	$(6) = -0.44 \pm 6.74$	−0.13		
	$(C_{aro}–H) = 13.05 \pm 0.71$	36.46		
	$(C_{aro}–C) = 12.26 \pm 3.51$	6.99		
	$(C=H_2) = 8.43 \pm 4.68$	3.60		
	$(C=CH) = 13.42 \pm 2.98$	9.04		

Correlation IV, in which the RMR is taken to be proportional to the heat of reaction of the oxidation of the hydrocarbon into carbon dioxide and hydrogen[10], is the only one to be rejected because of lack of fit. It has a very pronounced tendency to overestimate the calibration factors for saturates, and to underestimate those for aromatic hydrocarbons. Since the correlation is inadequate for hydrocarbons, it is not likely to be valid for oxygenated compounds[10].

A number of other correlations can be eliminated on the basis of the non-significance of some of the parameters, as revealed by their small t-values. This is the case for correlations III and V. In correlation III, the contribution of hydrogen atoms to the RMR of hydrocarbons appears to be non-significant. The correlation is reduced to correlation I by eliminating this parameter:

$$\frac{\mathrm{MW}(i)}{\mathrm{CF}(i)} = AN_{\mathrm{C}} + BN_{\mathrm{H}} = AN_{\mathrm{C}}$$

by eliminating the parameter B.

In the same way, correlation V turns into correlation VI:

$$\mathrm{CF}(i) \cdot \mathrm{MW}(i) = A\frac{[B + (-\Delta G^0)_{\mathrm{ox}}]^2}{[C + (-\Delta G^0)_{\mathrm{ox}}]} = A(-\Delta G^0)_{\mathrm{ox}}$$

by eliminating the parameters B and C.

In the group contribution methods X and XI, the number of contributions can be reduced by two, since the presence of a naphthenic ring apparently does not affect the response of an aliphatic carbon atom.

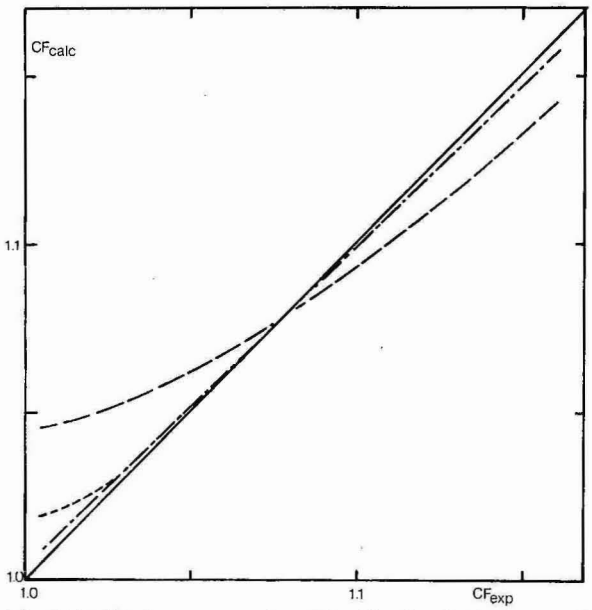

Fig. 5. Predicted *versus* experimental calibration factors. — —, Correlations I and VII; ----, Correlations II, VI and VIII; — · —, Correlations IX, X and XI.

As far as the group contribution methods are concerned, the best fit is obtained with correlations X and XI.

Further discrimination between these two is impossible. Since these correlations are derived from others that are already adequate (correlations VI and II, respectively) simply by adding parameters, intercorrelation between the parameters is high. This leads to extremely wide confidence intervals for the parameter estimates, as can be seen in Table VII. On the other hand, group contribution methods allow the closest prediction of CFs, as is evident from the average percentage error in Table VII and from Fig. 5. This figure also reveals that some of the remaining simplified correlations (I and VII) show a tendency to overestimate the CFs for aromatics. Correlation I (RMR proportional to N_C) is clearly an oversimplification. Since one of the main goals of calibrating is to arrive at an accurate ratio of saturates to aromatics, these correlations are discarded in favour of the correlations II (effective carbon number contributions), VI [$(-\Delta G^0)_{ox}$] and VIII (extension of VI). From the three resulting ones, correlation VI turns out to be the most efficient, combining a good fit with the lowest possible number of parameters.

CONCLUSIONS

It has been demonstrated that, in a reliable and precise analysis of complex hydrocarbon mixtures, calibration of detectors (flame ionization as well as thermal conductivity) is an absolute necessity. Calibration is even more necessary if heavier compounds are to be referred to a low-molecular-weight standard. It is not necessary to determine CFs for all the hydrocarbons analysed, as CFs on flame ionization detectors can be correlated. A new correlation, based on $(-\Delta G^0)_{ox}$ at 298K, has been presented and turns out to be very efficient. The use of detailed structural group contribution methods allows a very accurate prediction of CFs on flame ionization detectors from a limited number of calibration experiments.

ACKNOWLEDGEMENTS

J. L. Dierickx is grateful to the Belgian "Instituut tot aanmoediging van het Wetenschappelijk Onderzoek in Nijverheid en Landbouw" for a Research Fellowship.

P. M. Plehiers is grateful to the Belgian "Nationaal Fonds voor Wetenschappelijk Onderzoek" for a Research Assistantship.

REFERENCES

1 P. S. Van Damme and G. F. Froment, *Chem. Eng. Prog.*, 78(7) (1982) 77.
2 C. E. Van Camp, P. J. Clymans, P. S. Van Damme and G. F. Froment, *J. Chromatogr. Sci.*, 21 (1983) 259.
3 P. S. Van Damme, C. E. Van Camp, P. J. Clymans and G. F. Froment, *Oil Gas J.*, Sept 7 (1981) 124.
4 I. Halasz and W. Schneider, *Anal. Chem.*, 33 (1961) 979.
5 J. N. McTaggart and J. V. Mortimer, *J. Inst. Pet.*, 50 (1964) 255.
6 W. A. Dietz, *J. Gas Chromatogr.*, 5 (1967) 68.
7 E. R. Adlard, *Crit. Rev. Anal. Chem.*, 5 (1975) 1.
8 J. H. Bromly and P. Roga, *J. Chromatogr. Sci.*, 18 (1980) 606.

9 A. T. Blades, *J. Chromatogr. Sci.*, 11 (1973) 251.
10 E. M. Bulewicz, *Combust. Flame*, 11 (1967) 297.
11 A. J. Andreatch and R. Feinland, *Anal. Chem.*, 32 (1960) 1021.
12 J. C. Sternberg, W. S. Gallaway and D. T. L. Jones, in N. Brenner, J. E. Callen and M. D. Weiss (Editors), *Gas Chromatography*, Academic Press, New York, 1962, p. 231.
13 R. G. Ackman, *J. Gas Chromatogr.*, 2 (1964) 173.
14 R. G. Ackman, *J. Gas Chromatogr.*, 6 (1968) 497.
15 A. T. Blades, *Combust. Flame*, 12 (1968) 174.
16 B. A. Schaeffer, *Combust. Flame*, 13 (1969) 208.
17 E. M. Bulewicz, *Combust. Flame*, 13 (1969) 214.
18 R. C. Reid, J. M. Prausnitz and T. K. Sherwood, *The Properties of Gases and Liquids*, McGraw-Hill, New York, 3rd ed., 1977, pp. 224 and 629.
19 G. Perkins, jr., R. E. Laramy and L. D. Lively, *Anal. Chem.*, 35 (1963) 360.
20 S. W. Benson, *Thermochemical Kinetics*, Wiley, New York, 1976.
21 N. R. Draper and H. Smith, *Applied Regression Analysis*, Wiley, New York, 1966, 26.

Journal of Chromatography, 362 (1986) 175–185
Elsevier Science Publishers B.V., Amsterdam — Printed in The Netherlands

CHROM. 18 673

SIMPLE MODEL BASED ON SOLUBILITY PARAMETERS FOR LIQUID DESORPTION OF ORGANIC SOLVENTS ADSORBED ON ACTIVATED CARBON

JAN RUDLING
Research Department, National Board of Occupational Safety and Health, 171 84 Solna (Sweden)
(Received February 28th, 1986)

SUMMARY

Liquid desorption recoveries were studied on two carbons (SKC and Merck) commonly used for sampling of solvent vapours in air. For non-polar solvents it was found that carbon disulphide is an effective desorber as long as its surface free energy exceeds that of the adsorbed solvents. For polar solvents the recoveries with carbon disulphide are related to a parameter, ΔE_{DA}, that could be estimated from Hansen's solubility parameters. By using compounds with high ΔE_{DA} values as 5% mixtures in carbon disulphide recoveries could be raised to *ca.* 100% for 2-ethoxyethanol, butanol, acetone, dioxane and propyl acetate.

INTRODUCTION

The collection of organic solvent vapours on activated carbon followed by liquid desorption and gas chromatographic (GC) analysis has been used for a long time as a method to determine workers' exposure to industrial solvents. As early as 1964 Otterson and Guy[1] concluded that the use of carbon disulphide (CS_2) as desorbing agent resulted in almost complete recoveries for vapours of styrene, xylene and perchloroethylene collected on activated carbon. Slightly lower recoveries were obtained with toluene and benzene as desorbing agents, and the use of mesitylene and xylene yielded poorer results. CS_2 was used throughout the extensive study conducted by the National Institute for Occupational Safety and Health (NIOSH)[2] for desorption of non-polar solvents. For most aliphatic, aromatic and halogenated solvents recoveries of *ca.* 100% were obtained: exceptions included styrene, naphthalene, tetrachloroethane and tetrabromoethane.

The NIOSH study clearly demonstrated that for polar solvents, such as alcohols, ketones and ethers, CS_2 was not a good choice. A significant increase could in many cases be obtained by addition of a small amount of an alcohol, *e.g.* methanol. Other desorbing agents, such as dimethylformamide (DMF) in conjuction with a backflush technique[3] or 5% methanol in dichloromethane (photoionization detector)[4], have been found to increase recoveries to *ca.* 100%. However, with these procedures several common non-polar solvents, such as toluene and benzene, are not quantitatively recovered.

0021-9673/86/$03.50

Most suggestions concerning desorbing agents have been made on purely empirical grounds. As far as we know no systematic approach to liquid desorption of solvent vapours from activated carbon has been published. In spite of the difficulty of finding a useful model for an adsorbent that is heterogenous with regard to the chemical nature of the sites as well as the size and shape of the micropores responsible for most of the adsorption, a coarse model is valuable since it limits the number of possible desorbing agents to test. In practice, further limitations are set by the chromatographic conditions since the desorbing mixture has to be chosen so that it does not interfere with peaks emanating from the adsorbed vapours.

The purposes of this paper are to relate adsorption on both the hydrophobic and the hydrophilic parts of the surface to available physical–chemical parameters, and to apply the results to liquid desorption.

THEORY

Briefly, activated carbon consists of basal carbon layers of a "graphite-like" structure, with a hydrophobic surface, and of surface oxides located on the reactive edges of the carbon layers, giving a hydrophilic surface[5]. Usually the hydrophobic surface amounts to more than 90% of the available adsorption area.

The interaction between non-polar surfaces and liquids is predominately due to dispersion forces. The magnitude of the dispersive part of the free energy of interaction, $-W_A^d$, may be estimated[6] from eqn. 1:

$$W_A^d = 2\,(\gamma_i^d \cdot \gamma_s^d)^{\frac{1}{2}} \tag{1}$$

where W_A^d is dispersive part of the work of adhesion and γ_i^d and γ_s^d are the dispersive parts of the surface free energies of the liquid and solid, respectively. For non-polar surfaces, eqn. 1 is a good estimate of the total work of adhesion, W_A. For the sake of simplicity this approximation will be used here.

The solubility parameter, δ, is defined as:

$$\delta^2 = \Delta E_v / V$$

where ΔE_v is the energy of vaporization and V is the molar volume. Hansen and Beerbower[7] have proposed, that on the basis of the different types of intermolecular interaction, the solubility parameter may be further subdivided into three independent components: one due to dispersion forces (δ_D), one due to dipole moments (δ_P) and one due to hydrogen bonding (δ_H). This subdivision is based on the notion that the polar interactions may be divided into contributions from the two phases in the same way as for the dispersion forces (eqn. 1). This assumption can be criticized on theoretical grounds, but the division has been found useful in practice and the parameters are available for almost all industrial solvents. Some examples are given in Tables I and II.

Beerbower[8] has found the following relation between the dispersive component of the surface tension and Hansen's dispersive solubility parameter:

$$\gamma^d = 0.0715 V^{1/3} \cdot \delta_D^2 \tag{2}$$

TABLE I

DATA FOR NON-POLAR COMPOUNDS

The table gives surface free energy, γ (mJ/m^2) (*Handbook of Chemistry and Physics*), dispersive solubility parameter[7], δ_D (cal/cm^3)$^{1/2}$, and molar volume, V (cm^3), for the non-polar organic solvents used in this study.

No.	*Compound*	γ	δ_D	V
1	Hexane	18.4	7.3	131.6
2	Octane	21.8	7.6	163.5
3	Cyclohexane	25.5	8.2	108.7
4	Dichloromethane	26.5	8.9	63.9
5	Carbon tetrachloride	27.0	8.7	97.1
6	Toluene	28.5	8.8	106.8
7	Benzene	28.9	9.0	89.4
8	*m*-Xylene	28.9	8.7*	121.2*
9	1,1,2,2-Tetrachloroethane	36.0	9.2	105.2
10	Tetrachloroethylene	31.7	9.3	101.1
11	Chlorobenzene	33.6	9.3	102.1
12	Styrene	32.1	9.1	115.6
13	Ethylbenzene	29.2	8.7	123.1
14	Bromoform	41.5	10.5	87.5
15	Nitrobenzene	43.9	9.8	102.7
16	1,1,2,2-Tetrabromoethane	49.7	11.1	116.8
17	Trichloroethylene	32.0	8.8	90.2
	Carbon disulphide	32.3	10.0	60.0

* Value for *o*-xylene.

where V is the molar volume and δ_D is Hansen's dispersive solubility parameter. This relation can be used to estimate the dispersive component for polar liquids.

If γ_s^d is assumed to be constant, the dispersive part of the work of adhesion (and indirectly the adsorption strength) should be a function of the surface free energy for the liquid only, or in terms of Beerbower's relation a function of $V^{1/3} \cdot \delta_D^2$. For the use of CS_2 as a desorbing agent for non-polar solvents, the recovery would be expected to be dependent on the surface free energy of the adsorbate, which could be considered to be in the liquid state owing to condensation in the micropores. Compounds with low surface free energy, *e.g.* hexane, are not expected to work well as desorbing agents, in contrast to benzene or CS_2.

If we now consider the hydrophilic part of the surface, "acid–base" interactions (electron donor–acceptor interactions) are generally considered to be the most important forces for adsorption of polar compounds[9,10]. Adsorption of "acidic and basic" polymers is well correlated with the donor–acceptor properties of the solvents used. According to Jensen[11] and others, the donor (basic) and acceptor (acidic) properties of a liquid can be expressed by two numbers, donor number (DN) and acceptor number (AN). These numbers are determined experimentally by measuring the strength of interaction with a standard acid (gives DN) and a standard base (gives AN). It is recognized that DN and AN give a description with a closer relation to molecular parameters of the polar interactions than δ_P and δ_H. Unfortunately DN and AN are known for relatively few solvents: some examples are given in Table II.

TABLE II

DATA FOR POLAR COMPOUNDS

The table gives donor numbers (DN) and acceptor numbers (AN)[11]; Hansen's solubility parameters[7], δ $(cal/cm^3)^{1/2}$, ΔE_{DA} values (kcal/mol, calculated with eqn. 3) and molar volume, V (cm^3), for the polar solvents used in this study.

No.	*Compound*	*DN*	*AN*	*Solubility parameter*			ΔE_{DA}	V
				δ_D	δ_P	δ_H		
1	Ethyl formate	–	–	7.6	4.1	4.1	2.7	80.2
2	Methyl acetate	16.5	–	7.6	3.5	3.7	2.1	79.7
3	Ethyl acetate	17.1	–	7.7	2.6	3.5	1.9	98.5
4	Butyl acetate	–	–	7.7	1.8	3.1	1.7	132.5
5	2-Ethoxyethyl acetate	–	–	7.8	2.3	5.2	4.4	136.2
6	Tetrahydrofuran	20.0	8.0	8.2	2.8	3.9	1.9	81.7
7	*p*-Dioxane	14.8	10.8	9.3	0.9	3.6	1.2	85.7
8	Acetone	17.0	12.5	7.6	5.1	3.4	2.8	74.0
9	Butanol	–	–	7.8	2.8	7.7	6.1	91.5
10	Propanol	–	–	7.8	3.3	8.5	6.3	75.2
11	Ethanol	20.5	37.1	7.7	4.3	9.5	6.4	58.5
12	Cyclohexanol	–	–	8.5	2.0	6.6	5.0	106.0
13	Diacetone alcohol	–	–	7.7	4.0	5.3	5.5	124.2
14	2-Ethoxyethanol	–	–	7.9	4.5	7.0	6.7	97.8
15	Acetonitrile	14.1	18.9	7.5	8.8	3.0	4.5	52.6
16	Dimethylformamide	26.6	16.0	8.5	6.7	5.5	5.8	77.0
	2-Butoxyethanol	–	–	7.8	2.5	6.0	5.6	131.6
	Diethylene glycol monoethyl ether	–	–	7.9	4.5	6.0	7.4	130.9
	Nitrobenzene	4.4	14.8	9.8	4.2	2.0	2.2	102.7
	Benzyl alcohol	–	–	9.0	3.1	6.7	5.6	103.6
	Acetophenone	–	–	9.6	4.2	1.8	2.4	117.4

Ideally a good correlation of adsorption on the polar surface of activated carbon with the properties of the adsorbate should be based on an estimation of the DN and AN of the surface. This could possibly be done provided that we have a knowledge of the chemical nature of the adsorption sites. Attempts to reveal these structures were made by the use of electron spectroscopy for chemical analysis (ESCA) but these did not give the desired result.

However, another approach could be tried. It has been found that in many cases there is a good correlation between Hansen's polar solubility parameters (see Table II) and ΔE_{DA}[10], where $\Delta E_{DA} = DN \cdot AN/100$ (kcal/mol):

$$\Delta E_{DA} = V \cdot (\delta_P^2 + \delta_H^2)/1000 \qquad (3)$$

If it is assumed that all hydrophilic sites as an average have about the same donor and acceptor strength, the interaction energy as a geometric average of the DN and AN values (ΔE_{DA}) of the adsorbate would be expected to show some correlation with the observed adsorption in a solvent with high dispersive interactions like CS_2 (*i.e.* the polar interactions of the solvent with the surface are relatively small and only

CS_2 is adsorbed on the hydrophobic surface). For amphoteric solvents with about equal donor and acceptor strengths (alcohols) an overestimation of adsorption would probably be the result, and for solvents that are typically donors or acceptors an underprediction could be expected.

For a highly microporous adsorbent like activated carbon, there are phenomena related to the pore structure that could be of importance. In small pores (micropores less than 20 Å) the molecular diameter is of the same magnitude as the pore diameter. If the ratio of these two diameters is close to unity, the force field of the opposite pore wall contributes significantly to the adsorption energy[12]. Very small pores (or constrictions in the pore system) could be inaccessible to larger molecules. This pore size discrimination could be of importance when a small desorber molecule is substituted for a larger one. The micropore diffusion rate decreases considerably when the molecular diameter increases, and a long equilibration time would be the result.

The surface energy is given against air or the liquid's own vapour. The orientation of the molecule towards the surface is important[13]. A planar molecule such as benzene "fits the graphite-like" surface very well compared with branched aromatics such as butylbenzene. Hexane could be expected to interact more closely with the surface than cyclohexane, where the average distance to the surface of the atoms may be dependent on the "chair" or "boat" configuration of the molecule.

A desorption agent can work in two ways. First, it can displace the adsorbed compounds from the surface and thus decrease the number of available sites. Second, it can interact with the analyte in the solution thereby reducing the affinity of the adsorption sites. A good desorption agent usually combines these two properties. A compound that is strongly adsorbed should be a good displacing agent for compounds more weakly adsorbed, provided that adsorption takes place on the same type of sites.

EXPERIMENTAL

Two carbons SKC 120 (SKC, Eightyfour, PA, U.S.A.) and Merck (Nr. 9624) were used in this study: their characteristics are shown in Table III. Methods used for characterization have been described earlier[5].

Dried carbon (100 mg) was placed in a 3-ml screw-cap vial and the solvents (p.a. quality or better) were added from a syringe. After a delay of at least 24 h, samples were desorbed with 1.0 ml of desorbing agent. The equilibration time was

TABLE III

CHARACTERISTICS OF ACTIVATED CARBONS USED

	SKC	*Merck*
BET-surface area (m^2/g)	1120	1150
Pore volume (cm^3/g)	0.59	0.60
Micropore volume (cm^3/g)	0.43	0.37
Oxygen (% by weight)	*ca.* 8.7	*ca.* 10
pH in aqueous solution	9.7	5.7

ca. 24 h (with CS 2 h). Analysis was performed on a Varian 3400 gas chromatograph equipped with a flame ionization detector using non-polar or medium polar capillary columns (25 m × 0.2 mm I.D.). Samples were injected with a split injector and peak areas recorded with an Altex Chromatopak integrator.

RESULTS AND DISCUSSION

Recovery as a function of the surface free energy for a number of non-polar compounds (1 μl on 100 mg of carbon) desorbed with 1 ml of CS_2 is shown in Fig. 1. Surface free energy values have been obtained from *Handbook of Chemistry and Physics*. The same pattern was obtained for other loadings in the range 0.2–10 μl on 100 mg of carbon.

Aliphatic hydrocarbons, chlorinated aliphatics and aromatic hydrocarbons with surface free energy lower than that of CS_2 are easy to desorb, and recoveries are *ca.* 100%. Chlorobenzene and styrene, which have higher surface free energy, yield recoveries significantly less than 100%. As the surface free energy is further increased recoveries steadily fall. When compounds with about the same surface free energies are compared it is noticeable that halogenated aliphatic hydrocarbons have higher recoveries than aromatic compounds. None of these compounds is in a strict sense non-polar: halogenated compounds can act as electron acceptors and the π-electrons of the aromatics could be important. The atoms of the planar aromatic nucleus are also closer to the surface.

Recoveries obtained with hexane, cyclohexane, nitrobenzene, benzyl alcohol and acetophenone as desorbing agents are shown in Table IV. Cyclohexane gives extremely poor recoveries, and, as previously mentioned, this could be explained by the different conformations of the molecule. As anticipated, hexane is not an efficient desorbing agent: the recoveries obtained are also in this case a function of the surface free energy of the adsorbate. Of the three substituted aromatics, acetophenone and

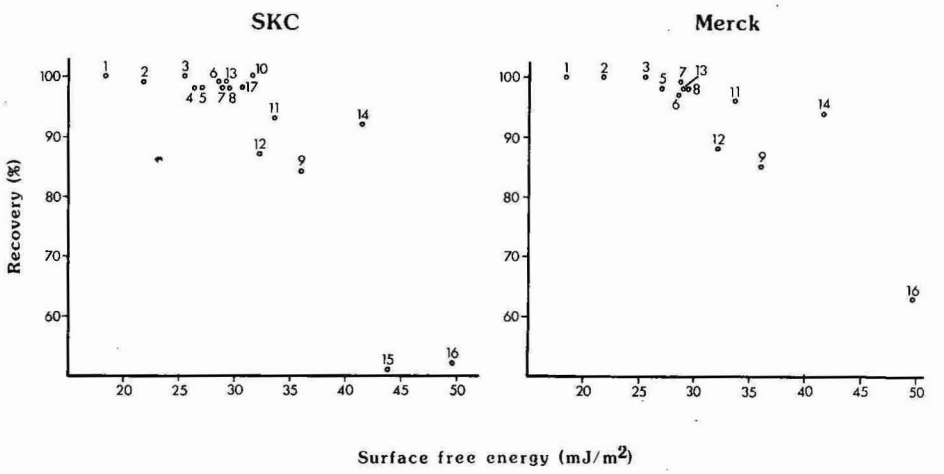

Fig. 1. Recovery as a function of the surface free energy for a number of non-polar compounds (1 μl added to 100 mg of carbon) desorbed with carbon disulphide. For key see Table I.

TABLE IV

EXPERIMENTS WITH DIFFERENT DESORBING AGENTS

The table shows recoveries for 1 μl of *n*-decane, toluene, styrene, trichloroethylene (TCE) and butanol on SKC and Merck (Mck) activated carbons using 1 ml of cyclohexane, hexane, benzyl alcohol, acetophenone and nitrobenzene as desorbing agents.

Desorbing agent	*Recovery (%)*									
	n-Decane		*Toluene*		*Styrene*		*TCE*		*Butanol*	
	SKC	*Mck*	*SKC*	*Mck*	*SKC*	*Mck*	*SKC*	*Mck*	*SKC*	*Mck*
Cyclohexane	8	–	4	–	2	–	–	–	–	–
Hexane	81	96	34	43	10	15	–	56	–	–
Benzyl alcohol	90	94	91	97	88	90	95	91	98	93
Acetophenone	97	97	100	101	96	94	99	102	101	98
Nitrobenzene	94	96	100	100	98	95	96	99	–	–

nitrobenzene yield higher recoveries than benzyl alcohol. The γ^d values calculated with Beerbower's relation are 32.3, 32.1 and 27.2, respectively. However, the interpretation of these numbers should not be stretched too far. A calculation for CS_2 gives $\gamma^d = 28$ mJ/m^2; the experimental value, γ, is 32.3, which shows that this relation is rather approximate. It is also interesting to note that acetophenone is a useful desorbing agent for polar compounds: recoveries for butanol are *ca.* 100%.

From a practical point of view none of these aromatics is especially suitable. Autosampler injections are unreliable (high viscosity?) and the long retention time is a problem. By using a backflush technique the latter problem might be solved. The results for decane could be an indication that 24 h of equilibration is not sufficient.

A scrutinization of Hansen's tables[7] does not reveal any attractive alternative to CS_2. In addition to its short retention time on most GC columns, CS_2 has another advantage, namely its low response on the flame ionization detector. Possible desorbing agents with higher surface free energy generally have high boiling points and viscosities.

Since the non-polar compounds that are difficult to desorb with CS_2 generally have low vapour pressures, the use of other adsorbents with lower capacity than activated carbon could be suggested. Nitrobenzene, for example, could be collected on porous polymers[14]. It is possible to desorb strongly adsorbed compounds from activated carbon, as has been demonstrated by Gu and Manes[15]. By the addition of naphthalene to the desorbing solvent they were able to desorb chlorinated polyaromatics. However, this procedure makes the analysis complicated.

Results obtained by other workers could also be explained in terms of the surface free energy of the desorbing agent, for dichloromethane $\gamma = 26.2$ and for DMF $\gamma^d = 22.0$ mJ/m^2 (calculated from Beerbower's relation). The latter value is probably too low. With dichloromethane the recovery for toluene was 85%[4]. With DMF the following results were obtained (compounds listed in order of increasing surface free energy): 1,2-dichloroethane ($\gamma = 24.2$ mJ/m^2) 93%, dichloromethane 91%, toluene 75%, benzene 81% and styrene 49%[3]. Thus, there is a good correlation between surface free energy and recovery.

In a study by Mueller and Miller, dichloromethane and trichloroethylene were desorbed with trichlorotrifluoroethane, chloroform and *o*-dichlorobenzene[16]. The first-mentioned solvent was, as could be expected (γ^d = 18.2 mJ/m^2), not efficient (recoveries 67% and 13%). Chloroform (γ = 27.1 mJ/m^2) was capable of quantitatively recovering dichloromethane, although lower recoveries were obtained for trichloroethylene. *o*-Dichlorobenzene yielded recoveries of *ca.* 90%, but the short equilibration time was probably not sufficient.

Recoveries for polar compounds (1 μl on 100 mg of carbon) as a function of ΔE_{DA} are given in Fig. 2. Although there is a fair amount of scatter, as could be expected, a definite relationship is established (r = −0.87 for both carbons). It should also be pointed out that for practical reasons, the recoveries were not obtained with equimolar amounts of adsorbate. For most compounds, 2-ethoxyethanol being an exception, only minor changes in the figure are expected if results for equimolar amounts are compared. Generally adsorption is stronger on the Merck carbon; this could be attributed to the higher oxygen content on this carbon (Table III) and to the fact that this carbon contains more acidic surface oxides[5]. In spite of these facts the same pattern is followed on both carbons. Some peculiarities could be stressed: dioxane is rather strongly adsorbed on Merck in contrast to SKC, and the difference between the alcohols and 2-ethoxyethanol is more pronounced on SKC.

If electron donors and acceptors are adsorbed on the same sites it should follow that compounds with high ΔE_{DA} values should be effective displacing agents. To put the matter to test, six solvents with different ΔE_{DA} values were prepared as 1% and 5% (by volume) mixtures in CS_2. Then 0.2–10 μl of butanol, 2-ethoxyethanol, acetone, *p*-dioxane and propyl acetate were added to the carbon and later desorbed with these mixtures. The test series on Merck was of more limited scope and comprised only butanol and 2-ethoxyethanol. The results (1 μl on 100 mg of carbon) are shown in Figs. 3 and 4. No values for dioxane are presented, but the results agreed very well with those for propyl acetate.

The efficiency of a desorbing agent is clearly related to its ΔE_{DA} value, although not as a simple function. As seen in Fig. 3 there is a slight "dip" for DMF, and in

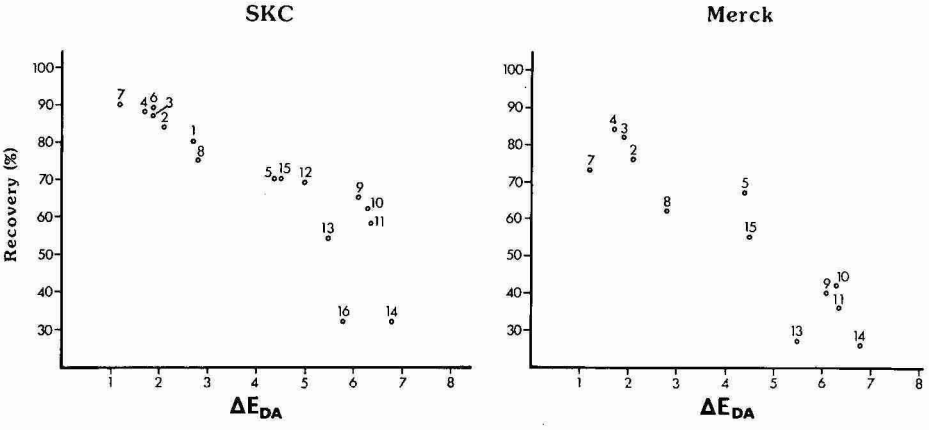

Fig. 2. Recovery as a function of ΔE_{DA} (see Table II) for a number of polar compounds (1 μl added to 100 mg of carbon) desorbed with carbon disulphide. For key see Table II.

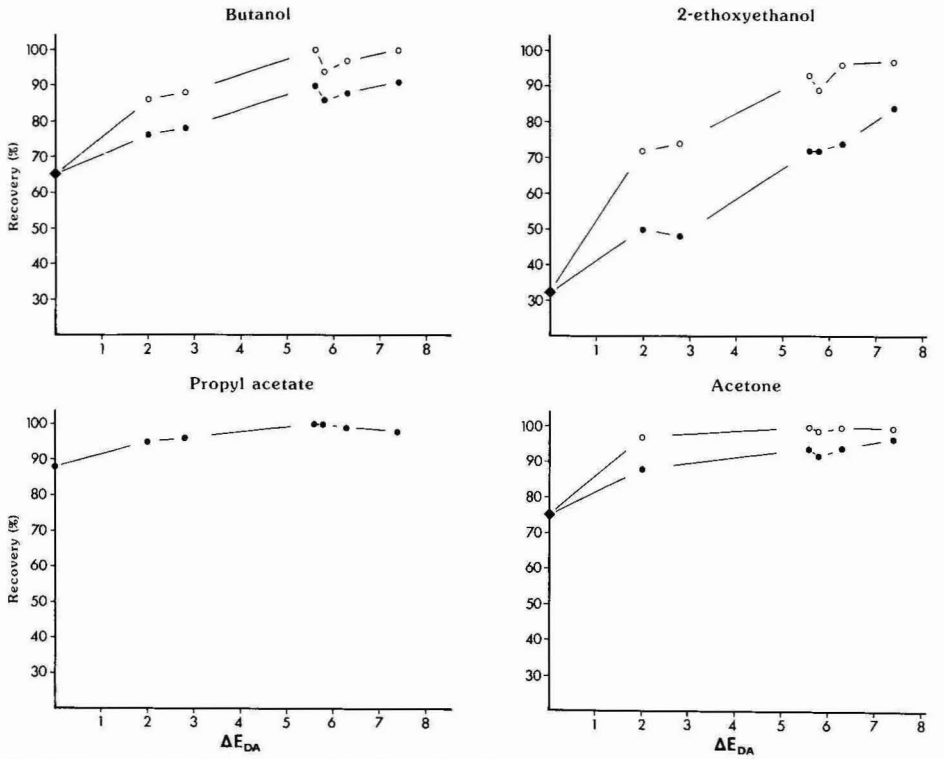

Fig. 3. Recoveries for 1 μl of butanol, 2-ethoxyethanol, acetone and propyl acetate on SKC carbon using 1% (●) and 5% (○) mixtures in carbon disulphide of the following solvents with ΔE_{DA} values given in Table II: methyl acetate, acetone, 2-butoxyethanol, dimethylformamide, ethanol and diethylene glycol monoethyl ether.

Fig. 4 a peak for ethanol (butanol) and DMF (2-ethoxyethanol). Surface heterogeneity and variations in donor–acceptor strength on the two carbons are possible explanations. Acetone (5%) gives about the same recoveries for butanol and 2-ethoxyethanol as 1% of the compounds with higher ΔE_{DA} values. For a solvent with a low ΔE_{DA} value the percentage added has to be increased in order to remove strongly retained adsorbates. Thus 50% acetone in CS_2 yields recoveries of 100% for butanol and 94% for ethyl cellosolve, whereas 50% dioxane is capable of raising recoveries for butanol to only 85%. Given a certain desorbing mixture, recoveries are related to the ΔE_{DA} values of the adsorbate. A strongly adsorbed compound, such as 2-ethoxyethanol, requires a higher ΔE_{DA} value/concentration of an addition compared with acetone for example.

It must be noted that the desorption of polar compounds requires a desorbing agent with sufficiently strong dispersive interactions with the hydrophobic surface, because otherwise the polar compounds would be adsorbed on this part of the surface. Ethanol or methanol would therefore not work well if used as desorbing agents by themselves.

The demonstrated relationships between recovery and surface free en-

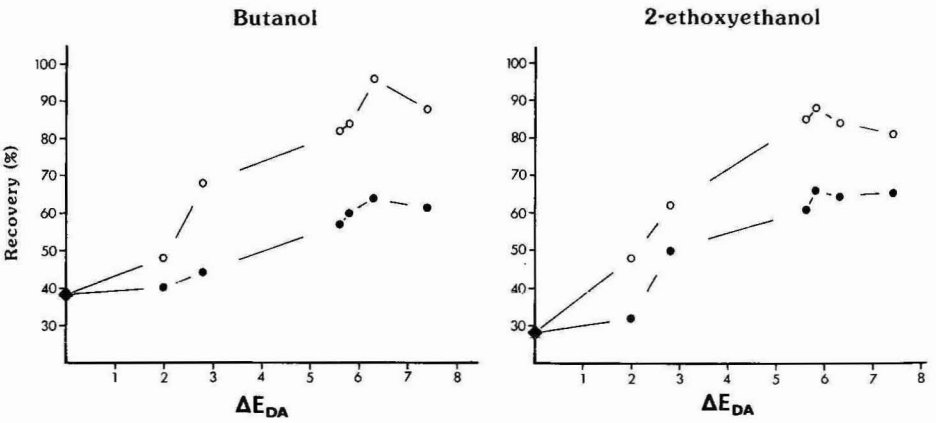

Fig. 4. Recoveries for 1 μl of butanol and 2-ethoxyethanol on Merck carbon using 1% (●) and 5% (○) mixtures in carbon disulphide of the following solvents with ΔE_{DA} values given in Table II: methyl acetate, acetone, 2-butoxyethanol, dimethylformamide, ethanol and diethylene glycol monoethyl ether.

ergy/ΔE_{DA} are rather approximate and cannot be used to predict recoveries for a certain desorbing system. The preferred uses of these relationships are to single out difficult compounds that could be used as touchstones for a desorbing agent, and to select suitable candidates for desorbing mixtures. This approach should increase experimental efficiency by limiting the number of experiments needed as new carbons and desorbing mixtures are tested.

ACKNOWLEDGEMENT

I am indebted to Professor Folke Ingman and Dr. Johan Roeraade at the Department of Analytical Chemistry of the Royal Institute of Technology, Professor Per Stenius at the Institute for Surface Chemistry, and Professor Ulf Ulfvarson at the Technical Unit of the Board for valuable discussions while this work was undertaken, and for helpful comments when the manuscript was in preparation.

REFERENCES

1 E. J. Otterson and C. U. Guy, *Transactions of the 26th Annual Meeting of the American Conference of Governmental Industrial Hygienists, Philadelphia, PA*, American Conference of Governmental Industrial Hygienists, Cincinnati, OH, 1964.
2 D. G. Taylor, R. E. Kupel and J. M. Bryant, *Documentation of the NIOSH Validation Tests*, DHEW (NIOSH) Publication No. 77–175, U.S. Government Printing Office, Washington, DC, 1977.
3 I. Johansen and J. F. Wendelboe, *J. Chromatogr.*, 217 (1981) 317.
4 J. C. Posner, *Am. Ind. Hyg. Assoc. J.*, 42 (1981) 647.
5 J. Rudling and E. Björkholm, *Am. Ind. Hyg. Assoc. J.*, in press.
6 F. M. Fowkes, *J. Colloid Interface Sci.*, 28 (1968) 493.
7 C. M. Hansen and A. Beerbower, *Encyclopedia of Chemical Technology, Supplemental Volume*, Wiley, New York, 2nd ed., 1971, pp. 889–910.
8 A. Beerbower, *J. Colloid Interface Sci.*, 35 (1971) 126.
9 F. M. Fowkes and M. A. Mostafa, *Ind. Eng. Chem. Prod. Res. Dev.*, 17 (1978) 3.
10 W. B. Jensen, *Chemtech*, 12 (1982) 755.

11 W. B. Jensen, *The Lewis Acid Base Concepts*, Wiley Interscience, New York, 1980, p. 235.
12 S. J. Gregg and K. S. W. Singh, *Adsorption, Surface Area and Porosity*, Academic Press, London, 2nd ed., 1982, p. 207.
13 A. V. Kiselev, *Discuss Faraday Soc.*, 40 (1965) 228.
14 K. Andersson, J-O. Levin and C-A. Nilsson, *Chemosphere*, 12 (1983) 377.
15 T. Gu and M. Manes, *Environ. Sci. Technol.*, 18 (1984) 55.
16 F. X. Mueller and J. A. Miller, *Am. Ind. Hyg. Assoc. J.*, 40 (1979) 380.

Journal of Chromatography, 362 (1986) 187–196
Elsevier Science Publishers B.V., Amsterdam — Printed in The Netherlands

CHROM. 18 680

FACTORS CONTRIBUTING TO INTRINSIC LOADING CAPACITY IN SILICA-BASED PACKING MATERIALS FOR PREPARATIVE ANION-EXCHANGE PROTEIN CHROMATOGRAPHY*

M. A. ROUNDS, W. KOPACIEWICZ and F. E. REGNIER*
Department of Biochemistry, Purdue University, West Lafayette, IN 47907 (U.S.A.)
(Received February 27th, 1986)

SUMMARY

Properties of the matrix and stationary phase which affect the intrinsic loading capacity of silica-based packing materials for preparative anion-exchange chromatography of proteins were investigated.

Polyethyleneimine-coated controlled porosity glass beads ranging from 100 to 2000 Å in pore diameter were used to evaluate the effects of pore diameter and surface area. Protein binding was found to depend on accessible, rather than total, support surface area. Consequently, wide-pore, high surface area media provide maximum intrinsic loading capacity.

Increasing the number of positively charged sites on the stationary phase by increased coating or by quaternization of amines increases hemoglobin-binding capacity.

INTRODUCTION

In selecting a silica-based matrix for surface-mediated preparative chromatography of proteins, materials of high 'intrinsic loading capacity" are desirable. Intrinsic loading capacity has been defined as the maximum amount of solute that can be loaded onto a medium (per unit of mass or volume) without regard to chromatographic separation[1]. This inherent characteristic of a sorbent is useful both for investigating media contributions to protein adsorption and comparing operational loading capacity of columns. It is the purpose of this paper to identify some physical and chemical factors which contribute to intrinsic loading capacity in anion-exchange chromatographic packing materials.

Ion-exchange chromatography requires interaction between solutes and the support surface. Thus, the capacity of such a sorbent depends, in part, on its surface area. Change *et al.*[2] have shown that binding capacity is also influenced by support pore diameter. A diethylaminoethyl-containing stationary phase was bonded to con-

* This is Journal Paper Number 10 331 from the Purdue University Agricultural Experiment Station.

0021-9673/86/$03.50

trolled porosity glass beads of 100, 240 or 550 Å pore diameter. Hemoglobin (Hb) ion-exchange capacity (expressed as mg Hb/cm^3) was highest for the 240 Å support, even though its surface area (130 m^2/g) is less than that of the 100 Å pore diameter media (170 m^2/g). It was hypothesized that the relatively large Hb molecule could not reach all available ion-exchange groups. Lowest ion-exchange capacity was exhibited by the 550 Å beads. Although these larger pore diameter media should permit better access, lower surface area (70 m^2/g) means fewer ligands are available for binding protein.

These results suggested that ion-exchange fractionation on supports having pore diameters similar to solute molecular dimensions is actually a combination of ion-exchange and size-exclusion chromatography. Size discrimination by ion-exchange media can be overcome by the use of large pore diameter particles. Pore diameters of 1000 Å (or greater) should allow molecules over 10^5 daltons to have nearly complete access to the internal surface[3]. Unfortunately, since the surface area of these materials is low, they are of relatively low ion-exchange capacity. Techniques for overcoming this problem via polymeric coatings were examined by Vanacek and Regnier[3].

In the present work, pore diameter and surface area effects were further investigated using controlled porosity glass (CPG) beads ranging from 100 to 2000 Å in pore diameter. Controlled porosity glass was chosen because these media are of narrow pore-size distribution and constant geometry[4]. The beads were coated with polyethyleneimine (PEI)[5] and their binding capacities for three proteins of different molecular weight were determined by means of static assays. Four (PEI-coated) commercial silicas of widely varying surface area were also evaluated for Hb-binding capacity in order to examine general applicability of the CPG data.

Stationary phase contributions to intrinsic binding capacity were studied using the same PEI coating on silica. Several modifications of the basic coating method[6] produced anion-exchange stationary phases of varying ligand density and amine type. Comparisons were made using Hb.

MATERIALS AND METHODS

Support materials

CPG beads of 100, 240 and 550 Å pore diameter were purchased from Pierce (Rockford, IL, U.S.A.). Those of 1000 and 2000 Å pore diameter were purchased from Electro-Nucleonics (Fairfield, NJ, U.S.A.). All were 37–74 μm particles. Surface areas, as specified by the manufacturer, are listed in Table I.

Vydac 101TPB (5.5 or 15–20 μm particles) silica was a gift from The Separations Group (Hesperia, CA, U.S.A.). PQ 200 Å and 270 Å experimental silicas were gifts from The PQ Corporation (Valley Forge, PA, U.S.A.). Serva Si-200 silica was obtained from Serva Fine Biochemicals (Westbury, NY, U.S.A.). Pharmacia Fine Chemicals (Piscataway, NJ, U.S.A.) provided A-50-120 DEAE Sephadex (40–120-μm particles).

Reagents

Polyethyleneimine-6 and 1,3-diglycidylglycerol were supplied by Polysciences (Warrington, PA, U.S.A.). Methyl iodide and "glycidol" (GLY) (1,2-epoxy-3-hy-

droxypropane) were purchased from Aldrich (Milwaukee, WI, U.S.A.). Eastman-Kodak (Rochester, NY, U.S.A.) supplied 1,2-epoxy-3-(*p*-nitrophenoxy)propane (ENPP), 1,2,2,6,6-pentamethylpiperidine and Coomassie Brilliant Blue G-250 dye (CI 42655; for Bradford assay).

Inorganic reagents and solvents were AR grade or of comparable quality.

Biochemicals

Proteins emplyed were: horse heart myoglobin (MYO; 17 500; 7.3); bovine hemoglobin (Hb; 64 500; 6.8); equine ferritin (FER; 440 000; 4.3); bovine serum albumin (BSA; 69 000; 5.0) and egg white ovalbumin (OVA; 43 500; 4.7). Numerical values in parentheses refer to molecular weight and isoelectric point[7,8], respectively. All were purchased from Sigma (St. Louis, MO, U.S.A.) except FER which was obtained from Pharmacia Fine Chemicals. The proteins used to investigate pore diameter and surface area effects were twice crystallized or of equivalent purity. "Crude" bovine Hb was used for binding assays on coated silicas.

Intrumentation

A Perkin-Elmer Model 55 spectrophotometer (Perkin-Elmer, Norwalk, CT, U.S.A.) and a Spectronic 70 (Bausch and Lomb, Rochester, NY, U.S.A.) were used to measure concentrations in protein-binding assays.

Application and modification of stationary phases

All support materials were coated with polyethyleneimine (PEI)-6, a branched-chain polyamine of molecular weight *ca.* 600, based on the method of Alpert and Regnier[5]. CPG beads and silicas were coated with one percent PEI-6 (10% for high ligand lensity material) and cross-linked with five percent diglycidylglycerol (in methanol) as described by Kopaciewicz *et al.*[6]. Subsequent epoxide derivatization of this weak anion-exchange coating, with "glycidol" or 1,2-epoxy-3-(*p*-nitrophenoxy) propane[6], produced the GLY and ENPP stationary phases, respectively.

The quaternary amine strong anion-exchange packing material was prepared as follows: 0.8 g of PEI-coated silica was suspended in 4.5 ml of dry dimethylformamide (DMF) to which had been added 105 µl of 1,2,2,6,6-pentamethylpiperidine[9]. After brief sonication, 0.5 ml of methyl iodide was added. This suspension was heated in an oil bath at 60°C overnight. The support material was isolated in a sintered glass funnel and washed successively with water, methanol, triethylamine and methanol. After 0.5 h in the funnel, the methylated polyamine-coated silica was dried in a vacuum dessicator.

Static protein-binding capacity assay

Static assays with Hb and other proteins were performed as described by Kopaciewicz *et al.*[6] except that the ionic desorption solution was 1.0 *M* in sodium chloride (instead of 0.5 *M*). Data reported are total desorbed protein (ionic + non-ionic) in mg/g support material. For all assays on the controlled porosity glass beads, aliquots of the desorption solutions were analyzed by the Bradford method[10] using appropriate standard curves (absorbance at 595 nm *vs.* µg protein). Experimental error was within 5%.

RESULTS AND DISCUSSION

Identifying factors which contribute to the intrinsic loading capacity of a column packing material required the use of media in which particle size, pore diameter, surface area and the chemical nature of the stationary phase could be controlled. This was accomplished by application of an adsorbed polyamine coating[5] to either CPG beads or silica of known dimensions.

Pore diameter and surface area effects

As an extension of the work previously discussed[2], the effects of pore diameter and surface area on intrinsic loading capacity were investigated using 100–2000 Å CPG beads. Since seventy percent of the proteins reported in the literature are acidic[7], an anion-exchange stationary phase was prepared by applying a "thin" coating of PEI to the beads. The polyamine coating itself has been shown to consume pore volume[3]; thus, manufacturer's specified pore diameters and surface areas were corrected to account for the thickness of the PEI layer (see Table I).

Hemoglobin-binding capacity assays were performed on the coated beads. When these data (mg Hb/g support) were plotted (Fig. 1), the same trend noted earlier was seen. Highest Hb loading was achieved with supports of intermediate pore diameter and surface area. (The same was true for Hb bound to uncoated beads at pH 6.0; data not shown.) Since the initial study utilized a different type of ion-exchange stationary phase, Chang's[2] hypothesis appears to be generally applicable. A mathematical statement of this concept is developed below.

The total surface area of a chromatographic support (A_t, in m^2/g) is the sum of the internal (A_i) and external (A_e) surface areas. More than 95% of the surface area of a porous media is internal[2,11]; consequently, A_t is essentially equal to A_i. Before a protein can bind to the surface of this support material, it must diffuse into

TABLE I

PHYSICAL CHARACTERISTICS OF CONTROLLED POROSITY GLASS BEADS BEFORE AND AFTER COATING WITH POLYETHYLENEIMINE

CPG beads were coated with 1% PEI-6 (5% diglycidylglycerol to cross-link)[6] to produce a weak anion-exchange stationary phase.

*Support material**	*Pore diameter (Å)***		*Surface area (m^2/g)****	
	Mfr's	*Coated*	*Mfr's*	*Coated*
CPG-100	100	60	170	102
CPG-240	240	200	130	108
CPG-550	550	510	70	65
CPG-1000	1000	960	26.1	25
CPG-2000	2000	1960	8.2	8

* Particle size = 37–74 μm for all.

** Based on the data of Vanacek and Regnier[3], a thickness of 20 Å was assumed for the 1% PEI coating; thus, manufacturer's (Mfr's) pore diameters decreased by 40 Å upon application of the coating.

*** If the pore is treated as a cylinder, total surface area decreases linearly with pore diameter upon coating. Surface area of the coated media was estimated by multiplying Mfr values by the ratio for coated/uncoated pore diameter.

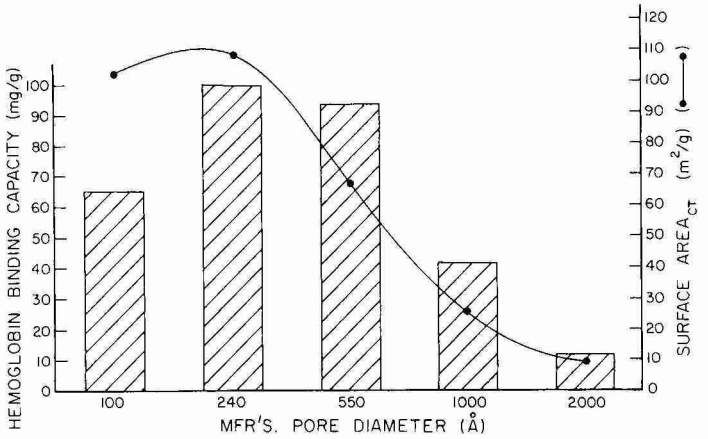

Fig. 1. Hemoglobin-binding capacities of PEI-coated controlled porosity glass beads of varying pore diameter. Surface areas (connected by solid line) of the coated (CT) supports were estimated as explained in Table I. Coating and assay procedures were as described in Materials and methods with Hb quantitated by the Bradford assay.

the matrix pore. If access to A_i is restricted, intrinsic loading capacity will be a function of the available or accessible surface area (A_{ac}) rather than A_t. As suggested by Regnier[11], this may be expressed as

$$A_{ac} = K_{ac}A_t \quad (1)$$

where A_{ac} is the accessible surface area of a support in m^2/g, A_t is the total surface area and K_{ac} is a protein-specific surface accessibility coefficient which varies from zero to one (complete access). A precedent for this concept is found in size-exclusion chromatography where the size-exclusion distribution coefficient is considered to be a measure of the differential permeability of a solute into the matrix pore volume[12]. Eltekov and co-workers[13,14] have studied polymer adsorption on various supports including porous silicas and have shown that this phenomenon is dependent on pore size.

In order to compare sorbents of different surface areas, the protein-binding capacity of a given medium may be divided by the total surface area of that sorbent to obtain a specific binding capacity (S). When S is the specific protein binding capacity in a non-size discriminating system (under saturating conditions), it is designated S'. The value of S' will not be the same for all proteins due to differences in equilibrium constants, molecular size and charge, etc.

If S' is known for a protein, then the relative accessibility of any medium to that protein may be expressed by K_{ac}, the accessibility coefficient, where

$$K_{ac} = S/S' \quad (2)$$

Assuming eqns. 1 and 2 are valid, the following relationship between intrinsic loading capacity (L_i) and accessible surface area is proposed

$$L_i = S' A_{ac} = S' K_{ac} A_t \quad (3)$$

TABLE II

SPECIFIC BINDING CAPACITIES AND ACCESSIBILITY COEFFICIENTS FOR THREE PROTEINS ON PEI-COATED CONTROLLED POROSITY GLASS BEADS OF VARYING PORE DIAMETER

Support material coated with 1% PEI-6. See Table I for pore diameters and estimated total surface areas of the coated media.

Support material	*Specific binding capacity, (S)**			*Accessibility coefficient, (K_{ac})***		
	MYO	*Hb*	*FER*	*MYO*	*Hb*	*FER*
CPG-100	8.0	9.7	0	0.6	0.4	0
CPG-240	6.0	14.4	0	0.4	0.6	0
CPG-550	10.0	22.5	16.0	0.7	1.0	0.4
CPG-1000	14.8	26.0	38.0	1.0	1.0	1.0
	$S' = 14.3$	23.6	39.6			
CPG-2000	13.8	21.2	41.2	1.0	1.0	1.0

* Specific binding capacity (S) in nmol/m^2 was calculated by dividing static binding capacity (expressed as nmol protein/g support) by surface area (m^2/g) of the coated support.

** $K_{ac} = S/S'$.

To test these relationships, additional static binding assays were performed, using proteins of different molecular weight. Specific binding capacities (see Table II) for MYO (MW = 17 500), Hb (MW = 64 500), and FER (MW = 440 000) are shown in Fig. 2. If each protein had equal access to the internal surface area, there would be no difference in S for a given protein on different pore diameter matrices. While S for the smallest protein, MYO, is reasonably independent of pore size, S for both Hb and FER varies directly with pore diameter. Similar S values were exhibited by the 1000 and 2000 Å beads for each of these as well as several other proteins (data not shown). This confirms that media having $\geq$ 1000 Å pore diameters do not distinguish proteins on the basis of size in the range tested. Consequently, S values on

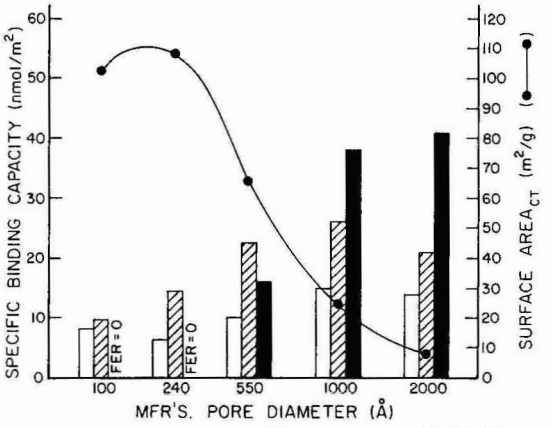

Fig. 2. The influence of pore diameter on specific binding capacity (calculated as described in Table II). Surface areas of the PEI-coated CPG beads (connected by solid line) were estimated as explained in Table I. □ = MYO; ▨ = Hb; ■ = FER. Binding assays were performed as described in Materials and methods with all proteins quantitated by the Bradford assay.

the 1000 and 2000 Å supports were averaged to provide an estimate of S' for each of the three proteins studied (see Table II). (On the basis of size, one might expect FER to occupy more surface, thereby decreasing the number of molecules bound per unit area; this would be true, however, only if all proteins adsorbed as a monolayer.) Accessibility coefficients, K_{ac}, calculated for MYO, Hb and FER on the 100, 240 and 550 Å pore diameter CPG beads (Table II) suggest that K_{ac} is inversely related to the ratio of molecular size to pore size.

Finally, protein accessibility coefficients (K_{ac}) and total surface areas (A_t, corrected for coating thickness as explained in Table I) were used to calculate (by eqn. 1) the surface area accessible (A_{ac}) to these three proteins. The results are shown in Fig. 3 where A_{ac} is plotted against pore diameter (corrected for coating thickness). According to eqn. 3, intrinsic loading capacity is directly proportional to accessible surface area. Thus, Fig. 3 suggests that maximum loading capacity for different proteins will be achieved on supports of varying pore diameter. Proteins of intermediate size such as Hb should exhibit maximum adsorption on 200–400 Å pore diameter supports. (Curves similar to that for Hb were also obtained for BSA, MW = 69 000 and OVA, MW = 43500; data not shown.) Large proteins such as FER will require large pore diameter materials and small proteins, small pore diameter media. Consequently, support materials of very high surface area and small pore diameter may actually have less intrinsic loading capacity than a medium of lower surface area but larger pore diameter.

Commercial silicas

The results discussed above may be used to explain differences in Hb-binding capacity observed with four (PEI-coated) commercial silicas (Table III). The Serva and PQ support materials bound considerably more Hb than Vydac silica. Vydac 101TPB (300 Å) silica is a very high-quality analytical support of relatively low surface area (80 m^2/g) which will withstand pressures in excess of 700 atm. By increasing pore volume, the manufacturers of Si-200 and the two PQ silicas have maintained macroporosity and enhanced protein binding capacity. The tradeoff, of course, is

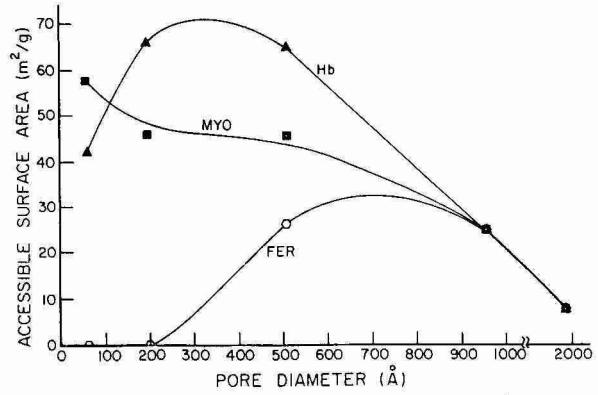

Fig. 3. The influence of pore diameter on support surface area accessible to three proteins of different molecular weight. Protein accessibility coefficients (Table II) and total surface areas (corrected for coating thickness) were used to calculate (eqn. 1) the surface areas accessible to MYO, Hb, and FER on PEI-coated CPG beads of varying pore diameter.

TABLE III

HEMOGLOBIN-BINDING CAPACITIES OF (PEI-COATED) COMMERCIAL SILICAS OF VARYING SURFACE AREA

All supports were coated with 1% PEI-6 (5% diglycidylglycerol to cross-link). The two PQ silicas were experimental materials.

Silica	*Particle size (μm)*	*Pore diameter* (Å)*	*Surface area* (m^2/g)*	*Hb-binding capacity** (mg Hb/g)*
Vydac 101TPB	15–20	300	80	27
PQ-270 Å	20	270	200	103
PQ-200 Å	20	200	272	134
Serva Si-200	30	250	290	123

* As specified by manufacturer (see Materials and methods).
** Ionically desorbed Hb quantitated directly at 410 nm.

decreased pressure stability (we have found these materials stable to 200 atm). Since 15–30 μm particles do not require high operating pressure, however, the lower pressure stability of these silicas should not preclude their use in large preparative columns. (When compared on a volumetric basis, the Hb-binding capacities of the Serva and PQ silicas were equal to or greater than that of Pharmacia A-50-120 DEAE Sephadex; data not included.)

Stationary phase contributions

Previous work[6] has suggested that both the chemical nature and ligand density of an ionic stationary phase can influence protein adsorption. Several stationary phases which varied in charge density and amine type (Table IV) were generated by modification of the basic PEI coating as described in Materials and methods. These (silica-based) anion-exchange packing materials were analyzed for Hb-binding capacity. The influence of ligand density was clearly demonstrated by the low and high ligand density materials; the latter, with more charged amine, exhibited greater protein binding capacity. Chromatographic retention was also increased on this stationary phase (data not shown). A second route to high loading capacity with PEI-coated media appears to be quaternization of low ligand density stationary phases. When such a matrix was exhaustively methylated, Hb-binding capacity increased to that of the high ligand density material. In contrast, derivatization with GLY or ENPP reduced Hb-binding capacity.

These results may be explained in terms of both ionic and steric effects about the stationary phase ion-exchange moiety. Adsorption of a protein at a surface is an equilibrium process which depends on solute concentration, ligand density, fraction of the surface covered with solute molecules and the equilibrium constant. An increased number of amine groups shifts the equilibrium constant in favor of adsorption of protein. Alpert and Regnier[5] have shown that only a portion of the amines on the adsorbed PEI-6 coating is ionized at pH 8. Exhaustive methylation converts primary and secondary amines to quaternary amine salts. The resulting increase in surface charge promotes protein binding. In contrast, increasing the distance between charged centers on the support and the solute decreases the strength of adsorption,

TABLE IV

EFFECT OF STATIONARY PHASE COMPOSITION ON Hb-BINDING CAPACITY

Application of a polyamine coating produces an anion-exchange stationary phase which may vary in amine content, *i.e.* ligand density. Further reaction with electrophiles such as methyl iodide or monofunctional epoxides (*e.g.* GLY or ENPP) modifies amine nitrogens as shown below. R and R′ denote remainder of the cross-linked matrix.

Description	*Abbreviation*	*Hb-binding capacity***	*Structure*
"Low" ligand density* (250 μmol amine/g support)	LLD	47	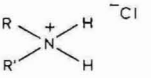
"High" ligand density (550 μmol amine/g support)	HLD	62	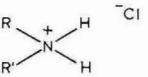
Quaternary amine (250 μmol amine/g support)	QME	69	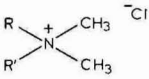
Glycidol-modified LLD (250 μmol amine/g support)	GLY	29	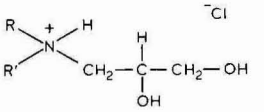
Nitrophenyl-modified LLD (250 μmol amine/g support)	ENPP	37	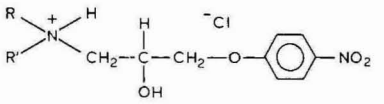

* Ligand density of the base coating was estimated using the picric acid assay[5].

** Total desorbed Hb (quantitated directly at 410 nm) in mg Hb/g support.

reducing the amount of protein bound. The introduction of bulky groups around charged centers on the ion-exchange matrix by derivatization with GLY or ENPP reduces loading capacity, possibly due to steric effects[6]. It should be noted that although such derivatives may exhibit lower loading capacities, they can provide unique chromatographic selectivity[6].

CONCLUSIONS

The intrinsic loading capacity of an anion-exchange chromatographic medium is determined by both porosity of the matrix and the chemical nature of the stationary phase. The contributions of pore diameter and surface area were investigated by means of static protein binding assays using PEI-coated controlled porosity glass beads of 100–2000 Å pore diameter. In agreement with earlier findings[2], maximum Hb adsorption was exhibited by media of intermediate pore diameter and surface area. Apparently, the internal surface area of the smallest pore diameter support was not completely accessible to this protein. To investigate this hypothesis, the binding of a small (MYO) and a large (FER) protein by these media was also measured. FER (MW = 440 000) did not bind to either the 100 Å or 240 Å CPG, while MYO (MW = 17 500) exhibited maximum adsorption on the 100 Å material. Specific binding capacities (nmol protein/m^2 surface area) were determined and used to calculate accessibility coefficients (K_{ac}) for each protein with respect to various pore

diameter supports. The product of K_{ac} and support surface area provided an estimate of accessible surface area (A_{ac}). The maximum surface area accessible to Hb (MW = 64 500) was available from supports of 200–400 Å pore diameter. Larger and smaller pore diameter media provided maximum A_{ac} for the binding of larger and smaller proteins, respectively. Obviously, both pore diameter and protein size are important considerations with regard to maximizing the intrinsic loading capacity of ion-exchange supports. Pores must be big enough to permit complete access of the protein(s) of interest, but not so large as to unnecessarily sacrifice the surface upon which binding takes place.

In addition to physical properties of the matrix, stationary phase composition also plays a role in protein binding. High ligand density coatings adsorbed more protein than low ligand density surfaces as a result of the increased availability of charged sites. Exhaustive methylation of amines also increased Hb binding by increasing surface charge. In contrast, the addition of monofunctional epoxides to stationary phase amines decreased protein loading capacity. It has been postulated that the addition of such moieties sterically inhibits protein binding[6].

The above findings imply that pore diameter, surface area and stationary phase composition must all be considered relative to the protein of interest in order to maximize intrinsic loading capacity. Unfortunately, this is not always possible due to the proprietary nature of many commercial packing materials. However, an understanding of the basic concepts discussed may facilitate the selection of media for preparative anion-exchange chromatography of proteins.

ACKNOWLEDGEMENTS

We thank The Separations Group and The PQ Corporation for their generous gifts of silica. Appreciation is also expressed to Dr. Bernard Axelrod and Dr. Rainer Bischoff for their thoughtful comments regarding this manuscript, and to P. Andrew Tice for related chromatographic applications. This work was supported by NIH Grant GM25431.

REFERENCES

1 M. A. Rounds, W. Kopaciewicz and F. E. Regnier, *The Fourth International Symposium on HPLC of Proteins, Peptides, and Polynucleotides, Baltimore, MD, December 10–12, 1984*, Abstract No. 812.
2 S. H. Chang, R. Noel and F. E. Regnier, *Anal. Chem.*, 48 (1976) 1839.
3 G. Vanacek and F. E. Regnier, *Anal. Biochem.*, 121 (1982) 156.
4 W. Haller, *Nature (London)*, 206 (1965) 693.
5 A. Alpert and F. E. Regnier, *J. Chromatogr.*, 185 (1979) 375.
6 W. Kopaciewicz, M. A. Rounds and F. E. Regnier, *J. Chromatogr.*, 318 (1985) 157.
7 P. G. Righetti and T. Caravaggio, *J. Chromatogr.*, 127 (1976) 1.
8 W. Kopaciewicz and F. E. Regnier, *Anal. Biochem.*, 126 (1982) 8.
9 H. Z. Sommer, H. I. Lipp and L. L. Jackson, *J. Org. Chem.*, 36 (1971) 824.
10 M. M. Bradford, *Anal. Biochem.*, 72 (1976) 248.
11 F. E. Regnier, *Anal. Biochem.*, 126 (1982) 1.
12 L. R. Snyder and J. J. Kirkland, *Introduction to Modern Liquid Chromatography*, Wiley, New York, 1979.
13 Y. A. Eltekov and A. V. Kiselev, *J. Polym. Sci., Part C*, 61 (1977) 431.
14 Y. A. Eltekov and A. S. Nazansky, *J. Chromatogr.*, 116 (1976) 99.

Journal of Chromatography, 362 (1986) 197–207
Elsevier Science Publishers B.V., Amsterdam — Printed in The Netherlands

CHROM. 18 663

PREPARATION AND GEL PERMEATION CHROMATOGRAPHIC PROPERTIES OF POROUS SPHERES FROM POLY(γ-METHYL OR γ-BENZYL L-GLUTAMATE)

HIROTAKA IHARA, TAKASHI YOSHINAGA and CHUICHI HIRAYAMA*
Department of Synthetic Chemistry, Faculty of Engineering, Kumamoto University, Kumamoto 860 (Japan)
(Received March 17th, 1986)

SUMMARY

Porous spheres with average diameters of 5–300 μm have been prepared for the first time from poly(γ-methyl or γ-benzyl L-glutamate) alone, and their gel permeation chromatographic properties, both without further modification and after cross-linking with appropriate agents, have been examined. The polypeptide spheres were prepared by gradually removing the solvent from the suspension particles containing polypeptide. The particle size and porosity were controlled with ease by adjusting the viscosity of the peptide solution and suspension medium, and by selecting additional diluents in the sphering (solidification) process, respectively. The spheres of poly(γ-methyl L-glutamate) can not only withstand a remarkably high flow-rate, but also show typical gel permeation chromatographic behaviours in both aqueous and organic systems. These good properties are attributable to inter- and intramolecular hydrogen bonding based on the formation of specific polypeptide conformations.

INTRODUCTION

Packing materials for gel permeation chromatography (GPC) are classified into those for aqueous and organic media, according to whether they are made from neutral polysaccharides or water-soluble synthetic polymers and polystyrene, respectively. The former type have been widely used for the analysis and separation not only of water-soluble polymer samples, but also of biological materials, *e.g.* proteins, nucleic acids and viruses.

Since it was first reported in 1959 that hydrophilic gels can be synthesized from dextran[1], many gels for aqueous GPC have been prepared from a variety of hydrophilic polymers, such as agar[2,3], cellulose[4], poly(acrylamide)[5,6] and poly(vinyl alcohol)[7,8]. However, they are not free of defects: for example, most of the hydrophilic gels with a large exclusion molecular weight (M_{lim}) cannot be used at high flow-rate condition, because the larger the value of M_{lim} the worse the pressure resistance. This is an unavoidable defect of gel(swelling)-type packings. On the other hand, we have succeeded in making porous and spherical particles of cellulose by a unique

0021-9673/86/$03.50

method[9–12]. This packing is very rigid and shows a higher pressure-resistance than any other available product. We consider that these excellent properties are due to intermolecular hydrogen bonding in cellulose.

This paper reports the production of novel packings for GPC from poly(γ-methyl or γ-benzyl L-glutamate), abbreviated as PMLG and PBLG. The former in particular can not only withstand a surprisingly high flow-rate, but also shows typical GPC behaviour in both aqueous and organic systems. These properties are attributed to the fact that the polypeptide is hydrophilic in chemical structure, but shows affinity and insolubility for most organic solvents by forming a specific conformation, such as β-structure and α-helix.

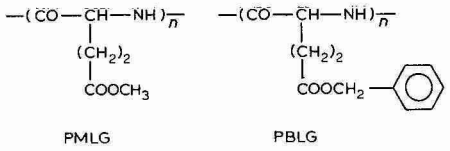

PMLG PBLG

EXPERIMENTAL

Preparation of polypeptide spheres

PMLG and PBLG were synthesized by the polymerization of carboxyanhydrides of γ-methyl and γ-benzyl L-glutamate in 1,2-dichloroethane and tetrahydrofuran, respectively. Commercial PMLG solution was also used as received.

Porous and spherical particles of these polypeptides were prepared as follows. A 1,2-dichloroethane solution of PMLG obtained by polymerization was diluted with 1,2-dichloroethane containing 2–10 wt.% of decahydronaphthalene (or diethylbenzene, 1-octanol, etc.) to give a 2.0–3.5 wt.% solution. This solution was suspended in a 0.5–5.0 wt.% solution of aqueous poly(vinyl alcohol) (viscosity, 40–46 cP; degree of saponification, 86.5–89 mol%). The mixture was stirred at a fixed speed (500–1000 rpm) at 40°C for 12–24 h to remove the dichloroethane. The spherical particles produced after filtration were washed successively with water, hot water, ethanol, and ether, to give a 50–90% yield of PMLG spheres of average diameter 5–300 μm. PBLG particles were obtained by a similar procedure from a dichloromethane solution.

These polypeptide spheres were cross-linked as required by transesterification with diol. The spheres were placed in a three-necked flask fitted with a stirrer, a condenser for azeotropic distillation and a thermometer. Decahydronaphthalene–chloroform (3:1), 0.2 equiv. of sulphuric acid and 0.5 equiv. of triethylene glycol were added and the mixture was stirred at 65°C with addition of fresh chloroform as necessary. Spheres cross-linked by triethylene glycol were obtained by filtering and washing with water and methanol. The yield was 90–100%.

Gel permeation chromatography

PMLG spheres prepared by our procedure and commercial packings from Sephadex, Sepharose and Bio Gel-P (for comparison) were packed into glass columns (15 × 0.5 cm I.D.) and stainless-steel columns (15 × 0.8 cm I.D.). The chromatograph included a Waters Assoc. 6000 p.s.i. pump (Model 510) and a Shodex refracto

monitor (SE-11). A homologous series of dextran and maltose in water and polystyrene in tetrahydrofuran was used as permeable substances. The calibration curves were obtained by plotting the average molecular weight against the peak elution volumes. The slope of the centre part of the curve is given by the equation[13]:

$$\log M = \beta - \alpha (V_e/V_t) \quad (1)$$

where V_t is the total volume of the gel bed and V_e is the eluting volume of a substance with molecular weight M. The excluded molecular weight, M_{lim}, was obtained by extrapolating the linear part of the log M *versus* V_e curve to $V_e = V_0$, where V_0 is outer volume of the gel bed.

Other measurements

Differential scanning calorimetry (DSC) of wet particles from which free water (or medium) is removed by centrifuging (200 *g*, 3 min), was carried out using a Seiko I & E SSC-580/DSC-10 instrument. The PMLG particles were sealed in an Al sample pan and DSC thermograms were obtained at a heating rate of 2°C min^{-1}.

The measurement of the degree of swelling (wet ml/dry ml) and solvent was carried out as previously reported[14]. Solvents used in the measurements were the same as those in the GPC operation.

RESULTS AND DISCUSSION

Polypeptide spheres

The polypeptide spheres are produced by the gradual evaporation of the solvent from the suspension (or emulsion) containing the polypeptide and the diluent. Consequently, the size of the spheres depends on the volume of the size of suspension and the concentration of polypeptide. These factors can be controlled by adjusting the initial concentrations of polypeptide and poly(vinyl alcohol) in the aqueous solution, and the stirring speed. In this study, they were controlled mainly by varying the concentration of the suspension media. For example, PMLG spheres with the average diameters of 44–105 μm and 5–10 μm were obtained from 2 wt.% and 5 wt.% of poly(vinyl alcohol) aqueous solution, respectively. As a result, we succeeded in preparing polypeptide spheres with average diameters of 5–300 μm. These sizes are suitable for chromatography.

Typical optical photographs and electron micrographs of PMLG and PBLG particles prepared by this procedure are shown in Fig. 1. The shape is spherical and uneven. This unevenness of the surface indicates partial crystallization of polypeptide in the sphering process from suspension. The existence of polypeptide crystals is indicated by the glittering observed under a polarization microscope.

The properties of PMLG spheres were investigated. These particles were insoluble in the usual chromatographic solvents without further treatment such as cross-linking: *e.g.*, water, methanol, ethanol, 2-propanol, acetonitrile, tetrahydrofuran, benzene, ether, hexane and hexane mixtures (but they swelled remarkably and because distorted in chloroform, 1,2-dichloroethane and dioxane). This insolubility is a characteristic property of polypeptides. Generally, polypeptides of random coil and α-helical form dissolve in polar solvents, but polypeptides with the β-structure

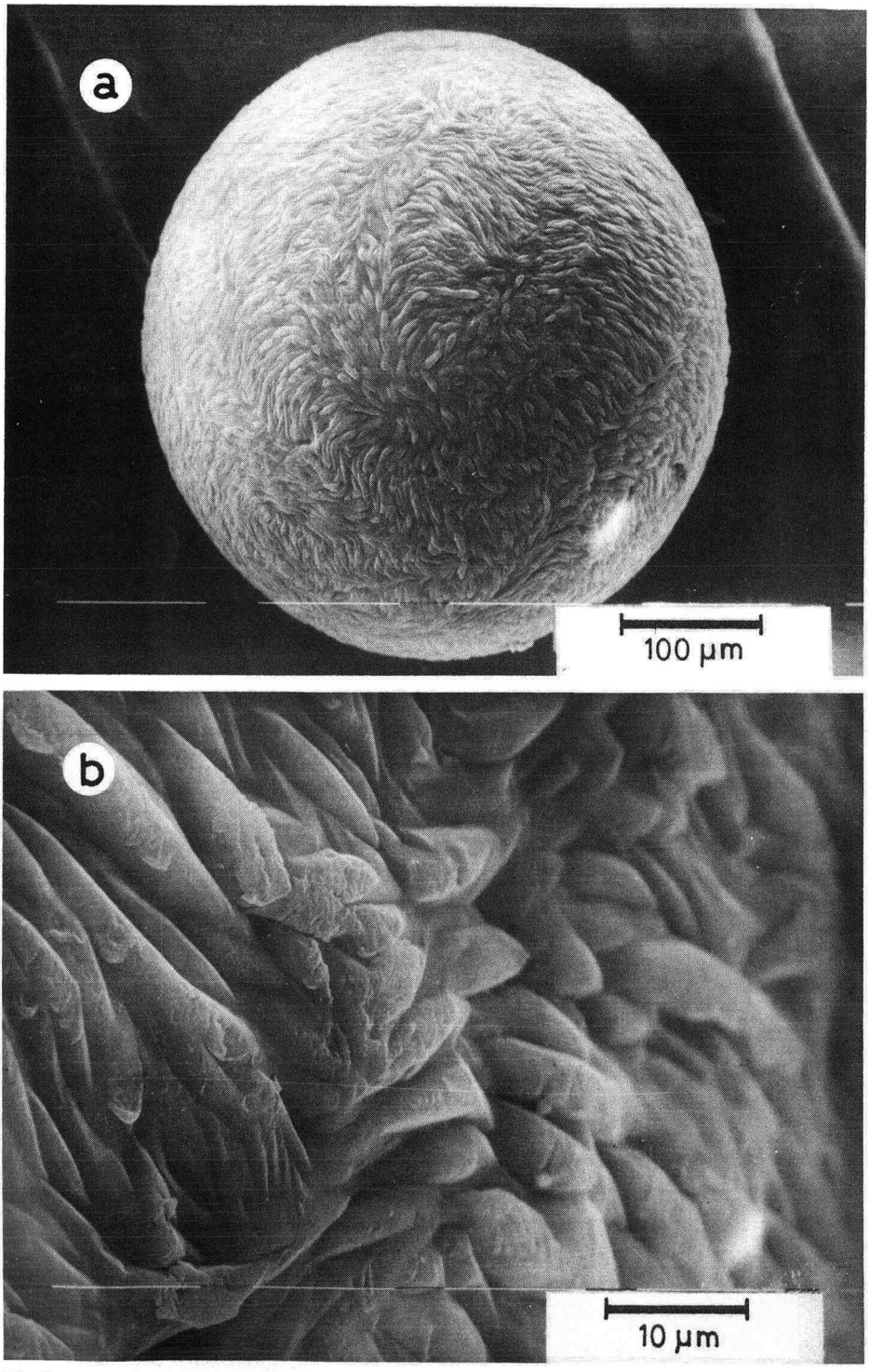

Fig. 1.

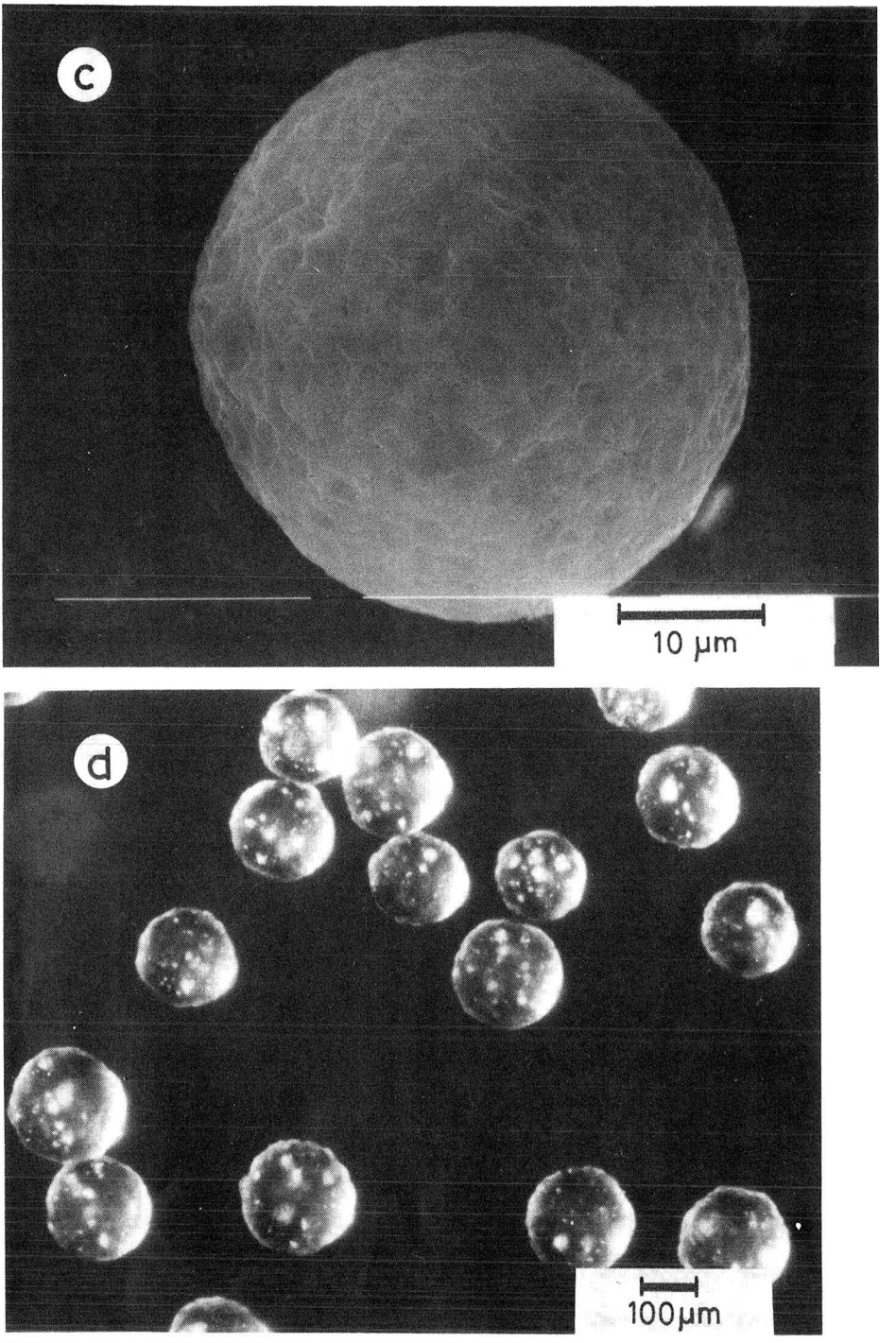

Fig. 1.

(Continued on p. 202)

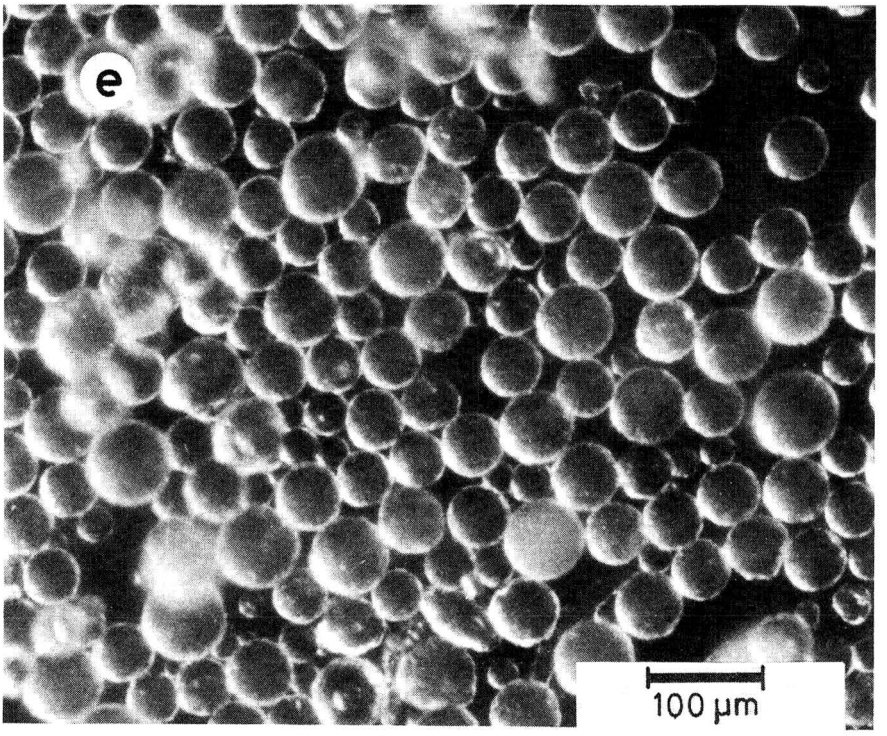

Fig. 1. Electron micrographs (a, b and c) and optical photographs (d and e) of polypeptide spheres: (a), (b) and (d) are pictures of non-porous PBLG spheres; (c) and (e) show non-cross-linked PMLG spheres B-13 and B-3, respectively.

are insoluble in most solvents because of strong intermolecular hydrogen bonding. This hydrogen bonding of the β-structure cannot be destroyed by the usual solvent[15]. As shown in Fig. 2, the production of β-structure was confirmed by IR spectroscopy. PMLG spheres showed absorption bands characteristic of the carbonyl group at 1685 cm^{-1} (anti-parallel β-structure) and 1630 cm^{-1} (parallel β-structure) as well as at 1650 cm^{-1} (α-helix)[16]. Thus, the insolubility of PMLG spheres is attributable to the formation of β-structure.

PMLG spheres were cross-linked as required by transesterification with diol. The resulting particles show different solubility from non-cross-linked particles, although the exact degree of cross-linking is difficult to determine because of the contamination of mono-substituent. The cross-linked particles are insoluble even in hot chloroform (Table I). The insolubility of the cross-linked particles seems to be unrelated to β-structure, because the absorption bands due to β-structures decreased or disappeared (*cf.* Fig. 2c). The β-structure may have disappeared in the cross-linking process because the cross-linking reaction was carried out in a chloroform mixture, which is predisposed to the α-helix form[15].

The cross-linking process is significant not only because the spheres are insolubilized, but also because the general properties are altered. For example, the PMLG spheres became more hydrophilic, after being cross-linked by poly(ethylene glycol). The exclusion molecular weight and the porosity became very small, after complete

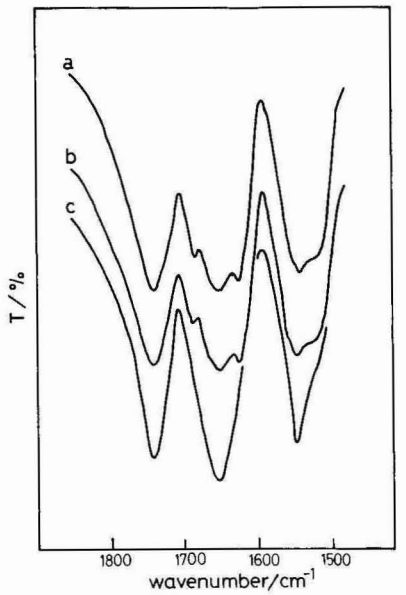

Fig. 2. IR spectra of PMLG spheres: (a) material PMLG (powder after reprecipitation from methanol); (b) porous PMLG spheres (B-9); (c) cross-linked PMLG spheres (C).

cross-linking by an equimolar solution of ethylene glycol for the methoxycarbonyl group of PMLG. Therefore, the GPC ability of the PMLG spheres was examined without prior cross-linking treatment, unless stated otherwise.

Gel permeation chromatography in aqueous solution

The chromatographic properties were investigated using PMLG spheres with diameters of 25–44 μm because of the ease of packing into a column. We examined PMLG particles that were sphered in the absence or the presence of a diluent, *e.g.* decahydronaphthalene or diethylbenzene. Fig. 3 shows typical calibration graphs for GPC in aqueous solution. Table II summarizes the exclusion molecular weights (M_{lim}) and porosities, which were estimated from the graphs of Fig. 3 and some physical properties of PMLG spheres. The porosity was determined[8,9] from eqn. 2:

TABLE I

DEGREE OF SWELLING (*Sd*) OF PMLG SPHERES

Sphere B-12 was prepared using 100% of decahydronaphthalene; sphere C was cross-linked using triethylene glycol.

Sphere No.	*Cross-linking*	*Porosity (%)*	*Sd (wet ml/dry ml)*			
			Water	*Ethanol*	*Chloroform*	*Hexane*
A	No	12	1.0	1.2	Distorted*	1.0
B-12	No	61	2.1	2.4	Distorted*	2.6
C	Yes	60	2.4	2.8	3.1	2.0

* Remarkably large degree of swelling.

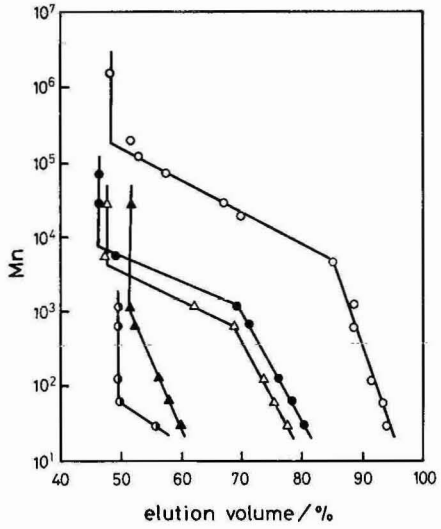

Fig. 3. Typical calibration curves of GPC for PMLG spheres in aqueous solution: ○ = B-15; ● = B-12; △ = B-10; ▲ = B-2; ◑ = A.

TABLE II

VALUES OF M_{lim}, POROSITY AND *Sd* OF PMLG SPHERES IN AQUEOUS SOLUTION

Sphere No.	*Diluent*		*Sd for water (wet ml/dry ml)*	M_{lim} *for dextran*	*Porosity (%)*
	Type	*wt.%*			
A	None	0	1.0	60	12
B-1	Butyl acetate	100	1.1	100	19
B-2	1-Hexanol	100	1.0	1000	16
B-3	1-Octanol	100	1.2	1000	37
B-4	1-Octanol	300	1.3	10 000	59
B-5	Toluene	100	1.1	150	14
B-6	*o*-Xylene	100	1.2	150	17
B-7	*m*-Xylene	100	1.2	150	32
B-8	*p*-Xylene	100	1.2	150	20
B-9	Diethylbenzene	100	1.5	6000	60
B-10	Diethylbenzene	200	1.8	6000	55
B-11	Diethylbenzene	300	1.7	6500	60
B-12	Decahydro-naphthalene	100	1.9	8100	61
B-13	Decahydro-naphthalene	200	2.1	40 000	74
B-14	Decahydro-naphthalene	300	2.1	120 000	83
B-15	Methyl dodecanoate	100	2.1	200 000–2 000 000	82

$$\text{Porosity} = \frac{V_{^2H_2O} - V_0}{V_t - V_0} \times 100\ (\%) \quad (2)$$

where $V_{^2H_2O}$ is the elution volume of ^2H_2O.

The type and the amount of a diluent directly affect the value of M_{lim} and the porosity. In the absence of a diluent, these values are only 60 and 12%, respectively. These spheres can be assumed to be non-porous, in contrast to the triacetates of cellulose[9,10] and pullulan[17], which have porosities of 40% and 90% even in the absence of a diluent. This is probably due to the strong cohesion of PMLG in the sphering process.

The effects of a diluent are remarkable in decahydronaphthalene, diethylbenzene, 1-octanol and methyl dodecanoate. For example, when 100–300% of decahydronaphthalene was used as a diluent, M_{lim} and porosity increased from 8100 to 120 000 and from 61% to 83%, respectively. The largest value of M_{lim}, 10^6, was obtained by the use of methyl dodecanoate, although values of M_{lim} were difficult to reproduce. In any case, the role of methyl dodecanoate as a diluent should be clarified by further studies because the diluent effects are surprising and significant.

On the contrary, when the diluent is butyl acetate, 1-hexanol, toluene or xylene, the effect is scarcely observable. These solvents increase the value M_{lim} and the porosity to some degree in the case of the sphering of cellulose triacetate[9,10]. This indicates that the PMLG spheres are reticulated only by specific diluents because of the strong cohesion effect.

The different diluents produce different effects on the degree of swelling of PMLG spheres. The non-porous spheres did not swell in water ($Sd = 1$), but the porous spheres prepared with the use of decahydronaphthalene doubled in size on swelling. In contrast, in the case of porous spheres prepared with the use of 1-octanol the value of Sd is only 1.3. Therefore, it is clear that two different types of sphere, swelling gel-type and permanent porous resin-type, can be produced. However, the formation mechanism is not yet clear.

As a result, we succeeded in the preparation of non-porous and porous PMLG spheres with a series of M_{lim} values from 10^3 to 10^6. These values are suitable to GPC.

Amphiphilicity

Fig. 4 shows calibration graphs for GPC in water and tetrahydrofuran. As shown in figure, PMLG spheres give typical GPC behaviour even in the organic system, and the calibration pattern is closely similar to that in the aqueous system. This indicates that PMLG spheres are amphiphilic and the reticular structure does not change even in organic systems.

This amphiphilicity was shown calorimetrically. As shown in Fig. 5, the melting behaviour of solvent containing in the spheres was examined by DSC. The DSC thermogram of the PMLG spheres containing water gives only a melting peak due to water (Fig. 5a). When these particles were washed with methanol in a column for 10 min, this peak disappeared (Fig. 5b). After the particles were washed with benzene, a peak due to benzene was observed (Fig. 5c). Even when water was replaced by dioxane, such peak-transfer was observed. Thus it is clear that the PMLG spheres are chromatographically amphiphilic also.

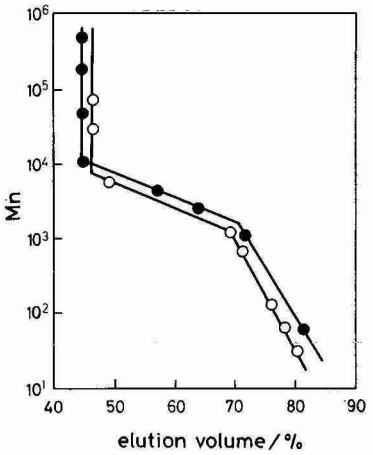

Fig. 4. Calibration graphs of GPC of PMLG sphere B-12 in tetrahydrofuran and water: ● = tetrahydrofuran; ○ = water.

Flow-rate properties

The PMLG spheres are insoluble in the usual chromatographic solvents. This property produces a remarkably high flow-rate for the chromatographic process. Fig. 6 shows the relationship between the pressure drop and the flow-rate for the PMLG spheres prepared using 100% of decahydronaphthalene as a diluent. The PMLG spheres easily reached 30 ml min^{-1} cm^{-2} (corresponding to *ca.* 6 ml min^{-1} at 5 mm I.D.)

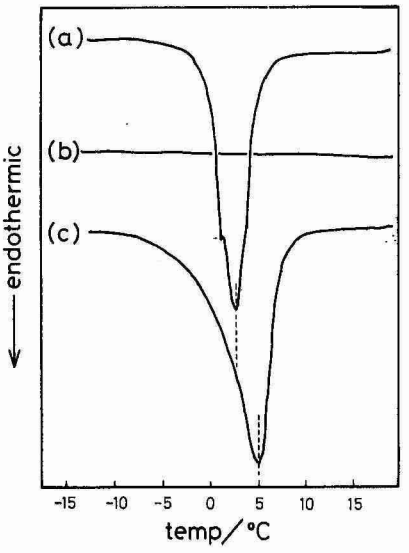

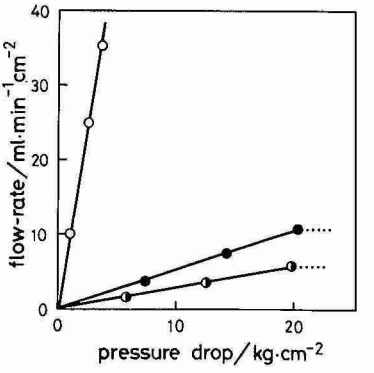

Fig. 5. DSC thermograms of PMLG spheres containing the medium for GPC: (a) water; (b) methanol; (c) benzene.

Fig. 6. Relationship between flow-rate and pressure drop in aqueous solution: ○ = PMLG spheres (B-12, size 25–44 μm, M_{lim} 8100); ● = Sephadex G-25 (size 44–105 μm, M_{lim} 5000); ◑ = Sephadex G-50 (size 44–105 μm, M_{lim} 10 000).

in water, but the corresponding commercial packings reached a limit at 2 ml min^{-1} (at 5 mm I.D.). This lower pressure-resistance of the commercial products is caused by their large degree of swelling. The PMLG spheres are rigid and the degree of swelling is small, regardless of whether they are cross-linked.

CONCLUSION

Porous spheres from synthetic polypeptides alone were prepared for the first time by our unique method. The particle size, the porosity and the pore size are controlled with ease by controlling the preparation conditions. The polypeptide spheres obtained are very rigid, insoluble in most chromatographic solvents and tolerate high flow-rates without further treatment.

If the spheres are cross-linked by transesterification with diol compounds the solvent-resistance increases.

In addition, it was confirmed that the spheres can be used in both aqueous and organic systems for GPC, and the eluent replacement was very easy.

These properties are attributable to the fact that the polypeptide shows amphiphilicity and insolubility, due to the formation specific conformations such as β-structure and α-helix.

Research into the application of polypeptide spheres to high-performance liquid chromatography has just begun, and we shall investigate further modifications and applications to affinity chromatography for biochemical and medical research as well as GPC.

ACKNOWLEDGEMENTS

We thank Mr. Yoichi Onitani for his capable assistance. This work was partially supported by a Grant-in-Aid for Scientific Research from the Japanese Ministry of Education.

REFERENCES

1 P. Flodin and B. Ingelman, *U.S. Pat.*, 3 042 667 (1959); J. Prath and P. Flodin, *Nature (London)*, 183 (1959) 1657.
2 A. Polson, *Biochim. Biophys. Acta*, 50 (1961) 565.
3 J. Killander, *Biochim. Biophys. Acta*, 93 (1964) 1.
4 H. Determan, H. Rehner and T. Wieland, *Makromol. Chem.*, 114 (1968) 263.
5 S. Hjerten and R. Mosbach, *Anal. Chem.*, 3 (1962) 109.
6 K. Sun and A. H. Sehon, *Can. J. Chem.*, 43 (1965) 969.
7 Y. Motozato, C. Hirayama and K. Matsumoto, *Nippon Kagaku Zasshi*, 74 (1971) 1904.
8 C. Hirayama and Y. Motozato, *Nippon Kagaku Kaishi*, (1972) 1087.
9 Y. Motozato, K. Matsumoto and C. Hirayama, *Nippon Kagaku Kaishi*, (1981) 1883.
10 Y. Motozato and C. Hirayama, *J. Chromatogr.*, 298 (1984) 499.
11 Y. Motozato and Chisso Co. Ltd., *U.S. Pat.*, 4 312 980 (1982).
12 Y. Motozato and Chisso Co. Ltd., *Eur. Pat.*, 0 025 639 (1982).
13 K. A. Granath and P. Foldin, *Makromol. Chem.*, 48 (1961) 160.
14 Y. Motozato, C. Hirayama, K. Morodomi and N. Kunitake, *Nippon Kagaku Kaishi*, (1973) 79.
15 Y. Fujimoto (Editor), *Poly Amino Acids*, Kodansha, Tokyo, 1974, p. 129.
16 E. R. Brout and A. Asadourian, *J. Am. Chem. Soc.*, 78 (1956) 955.
17 Y. Motozato, H. Ihara, T. Tomoda and C. Hirayama, *J. Chromatogr.*, 355 (1986) 434.

Journal of Chromatography, 362 (1986) 209–216
Elsevier Science Publishers B.V., Amsterdam — Printed in The Netherlands

CHROM. 18 667

3,4-DIHYDRO-6,7-DIMETHOXY-4-METHYL-3-OXO-QUINOXALINE-2-CARBONYL CHLORIDE AS A HIGHLY SENSITIVE FLUORESCENCE DERIVATIZATION REAGENT FOR ALCOHOLS IN HIGH-PERFORMANCE LIQUID CHROMATOGRAPHY

TETSUHARU IWATA, MASATOSHI YAMAGUCHI, SHUUJI HARA and MASARU NAKAMURA*

Faculty of Pharmaceutical Sciences, Fukuoka University, Nanakuma, Jonan-ku, Fukuoka 814-01 (Japan)

and

YOSUKE OHKURA

Faculty of Pharmaceutical Sciences, Kyushu University 62, Maidashi, Higashi-ku, Fukuoka 812 (Japan)

(First received February 6th, 1986; revised manuscript received March 19th, 1986)

SUMMARY

3,4-Dihydro-6,7-dimethoxy-4-methyl-3-oxo-quinoxaline-2-carbonyl chloride was found to be a highly sensitive fluorescence derivatization reagent for primary and secondary alcohols in high-performance liquid chromatography. Its reactivity was investigated for benzyl alcohol, *n*-hexanol and cyclohexanol. The reagent reacts with the alcohols in benzene to produce the corresponding fluorescent esters, which can be separated on a reversed-phase column, YMC Pack C_8, with aqueous 70% (v/v) methanol; the detection limits for the alcohols were 2–3 fmol for an injection volume of 10 μl. The reagent also reacts with hydroxysteroids with primary and/or secondary alcoholic group(s) to form fluorescent derivatives. Tertiary alcohols, hydroxycarboxylic acids and phenols do not give fluorescent derivatives under these conditions.

INTRODUCTION

Many fluorescence derivatization reagents have been developed for the determination of alcohols by high-performance liquid chromatography (HPLC), *e.g.* 4-dimethylamino-1-naphthoylnitrile[1], (+)- and (−)-2-methyl-1,1′-binaphthalene-2′-carbonyl nitriles[2], 2-dansylethyl chloroformate[3], 1- and 9-anthroylnitriles[4], 3- and 4-chloroformyl-7-methoxy-[5], 7-[(chlorocarbonyl)methoxy]-4-methyl-[6] and 4-diazomethyl-7-methoxycoumarins[7], 7-methoxycoumarin-3- and -4-carbonyl azides[8], 2-(4-isocyanatophenyl)-6-methyl-benzothiazole[9,10] and naphthyl isocyanate[11]. HPLC methods with these reagents are not always satisfactory with respect to sensitivity; the reagents do not permit the determination of alcohols at the femtomole level per injection volume except for 7-methoxycoumarin-3-carbonyl azide.

We have previously reported that 3,4-dihydro-6,7-dimethoxy-4-methyl-3-oxo-

0021-9673/86/$03.50

TABLE I

3,4-DIHYDRO-6,7-DIMETHOXY-3-OXO-QUINOXALINES AND THEIR ANALYTICAL DATA

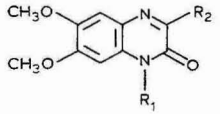

Compound	R_1	R_2	*Yield (%)*	*Appearance**	*m.p. (°C)*	*Formula*	*Analysis (%) calc. (found)*		
							C	*H*	*N*
DQ-COOH	H	COOH	55.9	ON	268	$C_{11}H_{10}N_2O_5$	52.80 (52.71	4.00 4.02	11.20 11.13)
DMEQ-$COOCH_3$	CH_3	$COOCH_3$	14.3	YN	164	$C_{13}H_{14}N_2O_5$	56.12 (56.13	5.04 5.04	10.07 9.98)
DMEQ-COOH	CH_3	COOH	78.6	YN	222	$C_{12}H_{12}N_2O_5$	54.54 (54.51	4.54 4.52	10.60 10.58)
DMEQ-COCl	CH_3	COCl	96.0	ON	261	$C_{12}H_{11}N_2O_4Cl$	50.97 (50.94	3.89 3.77	9.91 9.81)
I	CH_3	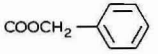	11.0	ON	193	$C_{19}H_{18}N_2O_5$	64.41 (64.32	5.08 5.10	7.91 7.98)
II	CH_3	$COOC_6H_{13}$	6.10	PYN	198	$C_{18}H_{24}N_2O_5$	62.02 (61.80	6.90 7.08	8.05 8.17)
III	CH_3	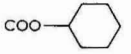	17.0	PYN	190	$C_{18}H_{22}N_2O_5$	62.42 (62.46	6.36 6.51	8.09 8.17)

* O = orange; p = pale; y = yellow; N = needles.

quinoxaline (DMEQ) derivatives fluoresce highly intensely in aqueous methanol and acetonitrile[12], and thus we developed 2-bromomethyl-DMEQ as a fluorescence derivatization reagent for carboxylic acids in HPLC[12]. Recently, we found that DMEQ-2-carboxylic acid (DMEQ-COOH; Table I) also gives an intense fluorescence in aqueous methanol and acetonitrile. Thus, DMEQ-2-carbonyl chloride (DMEQ-COCl; Table I) was synthesized as a fluorescence derivatization reagent for alcohols. In order to investigate its reactivity with alcohols, we have used benzyl alcohol, *n*-hexanol and cyclohexanol as model primary and secondary alcohols. DMEQ-COCl reacts with these alcohols in benzene to produce the corresponding fluorescent esters. The esters are separated on a reversed-phase column with aqueous methanol. The reactivity of DMEQ-COCl with various other alcohols (tertiary alcohols, hydroxysteroids and hydroxycarboxylic acids) has also been examined.

EXPERIMENTAL

Apparatus

Uncorrected fluorescence spectra and intensities were measured with a Hitachi 650-60 spectrofluorimeter in 10 × 10 mm quartz cells; spectral bandwidths of 10 nm were used in both the excitation and emission monochromators. Quantum yields of fluorescence were obtained on the fluorimeter by the method of Parker and Rees[13].

Infrared (IR) spectra were recorded with a Shimadzu 430 spectrophotometer using potassium bromide pellets. ^{1}H nuclear magnetic resonance (NMR) spectra were obtained with a Hitachi R-90H spectrometer at 90 MHz using a *ca.* 5% (w/v) solution of [$^2H_6$]dimethyl sulphoxide containing tetramethylsilane as an internal standard.

Field desorption-mass spectra (MS) were taken with a Jeol DX-300 spectrometer. Uncorrected melting points were measured with a Yazawa melting point apparatus.

Reagents and materials

All chemicals were of analytical reagent grade, unless noted otherwise. Deionized and distilled water was used. Organic solvents were distilled and dried in the usual manner. 1,2-Diamino-4,5-dimethoxybenzene monohydrochloride was prepared as described previously[14]; it is now available from Dojindo Labs. (Kumamoto, Japan).

Synthesis of DMEQ-COCl

1,2-Diamino-4,5-dimethoxybenzene monohydrochloride (8 g, 40 mmol) and α-ketomalonic acid (8 g, 44 mmol) were dissolved in 200 ml of 0.5 *M* hydrochloric acid. The mixture was heated for 2 h in a boiling water-bath. The precipitates that separated on cooling the mixture in ice-water were filtered off, washed with water and then recrystallized from aqueous 90% (v/v) 1,4-dioxane to give 3,4-dihydro-6,7-dimethoxy-3-oxo-quinoxaline-2-carboxylic acid (DQ-COOH;Table I).

DQ-COOH (5.5 g, 22 mmol) in 50 ml of anhydrous methanol was treated with ethereal diazomethane solution prepared by the established method[15]. The reaction mixture was evaporated to dryness *in vacuo*. The residue dissolved in 30 ml of chloroform was purified by column chromatography (25 × 5.7 cm I.D.) on silica gel 60

(*ca.* 130 g, 70–230 mesh; Japan Merck, Tokyo, Japan) with *n*-hexane–ethyl acetate (1:1, v/v) as eluent to give methyl DMEQ-2-carboxylate (DMEQ-$COOCH_3$; Table I).

DMEQ-$COOCH_3$ (2.5 g, 9.5 mmol) was dissolved in 200 ml of 1.0 *M* sodium hydroxide. The solution was allowed to stand at room temperature for *ca.* 70 min and then washed five times with 200 ml of ethyl acetate. The aqueous layer was neutralized with dilute hydrochloric acid and the resulting precipitates were collected by filtration and recrystallized from aqueous 80% (v/v) 1,4-dioxane to give DMEQ-COOH (Table I).

A solution of DMEQ-COOH (1 g, 3.6 mmol) in 20 ml of freshly distilled thionyl chloride was refluxed for 1 h and cooled. The precipitates formed on adding *ca.* 50 ml of light petroleum (b.p. 30–60°C) were collected by filtration and recrystallized from benzene–light petroleum (9:1, v/v) to give DMEQ-COCl (Table I).

DMEQ-COCl was stable in the crystalline state for three months or longer when kept dry in the dark at room temperature. The reagent dissolved in benzene could be used for a week when stored in a refrigerator at 5°C.

Preparation of the fluorescent compounds from benzyl alcohol, n-hexanol and cyclohexanol

DMEQ-COCl (100 mg, 0.35 mmol) and an alcohol (0.35 mmol) were dissolved in 10 ml of benzene. The solution was placed in a screw-capped test-tube (20 ml) and heated at 100°C for 1 h and cooled. The reaction mixture was evaporated to dryness *in vacuo*. The residue, dissolved in 5 ml of chloroform, was chromatographed on a silica gel-60 column (25 × 2.7 cm I.D.) with *n*-hexane–ethyl acetate (1:1, v/v). The main fraction was evaporated to dryness *in vacuo*, and the residue was recrystallized from methanol to give the corresponding product (I, II or III; Table I).

Derivatization procedure

To 0.5 ml of a test solution of alcohols in benzene (from 20 pmol to 25 nmol each per 0.5 ml) placed in a PTFE screw-capped reaction vial (2 ml) was added 0.5 ml of 3 m*M* DMEQ-COCl in benzene. The vial was tightly closed and heated at 100°C for 40 min in the dark. After cooling, 20 μl of the reaction mixture was diluted with 2 ml of methanol, and the resulting solution (10 μl) was injected into the chromatograph. For the reagent blank, 0.5 ml of benzene in place of a test solution was subjected to the same procedure.

HPLC apparatus and conditions

A Waters 510 high-performance liquid chromatograph equipped with a U6K universal injector (10-μl loop) and a Hitachi F1100 fluorescence spectrometer equipped with a 12-μl flow-cell operated at the excitation wavelength of 400 nm and the emission wavelength of 500 nm were used. The column was a YMC Pack C_8 (150 × 6 mm I.D.; particle size, 10 μm; Yamamura Chemical Labs., Kyoto, Japan). It can be used for more than 1000 injections with only a small decrease in the theoretical plate number, when washed with methanol every day after analyses. The mobile phase used for the separation of the DMEQ derivatives of the examined alcohols was aqueous 70% (v/v) methanol at a flow-rate of 2.0 ml/min (*ca.* 90 kg/cm^2). The column temperature was ambient (15–25°C).

RESULTS AND DISCUSSION

Fluorescent products of reaction between alcohols and DMEQ-COCl

The reaction products from benzyl alcohol, *n*-hexanol and cyclohexanol were confirmed as the corresponding DMEQ-2-carboxylates, compounds I, II and III, respectively, by IR, MS and NMR data (Table I).

Fluorescence properties of DMEQ derivatives

The fluorescence properties of the DMEQ derivatives in methanol, acetonitrile and water, which have widely been used as components of mobile phases in reversed-phase HPLC, were examined. The DMEQ esters of alcohols (DMEQ-$COOCH_3$ and compounds I–III) showed almost the same fluorescence excitation and emission maxima; the maxima are almost independent of the kind of the alcohol and of the solvent. On the other hand, the fluorescence intensities (or the quantum yields) in acetonitrile were smaller than those in methanol and water. The intensity of DMEQ-COOH in these solvents was low compared with that of the DMEQ esters (Table II).

HPLC conditions

The separation of DMEQ derivatives of benzyl alcohol, *n*-hexanol and cyclohexanol was studied on a reversed-phase column, YMC Pack C_8, with aqueous methanol. At methanol concentrations higher than 80% (v/v), the peak for the DMEQ derivative of benzyl alcohol partially overlapped an unknown peak (Fig. 1, peak 4), whereas methanol concentrations of 60–65% (v/v) caused a delay in elution with broadening of the peaks. Optimum separation was attained by using aqueous 70% (v/v) methanol. Fig. 1 shows a typical chromatogram obtained with the alcohols.

Derivatization conditions

Benzene as a solvent for the derivatization reaction provided the most intense peaks for the alcohols examined, and toluene gave less intense peaks (*ca.* 70% of those in benzene). On the other hand, the fluorescence reaction was very limited in chloroform, dimethyl sulphoxide, dimethylformamide, tetrahydrofuran, ethyl acetate, acetonitrile, acetone or 1,4-dioxane. Water interfered with the reaction owing to the decomposition of DMEQ-COCl. Thus, benzene was chosen for the procedure. Acceleration of the reaction was not observed in the presence of pyridine, trimethylamine, dimethylaminopyridine, N,N-diisopropylethylamine, potassium carbonate, potassium hydrogen carbonate or 18-crown-6.

The reaction of DMEQ-COCl with the alcohols occurred more rapidly with as the reaction temperature was increased. An example for cyclohexanol is shown in Fig. 2. The peak heights reached a maximum and constant after heating at 100–150°C for 30 min. Thus, heating for 40 min at 100°C was employed in the procedure. The most intense peaks were obtained at reagent concentrations greater than *ca.* 2 m*M* and 3 m*M* was employed in the procedure. The DMEQ derivatives in the final mixture were stable for at least 72 h in daylight at room temperature.

Calibration curve, precision and detection limit

The relationships between the peak heights and the amounts of the individual

TABLE II

FLUORESCENCE PROPERTIES OF DMEQ DERIVATIVES IN METHANOL, ACETONITRILE AND WATER

Compound	*Excitation maximum (nm)*			*Emission maximum (nm)*			*Relative fluorescence intensity**			*Quantum yield*		
	Methanol	*Acetonitrile*	*Water*	*Methanol*	*Acetonitrile*	*Water*	*Methanol*	*Acetonitrile*	*Water*	*Methanol*	*Acetonitrile*	*Water*
DMEQ-$COOCH_3$	399	397	406	503	487	512	99	73	83	0.99	0.65	0.86
DMEQ-COOH	400	413	379	479	489	480	17	24	16	0.16	0.06	0.16
DMEQ-COCl**	–	401	–	–	473	–	–	76	–	–	0.76	–
I	400	399	408	501	489	503	100	74	84	0.99	0.67	0.85
II	399	394	406	501	488	509	97	61	84	0.95	0.56	0.87
III	399	396	408	502	486	513	78	52	85	0.89	0.56	0.84

* The fluorescence intensity was measured at the excitation and emission maxima. The intensity of compound I in methanol was taken as 100.

** DMEQ-COCl reacted partly with methanol to produce DMEQ-$COOCH_3$ even at room temperature, and decomposed with water to form DMEQ-COOH.

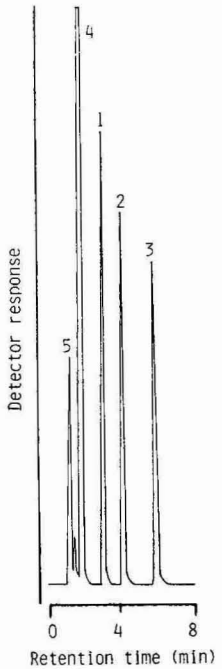

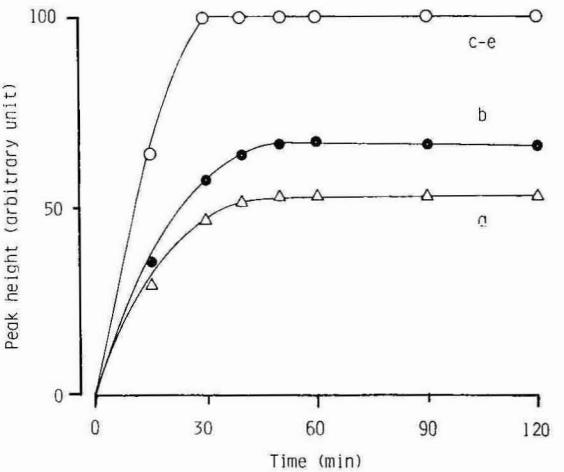

Fig. 1. Chromatogram of DMEQ derivatives of benzyl alcohol, *n*-hexanol and cyclohexanol. A portion (0.5 ml) of a mixture of the alcohols (1.0 nmol each per ml) was treated according to the described procedure. Peaks: 1 = benzyl alcohol; 2 = cyclohexanol; 3 = *n*-hexanol; 4 and 5 = unknown (probably due to decomposition products of DMEQ-COCl).

Fig. 2. Effect of reaction time and temperature on the peak height. Portions (0.5 ml) of cyclohexanol (1.0 nmol/ml) were treated as in the procedure at various temperatures. Temperatures: a = 60°C; b = 80°C; c = 100°C; d = 130°C; e = 150°C.

alcohols were linear from 2 fmol to at least 2.5 pmol per 10-μl injection volume (corresponding to 20 pmol to 25 nmol in 0.5 ml of a test solution). The precision was established by repeated determinations ($n = 10$) using a mixture of the three alcohols (25 nmol each per 0.5 ml). The coefficients of variation were 0.7, 1.2 and 0.9% for benzyl alcohol, *n*-hexanol and cyclohexanol, respectively. The detection limits for the alcohols were 2–3 fmol for an injection volume of 10 μl, at a signal-to-noise ratio of 2. The sensitivity is comparable with that of the method using 7-methoxycoumarin-3-carbonylazide[8], and much higher than those of the methods with the other fluorescence derivatization reagents[1–11].

Reaction of DMEQ-COCl with other substances

Many hydroxysteroids reacted with DMEQ-COCl under the derivatization conditions recommended for the formation of fluorescent derivatives. The retention times and detection limits for the DMEQ derivatives of the compounds are shown in Table III. Tertiary alcohols (2-methyl-2-propanol, 2-methyl-2-butanol and 4-androsten-17α-ethynyl-17β-ol-3-one) and hydroxycarboxylic acids (lactic and malic acids) did not fluoresce. Other substances, such as carboxylic acids, seventeen different L-α-amino acids, aldehydes, ketones, phenols and sulphydryl compounds gave

TABLE III

RETENTION TIMES AND DETECTION LIMITS FOR DMEQ DERIVATIVES OF HYDROXY-STEROIDS

Compound	*Retention time (min)*	*Detection limit (fmol/10 µl)*
4-Pregnen-21-ol-3,11,20-trione (1-dehydrocorticosterone)	3.4	12.6
4-Pregnen-21-ol-3,20-dione (deoxycorticosterone)	6.6	8.4
5-Pregnen-3β-ol-20-one (pregnenolone)	28.8	15.2
1,3,5(10)-Estratriene-3,17α-diol (17α-estradiol)	9.6	10.4
5-Androsten-3β-ol-17-one (dehydroisoandrosterone)	13.5	6.6
5-Cholesten-3β-ol (cholesterol)*	4.9	4.6
5α-Cholestan-3β-ol (cholestanol)	5.4	7.5

* Methanol was used as a mobile phase for the separation of the DMEQ derivatives of these compounds. When the mobile phase in the described procedure was used, the DMEQ derivatives were strongly retained on the column and not eluted.

no fluorescent derivatives. Therefore, DMEQ-COCl should be useful as a fluorescence derivatization reagent in HPLC of primary and secondary alcohols.

REFERENCES

1 J. Goto, S. Komatsu, N. Goto and T. Nambara, *Chem. Pharm. Bull.*, 29 (1981) 899.
2 J. Goto, N. Goto and T. Nambara, *Chem. Pharm. Bull.*, 30 (1982) 4597.
3 A. Takadate, M. Iwai, H. Fujino, K. Tahara and S. Goya, *Yakugaku Zasshi*, 103 (1983) 962.
4 J. Goto, N. Goto, F. Shamsa, M. Saito, S. Komatsu, K. Suzaki and T. Nambara, *Anal. Chim. Acta*, 147 (1983) 397.
5 C. Hamada, M. Iwasaki, N. Kuroda and Y. Ohkura, *J. Chromatogr.*, 341 (1985) 426.
6 K. E. Karlsson, D. Wiesler, M. Alasandro and M. Novotny, *Anal. Chem.*, 57 (1985) 229.
7 A. Takadate, T. Tahara, H. Fujino and S. Goya, *Chem. Pharm. Bull.*, 30 (1982) 4120.
8 A. Takadate, M. Irikura, T. Suehiro, H. Fujino and S. Goya, *Chem. Pharm. Bull.*, 33 (1985) 1164.
9 R. Wintersteiger, G. Gamse and W. Pacha, *Fresenius' Z. Anal. Chem.*, 312 (1982) 455.
10 O. S. Wolfbeis and H. Marhold, *Monatsh. Chem.*, 114 (1983) 599.
11 R. Wintersteiger, G. Wenninger-Weinzierl and W. Pacha, *J. Chromatogr.*, 237 (1982) 399.
12 M. Yamaguchi, S Hara, R. Matsunaga, M. Nakamura and Y. Ohkura, *J. Chromatogr.*, 346 (1985) 227.
13 C. A. Parker and W. T. Rees, *Analyst (London)*, 85 (1960) 587.
14 M. Nakamura, M. Toda, H. Saito and Y. Ohkura, *Anal. Chim. Acta*, 134 (1982) 39.
15 H. Schlenk and J. L. Gellerman, *Anal. Chem.*, 32 (1960) 1412.

Journal of Chromatography, 362 (1986) 217–226
Elsevier Science Publishers B.V., Amsterdam — Printed in The Netherlands

CHROM. 18 658

CHROMATOGRAPHIC ANALYSIS OF 4-DIMETHYLAMINOAZOBENZENE-4′-SULPHONYL AND 4-NAPHTHALENE-1-AZO-(4′-DIMETHYLAMINOBENZENE)SULPHONYL DERIVATIVES OF ALIPHATIC ALCOHOLS

T. WOLSKI*, W. GOŁKIEWICZ and G. BARTUZI
Technological Laboratory, Department of Inorganic and Analytical Chemistry, Medical Academy, 20-209 Lublin (Poland)
(First received November 14th, 1985; revised manuscript received March 17th, 1986)

SUMMARY

Seven 4-dimethylaminoazobenzene-4′-sulphonyl (dabsyl) and 4-naphthalene-1-azo-(4′-dimethylaminobenzene)sulphonyl (dabnsyl) derivatives of aliphatic alcohols have been analysed chromatographically in adsorption and reversed-phase systems. It has been found, rather unexpectedly, that the derivatives can be separated in both types of system. The results obtained for dabsyl and dabnsyl derivatives of aliphatic alcohols satisfy the well-known equations describing the influence of the mobile phase concentration on the capacity factor k'. The influence on the dabsylation and dabnsylation yield of the molar ratio of the derivatizing reagent to the substrate, and of the pH value of the reaction medium, has been examined.

INTRODUCTION

Derivatization is a widely applied procedure during various chromatographic operations. Its use enables detection, enhances sensitivity and improves the selectivity of an analytical separation, mainly thanks to a decrease in the polarity of the substances examined[1–3].

Alcohols and phenols are strongly polar compounds because of the presence of the hydroxyl group. Hence alcohols are good solvents for various organic and inorganic compounds. They are also applied as components of mobile phases in thin-layer chromatography (TLC) and high-performance liquid chromatography (HPLC). The use of alcohols as solvents is sometimes limited owing to the reactivity of the hydroxyl group.

The hydroxyl group is a functional element of many naturally occurring compounds; however, these compounds predominantly have a complex structure and also contain other groups, *e.g.* aldehyde, carboxyl and amine.

Detection of the hydroxyl group is still not a completely solved analytical problem. None of applied reactions for this group is sufficiently characteristic to allow unambiquous confirmation on the basis of a single test of the presence of the hydroxyl group. Several reactions are necessary[4].

0021-9673/86/$03.50

The liquid chromatographic analysis of aliphatic alcohols is usually performed by the gel chromatographic method on Sephadex[5,6] with the use of a refractometric detector[6]. Another possibility is derivatization of alcohols with phenyl isocyanate[7] or naphthyl isocyanate[8], and subsequent analysis of the derivatives by adsorption[8] or reversed-phase chromatography[7]. Parkin and Lau[9] have separated aliphatic alcohols by the reversed-phase method, and used for their detection various substances absorbing UV radiation at 270 nm.

It is known that dabsyl chloride (DABS-Cl, 4-dimethylaminoazobenzene-4'-sulphonyl), which has recently been applied in analytical practice[10], reacts with amino, hydroxyl and sulphydryl groups; hence it can be used as derivatizing reagent for alcohols. Examples of the application of DABS-Cl in chromatographic analysis have been presented in numerous publications. Lammens and Verzele[11] and Chang *et al.*[12] have described a rapid and easy method for the chromatographic analysis of amino acids. Lin and Wang[13] have determined amino acids in urine. Other authors have applied dabsyl chloride to the determination of primary and secondary amines[14] and sphingosine[15].

Recently we have suggested a new derivatizing reagent, dabnsyl chloride (DABNS-4-Cl, 4-naphthalene-1-azo-(4'-dimethylaminobenzene)sulphonyl chloride)[16,17] for amino acid analysis. The compound is a modification of dabsyl chloride.

Both DABS-Cl and DABNS-4-Cl react not only with amino groups but also with hydroxyl groups of phenols and alcohols. That is why the compounds seem to be good reagents for alcohol analysis. Studies of the reaction of aliphatic alcohols with DABS-Cl and DABNS-4-Cl can also give information on the reactivity of alcoholic and phenolic hydroxyl groups of amino acids (*e.g.* serine and tyrosine) with these reagents. The data are useful during derivatization of polyfunctional amino acids and help to determine whether mono- or polysubstituted derivatives are formed.

EXPERIMENTAL

Dabsyl chloride reacts with aliphatic alcohols according to the reaction shown in eqn. 1:

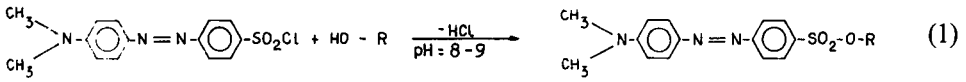

(1)

where R is an alkyl chain.

The reaction between dabnsyl chloride and aliphatic alcohols[16,17] is similar:

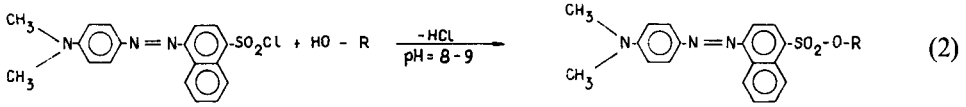

(2)

The derivatives obtained in both reactions are coloured solids of good solubility in organic solvents. The conditions for alcohol (Polish Reagents, POCh Gliwice) dabsylation are similar to those for amino acid derivatization[10,18].

Derivatives of alcohols used as standards were prepared in the following way.

Pure alcohol (1 cm^3) was mixed with 10 cm^3 of 0.1 *M* sodium hydrogen carbonate and 20 cm^3 of acetone solution of DABS-Cl or DABNS-4-Cl (10 $\mu mol/cm^3$),

and the reaction mixture was allowed to react at 343 K in a water-bath for 10 min under reflux. The mixture was cooled, and the derivative was extracted with diethyl ether. The DABS-ONa or DABNS-4-ONa, which originated from DABS-Cl and DABNS-4-Cl, respectively, was re-extracted from the organic phase with citrate buffer (pH 3). The diethyl ether was evaporated off and the solid derivative was obtained. Quantity determination of DABS- and DABNS-4-alcohols showed that the molar ratio of derivatizing reagent to alcohol lay in the range 2:1 to 16:1.

The conditions for serine (produced by E. Merck, Darmstadt, F.R.G.) dabnsylation are the same as for its dabsylation, and are described elsewhere[10,18].

The experiments were carried out using a liquid chromatograph Type 302 (Institute of Physical Chemistry of the Polish Academy of Sciences, Warsaw), which consisted of a syringe pump, a UV detector (fixed wavelength 254 nm) and a four-port injection valve. Two 250 × 4 mm I.D. stainless-steel columns (ZOCh, Lublin, Poland) packed with 10 μm LiChrosorb Si 60 and LiChrosorb RP-18 (E. Merck) were used for measurements of capacity factors.

The dead volume of the column packed with LiChrosorb Si 60 was calculated after injection of a heptane solution of benzene. The determination was performed at various concentrations of ethyl acetate in the mobile phase. The dead volume of the column packed with LiChrosorb RP-18 was calculated after injection of an aqueous solution of potassium chloride when the mobile phase consisted of methanol–water (60:40, v/v).

RESULTS AND DISCUSSION

Structural effects in molecules of organic compounds can exert an influence on the separation selectivity of adsorption chromatography[19]. On the other hand it is known that organic compounds that differ by only one $-CH_2-$ group in an alkyl chain are separated with difficulty in typical adsorption systems[19,20]. That is why DABS- and DABNS-4 derivatives of aliphatic alcohols differing by only one $-CH_2-$ group could be expected to have poor selectivity in adsorption chromatographic systems too. However, the experiments performed show that separation is possible. Fig. 1 shows that the DABS derivatives of alohols can be separated without difficulty. Jusiak and Soczewiński[21] suggested that dabsyl derivatives of aliphatic amines are adsorbed by the $-SO_2-$ group (structure 1); so it can be assumed that differentiation of capacity factors k' of the alcohol derivatives is caused by the steric hindrance due to the alkyl chain of each alcohol. Soczewiński and Golkiewicz[22,23], Snyder[24], Ościk *et al.*[25] and Jandera and Churaček[26] have all shown that the following equation is appropriate for adsorption chromatography:

$$\log k' = \log k'_S - n \log X_S \qquad (3)$$

where k' is the capacity factor, n is the slope of the plot corresponding to eqn. 3 ($n = A_S/n_b$ is the ratio of the molecular areas on the adsorbent surface occupied by the solute A_S and the solvent n_b), and X_S is the mole fraction of the stronger solvent S in the binary mobile phase.

Figs. 2 and 3 show the correlation between the logarithm of the capacity factor k' and the logarithm of the concentration of the more polar solvent S in the binary

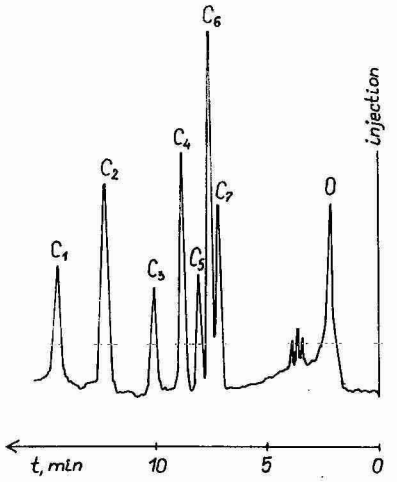

Fig. 1. HPLC chromatogram of seven DABS-alcohols. Stationary phase, LiChrosorb Si 60 (10 μm); mobile phase, *n*-heptane–ethyl acetate (85:15, v/v); stainless steel column, 250 × 4 mm I.D.; flow-rate, 1.2 cm^3/min; detection at 254 nm. Peaks: C_1 = DABS-methanol; C_2 = DABS-ethanol; C_3 = DABS-propanol; C_4 = DABS-butanol; C_5 = DABS-pentanol; C_6 = DABS-hexanol; C_7 = DABS-heptanol; 0 = DABS-Cl.

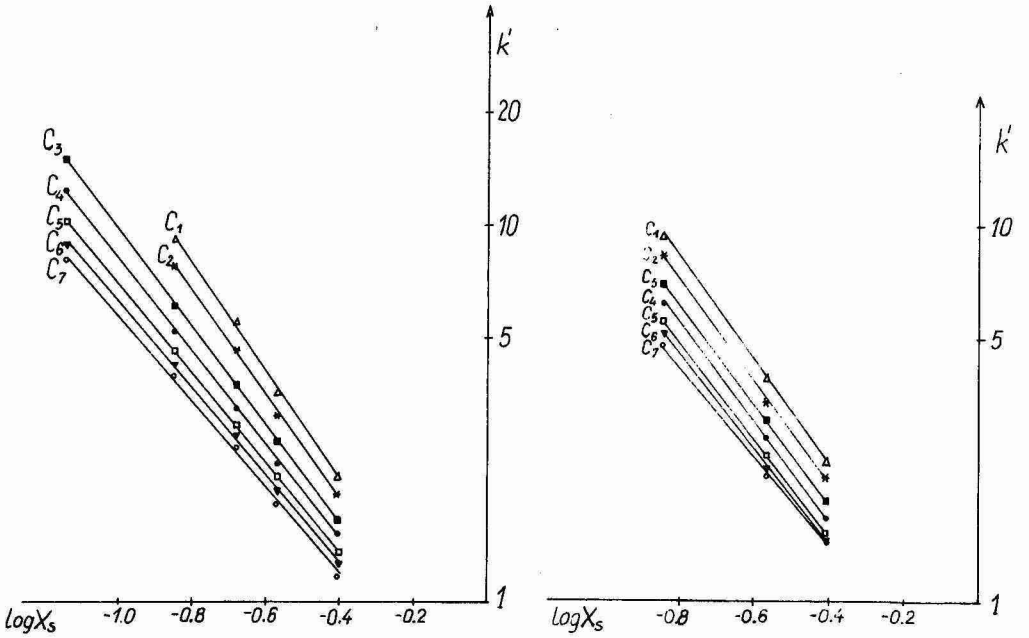

Fig. 2. The log k' *vs.* log X_S relationship for some DABS-alcohols. Polar solvent, ethyl acetate; diluent, *n*-heptane. Notation of compounds as in Fig. 1.

Fig. 3. The log k' *vs.* log X_S relationship for some DABNS-4-alcohols. Conditions as in Fig. 1. Notation of compounds: C_1 = DABNS-4-methanol; C_2 = DABNS-4-ethanol; C_3 = DABNS-4-propanol; C_4 = DABNS-4-butanol; C_5 = DABNS-4-pentanol; C_6 = DABNS-4-hexanol; C_7 = DABNS-4-heptanol.

TABLE I

ABSOLUTE SLOPES FOR THE PLOTS OF log k' OF DABS- AND DABNS-4 DERIVATIVES OF ALCOHOLS, AGAINST LOGARITHM OF MOLE FRACTION OF ETHYL ACETATE (NORMAL PHASE) AND VOLUME FRACTION OF METHANOL (REVERSED PHASE)

Solute	*Code*	*n-Heptane–ethyl acetate on SiO_2*		*Water–methanol on RP-18*
		DABS	*DABNS-4*	*DABNS-4*
Methanol	C_1	1.45	1.36	4.05
Ethanol	C_2	1.37	1.33	4.68
Propanol	C_3	1.30	1.31	5.31
Butanol	C_4	1.24	1.28	5.95
Pentanol	C_5	1.19	1.25	6.55
Hexanol	C_6	1.15	1.22	7.20
Heptanol	C_7	1.12	1.19	7.83

mobile phase. The linear correlation log $k' = f(\log X_S)$ obtained for both DABS- and DABNS-4 derivatives proves that the chromatographic behaviour of the compounds is accurately described by eqn. 3.

The values of the plot slopes n compiled in Table I also seem to confirm that adsorption of the derivatives is caused by the $-SO_2-O-$ group. If it is assumed, according to the Snyder theory[19,24], that the slope n in eqn. 3 equals the ratio of the areas of the adsorbed solute and solvent, the n value in the case of DABS- and

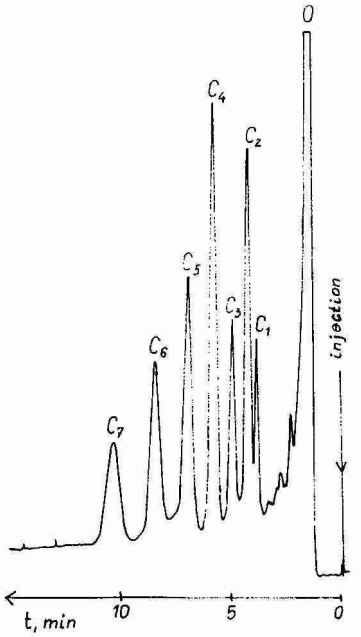

Fig. 4. HPLC chromatogram of seven DABNS-4-alcohols. Stationary phase, silica gel ODS (10 μm); mobile phase, water–methanol (90:10, v/v). Notation of compounds as in Fig. 3; 0 = DABNS-4-OH.

DABNS-4 derivatives of aliphatic alcohols and ethyl acetate should be very high. The n values in the range 1.12–1.45 indicate that only one group, probably the $-SO_2-O-$ group, occupies the space on the adsorbent surface but the rest of the molecule is in the bulk phase.

The slopes of the plots describing the correlation $\log k' = f(\log X_S)$ differ slightly and decrease as the alkyl chain lengthens (Table I).

The differences in the slopes for DABNS-4 derivatives of neighbouring alcohol homologues are constant and equal to 0.03 units, but for DABS derivatives they decrease regularly as the alkyl chain lengthens (notice that the differences in slopes are 0.08, 0.07, 0.06... between the pairs DABS-methanol and -ethanol, -ethanol and -propanol, -propanol and -butanol, etc., respectively).

When preparing DABS- and DABNS-4 derivatives of alcohols we expected that they would be easily separated by reversed-phase chromatography. These expectations are confirmed by the chromatogram (Fig. 4).

The molecular mechanism of adsorption on adsorbents with a chemically bonded stationary phase is a matter of controversy. It has been shown experimentally that generally $\log k'$ is approximately a linear function of the volume fraction of a modifier[21,27,28] in the binary mobile phase:

$$\log k' = \log k'_w - n\varphi \tag{4}$$

where the subscript w denotes pure water and φ is the volume fraction of the modifier.

Sometimes, in the case of a wider range of concentrations, curved lines described by a quadratic equation[29]:

$$\ln k' = A\varphi^2 + B\varphi + C \tag{5}$$

are obtained (A, B and C are empirical coefficients of the quadratic equation).

It is of interest that our results confirm the validity of eqns. 4 and 5. The correlation for DABS derivatives of alcohols in the system LiChrosorb RP-18–methanol–water is curvilinear (Fig. 5) and accurately described by eqn. 5[29], but in the case of DABNS-4 derivatives, chromatographed in the same system, the correlation obtained is rectilinear according to eqn. 4.

An analysis of the slopes described by the equation $\log k' = f(\varphi)$ and shown in Table I (reversed phase), is also of interest. The values of the slopes increase regularly from 4.05 to 7.83 for DABNS-4-methanol to DABNS-4-heptanol, respectively (Fig. 6). The increase in the slope value corresponding to one $-CH_2-$ group is constant and equals 0.63 units. It is noteworthy that in theories of gradient elution the value of the slope is of great importance during elaboration of optimum conditions of the chromatographic analysis[30,31].

Quantitative determination of DABS- and DABNS-4-alcohols was performed chromatographically using an external standard method. A rectilinear relationship between peak heights and concentrations of the alcohol derivatives in the range 0.01–0.2 mg/cm^3 was obtained.

Quantitative determination of alcohols in the form of their derivatives with dabsyl and dabnsyl chloride was performed mainly in order to establish to what extent alcoholic hydroxyl groups of amino acids can react with these reagents.

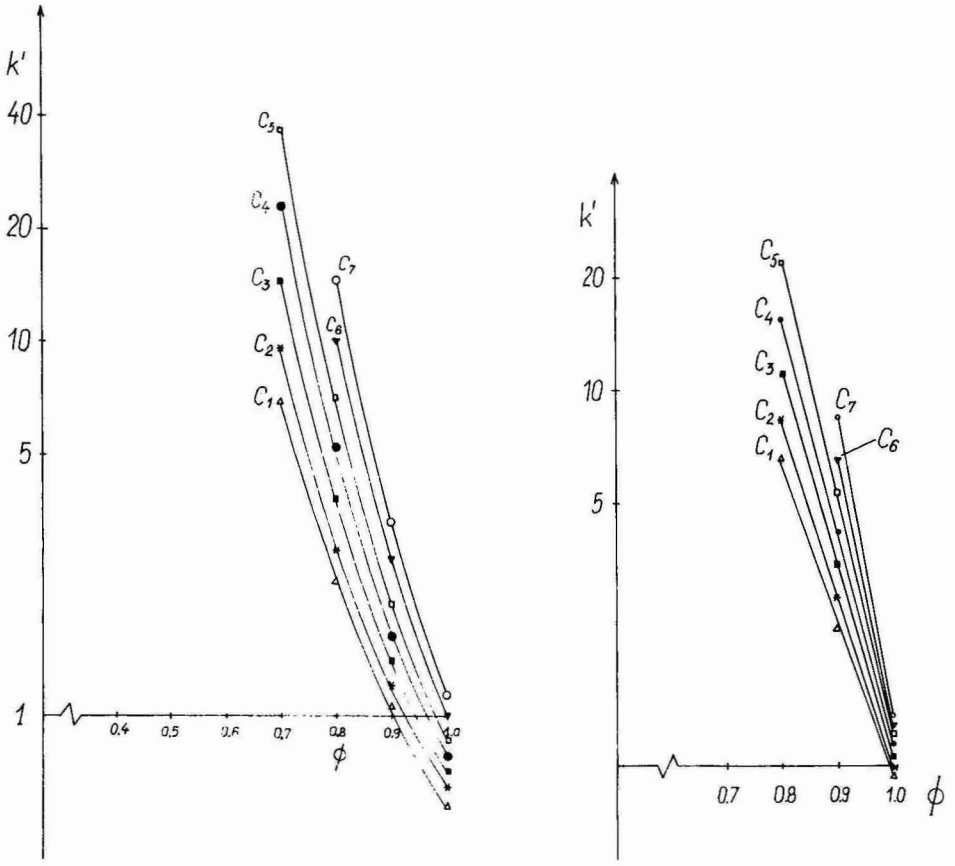

Fig. 5. The plots of log k' *vs.* volume fraction of methanol for some DABS-alcohols. Mobile phase, water–methanol. Notation of compounds as in Fig. 1.

Fig. 6. The plots of log k' *vs.* volume fraction (φ) of methanol for some DABNS-4-alcohols. Mobile phase, water–methanol. Notation of compounds as in Fig. 3.

Initially the influence of the pH of the reaction medium on the dabsylation yield was examined. It turned out that maximum yield was attained at pH 9, the same as in the case of amino acid derivatization.

Next the influence of the reagent excess on the dabsylation and dabnsylation yield was investigated. The reactions were performed with various molar ratios of derivatizing reagent to alcohol. The derivatization reactions of alcohol proceed with a very low yield (Fig. 7), so dabsyl and dabnsyl chloride cannot be applied to the quantitative determination of alcohols. The problem of the formation of disubstituted derivatives of amino acids may have a significant influence on the results of chromatographic analysis of amino acids containing both $-NH_2$ and $-OH$ groups: it is known that both groups react with dabsyl chloride.

Lin and Chang[10] and Chang *et al.*[32] have suggested that disubstituted derivatives of amino acids can be formed with a great excess of dabsyl chloride; the molar ratio of dabsyl chloride to amino acid should be 5:1 or even 40:1.

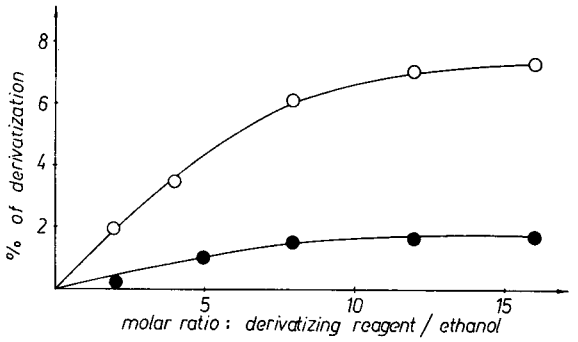

Fig. 7. Dependence of the yield of ethanol derivatization on the molar ratio of reagent to alcohol. Key: 0 = DABS-ethanol; ● = DABNS-4-ethanol.

It is interesting that in the case of derivatization with DABNS-4-Cl, the dabnsylation yield even with a great excess of the reagent does not exceed 2%. The low yield of dabnsylation of alcoholic hydroxyl groups and the high yield (95–100%) of dabnsylation of amino groups[33], seem to prove that DABNS-4-Cl is a more selective derivatizing reagent for amino acids than DABS-Cl.

This conclusion is confirmed by results obtained during serine derivatization with excess amounts of DABS-Cl and DABNS-4-Cl (molar ratio of derivatizing reagent to serine = 15:1). Two peaks of the derivatives were obtained on chromatographic analysis of DABS-serine. The capacity factor for the less retained peak was almost identical with the k' value of DABS-alanine: this suggests that the serine was contaminated with alanine. After addition of DABS-Ala to DABS-Ser (Fig. 8a) three peaks of derivatives were observed: DABS-Ala, monosubstituted DABS-Ser and probably disubstituted DABS-Ser.

The low yield of the reaction between DABNS-4-Cl and ethanol suggests that the peak of disubstituted DABNS-4-Ser should be considerably lower than that of disubstituted DABS-Ser. Fig. 8b shows a chromatogram of DABNS-4-Ser spiked with DABNS-4-Ala. The peak of disubstituted serine is indeed very small, which confirms the earlier supposition of low reactivity of DABNS-4-Cl with alocholic hydroxyl groups.

It is noteworthy that if quantitatively determined amino acids forms mono- and disubstituted derivatives (two peaks on the chromatogram), the quantitative results obtained on the basis of the monosubstituted derivative will be several per cent lower than they should be.

The results obtained permit us to draw some conclusions concerning the derivatization of bifunctional amino acids such as serine. In the case of serine dabsylation and dabnsylation, it is mainly the amino group that participates in the reaction to form the monosubstituted derivative. With large excesses of derivatizing reagents, the hydroxyl group can also react and form small amounts of disubstituted serine. Such amounts of disubstituted derivatives are sometimes chromatographically revealed as unidentified peaks.

It has been shown[33] that DABS-Cl reacts with phenolic hydroxyl groups of phenolic acids and amino acids in good yield.

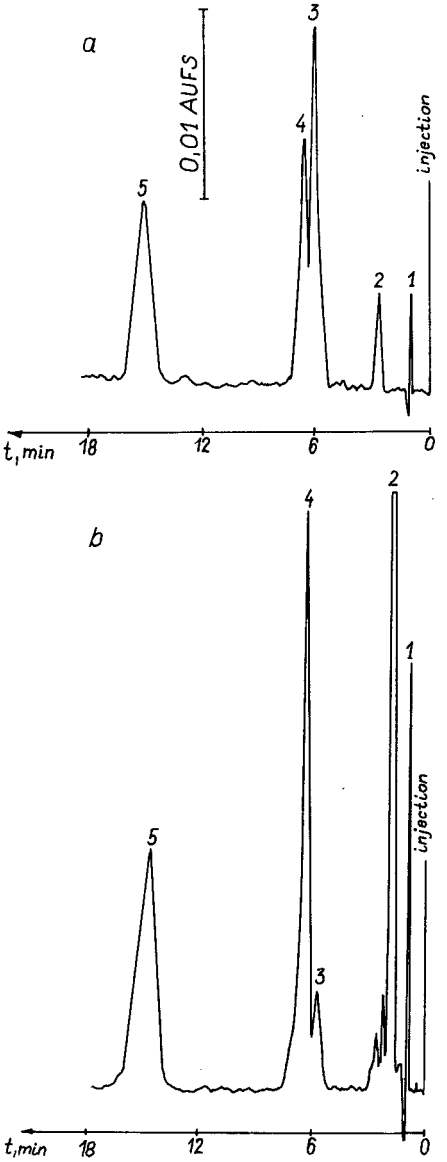

Fig. 8. HPLC chromatogram of mono- and disubstituted derivatives of serine spiked with alanine derivative. Conditions as in Fig. 1, except the mobile phase, *n*-heptane–acetone–acetic acid (75:20:5, v/v). (a) DABS-Ser spiked with DABS-Ala; peaks: 1 = solvent; 2 = DABS-Cl; 3 = disubstituted DABS-Ser; 4 = DABS-Ala; 5 = monosubstituted DABS-Ser. (b) DABNS-4-Ser spiked with DABNS-4-Ala; peaks: 1 = solvent; 2 = DABNS-4-Cl; 3 = disubstituted DABNS-4-Ser; 4 = DABNS-4-Ala; 5 = monosubstituted DABNS-4-Ser.

CONCLUSIONS

Both DABS-Cl and DABNS-4-Cl are good reagents for amino[10,16–18,32] as well as phenolic hydroxyl groups[33], but considerably worse for alcoholic hydroxyl

groups. The derivatization yield of aliphatic alcohols does not exceed 10% and 2% with DABS-Cl and DABNS-4-Cl, respectively. This means that in the case of amino acids with both amino and hydroxyl groups (*e.g.* serine), mainly monosubstituted derivatives are formed as a result of reaction between the amino group and dabsyl chloride.

However, in the presence of a large excess of derivatizing reagent, disubstituted derivatives can be formed (Fig. 8a and b); this effect is more noticeable for DABS-Cl than for DABNS-4-Cl.

Dabsyl and dabnsyl derivatives of aliphatic alcohols can be separated by liquid–solid or reversed-phase chromatography.

In spite of poor yields, DABS-Cl or DABNS-4-Cl can be used for the detection of compounds with primary alcoholic hydroxyl groups.

REFERENCES

1 J. F. Lawrence and R. W. Frei, *Chemical Derivatization in Liquid Chromatography*, Elsevier, Amsterdam, 1976.
2 K. Blau and G. King (Editors), *Handbook of Derivatives for Chromatography*, Heyden and Son, London, 1977.
3 R. W. Frei, *J. Chromatogr.*, 165 (1979) 75.
4 P. Mastalerz, *Organic Chemistry*, PWN, Warszawa, 1984, pp. 357–431.
5 T. Barth, K. Tjessem and A. Aaberg, *J. Chromatogr.*, 214 (1981) 83.
6 K. Ujimoto and H. Kurihara, *J. Chromatogr.*, 208 (1981) 183.
7 B. Bjorkqvist, *J. Chromatogr.*, 218 (1981) 65.
8 R. Wintersteiger, G. Wenninger-Weinzierl and W. Pacha, *J. Chromatogr.*, 237 (1982) 399.
9 J. E. Parkin and H. T. Lau, *J. Chromatogr.*, 314 (1984) 488.
10 K. J. Lin and J. Y. Chang, *Anal. Chem.*, 47 (1975) 1634.
11 J. Lammens and M. Verzele, *Chromatographia.*, 11 (1978) 376.
12 J. Y. Chang, R. Knecht and D. G. Braun, *Biochem. J.*, 203 (1982) 803.
13 J. K. Lin and Ch. H. Wang, *Clin. Chem.*, 26/5 (1980) 579.
14 J. K. Lin and Ch. Ch. Lai, *Anal. Chem.*, 52 (1980) 630.
15 G. Rosenfelder, J.-Y. Chang and D. G. Braun, *J. Chromatogr.*, 272 (1983) 21.
16 T. Wolski, W. Golkiewicz, Z. Grodzicki and G. Bartuzi, *Chem. Anal. (Warsaw)*, 30 (1985) 291.
17 T. Wolski, W. Golkiewicz, and E. Partyka, in preparation.
18 T. Wolski, W. Golkiewicz and A. Rompała, *Chem. Anal. (Warsaw)*, 25 (1980) 583.
19 L. R. Snyder, *Principles of Adsorption Chromatography*, Marcel Dekker, New York, 1968.
20 L. R. Snyder and H. D. Warren, *J. Chromatogr.*, 15 (1964) 344.
21 J. Jusiak and E. Soczewiński, *J. Chromatogr.*, 248 (1982) 263.
22 E. Soczewiński, *Anal. Chem.*, 41 (1969) 179.
23 E. Soczewiński and W. Golkiewicz, *Chromatographia.*, 4 (1971) 501.
24 L. R. Snyder, *Anal. Chem.*, 46 (1974) 1384.
25 J. Ościk, J. K. Różyło, B. Ościk-Mendyk and M. Jaroniec, *Chromatographia.*, 4 (1981) 95.
26 P. Jandera and J. Churaček, *J. Chromatogr.*, 91 (1974) 223.
27 M. Bieganowska and E. Soczewiński, in R. Franke and P. Oehme, (Editor), *Quantitative Structure–Activity Analysis*, Academia Verlag, Berlin, 1978, p. 29.
28 L. R. Snyder, J. W. Dolan and J. R. Gant, *J. Chromatogr.*, 165 (1979) 3.
29 P. J. Schoenmakers, H. A. Billiet and L. de Galan, *J. Chromatogr.*, 185 (1979) 179.
30 L. R. Snyder, in Cs. Horváth (Editor), *High Performance Liquid Chromatography*, Academic Press, New York, Vol. 1, 1980.
31 P. Jandera and J. Churaček, *Adv. Chromatogr.*, 19 (1980) 126–260.
32 J. Y. Chang, R. Knecht and D. G. Braun, *Biochem. J.*, 199 (1981) 547.
33 T. Wolski, W. Golkiewicz, G. Bartuzi and J. Lobarzewski, in H. Kalasz and L. S. Ettre (Editors), *Fifth American-Eastern European Symposium on Liquid Chromatography, Budapest, 1985*, Akademiai Kiado, Budapest, in press.

Journal of Chromatography, 362 (1986) 227–234
Elsevier Science Publishers B.V., Amsterdam — Printed in The Netherlands

CHROM. 18 679

ANALYSIS OF ALKYLTRIMETHYL- AND DIALKYLDIMETHYLAMMONIUM COMPOUNDS BY GAS CHROMATOGRAPHY

SUKEJI SUZUKI*, MASAMI SAKAI, KAZUO IKEDA, KENICHIRO MORI, TAKASHI AMEMIYA and YOHYA WATANABE

Tokyo Metropolitan Research Laboratory of Public Health, 3-24-1, Hyakunincho, Shinjuku-ku, Tokyo 160 (Japan)

(First received February 11th, 1986; revised manuscript received March 22nd, 1986)

SUMMARY

A method for the determination of long-chain alkyltrimethylammonium chlorides (I–VII) and dialkyldimethylammonium chlorides (VIII, IX) by gas chromatography has been developed. The Hofmann degradation of I–IX with potassium *tert.*-butoxide in benzene–dimethyl sulphoxide (8:2) under reflux for 30 min gave quantitatively the corresponding 1-olefin. The 1-olefins obtained were measured by gas chromatography on a 5% SE-30 column. The proposed method could be applied to the analysis of these compounds in household products such as hair rinses, fabric softeners and antistatic aerosols.

INTRODUCTION

Cationic surfactants of the long-chain alkyltrimethylammonium and dialkyldimethylammonium types are widely employed in toiletry and household products such as hair rinses, hair treatments and fabric softeners. These ammonium compounds are usually homologous mixtures of C_{10}–C_{18} alkyl groups and are present at the level of 1–5% in hair rinses and many other commercial household products.

The determination of the type and homologous distributions of cationic surfactants is difficult due to their high polarities. Therefore, only a few analyses of these compounds have been reported. Kawase *et al.*[1,2] described the analysis of alkyltrimethylammonium compounds by flow injection analysis techniques and of dialkyldimethylammonium compounds by high-performance liquid chromatography. Metcalfe[3] attempted the determination of alkyltrimethyl- and dialkyldimethylammonium compounds by Hofmann degradation and with gas chromatography (GC) by direct injection on an alkali-treated column. Kojima and Oka[4] reported the lithium aluminium hydride reduction of these two types of ammonium compounds to alkyldimethylamines and dialkylmethylamines for GC analysis. However, the reduction products or thermal decomposition products obtained by such conversion methods were mainly the tertiary amines, not the corresponding 1-olefins.

This paper describes a new method for the convenient GC determination of

0021-9673/86/$03.50

cationic surfactants of the alkyltrimethylammonium and dialkyldimethylammonium types by Hofmann degradation. The non-volatile cationic surfactants were converted with potassium *tert.*-butoxide into the corresponding volatile 1-olefins amenable to GC.

EXPERIMENTAL

Apparatus

GC was carried out using an Hitachi Model 163 gas chromatograph fitted with an hydrogen flame ionization detector. Peak area measurements were obtained by a Shimadzu Chromatopac C-RIA digital integrator. Gas chromatography–mass spectrometry (GC–MS) was performed on a JEOL JMS-D300 instrument equipped with an Hewlett-Packard gas chromatograph. The mass spectra were recorded at 70 eV in the electron-impact ionization mode. Nuclear magnetic resonance (NMR) spectroscopy was carried out with a JEOL JNM-FX 270 instrument (^{1}H, 269.65 MHz; ^{13}C, 67.80 MHz). The spectra were recorded for solutions in deuterochloroform. Chemical shifts, δ (ppm), are downfield from tetramethylsilane as internal standard.

Reagents

Alkyltrimethylammonium chlorides with C_{12} (I), C_{14} (II), C_{16} (III) and C_{18} (IV) alkyl groups were purchased from Tokyo Kasei Kogio (Tokyo, Japan). Alkyltrimethylammonium chlorides with C_{20} (V), C_{22} (VI) and C_{24} (VII) alkyl groups and dialkyldimethylammonium chlorides with C_{16} (VIII) and C_{18} (IX) alkyl groups were obtained from Kao Soap Co. (Tokyo, Japan). Standard solutions were prepared by dissolving each ammonium compound in ethanol.

All other chemicals employed were of analytical grade.

Degradation procedure A for I–IX

An ethanolic solution containing 0.5–4 mg of compounds I–IX was placed in a 100-ml Kjeldahl type flask and evaporated to dryness under reduced pressure. A 100-mg amount of potassium *tert.*-butoxide and 25 ml of benzene–dimethyl sulphoxide (DMSO) (8:2) were added. The solution was refluxed on water-bath for 30 min. After cooling the flask to room temperature, the reaction solution was transferred to a 100-ml separating funnel. The flask was rinsed with two 5-ml portions of benzene. The rinsing solutions were added to the reaction solution and then washed with two 20-ml portions of 5% hydrochloric acid and with 10 ml of water. The benzene layer was separated, 1 ml of *n*-nonane was added and then evaporated to about 1 ml under reduced pressure. This residue was made up to 5 ml with hexane and 5 μl of the solution were injected into the gas chromatograph.

In the case of compounds VIII and IX, because alkyldimethylamine was obtained together with the 1-olefin, the hexane solution was subjected to further clean-up by silica gel column chromatography (silica gel 60, 2 g; 6 cm × 1 cm I.D.) with hexane to remove the alkyldimethylamine. The 1-olefin was eluted with 30 ml of hexane. To the hexane eluate was added 1 ml of *n*-nonane and then evaporated to about 1 ml under reduced pressure. This residue was dissolved in hexane as described above.

Degradation procedure B for samples such as hair rinse and fabric softener

All the samples containing the cationic surfactants I–IX were dissolved in a mixture of ethanol and benzene to yield 0.1–1.0% solutions of appropriate concentration for the GC determinations. Each solution (10 ml) was placed in a 100-ml Kjeldahl type flask, and degraded with potassium *tert.*-butoxide as described in procedure A. The reaction solution was evaporated under reduced pressure to remove the benzene, 10 ml of hexane were added and the mixture was transferred to a 100-ml separating funnel. The flask was rinsed with two 5-ml portions of hexane. The pooled hexane solutions were washed with 20 ml of 5% hydrochloric acid. The hexane layer was subjected to silica gel column chromatography, and the solution for the GC determinations prepared as in procedure A.

GC conditions

GC was carried out on a glass column (2 m × 3 mm I.D.) packed with 5% SE-30 on Chromosorb W AW DMCS (80–100 mesh) with a nitrogen flow-rate of 40 ml/min. The injection port and detector temperatures were 250°C. The column oven temperatures were as follows: (1) for identification of the degradation products, increased from 160 to 270°C at a rate of 6°C/min then isothermal until the end of the chromatogram; (2) for the examination of optimum reaction conditions, isothermal at 160°C; (3) for the construction of calibration curves, isothermal at 130°C (I), 150°C (II), 170°C (III, VIII), 190°C (IV, IX), 210°C (V), 230°C (VI) and 250°C (VII).

RESULTS AND DISCUSSION

Identification of degradation products

The ammonium compounds (I–IX, 30 mg) shown in Scheme 1 were degraded according to procedure A. The degradation products were identified by GC–MS and NMR spectroscopy after their isolation from the reaction mixture by silica gel col-

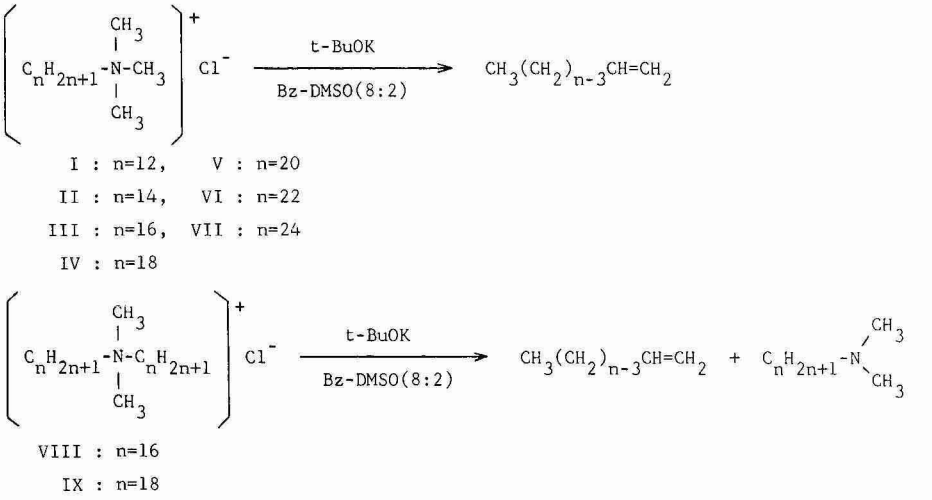

Scheme 1. t-BuOK = potassium *tert.*-butoxide; Bz = benzene.

umn chromatography. Each product from compounds I–VII gave one peak on the temperature-programmed gas chromatogram. Typical gas chromatograms of II, IV and VI are shown in Fig. 1. The mass spectra of the degradation products corresponding to peaks 1, 2 and 3 exhibited molecular ion peaks, M^+, at *m/z* 196, 252 and 308, respectively. The ^1H NMR spectra of the degradation products indicated the presence of methyl (δ 0.88 ppm, 3H, t, J = 6.6 Hz) and $-CH=CH_2$ groups (4.95, 2H, m; 5.80, 1H, m). These were also suggested by the signals at δ 14.2 (q), 114.1(t) and 139.3(d) ppm, and the signals of long-chain alkyl group were observed at 22.7(t), 29.0(t), 29.2(t), 29.4(t), 29.6(t), 29.7(t), 32.0(t) and 33.8(t) ppm in the ^{13}C NMR spectra. Therefore, the degradation products of compounds II, IV and VI were identified as 1-tetradecene, 1-octadecene and 1-docosene. The yield was 92–107% for 1-olefins.

On the degradation of compounds I, III, V and VII, each product was identified as 1-dodecene, 1-hexadecene, 1-eicosene and 1-tetracosene based on GC–MS and NMR spectral data, respectively.

The degradation products of compounds VIII and IX gave two peaks on the gas chromatograms as shown in Fig. 2. Peaks 4 and 5 were identified as 1-hexadecene and 1-octadecene by GC–MS and NMR spectroscopy. On the other hand, the degradation products corresponding to peaks 6 and 7 gave M^+ at *m/z* 269 and 297 in

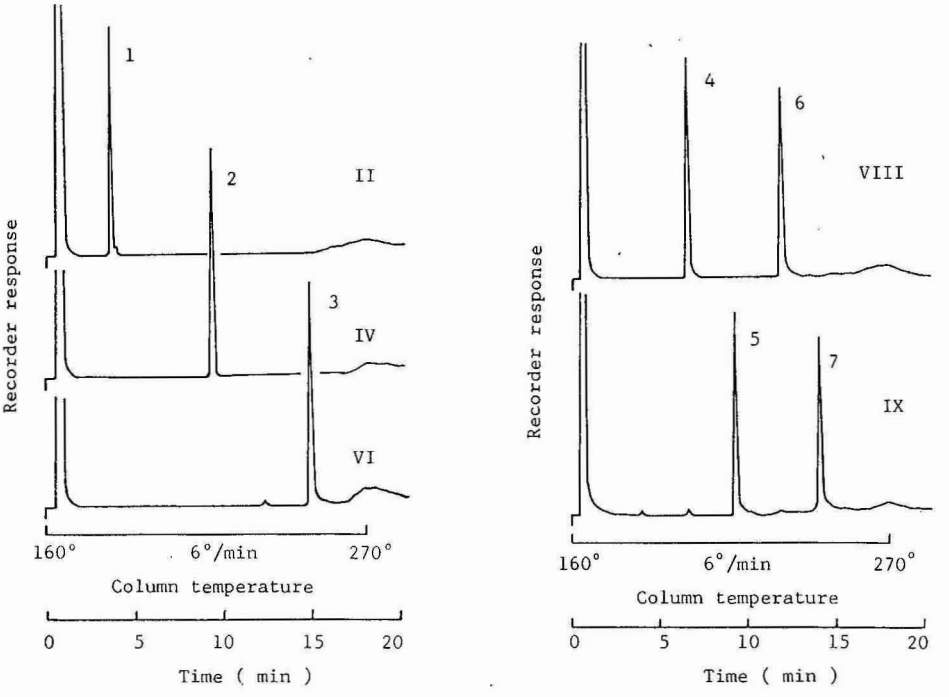

Fig. 1. Temperature-programmed gas chromatograms of 1-olefins derived from alkyltrimethylammonium chlorides (II, IV and VI). Peaks: 1 = 1-tetradecene; 2 = 1-octadecene; 3 = 1-docosene.

Fig. 2. Temperature-programmed gas chromatograms of 1-olefins and alkyldimethylamines derived from dialkyldimethylammonium chlorides (VIII and IX). Peaks: 4 = 1-hexadecene; 5 = 1-octadecene; 6 = hexadecyldimethylamine; 7 = octadecyldimethylamine.

the mass spectrum, and showed ^{1}H NMR signals due to a methyl group (0.88, 3H, t, J = 6.6 Hz) and two equivalent methyl groups bonded to a nitrogen atom (2.21, 6H, s). The ^{13}C NMR spectra also showed the presence of a methyl group at 14.2(q) ppm, long-chain alkyl group at 22.8(t), 27.7(t), 28.0(t), 29.6(t), 29.9(t) and 32.1(t) ppm and methyl and methylene groups bonded to a nitrogen atom at 45.5(q) and 60.1(t) ppm. Therefore, the degradation products were identified as hexadecyldimethylamine for peak 6 and octadecyldimethylamine for peak 7. The yield was 96–98% for 1-olefins and 93–98% for alkyldimethylamines.

In the Hofmann degradation of compounds I–IX, the corresponding 1-olefins were formed as the main product with release of tertiary amine based on β-elimination as shown in Scheme 1. Tanaka *et al.*[5] reported that alkyltrimethyl- and dialkyldimethylammonium salts yielded the 1-olefin and the tertiary amine, *i.e.*, alkyldimethylamine and dialkyldimethylamine, upon Hofmann degradation involving demethylation in the presence of sodium methoxide in dimethylformamide. The described method involving potassium *tert.*-butoxide provided a more selective β-elimination reaction than that with sodium methoxide as attempted by Tanaka *et al.*[5] It was confirmed that this mechanism consisted exclusively of the olefin-forming β-elimination at the nitrogen-bonded alkyl chain in compounds I–IX.

Optimum reaction conditions

The conditions for Hofmann degradation with potassium *tert.*-butoxide were examined. GC analysis of 1-olefins formed from 2 mg of compounds I–IV was performed under isothermal conditions at 160°C. Fig. 3 shows the effect of amount of potassium *tert.*-butoxide on the degradation. The results indicated that the 1-olefins were formed quantitatively when more than 60 mg of potassium *tert.*-butoxide were employed. Thus, the amount of potassium *tert.*-butoxide was set at 100 mg for the degradation of compounds I–IX. In the presence of this amount, the formation of 1-olefins was slightly increased by increasing the concentration of DMSO in benzene

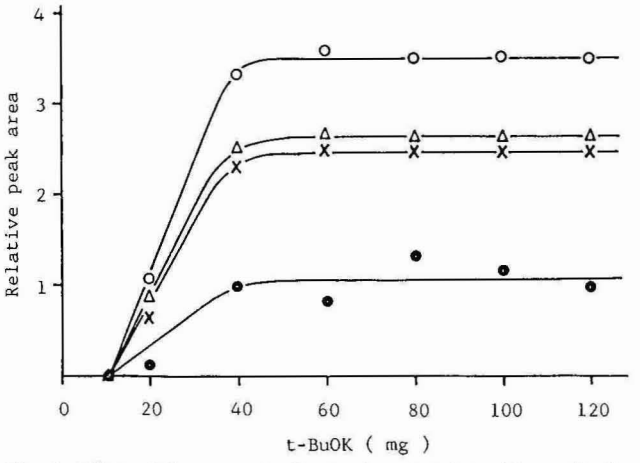

Fig. 3. Effect of the amount of potassium *tert.*-butoxide on the formation of 1-olefins from alkyltrimethylammonium chlorides. GC column temperature: 160°C. ●–●, I; ×–×, II; △–△, III and ○–○, IV.

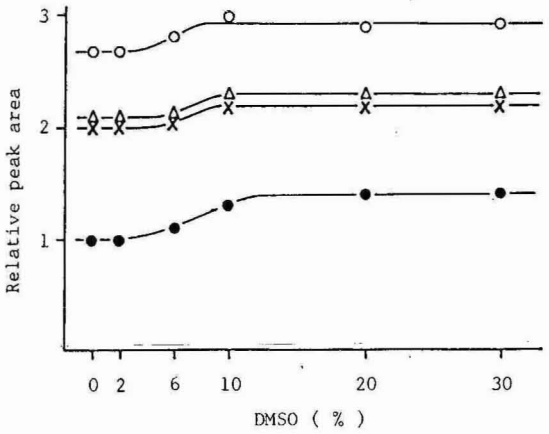

Fig. 4. Effect of DMSO concentration on the formation of 1-olefins from alkyltrimethylammonium chlorides (I–IV). GC column temperature and symbols as in Fig. 3.

and fairly constant on the addition of more than 10% of DMSO (Fig. 4). Benzene–DMSO (8:2) was chosen as the reaction solvent. As shown in Fig. 5, the reaction time for the degradation with 100 mg of potassium *tert.*-butoxide in 25 ml of benzene–DMSO (8:2) solution was 20 min. From these results, the recommended reaction conditions were as follows: 100 mg potassium *tert.*-butoxide; 20% DMSO in benzene; reaction time, 30 min.

Modification of analytical procedure

The procedure was modified for application to the determination of compounds I–IX in hair rinses and fabric softeners.

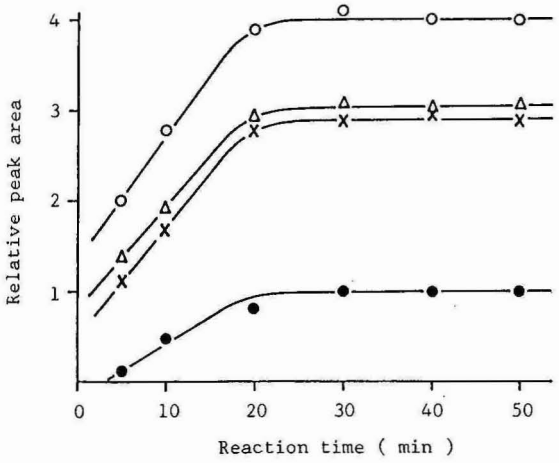

Fig. 5. Effect of reaction time on the formation of 1-olefins from alkyltrimethylammonium chlorides (I–IV). GC column temperature and symbols as in Fig. 3.

The potassium *tert.*-butoxide was inactivated by the presence of water contained in hair rinses or in ethanol used as solvent for the preparation of the sample solution, and the yield of 1-olefins was decreased. Thus, the sample solution made up with ethanol was completely evaporated to dryness under reduced pressure before degradation and freed from water and ethanol.

When the reaction solution was directly washed with 5% hydrochloric acid as in procedure B, shaking of the two phases frequently caused emulsification. The benzene layer was extremely difficult to separate from the aqueous emulsion of the examined hair rinses. Therefore, the reaction solution was freed from benzene under reduced pressure. The 1-olefin formed was extracted with hexane. However, the gas chromatograms of the hexane extracts were complicated with alkyldimethylamine derived from compounds VIII and IX and by interference, *e.g.*, from long-chain fatty alcohols such as cetyl alcohol and stearyl alcohol contained as emulsifier in hair rinses. Thus, the extracts were subjected to silica gel column chromatography for the removal of the tertiary amines and alcohols, as in procedure B.

Calibration curve

As shown in Fig. 6, the calibration curves of peak heights *vs.* concentration for compounds I–IX treated as in procedure B passed through the origin and showed good linearity over the range of 100–800 ppm. The GC measurements were carried out under isothermal column conditions where the 1-olefin appeared at a retention time of about 5 min. The detection limit for each ammonium compound from I–IX was approximately 40 ppm.

Application to practical product analysis

Recovery tests were performed by adding known amounts of compounds II, IV, VII and IX to a laboratory-made hair rinse as shown in Table I. Average recoveries in three experiments were 96.3–102.0% for II, IV and VI, and 96.3–101.6% for

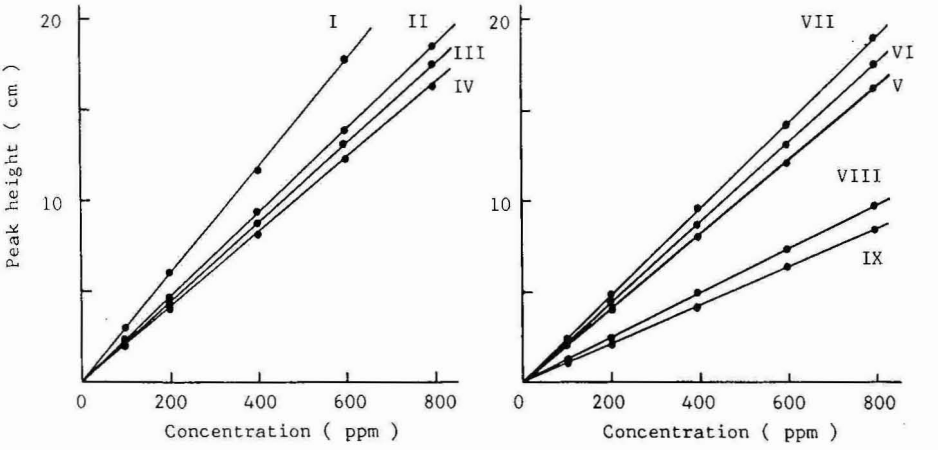

Fig. 6. Calibration curves for alkyltrimethyl- and dialkyldimethylammonium chlorides. Column temperatures: I, 130°C; II, 150°C; III, 170°C; IV, 190°C; V, 210°C; VI, 230°C; VII, 250°C; VIII, 170°C; IX, 190°C.

TABLE I

RECOVERIES OF ALKYLTRIMETHYL- AND DIALKYLDIMETHYLAMMONIUM CHLORIDES FROM HAIR RINSE

The quaternary ammonium chlorides were added to 0.5 g of laboratory-made rinse, the composition of which is as follows: 0.5% cetyl alcohol; 4% propylene glycol; 1% methylcellulose (mol.wt. 4000), colour and perfume q.s.; made up with purified water.

Compound	*Added (mg)*	*Average recovery (n=3) (%)*	*C.V. (%)*
II	1.0	97.0	2.9
	2.0	102.0	1.0
	3.0	97.0	3.0
IV	1.0	98.1	1.5
	2.0	96.4	1.7
	3.0	96.9	2.0
VI	1.0	101.7	1.7
	2.0	98.3	1.0
	3.0	98.3	1.0
VIII	1.0	98.7	1.9
	2.0	96.3	2.7
	3.0	101.6	1.6
IX	1.0	101.0	1.0
	2.0	100.0	1.4
	3.0	100.0	1.0

VIII and IX using the entire procedure B. A good reproducibility was obtained, and the coefficient of variation (C.V.) was less than 3.0%. Table I demonstrates that the proposed method can be applied to commercial product analysis.

REFERENCES

1 J. Kawase, *Anal. Chem.*, 52 (1980) 2124.
2 J. Kawase, Y. Takao and K. Tsuji, *J. Chromatogr.*, 262 (1983) 293.
3 L. D. Metcalfe, *J. Am. Oil Chem. Soc.*, 40 (1963) 25.
4 T. Kojima and H. Oka, *Nippon Kagaku Kaishi*, 71 (1968) 1844.
5 S. Takano, C. Takasaki, K. Kunihiro and M. Yamanaka, *J. Am. Oil Chem. Soc.*, 54 (1977) 139.

Journal of Chromatography, 362 (1986) 235–242
Elsevier Science Publishers B.V., Amsterdam — Printed in The Netherlands

CHROM. 18 678

HIGH-PERFORMANCE LIQUID CHROMATOGRAPHY OF SUGARS ON A MIXED CATION-EXCHANGE RESIN COLUMN

J. A. M. VAN RIEL and C. OLIEMAN*
Netherlands Institute for Dairy Research (NIZO), Kernhemseweg 2, P.O. Box 20, 6710 BA Ede (The Netherlands)
(First received January 27th, 1986; revised manuscript received March 26th, 1986)

SUMMARY

The separation of mono-, di-, and trisaccharides on a cation-exchange 6% cross-linked resin column in the silver form (HPX-65A) is described. Acid-catalysed hydrolysis of sugars at elevated column temperatures could be suppressed by partially converting the column into the lead(II) form. The selectivity can be influenced by varying the ratio of the counter-ions. The use of this column connected in series with a cation-exchange 8% cross-linked resin column in the lead(II) form enabled the separation of sucrose, maltose, lactose, glucose, galactose, and fructose. The presence of the combinations maltotriose–sucrose and lactulose–glucose requires additional analysis on an unmodified HPX-65A column.

INTRODUCTION

The most prominent carbohydrate of milk is lactose, but traces of the monosaccharides glucose and galactose and other (poly)saccharides are also present. In dairy products lactose may be hydrolysed to D-glucose and D-galactose by enzymes. The determination of these three sugars by high-performance liquid chromatography (HPLC) should be performed on diol-modified silica or cation-exchange resin columns[1]. The accuracy and reproducibility of the determination of lactose in milk have been studied, and the results obtained by HPLC were compared with those found by polarimetry, enzymatic assay and reductometry (Luff-Schoorl)[2]. Since HPLC gave the same levels for lactose in milk as the enzymatic assay and is capable of measuring several sugars in one analysis, it is the method of choice.

In addition to the carbohydrates naturally present in dairy products, other sugars or sugar-containing components may be added in order to give the food product more desirable properties. The sugars encountered most frequently are sucrose, fructose, maltose and maltodextrins. The HPLC analysis of sugars in foods such as dairy products has been studied by several groups[3–6]. In these cases only a limited number of sugars was investigated or a marginal separation between some types of sugar was obtained. Diol-modified silica columns fail to give sufficient resolution for galactose and glucose, whereas the cation-exchange columns show insuf-

0021-9673/86/$03.50

ficient separation between the disaccharides. This implies that foods with an unknown or complicated sugar composition should be analysed on a diol-modified silica column and also on a cation-exchange resin column. The use of an acetonitrile-rich solvent in combination with a cation-exchange resin column gives sufficient resolution of sucrose, maltose and lactose[7]. However, many commercial cation-exchange resin columns do not tolerate the high content of acetonitrile (70–80%) in the eluent. Moreover, the sensitivity is considerably reduced, owing to the unfavourable refractive index of acetonitrile and to the high pressure-dependence of this index, giving a noisy baseline, caused by pump pulsation. The toxic properties of acetonitrile and the limited solubility of sugars in this eluent also make it less attractive.

Scobell and Brobst[8] described the preparation and application of a silver-loaded cation-exchange resin column with an intermediate cross-linking of 6%. Silver ions form monodentate complexes, which are stronger with disaccharides than with monosaccharides. This type of column is able to separate the disaccharides and to give reasonable separations for the monosaccharides.

Recently, a commercial version of this column became available and this prompted us to investigate its usefulness for the analysis of sugars, especially in dairy products.

TABLE I

RETENTION TIMES (min) OF SUGARS ON CATION-EXCHANGE RESIN COLUMNS AT VARIOUS TEMPERATURES

D = decomposition.

Sugar	*HPX-65A column*				*HPX-87P column*		
	25°C	*45°C*	*65°C*	*85°C*	*65°C*	*85°C*	*95°C*
Maltotriose	11.33	10.66	10.23	9.87	10.42	9.86	9.70
Stachiose	10.60	9.92 (D)	D	D	8.99	8.78	8.78
Gentiobiose	11.75	11.46	11.18	11.01	9.69	9.62	9.55
Cellobiose	12.12	11.71	11.39	11.17	10.19	10.06	9.98
Maltose	12.30	11.87	11.56	11.31	10.99	10.66	10.57
Melezitose	10.02	9.76 (D)	D	D	9.15	9.08	9.08
Raffinose	11.18	10.64 (D)	D	D	9.59	9.40	9.37
Melibiose	14.06	13.31	12.82	12.46	11.54	11.20	11.10
Lactose	14.18	13.42	12.87	12.47	11.25	10.97	10.80
Lactulose	17.10	15.38	14.26	13.40	13.74	12.70	12.37
Sucrose	11.44	11.23 (D)	D	D	10.29	10.16	10.12
Glucose	13.88	13.76	13.59	13.47	12.37	12.24	12.17
Tagatose	13.52	13.74	13.71	13.70	23.07	21.02	20.08
Xylose	14.30	14.16	13.94	13.82	13.54	13.26	13.13
Fructose	17.09	16.06	15.27	14.71	17.92	16.27	15.68
Galactose	16.78	16.04	15.48	15.06	14.60	14.10	13.88
Mannose	16.66	16.10	15.57	15.22	16.75	15.82	15.50
Arabinose	17.60	16.77	16.11	15.59	16.22	15.27	14.85
Fucose	18.21	17.84	17.32	16.83	16.12	15.48	15.15
Rhamnose	14.72	14.80	14.66	14.56	14.67	14.34	14.17

EXPERIMENTAL

Chemicals and materials

All reference standard solutions were prepared from analytical-reagent grade chemicals (Fluka, Buchs, Switzerland; Merck, Darmstadt, F.R.G.; Sigma, St. Louis, MO, U.S.A.; BDH, Poole, U.K.). For injection the samples were dissolved in doubly-distilled water. The compounds investigated are listed in Table I. All chemicals used in sample clean-up were of reagent-grade quality. Analytical grade cation-exchange resin (H^+, AG 50W-X4, <400 mesh; Bio-Rad Labs., Richmond, U.S.A.) and anion-exchange resin (base form, AG 3-X4A, 200–400 mesh; Bio-Rad) were used to pack the pre-column. The clean-up solution of Biggs and Szijarto[9] contained 91.0 g of zinc acetate dihydrate, 54.6 g of phosphotungstic acid 24-hydrate and 58.1 ml of glacial acetic acid per litre of doubly-distilled water.

Apparatus

A Waters Assoc. Model 6000 A pump with a Wisp 710B automatic sample injector was used in combination with an Erma Optical Works ERC-7510 refractive index detector and a Kipp Analytica 9222 column oven. Chromatograms were recorded and integrated with a Spectra-Physics SP4200 data system. The separations

TABLE II

RETENTION TIMES (min) OF SUGARS ON A MIXED SILVER–LEAD ION-EXCHANGE RESIN COLUMN AT VARIOUS TEMPERATURES AND SILVER–LEAD RATIOS

Sugar	*Percentage lead in column regenerating solvent: % (mol Pb/mol Ag)*					
	7.5	*3*	*1.5*			
	65°C	*65°C*	*25°C*	*45°C*	*65°C*	*85°C*
Maltotriose	12.37	12.13	13.86	12.83	12.10	11.60
Stachiose	13.35	11.40	12.67	11.83	11.33	10.98
Gentiobiose	12.75	12.30	12.86	12.47	12.27	12.03
Cellobiose	12.97	12.58	13.31	12.87	12.58	12.28
Maltose	13.25	12.97	13.89	13.37	12.93	12.63
Melezitose	11.18	10.97	11.44	11.13	10.93	10.82
Raffinose	14.02	11.85	12.90	12.20	11.78	11.52
Melibiose	14.87	15.83	15.60	14.83	14.28	13.85
Lactose	14.67	14.15	15.31	14.63	14.08	13.65
Lactulose	16.78	16.43	20.55	17.85	16.38	15.27
Sucrose	12.43	12.20	12.73	12.37	12.17	12.00
Glucose	14.78	14.52	14.54	14.60	14.47	14.30
Tagatose	19.00	20.53	23.20	21.32	20.57	19.22
Xylose	15.20	15.03	15.56	15.23	15.05	14.78
Fructose	17.77	17.95	21.83	19.37	17.98	16.87
Galactose	17.05	16.75	18.30	17.30	16.72	16.17
Mannose	18.00	18.00	20.15	18.78	18.02	17.23
Arabinose	17.73	17.58	19.93	18.50	17.58	16.78
Fucose	18.55	18.17	19.38	18.67	18.17	17.53
Rhamnose	16.12	16.07	16.45	16.20	16.08	15.77

were performed on a HPX-65A (11 μm) and a HPX-87P (9 μm) (30 × 0.78 cm, Bio-Rad Labs.), used individually or connected in series. A pre-column from Waters Assoc. having an enlarged I.D. of 7 mm and equipped with flow-distributors was packed with a dry mixture of cation- and anion-exchange resins (10:15, mequiv.) and placed outside the column oven. The eluent reservoir was kept at 85°C. The eluent was filtered through a 0.45-μm Millipore filter.

Procedures

The sample clean-up according to Biggs and Szijarto[9] was carried out as follows. To a weighed amount of dairy product (*ca.* 2 g), 80 ml of distilled water and 25 ml of the Biggs solution were added, after which the volume was made up to 200 ml with water. The precipitate was filtered off (Whatman No. 40), the first 20 ml of the filtrate were discarded and 15 μl of the filtrate were injected.

The conversion of the HPX-65A column into the mixed-ion mode was carried out by pumping 400 ml of a solution of silver and lead(II) nitrate (total concentration $\approx$0.1 M) in the desired ratio (see Table II) through the column at room temperature. If the column developed a void at the top, it was carefully filled with a thick slurry of resin from an old HPX-87P column and converted again with the appropriate solution of silver and lead(II) nitrate.

RESULTS AND DISCUSSION

Since the determination of sugars is of interest not only for the analysis of dairy products, we have investigated the retention of twenty sugars on a silver-loaded intermediate cross-linked HPX-65A column at different column temperatures (Table I). Fig. 1 shows a separation at 85°C. Lower temperatures can be used with this type of column, because α and β anomers of glucose (oligosaccharide) are not resolved. Stachiose, melezitose, raffinose and sucrose showed multiple or broad peaks at temperatures above 25°C, owing to acid-catalysed hydrolysis due to sulphonic groups in the hydrogen form. Regeneration of the column with 0.1 *M* silver nitrate solution did not eliminate the decomposition of these sugars (Fig. 2). The analysis of samples containing one or more of these acid-sensitive sugars, can be performed only at room temperature. Under these conditions rather broad peaks are observed, owing to slower mass transfer. Moreover, the frequently occurring combinations lactose–glucose and galactose–fructose are not resolved.

For comparison we have analysed the same sugasrs on an HPX-87P column in the temperature range 65–95°C (Table I). Lower temperatures are not practical, because of increased separation of α and β anomers. The HPX-65A and the HPX-87P columns show different selectivities, and we have therefore investigated the possibility of using both columns connected in series. As a test sample a mixture of maltose, lactose, sucrose, glucose, galactose and fructose was used. The temperature of the HPX-65A was fixed at 25°C, but that of the HPX-87P was varied between 65°C and 95°C. Calculation of the resolution for critical pairs of sugars with the data of Table I and plate numbers did not suggest a satisfactory separation, which was confirmed by experiment.

We reasoned that the problem of acid-catalysed hydrolysis could be solved if the residual sulphonic groups in the hydrogen form of the HPX-65A column could

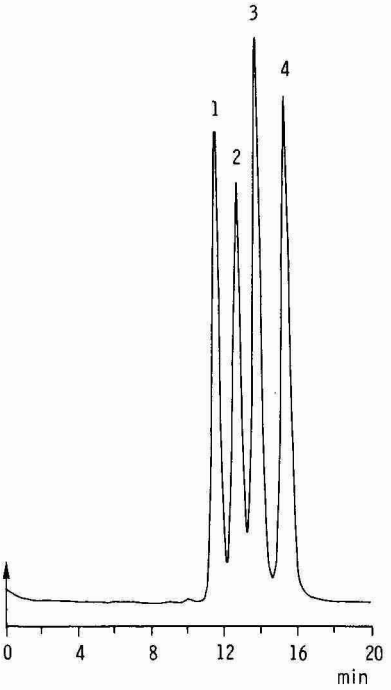

Fig. 1. Separation of maltose (1), lactose (2), glucose (3) and galactose (4) on an unmodified HPX-65A column at 85°C; flow-rate, 0.6 ml/min.

be converted into a neutral form, enabling its use at elevated temperatures for acid-sensitive sugars. The HPX-87P column does not display any sulphonic groups in the hydrogen form. Assuming that both resins are sulphonated in a similar way, resulting in the same number and distribution of sulphonic groups, the HPX-65A column should contain double the amount of silver ions in HPX-87P column, which contains lead(II) ions. The ionic radii of silver(I) and of lead(II) ions are comparable, which implies that the resin in the silver form contains twice the volume fraction, occupied by the ions, compared with the resin in the lead form, assuming that each lead(II) ion needs two sulphonic residues. Although the cross-linking of the resin used for the

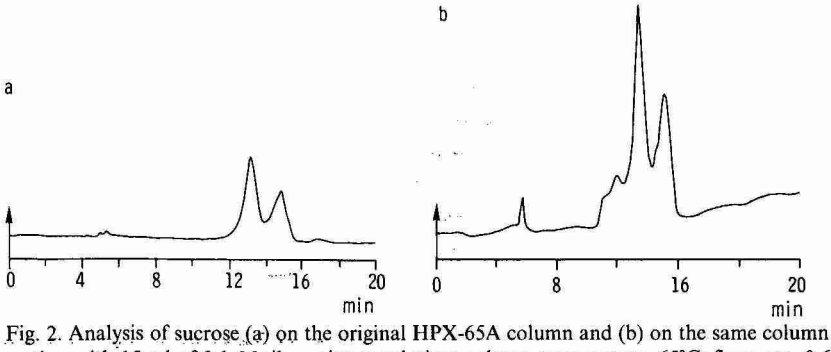

Fig. 2. Analysis of sucrose (a) on the original HPX-65A column and (b) on the same column after regeneration with 15 ml of 0.1 *M* silver nitrate solution; column temperature, 65°C; flow-rate, 0.6 ml/min.

HPX-65A is 6%, which is lower than for the HPX-87P (8%), the physical space might be insufficient to accommodate all the silver ions. Converting a cation-exchanger, which is necessarily partly in the silver form, by a small fraction into the lead form, could eliminate the presence of sulphonic groups in the hydrogen form, while maintaining the positive effects of the silver ions on the retention mechanism. This was accomplished by treating the HPX-65A column with mixtures of lead(II) and silver(I) nitrate solutions. Table II shows the retention of the sugars as a function of the column temperature and as a function of the percentage of lead(II) nitrate in the regenerating solvent. Acid-sensitive sugars such as sucrose and raffinose gave single, sharp peaks at 85°C, which proves the virtual absence of sulphonic residues in the hydrogen form. At 25°C some sugars show broad or double peaks, due to α and β anomer separation, which limits the use of the column at this temperature. The HPX-65A column, thus modified, remains stable for one week of continued use, provided that a mixed-bed ion-exchanger with excess anion-exchanger (see Experimental) is used. With the pre-column installed, a column temperature of 70°C and a flow-rate of 0.6 ml/min, a plate count of 3005 and an asymmetry factor of 0.85

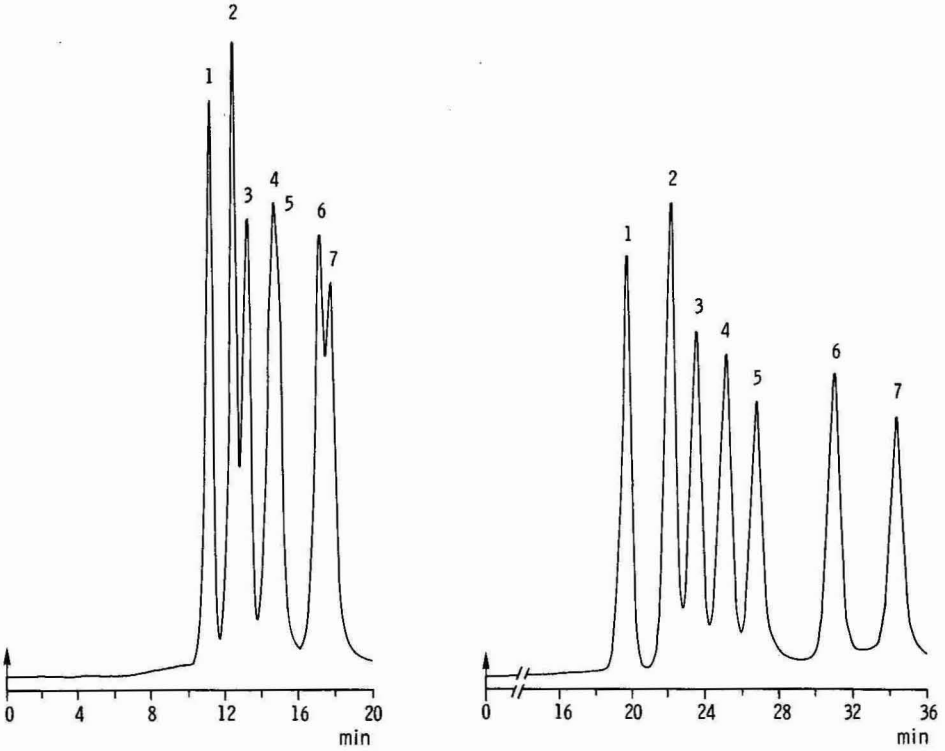

Fig. 3. Separation of melezitose (1), sucrose (2), maltose (3), lactose (4), glucose (5), galactose (6) and fructose (7) on a HPX-65A column, modified with 1.5 mol% lead(II)–silver nitrate solution; column temperature, 70°C; flow-rate, 0.6 ml/min.

Fig. 4. Separation of melezitose (1), sucrose (2), maltose (3), lactose (4), glucose (5), galactose (6) and fructose (7) on a dual column system, consisting of a modified HPX-65A column (see Fig. 3) and a HPX-87P column; column temperature, 70°C; flow-rate, 0.6 ml/min.

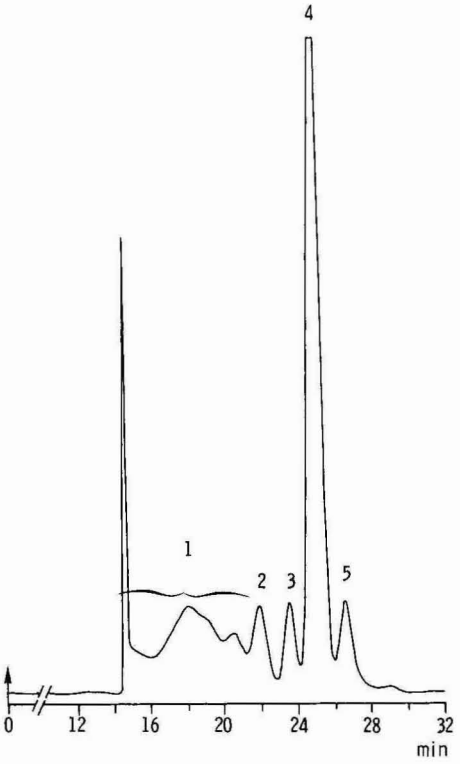

Fig. 5. Analysis of a baby-food containing lactose (4) and maltodextrins: malto-oligosaccharides (1), maltotriose (2), maltose (3) and glucose (5); 15 μl injection of a Biggs filtrate; for conditions see Fig. 4.

were obtained for lactulose. Without the pre-column these values were 3884 and 1.06, respectively. In this case the pre-column causes the peaks to front.

Fig. 3 shows a chromatogram of the separation of a mixture of sugars that occur frequently in dairy products. Melezitose was included as a suitable internal standard. Lactose and glucose are not resolved, and galactose and fructose are only partly separated. This cannot be improved by changing the column temperature (Table II). Although the selectivity for galactose and fructose increases with decreasing temperatures, the resolution does not increase, owing to peak broadening. The use of other ratios of silver to lead(II) did not improve the situation (Table II).

The problem of co-eluting pairs of sugars can be solved by connecting an HPX-87P column in series with a modified HPX-65A column, as was predicted by summing the retention times of the sugars on the individual columns (Tables I and II). If both columns are installed in the same oven, then the useful temperature range is dictated by that of the HPX-87P, being 65–85°C. The same set of sugars can be separated on this dual column system (Fig. 4) within 40 min. Two interferences might occur in the analysis of dairy products. Firstly, the presence of lactulose, which co-elutes with glucose. Lactulose is formed on strong heating of lactose-containing products. This reaction is strongly dependent on the pH. The presence of lactulose in dairy products can be determined with an HPX-87P column (Table I). Secondly, the

presence of maltotriose in sucrose-containing products. These sugars co-elute on the dual column system, as well as on the individual columns. However, maltotriose is well separated from other sugars (including maltotetraose) on an unmodified HPX-65A column. Fig. 5 shows the analysis of a baby-food, containing maltodextrins. For sample clean-up, the method of Biggs and Szijarto[9] has to be used since acetonitrile is retained strongly on the silver-loaded resin column.

CONCLUSION

We have found that a cation-exchange resin in the silver form with a cross-linking of 6% is suitable for the analysis of mono- and disaccharides. The column can be used at elevated temperatures, provided that sugars, which are sensitive to acid-catalysed hydrolysis, are absent. The use of this column in a mixed cation form can eliminate the adverse effects of sulphonic groups in the hydrogen form on acid-sensitive sugars. Moreover, it offers the additional possibility of influencing the selectivity of sugar separations by altering the ratio of the cations on the column. The analysis of sugars in foods has been improved by the use of a cation-exchange resin column in the silver–lead(II) form connected in series with a cation-exchange resin column in the lead(II) form. The presence of the combination of maltodextrins and sucrose, however, requires a separate analysis on an unmodified HPX-65A column. This is also the case when lactulose is present in heated dairy products, because it co-elutes with glucose.

REFERENCES

1 C. Brons and C. Olieman, *J. Chromatogr.*, 259 (1983) 79.
2 J. Koops and C. Olieman, *Neth. Milk Dairy J.*, 39 (1985) 89.
3 D. C. Woollard, *N. Z. J. Dairy Sci. Technol.*, 18 (1983) 209.
4 C. Vidal Valverde, C. Martin Villa and J. Herranz, *J. Dairy Sci.*, 67 (1984) 759.
5 J. R. Saucerman and C. E. W. Winstead, *J. Assoc. Off. Anal. Chem.*, 67 (1984) 899.
6 J. F. Pirisino, *J. Food Sci.*, 48 (1983) 742.
7 T. Kawamoto and E. Okada, *J. Chromatogr.*, 258 (1983) 284.
8 H. D. Scobell and K. M. Brobst, *J. Chromatogr.*, 212 (1981) 51.
9 D. A. Biggs and L. Szijarto, *J. Dairy Sci.*, 46 (1963) 1196.

Journal of Chromatography, 362 (1986) 243–253
Elsevier Science Publishers B.V., Amsterdam — Printed in The Netherlands

CHROM. 18 681

REVERSED-PHASE, ION-PAIR HIGH-PERFORMANCE LIQUID CHROMATOGRAPHIC SEPARATION OF AMINOETHANOL, CHOLINE AND RELATED COMPOUNDS, AND A DIRECT, QUANTITATIVE HIGH-PERFORMANCE LIQUID CHROMATOGRAPHIC ASSAY FOR CHOLINE IN PLANTS

JOHN GORHAM
Centre for Arid Zone Studies, Department of Biochemistry and Soil Science, University College of North Wales, Bangor, Gwynedd, LL57 2UW (U.K.)
(Received March 22nd, 1986)

SUMMARY

The separation of a wide range of aminoethanol and choline derivatives by ion-pair reversed-phase high-performance liquid chromatography on a styrene–divinylbenzene co-polymer stationary phase is described. Suppression of the conductivity of the eluent and electrical conductivity detection of the remaining cation provides a method for analyzing low concentrations of such compounds. Reineckate precipitation in conjunction with this method forms the basis of a rapid method for the quantitative analysis of choline in plant extracts. The method should also be useful for monitoring the concentrations of choline esters in pharmaceutical preparations, and for the purification of acetylcholine prior to analysis by more sensitive procedures.

INTRODUCTION

Various derivatives of aminoethanol and choline (trimethylaminoethanol) are of great importance in plant and animal biology. Phosphatidylaminoethanol (and its mono- and di-methyl derivatives) and phosphatidylcholine are important constituents of the phospholipid fractions of biological membranes, and choline esters are major neurotransmitters in animals. Several choline esters which are analogues of acetylcholine are of pharmaceutical interest. Aminoethanol and choline are precursors of the plant stress metabolite, glycinebetaine[1], and acetylcholine is also reported to occur in plants[2–5]. Chlorocholine chloride (CCC) is a synthetic plant growth retarder which has been reported to enhance salt tolerance[6,7].

Methods for the analysis of choline have been based on relatively non-specific precipitation of the periodide at high pH[8–11], scanning densitometry of thin-layer separations[12,13] or enzymatic reactions[14–16]. Gas–liquid chromatography (GLC) is not suitable for such highly polar compounds, but a number of methods have been developed for the analysis of choline and its esters which involve either chemical

0021-9673/86/$03.50

demethylation with benzenethiolate under strictly anhydrous conditions[17–27] or pyrolytic demethylation[28–32]. An alternative procedure for choline esters used potassium borohydride to hydrolyse the ester and reduce the liberated acid to an alcohol[33]. The resulting alcohols were separated by GLC on Carbowax 6000. A recent paper describes the use of a splitless capillary GC injector for the aminoethanol-catalysed demethylation of choline esters[34] and the separation of the products on bonded-phase fused-silica capillary columns. Direct high-performance liquid chromatographic (HPLC) separation of choline and acetylcholine have been used in conjunction with post-column enzymatic hydrolysis of the acetylcholine and oxidation of choline followed by electrochemical detection of the resulting hydrogen peroxide[35,36]. A more conventional approach to the chromatography of choline is the formation of UV-absorbing esters and their separation by ion-pair reversed-phase or cation-exchange HPLC[37,38].

The development of the method described in the present paper was stimulated by the need to separate metabolites of aminoethanol and choline in the course of radio-tracer experiments on the biosynthesis of glycinebetaine in plants. In particular, it was desirable to develop methods for the separation of the phosphorylated intermediates in the pathway between aminoethanol and glycinebetaine because of the number of different possible pathways between these two compounds[1,39]. Of the phosphorylated intermediates, phosphorylcholine presented the greatest problems because it cannot be analysed together with the other aminoethanols by derivatization of the amino group[40]. Another consideration was that the method should involve as few preliminary clean-up steps as possible, and preferably not require derivatization. Since few of the compounds in question possess any significant absorbance in the UV region, detection would be by refractive index or conductivity. The method described below uses ion-pair reversed-phase HPLC in conjunction with post-column supression of the conductivity of the eluent and detection of the cations in an electrical conductivity detector.

EXPERIMENTAL

Chemicals

The normal ion-pair reagent, hexanesulphonic acid, was purchased as a 100 mol m^{-3} solution from Dionex U.K. Methanesulphonic acid was purchased from Aldrich and a 100 mol m^{-3} stock solution was prepared with deionized water. This solution was treated with Dowex 50 (H^+ form) to reduce background conductivity. Glycinebetaine aldehyde (trimethylaminoacetaldehyde), trimethylaminoacetone, trimethylamino-3-methyl-2-butanone, trimethylaminopropan-1-ol, trimethylaminopropan-2-ol, triethylaminoethanol, diethylmethylaminoethanol and trimethylaminoacetaldehyde dimethyl acetal were synthesized as previously described[38]. Sulphocholine was produced by the action of concentrated sulphuric acid on choline[41].

High-performance liquid chromatography

HPLC was performed on a 200 × 4 mm I.D. Dionex MPIC-NS1 column with a Dionex MPIC-NG1 guard column, mounted in a Dionex 2010i ion chromatograph and connected to a cation fibre suppressor which was regenerated with 40 mol m^{-3} barium hydroxide. The conductivity detector was routinely operated at 30 μS full

scale deflection and the background conductivity was 5–9 μS. For the detection of glycinebetaine and trigonelline a Cecil CE 212A variable-wavelength monitor was connected to the end of the MPIC-NS1 column and operated at 200 nm. For gradient elution and method development a Spectra-Physics SP 8700 solvent delivery system replaced the Dionex pump. Injections were made either automatically with a 50-μl loop in a Dionex injection valve loaded and activated by a Pye 4700 autoinjector or manually through a 20-μl loop mounted in the Rheodyne injection valve of the SP 8700. Peak heights were determined with a Pye DP 88 integrator.

Extraction and purification of choline from plant material

Either plant material was extracted with propan-2-ol[38] or plant saps were obtained from freeze-thawed samples as previously described[42] and treated with propan-2-ol to precipitate proteins and inhibit enzyme activity[43]. Initially an ion-exchange procedure was used to purify the choline[37,38]. This involved passage through an anion exchanger, loading onto a cation exchanger, washing the cation exchanger with ammonium hydroxide and finally eluting the choline with hydrochloric acid. The main disadvantage of this procedure is the large quantity of ammonium chloride in the final eluate. This has previously been removed by drying the eluate and dissolving the choline with either methanol or acetonitrile[37,38]. It was subsequently found that precipitation with reineckate after reduction in volume *in vacuo* was more effective. A volume of 0.5 ml of a saturated solution of ammonium reineckate was added to the concentrated eluate (1 ml) together with 50 μl of trimethylamine hydrochloride solution (0.5 mg ml^{-1} in water) to act as a co-precipitant. After standing at 4°C for at least 1 h (preferably overnight) the mixture was centrifuged (9000 *g* for 1 min) in a 1.5-ml polypropylene microcentrifuge tube and the supernatant discarded. The reineckate ions were removed with an anion-exchange resin in methanol in a procedure similar to that described for the purification of acetylcholine from brain tissue[27]. In the present case, however, it was not necessary to maintain completely anhydrous conditions. Methanol (1 ml) was added to the microcentrifuge tube together with *ca.* 0.5 ml of Dowex 1 (OH^--form, 100 mesh) dried on a sintered glass funnel to remove surface water. The tube was then shaken mechanically for 10 min, making sure that the reineckate pellet was thoroughly suspended in the methanol. A pin was used to make a small hole in the base of the microcentrifuge tube and the methanolic solution was collected in a small glass vial. Another 1 ml of methanol was added to the microcentrifuge tube to wash the Dowex 1 beads and recover all of the choline. After evaporation to dryness in a stream of air, the purified extract was dissolved in 100 μl of water and centrifuged at 9000 *g* for 1 min before being injected into the high-performance liquid chromatograph. In most cases it was found that the ion-exchange steps could be omitted and the extract (or sap) treated directly with ammonium reineckate. Trimethylaminopropan-2-ol was found to be a suitable internal standard for the quantitative estimation of choline. The same procedure can be used to simultaneously purify choline and glycinebetaine from plant saps, provided that the sap is first acidified to pH 4 or below.

RESULTS AND DISCUSSION

Ion-pair reversed-phase HPLC has previously been used to separate choline

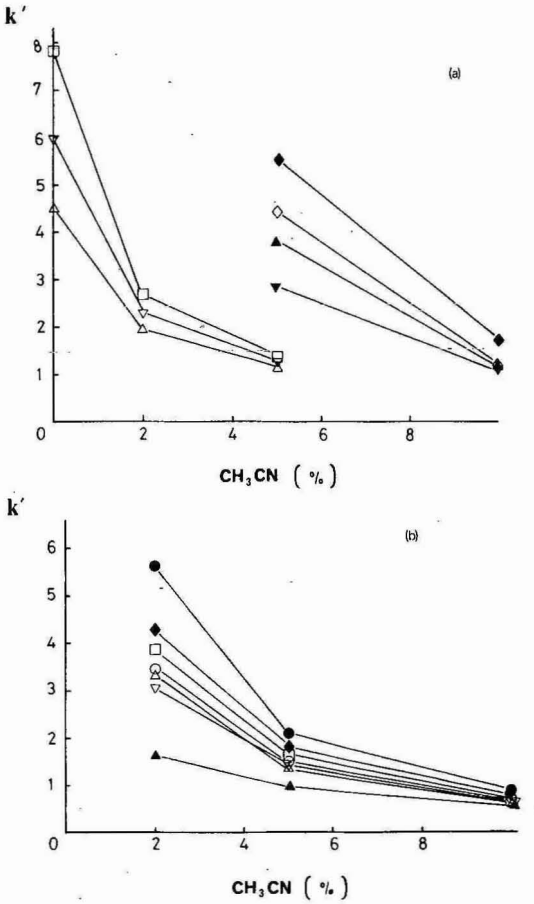

Fig. 1. Capacity factors (k') for a range of aminoethanol and choline analogues against acetonitrile concentration. (a) △ = Aminoethanol; ▽ = methylaminoethanol; □ = dimethylaminoethanol; ◆ = phosphorylcholine; ▲ = triethylaminoethanol; ▼ = acetylcholine; ◇ = glycinebetaine aldehyde. (b) ▲ = Ammonium; ▽ = choline; △ = trimethylaminopropan-1-ol; ◆ = trimethylaminopropan-2-ol; ● = diethylaminoethanol; ○ = dimethylaminopropan-1-ol; □ = dimethylaminopropan-2-ol.

esters on octadecylsilyl stationary phases bonded to silica[37,44]. A similar system (LiChrosorb 10 RP-18) gave broad peaks and poor resolution when used in conjunction with the reagents and detector used in the present investigation. Attempts to use a low-capacity strong cation-exchange column with the Dionex ion chromatograph were also unsuccessful. The Dionex MPIC-NS1 column used here is packed with a 10-μm, porous, neutral, highly cross-linked styrene–divinylbenzene co-polymer. This column has previously been used to separate methyl esters of betaines[45]. That an ion-pair reversed-phase partition mechanism is in operation is demonstrated by the low retention of the quaternary ammonium compounds in the absence of an ion-pair reagent, the increase in retention with increasing concentration or increasing chain length of the ion-pair reagent and the decrease in retention times with increasing concentrations of acetonitrile. The effect of acetonitrile on the ca-

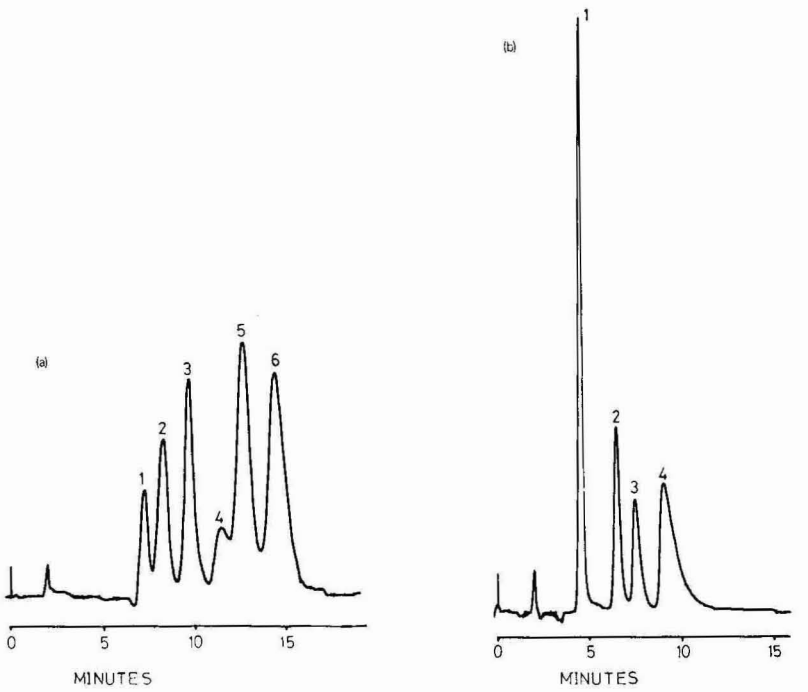

Fig. 2. Isocratic separation on Dionex MPIC-NS1 eluted with 2 mol m^{-3} hexanesulphonic acid. (a) 0.75% Acetonitrile; 1 = ammonium; 2 = aminoethanol; 3 = methylaminoethanol; 4 = dimethylaminoethanol; 5 = choline; 6 = trimethylaminopropan-1-ol. (b) 7% Acetonitrile; 1 = choline; 2 = acetylcholine; 3 = triethylaminoethanol; 4 = phosphorylcholine.

TABLE I

RETENTION TIMES (min) FOR AMINOETHANOL AND RELATED COMPOUNDS ON DIONEX MPIC-NS1 AND MPIC-NG1 COLUMNS ELUTED AT 1 ml min^{-1} WITH 2 mol m^{-3} HEXANESULPHONIC ACID CONTAINING VARIOUS AMOUNTS OF ACETONITRILE

Unretained compounds eluted after 2.5 min.

Compound	*Acetonitrile concentration*		
	0.6%	*2.1%*	*Gradient**
Aminoethanol	8.9	6.3	8.6
Methylaminoethanol	11.0	6.9	10.3
Dimethylaminoethanol	12.7	7.5	12.3
Diethylaminoethanol	>20.0	15.3	24.4
Dimethylaminopropan-1-ol	>15.0	9.3	15.4
Dimethylaminopropan-2-ol	>15.0	10.2	17.5

* Linear gradient between the following set points; 0 min, 0.6% acetonitrile; 9 min, 0.9% acetonitrile; 20 min, 3% acetonitrile; 30 min, 15% acetonitrile; 38 min, 30% acetonitrile.

TABLE II

RETENTION TIMES (min) FOR CHOLINE ANALOGUES

Conditions as in Table I

*Compound**	*Acetonitrile concentration*			
	0.6%	*2.1%*	*4.5%*	*Gradient*
Trimethylaminoethanol (choline)	13.1	7.9	5.1	13.4
Trimethylaminopropan-1-ol	15.9	9.1	5.5	15.4
Trimethylaminopropan-2-ol	21.2	10.9	6.0	19.4
Diethylmethylaminoethanol	>20.0	15.2	7.0	26.1
Triethylaminoethanol	⩾20.0	>20.0	9.5	29.5
(2-Chloroethyl)trimethylammonium (chlorocholine)	>20.0	16.6	7.8	26.1

* As the chloride or iodide salt.

pacity factors of a number of aminoethanol and choline derivatives is shown in Fig. 1. Addition of methanol or tetrahydrofuran similarly decreased retention times, but acetonitrile was found to give the best peak shape. An ion-pair reagent with a smaller hydrophobic side chain, methanesulphonic acid, was also used to decrease the retention times of the less polar compounds (Table VI).

Examples of isocratic separations of aminoethanol and choline derivatives are shown in Fig. 2. For choline eluted with 2 mol m^{-3} hexanesulphonic acid in 1.5% acetonitrile the efficiency of this system was *ca.* 5000 plates m^{-1}. Increasing the size of the hydroxy side-chain or of the substituents on the nitrogen atom increased retention times of both aminoethanol (Table I) and choline (Table II) analogues. Replacement of the hydroxy group with chlorine in chlorocholine also increased the retention time considerably (Table II).

The retention times of a number of choline esters are given in Table III. Increasing the size of the ester again increased the retention time for the organic esters. Phosphorylcholine eluted considerably later than sulphocholine. These two compounds have been implicated in phosphate and sulphate transport in plants[46,47] and

TABLE III

RETENTION TIMES (min) FOR CHOLINE ESTERS

Conditions as in Table I.

Compound	*Acetonitrile concentration*			
	4.5%	*10%*	*15%*	*Gradient*
Acetylcholine	7.5	4.1	3.1	27.0
Acetyl-B-methylcholine (methacholine)	11.2	4.8	3.2	30.5
Butyrylcholine	>20.0	9.4	4.2	35.0
Benzoylcholine	>20.0	>20.0	9.3	39.0
Phosphorylcholine	9.4	4.9	3.1	30.0
Choline-O-sulphate (sulphocholine)	8.0	4.2	3.1	25.0

TABLE IV

RETENTION TIMES (min) FOR QUATERNARY AMMONIUM ALDEHYDES

Conditions as in Table I.

Compound	*Acetonitrile concentration*	
	4.5%	*Gradient*
Trimethylaminoacetaldehyde (glycinebetaine aldehyde)	6.4	22.0
Trimethylaminoacetaldehyde dimethyl acetal	9.6	29.5
Trimethylaminoacetone	6.4	23.2
Trimethylamino-3-methyl-2-butanone	10.4	29.6

have been detected at high concentrations in the salt glands of *Avicennia*[48]. Table IV gives the retention times for a number of quaternary ammonium aldehydes including glycinebetaine aldehyde which is an intermediate in the biosynthesis of glycinebetaine from choline[1,39]. Data on the retention of a number of other compounds are shown in Table V. These data were obtained partly to provide information on possible interferences with the assays of choline and other compounds. The monovalent inorganic cations eluted before aminoethanol whereas the divalent inorganic cations were strongly retained, eluting between acetylcholine and phosphorylcholine. Amino acids and betaines gave very low responses in the conductivity detector. Since the aim of the present work was to provide a system for the analysis of intermediates in glycinebetaine biosynthesis, it was desirable to determine where glycinebetaine itself eluted. This was done by replacing the conductivity detector with a UV absorbance detector. Both glycinebetaine and trigonelline, the most common betaines in plants, eluted before aminoethanol and choline (Table V).

TABLE V

RETENTION TIMES (min) OF VARIOUS COMPOUNDS

Conditions as in Table I. ND = Not determined.

Compound	*Acetonitrile concentration*		
	0.6%	*4.5%*	*Gradient*
Sodium	6.2	3.5	6.2
Ammonium	7.3	4.4	7.3
Potassium	7.3	4.2	7.2
Calcium	ND	ND	29.2
Barium	ND	ND	29.0
Trimethylamine	7.5	5.0	11.7
Benzyltrimethylammonium	>20.0	>20.0	35.0
Methyl viologen	>20.0	16.5	32.3
Proline	ND	ND	–
Glycinebetaine*	ND	ND	3.6
Trigonelline*	ND	ND	7.4

* Detection by UV absorbance at 200 nm.

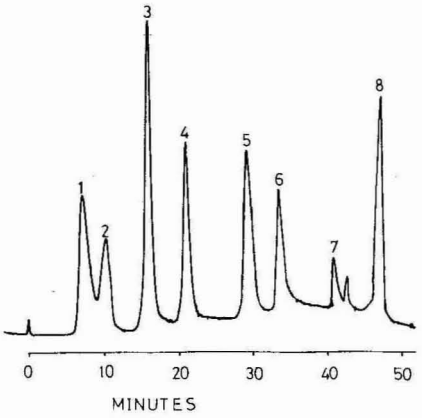

Fig. 3. Separation of choline and related compounds on Dionex MPIC-NS1 eluted with 2 mol m^{-3} hexanesulphonic acid and a gradient of acetonitrile concentration linear gradients between set points given in Table I. 1 = Ammonium; 2 = aminoethanol; 3 = choline; 4 = trimethylaminopropan-2-ol; 5 = acetylcholine; 6 = phosphorylcholine; 7 = butyrylcholine; 8 = benzoylcholine.

Because of the wide range of retention times displayed by the compounds used in this investigation the possibility of gradient elution was explored. Only a small rise in the background conductivity was observed when a gradient was run from 0.6 to 30% acetonitrile (Fig. 3). This gradient separated compounds ranging from ammonium to benzoyl choline in a single run. Retention data obtained with this gradient for most of the compounds investigated are shown in Tables I–V. Data obtained with 2 mol m^{-3} methanesulphonic acid and an acetonitrile gradient from 0 to 10% are given in Table VI. All compounds eluted much earlier with this ion-pair reagent, even when the concentration was increased to 5 mol m^{-3}.

The response of the conductivity detector for choline was linear between 0.5 and 20 nmol (regression coefficient, $r^2 = 0.9997$). Examples of choline separations in extracts of plant saps are shown in Fig. 4. The choline peak is well separated from the large peak of inorganic cations, and is the main peak eluting after 10 min. Trimethylaminopropan-2-ol, a possible internal standard for quantitative choline determinations, was completely separated from choline and did not coincide with any other peaks in the extract. Purification of choline by reineckate precipitation was

TABLE VI

RETENTION TIMES (min) FOR CHOLINE DERIVATIVES ELUTED WITH 2 mol m^{-3} METHANESULPHONIC ACID

Acetonitrile concentration gradient from 0 to 10% in 20 min.

Compound	*Retention time (min)*
Choline	2.6
Chlorocholine	2.8
Acetylcholine	3.1
Acetyl-β-methylcholine	4.5
Butyrylcholine	11.8

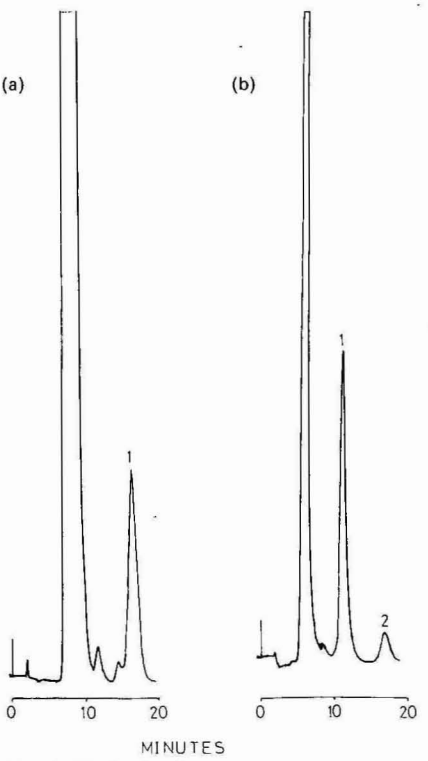

Fig. 4. Choline in plant saps treated with ammonium reineckate. (a) *Thinopyrum scirpeum*, 20-μl injection equivalent to 30 μl of sap. 30 μS full-scale deflection, 2 mol m^{-3} hexanesulphonic acid in 1% acetonitrile. (b) *Phaseolus aureus*, 20-μl injection equivalent to 10 μl of sap. 30 μS full-scale deflection, 2 mol m^{-3} hexanesulphonic acid in 1.2% acetonitrile. 1 = Choline; 2 = trimethylaminopropan-2-ol (internal standard).

found to be more convenient and more rapid than the ion-exchange procedures. The choline content was determined quantitatively in four samples of leaf sap from *Thinopyrum scirpeum* and four samples of sap from mung bean (*Phaseolus aureus*) cotyledons (Table VII). The variation within three replicate determinations was quite low and much less than the variation between the different samples. The results confirm the previous reports of high contents of choline in germinating mung beans[2].

The same purification technique was also used to determine simultaneously the contents of glycinebetaine and choline in control and salt-stressed plants of the hybrid wheat *Triticum aestivum* cv. Chinese Spring × *Thinopyrum bessarabicum*[49]. The isopropanol-treated expressed sap from the leaves was acidified with 50 μl of 1 mol[3] m^{-3} hydrochloric acid and treated with ammonium reineckate and trimethylamine hydrochloride as described above. Purified extract corresponding to 200 μl of sap was dissolved in 200 μl of water and 50-μl aliquots used for the determination of choline. Glycinebetaine contents were determined in 20-μl aliquots by cation-exchange HPLC as previously described[42]. Reineckate precipitation greatly reduced the interferences with the detection of glycinebetaine by this method compared with ion-exchange purification. The results of these analyses are presented in Table VIII

TABLE VII

QUANTITATIVE ESTIMATION OF CHOLINE IN SAPS OF *PHASEOLUS AUREUS* SEEDLINGS AND MATURE LEAVES OF *THINOPYRUM SCIRPEUM*

Values are means of three replicates ± standard errors.

Sample	*Choline (mmol m^{-3} sap)*	
	Phaseolus aureus	*Thinopyrum scirpeum*
1	1387 ± 8	563 ± 5
2	1907 ± 16	554 ± 15
3	1630 ± 15	547 ± 8
4	1600 ± 18	663 ± 5
Overall mean	1631 ± 107	582 ± 27

TABLE VIII

CHOLINE AND GLYCINEBETAINE IN SAP OF CONTROL AND SALT STRESSED HYBRID WHEAT (*TRITICUM AESTIVUM* cv. CHINESE SPRING × *THINOPYRUM BESSARABICUM*)

Values are means of four replicates ± standard errors.

Growth conditions	*Choline (mol m^{-3})*	*Glycinebetaine (mol m^{-3})*
Control (no salt)	0.727 ± 0.050	2.89 ± 0.22
200 mol m^{-3} sodium chloride + 10 mol m^{-3} calcium chloride	1.140 ± 0.080	9.75 ± 0.61
t-Test probability	0.007	0.000

and show the expected increase in glycinebetaine in salt-stressed plants. They also show a slight increase in the choline content of the plants grown at 200 mol m^{-3} sodium chloride + 10 mol m^{-3} calcium chloride.

The method described above should be useful not only for the analysis of choline itself but also for monitoring the concentrations of choline esters in pharmaceutical preparations[44,50]. While it is not sensitive or efficient enough for the determination of trace amounts of acetylcholine, it may be useful for preliminary purification prior to analysis by GLC. It also has potential uses in the separation of ^{14}C-labelled metabolites of aminoethanol, and in the analysis of the products of phospholipase *c* action on phospholipids. Divalent metal ions may, however, interfere with the determination of some choline esters, but can be removed by precipitating the quaternary ammonium compounds with ammonium reineckate. The main advantage of the method described above is that it can be used for the analysis of aqueous solutions without the need for derivatization.

ACKNOWLEDGEMENTS

The author wishes to acknowledge the financial support of the Overseas Development Administration of the United Kingdom, and the technical advice of M. Masters (Dionex U.K.).

REFERENCES

1 A. D. Hanson and W. D. Hitz, *Ann. Rev. Plant Physiol.*, 33 (1982) 163.
2 G. A. Miura and T.-M. Shih, *Physiol. Plant.*, 61 (1984) 417.
3 R. A. Fluck and M. J. Jaffe, *Phytochemistry*, 13 (1974) 2475.
4 E. Hartmann and H. Kilbinger, *Biochem. J.*, 137 (1974) 249.
5 E. Hartmann and H. Kilbinger, *Experientia*, 30 (1974) 1387.
6 A. H. El-Damaty, A. H. Kuhn and H. Linser, *Agrochimica*, 8 (1964) 129.
7 C. P. Marth and J. R. Frank, *J. Agric. Food Chem.*, 9 (1961) 359.
8 D. Speed and M. Richardson, *J. Chromatogr.*, 35 (1968) 497.
9 J. S. Wall, D. D. Christianson, R. J. Dimler and F. R. Senti, *Anal. Chem.*, 32 (1960) 870.
10 R. Storey and R. G. Wyn Jones, *Phytochemistry*, 16 (1977) 447.
11 C. M. Grieve and S. R. Grattan, *Plant Soil*, 70 (1983) 303.
12 C. Radeka, K. Genest and D. W. Hughes, *Arzneim.-Forsch.*, 21 (1971) 548.
13 J. Gorham, S. J. Coughlan, R. Storey and R. G. Wyn Jones, *J. Chromatogr.*, 210 (1981) 550.
14 M. Acara, B. Rennick, S. Lagraff and E. T. Schroeder, *Nephron*, 35 (1983) 241.
15 G. Von Puchwein and E. Mayr, *Landwirtsch. Forsch.*, 37 (1984) 53.
16 M. Gilberstadt and J. A. Russell, *Anal. Biochem.*, 138 (1984) 78.
17 M. K. Hise and C. M. Mansbach, *Anal. Biochem.*, 135 (1984) 78.
18 D. J. Jenden, I. Hanin and S. I. Lamb, *Anal. Chem.*, 40 (1968) 125.
19 N. R. Zahniser, D. Chou and I. Hanin, *J. Pharmacol. Exp. Ther.*, 200 (1977) 545.
20 D. J. Jenden, M. Roch and F. Fainman, *Life Sci.*, 23 (1978) 291.
21 I. Hanin and J. Scherberth, *J. Neurochem.*, 23 (1974) 819.
22 H. Kilbinger, *J. Neurochem.*, 21 (1973) 421.
23 J. W. Kosh, M. B. Smith, J. W. Sowell and J. J. Freeman, *J. Chromatogr.*, 163 (1979) 206.
24 H. E. Ward, J. J. Freeman, J. W. Sowell and J. W. Kosh, *J. Pharm. Sci.*, 70 (1981) 433.
25 H. E. Ward, J. W. Kosh and J. J. Freeman, *Neuropharmacology*, 20 (1981) 703.
26 C. G. Hammar, I. Hanin, B. Holmstedt, R. J. Kitz, D. J. Jenden and B. Karlen, *Nature (London)*, 220 (1968) 915.
27 I. Hanin and D. J. Jenden, *Biochem. Pharmacol.*, 18 (1969) 837.
28 P. I. A. Szilagyi, D. E. Schmidt and J. P. Green, *Anal. Chem.*, 40 (1968) 2009.
29 W. B. Stavinoha and S. T. Weintraub, *Anal. Chem.*, 46 (1974) 757.
30 F. Mikes, G. Boshart, K. Wuthrich and P. G. Glaser, *Anal. Chem.*, 52 (1980) 1001.
31 Y. Maruyama, M. Kusaka, J. Mori, A. Horikawa and Y. Hasegawa, *J. Chromatogr.*, 164 (1979) 121.
32 Y. Hasegawa, M. Kunihara and Y. Maruyama, *J. Chromatogr.*, 239 (1982) 335.
33 W. B. Stavinoha, L. C. Ryan and E. L. Treat, *Life Sci.*, 3 (1964) 689.
34 P. M. Findeis and S. O. Farwell, *J. High Res. Chromatogr. Chromatogr. Commun.*, 7 (1984) 19.
35 P. E. Potter, J. L. Meek and N. H. Neff, *J. Neurochem.*, 41 (1983) 188.
36 Y. Ikarashi, T. Sasahara and Y. Maruyama, *Nippon Yakurigaku Zasshi*, 84 (1984) 529.
37 D. N. Buchanan, F. R. Fucek and E. F. Domino, *J. Chromatogr.*, 181 (1980) 329.
38 J. Gorham and E. McDonnell, *J. Chromatogr.*, 350 (1985) 245.
39 S. J. Coughlan and R. G. Wyn Jones, *Planta*, 154 (1982) 6.
40 J. Gorham, in preparation.
41 E. Schmidt, *Justus Liebigs Ann. Chem.*, 337 (1904) 37.
42 J. Gorham, *J. Chromatogr.*, 287 (1984) 345.
43 J. Gorham, E. Budrewicz, E. McDonnell and R. G. Wyn Jones, *J. Exp. Bot.*, (1986) in press.
44 T. F. Woodman, B. Johnson and R. K. Marwaha, *J. Liq. Chromatogr.*, 5 (1982) 1341.
45 J. Gorham, *J. Chromatogr.*, 361 (1986) 301.
46 P. Nissen and A. A. Benson, *Science (Washington, D.C.)*, 134 (1961) 1759.
47 J. V. Maizel, A. A. Benson and N. E. Tolbert, *Plant Physiol.*, 31 (1956) 407.
48 A. A. Benson and M. R. Atkinson, *Fed. Proc., Fed. Am. Soc. Exp. Biol.*, 26 (1967) 394.
49 J. Gorham, B. P. Forster, E. Budrewicz, R. G. Wyn Jones, T. E. Miller and C. N. Law, *J. Exp. Bot.*, submitted for publication.
50 J. Rosenfeld, E. F. Juniper and F. E. Hargreave, *J. Chromatogr.*, 287 (1984) 433.

Journal of Chromatography, 362 (1986) 255–262
Elsevier Science Publishers B.V., Amsterdam — Printed in The Netherlands

CHROM. 18 659

SEPARATION AND QUANTITATION OF FERULIC ACID AND TYROSINE IN WHEAT SEEDS (*TRITICUM AESTIVUM*) BY REVERSED-PHASE HIGH-PERFORMANCE LIQUID CHROMATOGRAPHY

T. KUNINORI* and J. NISHIYAMA
Department of Natural Science, Osaka Women's University, 2-1 Daisen-cho, Sakai, Osaka 590 (Japan)
(First received February 10th, 1986; revised manuscript received March 18th, 1986)

SUMMARY

Separation and quantitation of free and bound ferulic acid and tyrosine in wheat seeds were undertaken by reversed-phase high-performance liquid chromatography. The first separation on the C_{18} column was followed by one or two successive separations of the collected peaks on the same column with different compositions of the mobile phase. The separated compounds were identified from their fluorescence spectra and thin-layer chromatographic profiles and estimated from their peak heights on the chromatograms obtained from the final step of separation. This paper describes a simpler, cheaper and more rapid method with no requirement for preliminary preparation of derivatives.

INTRODUCTION

The phenylpropane series of phenolic acids is widely distributed in plants in both free and bound form. Some are the basic structural units of lignin[1] and some inhibit fungal growth around roots[2]. Ferulic acid has been found to be a constituent of the cell walls of many plants[3–6]. The amino acid tyrosine is the most ubiquitous phenylpropane naturally occurring and it is a precursor of nitrogen-free phenylpropanes through the reaction of tyrosine ammonia lyase that is characteristic of *Gramineae*[7].

Geissman and Neukom[8] postulated that an oxidative mechanism in wheat flour pentosan, involving the radical coupling of ferulic acid, causes gelation of the soluble pentosans. They detected diferulic acid in wheat flour[9]. Neukom suggested that tyrosine residues are also responsible for phenolic coupling in the same way[10].

In the present work both phenylpropanes, tyrosine with high polarity and ferulic acid with lower polarity, were separated and quantitated effectively by successive chromatography on the same column without any pretreatment.

0021-9673/86/$03.50

EXPERIMENTAL

Materials

Bran, germ, and endosperm of *Triticum aestivum,* Canadian northern white wheat, Manitoba II, were milled by Nisshin Flour Milling. These samples were defatted by extraction with petroleum ether and air-dried. The defatted bran was ground using a ball mill before the next extraction. The samples were then extracted by refluxing with 70% aqueous methanol for 1 h. The combined filtrate was concentrated under reduced pressure and lyophilized. The lyophilized material is called the extract. All manipulation of the extracts and authentic compounds was done in the dark to prevent light-induced isomerization of ferulic acid[7]. The yields were 0.11, 0.25, and 0.013 g for 1 g of bran, germ, and endosperm, respectively.

In acid hydrolysis, the extract (20–200 mg) was heated with 3 ml of 2 *N* hydrochloric acid in an evacuated sealed tube at 100 ± 1°C for 2 h. The hydrolysate was evaporated to dryness under vacuum. In alkaline hydrolysis, the extract (200 mg) was heated with 500 μl of 1 *N* sodium hydroxide in an evacuated sealed tube at 60°C for 90 min.

Reversed-phase high-performance liquid chromatography (HPLC)

The chromatographic system (Japan Spectroscopic) included a Twincle pump, a variable-loop injector, and a UVIDEC-100 III UV Spectrophotometer. An analytical column (250 × 4.6 mm I.D.) packed with Fine Sil C_{18}-10 was used, with a mobile phase of methanol–0.033 *M* potassium dihydrogen phosphate–acetic acid (pH 3.5) and a flow-rate of 1 ml/min. The column effluent was monitored by the absorbance at 280 nm. To desalt the effluent, a preparative column (250 × 10 mm I.D.) packed with Fine Sil C_{18}-20 was used, with a mobile phase of methanol–water–acetic acid (pH 3.5) and a flow-rate of 4 ml/min. The extract and the dried acid hydrolysate were each dissolved in 40% methanol. The alkaline hydrolysate was acidified to pH 3.5 with 6 *N* hydrochloric acid.

A first separation was done on the analytical column using methanol–0.033 *M* potassium dihydrogen phosphate (pH 3.5) (40:60). After evaporation of the peak fraction corresponding to tyrosine or ferulic acid, a second separation was done. The concentration of methanol in the mobile phase was 10% and 30% for tyrosine and ferulic acid, respectively. A third separation was done for the tyrosine peak fraction collected from the second one using 0.033 *M* potassium dihydrogen phosphate (pH 3.5).

Fluorescence spectrometry

Each fraction containing tyrosine or ferulic acid was collected from the final step of chromatography and desalted by HPLC. The fluorescence was measured using a recorder attached to a Shimadzu Spectrofluorometer RF 510. For the ferulic acid fraction, the fluorescence intensity was stabilized by exposure to light of 330 nm for 30–60 min prior to each run.

Thin-layer chromatography (TLC)

The peak fraction of each extract thought to contain *ca.* 0.1 μg of tyrosine or ferulic acid was obtained from the final step of chromatography and desalted. It was

concentrated to a small volume and derivatized with dansyl chloride (Pierce, Rockford, IL, U.S.A.)[11]. The derivatives were placed on one corner of a polyamide-layered sheet (5 × 5 cm, Chen-Chin Trading, Taiwan). Two-dimensional chromatography[12] was done using water–90% formic acid (200:3) as solvent I, benzene–acetic acid (9:1) as solvent II, and ethyl acetate–methanol–acetic acid (20:1:1) as solvent III. The first development was done with solvent I; the second, at 90° to the first, with solvent II; and the third, in the same direction as the second, with solvent III. Fluorescent spots were located by exposing the test sheets under UV light at 365 nm using a fluorescence inspection lamp.

Exposure of ferulic acid peak fraction to UV light

The ferulic acid peak fraction prepared for fluorescence spectrometry was concentrated and exposed to 330-nm light in a quartz tube using the same spectrofluorometer with occasional stirring for different periods of time.

Estimation of tyrosine and ferulic acid

Tyrosine and ferulic acid were assayed from the peak heights of the corresponding fractions from the final step of chromatography. The minimum detectable amount was 0.2 μg for one injection (30 μl). Tyrosine was also assayed by fluorescence at 310 nm with excitation light of 280 nm, because there was linearity between the fluorescence intensity and the concentration of tyrosine in the range 0–5 μg/ml.

RESULTS AND DISCUSSION

HPLC of non-hydrolysed extracts of wheat seed fractions

The non-hydrolysed extract of endosperm was separated with methanol–0.033 *M* potassium dihydrogen phosphate (pH 3.5) (40:60) as shown in Fig. 1. Authentic substances appeared at the positions indicated with arrows: tyrosine slightly behind the solvent front and ferulic acid at 10 min. The fractions thought to contain tyrosine and ferulic acid are shaded and dotted in the figure, respectively. They were collected separately for the next step of chromatography. The second separation of the tyrosine fraction was followed by the third one. Fig. 2 is the chromatogram obtained from the third step using 0.033 *M* potassium dihydrogen phosphate (pH 3.5). The peak at 8.5 min was well resolved, and completely overlapped the peak of authentic tyrosine. The ferulic acid fraction shown as the dotted area in Fig. 1, when submitted to the second chromatographic step using methanol–potassium dihydrogen phosphate (pH 3.5) (30:70), gave a peak at 26 min (Fig. 3). This peak was clearly resolved and completely overlapped that of authentic ferulic acid.

When the same procedures were carriet out for the tyrosine and ferulic acid fractions of non-hydrolysed extracts of germ and bran, all these fractions were separated with good resolution in the final steps of chromatography.

Chromatography of hydrolysed extracts

Both acid[13] and alkali[14] have been used to liberate phenolic acids from sugar esters. Treatment with hydrochloric acid was found to decompose ferulic acid into a substance with a shorter retention time on HPLC, whereas treatment with sodium hydroxide led to a good recovery of ferulic acid. Tyrosine was recovered completely with no degradation after acid treatment.

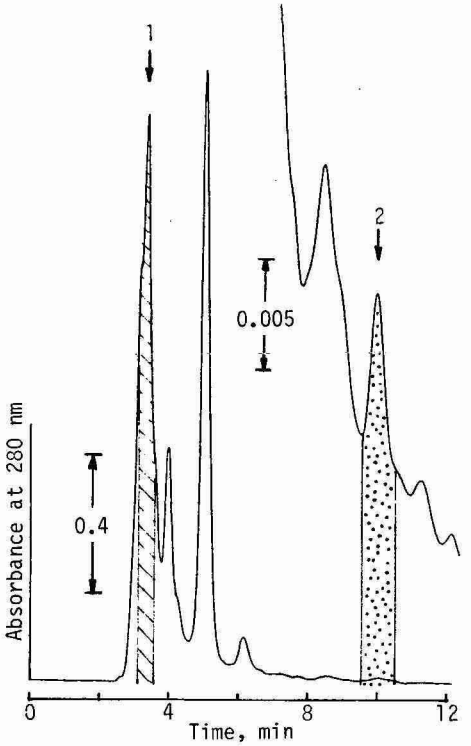

Fig. 1. HPLC profile of non-hydrolysed extract of endosperm (8 mg). Chromatographic conditions are given in the text. Authentic tyrosine (1) and ferulic acid (2) were eluted at the positions indicated with arrows.

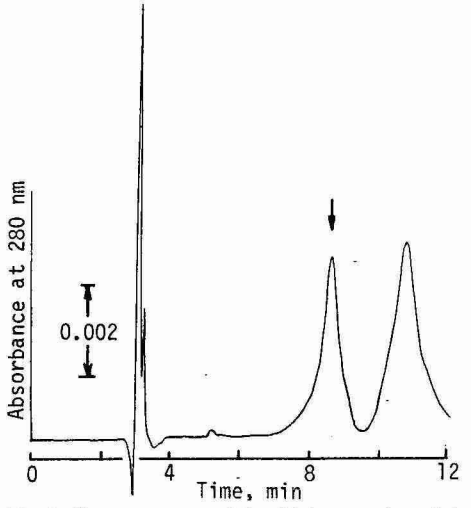

Fig. 2. Chromatogram of the third separation of the tyrosine peak collected by the successive chromatography of the first and the second step of non-hydrolysed endosperm extract (1.1 mg). Chromatographic conditions are given in the text. Authentic tyrosine was eluted at the position indicated with an arrow.

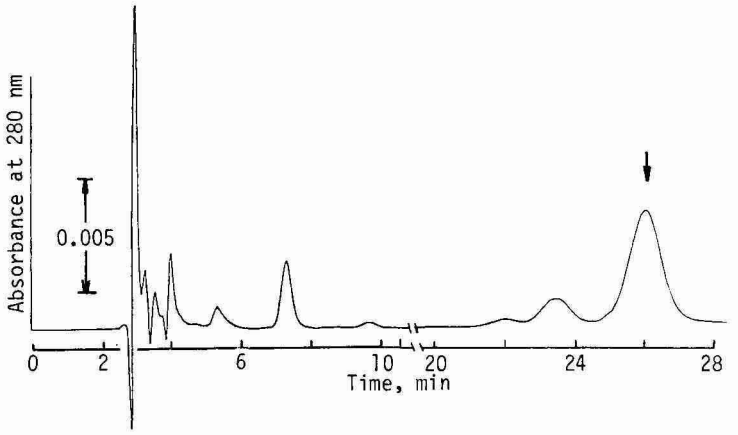

Fig. 3. Chromatogram of the second separation of the ferulic acid peak collected by the chromatography of the first step of non-hydrolysed endosperm extract (11.4 mg). Chromatographic conditions are given in the text. Authentic ferulic acid was eluted at the position indicated with an arrow.

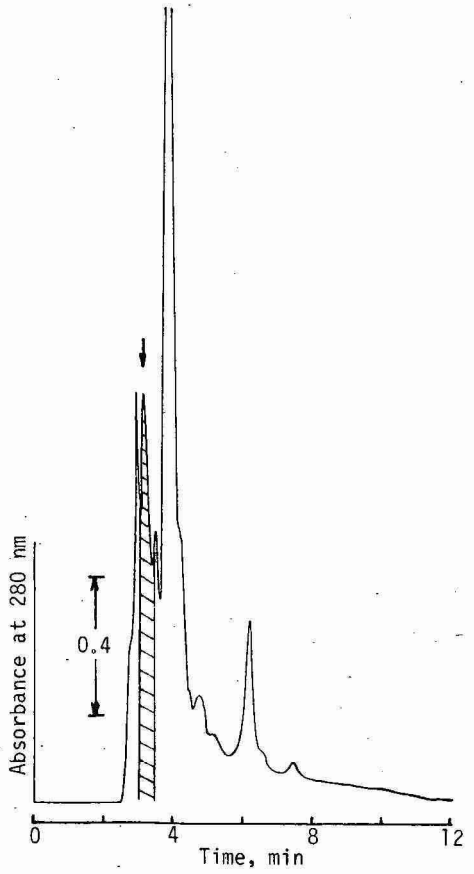

Fig. 4. HPLC profile of the acid hydrolysate of endosperm extract (4 mg). Chromatographic conditions are given in the text. Authentic tyrosine was eluted at the position indicated with an arrow.

Fig. 4 is the chromatographic profile of the acid hydolysate of the endosperm extract using the mobile phase methanol–potassium dihydrogen phosphate (pH 3.5) (40:60). The tyrosine peak fraction shown as the shaded area in the figure was successively separated by the second and third steps of chromatography. The peak at 8.5 min on the chromatogram of the third step was well resolved and completely overlapped that of authentic tyrosine.

Fig. 5 shows the chromatographic profile of the alkaline hydrolysate of the endosperm extract using the 40% methanol system. The ferulic acid fraction shown as the dotted area in the figure was collected and separated by the second step of chromatography. A well-resolved peak appeared at 26 min and overlapped the peak of authentic ferulic acid.

The tyrosine fraction from the acid hydrolysate and the ferulic acid fraction from the alkaline hydrolysate of bran or germ were separated with good resolution in the same way.

Identification of tyrosine and ferulic acid peaks separated by HPLC

Fluorescence characteristics for the peak fractions obtained from the final step of chromatography were identical with those of the authentic compounds: 280-nm excitation and 310-nm emission maxima for the tyrosine fraction, and 330-nm excitation and 440-nm emission maxima for the ferulic acid fraction.

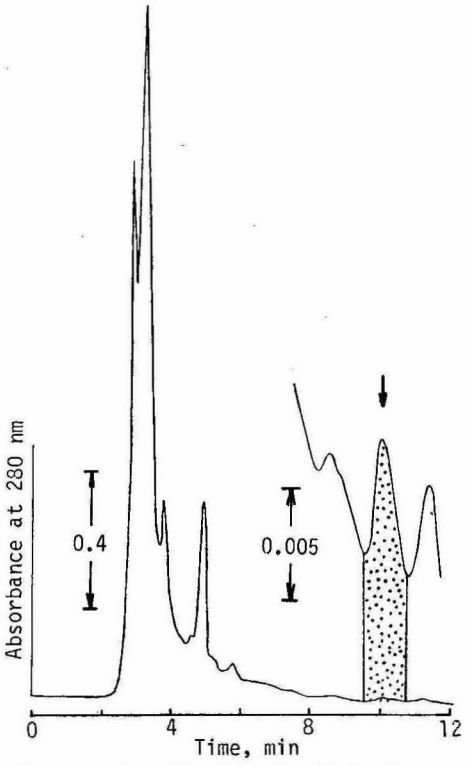

Fig. 5. HPLC profile of the the alkaline hydrolysate of endosperm extract (4 mg). Chromatographic conditions are given in the text. Authentic ferulic acid was eluted at the position indicated with an arrow.

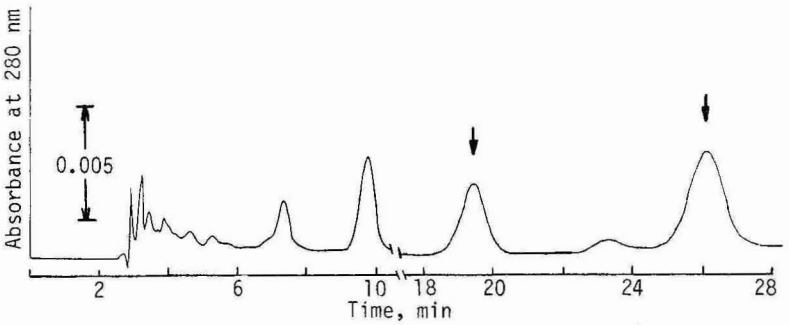

Fig. 6. HPLC profile of the ferulic acid peak of bran extract with irradiation. The peak fraction collected from the three steps of chromatography of bran extract (1.3 mg) was exposed to light of wavelength 330 nm for 30 min as described in the text. Chromatographic conditions are given in the text.

Fractions from the final separation step, when incubated with dansyl chloride and developed on the polyamide layer, gave bright yellow spots at R_F 0 and 0.74 for all tyrosine fractions coinciding with that of the dansyl derivative of authentic tyrosine. Dansyl ferulic acid was detected as orange spots at R_F 0 and 0.89 for all ferulic acid fractions and the authentic compound.

The *trans* isomer of ferulic acid is partially converted into the *cis* isomer by UV light[7,15], and this reaction was used to identify the ferulic acid peak substance. The ferulic acid peak collected from the three steps of chromatography, when submitted to HPLC with methanol–potassium dihydrogen phosphate (pH 3.5) (30:70) after 30-min irradiation with UV light, separated into two peaks. Retention times (min) were 19.5 and 26 (Fig. 6). After prolonged irradiation, the ratio of the peak height with a short retention time to that with the longer time approached the final ratio for the irradiated authentic ferulic acid (1.8).

Estimation of tyrosine and ferulic acid in endosperm, germ, and bran

The fluorescence characteristics, R_F values, and isomerization behaviour under UV irradiation all indicated that the peak fractions separated here by HPLC were tyrosine and ferulic acid. Thus, the amounts of free and methanol-soluble bound ferulic acid and tyrosine were estimated from the peak heights on the chromatograms of the final step (Table I). The amount of the bound form was estimated by sub-

TABLE I

TYROSINE AND FERULIC ACID DETERMINED FROM THE PEAK HEIGHTS SEPARATED BY SUCCESSIVE SEPARATION ON C_{18} COLUMN OF THE WHEAT SEEDS

Data are averages of four determinations ± S.D.

	Tyrosine (μg/g)		*Ferulic acid (μg/g)*	
	Free	*Bound*	*Free*	*Bound*
Bran	40.0 ± 2.6	Nil	14.2 ± 0.5	29.4 ± 1.3
Germ	37.5 ± 1.9	41.6 ± 1.83	2.80 ± 0.03	31.3 ± 1.6
Endosperm	4.06 ± 0.25	3.33 ± 0.24	0.114 ± 0.003	0.217 ± 0.008

tracting the amount of free form from that of the free plus bound form evaluated using the hydrolysed sample.

The amount of either form of ferulic acid was negligible in endosperm. The free form was present in considerable amounts in germ and bran, and the bound form was present in bran. Bran contains much cell-wall material, accounting for the higher levels of ferulic acid in this fraction. However, the levels found here were much smaller than that of the insoluble form in grain cell walls as reported in the literature: 4.8 mg/g of cell wall for wheat bran[16], 5.3 mg/g for shoots of Italian rye grass[4], and 9.1 mg/g for rice endosperm[5]. This low level of soluble ferulic acid probably arises from the formation of complexes in ripe seeds that are insoluble in the aqueous methanol used for extraction.

The amount of free tyrosine found in endosperm is comparable with that found in wheat flour by El-Dash and Johnson[17]. In germ and bran there was ten-fold more free tyrosine than in endosperm. There were similar amounts of soluble bound and free tyrosine in germ. The levels of tyrosine found in bran and germ are comparable with that of ferulic acid in bran. This may point indirectly to the function of tyrosine in the cell wall, where it may cross-link through the oxidative coupling of hydroxyl groups[10].

REFERENCES

1 A. C. Neish, in J. Bonner and J. E. Varner (Editors), *Plant Biochemistry*, Academic Press, London, New York, 1965, p. 581.
2 E. M. C. Turner, *J. Exp. Bot.*, 11 (1960) 403.
3 R. G. Fulcher, T. P. O'Brien and J. W. Lee, *Aust. J. Biol. Sci.*, 25 (1972) 23.
4 R. D. Hartley, *J. Sci. Food Agric.*, 23 (1972) 1347.
5 N. Shibuya, *Phytochemistry*, 23 (1984) 2233.
6 A. B. Durkee and P. A. Thivierge, *J. Food Sci.*, 42 (1977) 551.
7 A. C. Neish, *Phytochemistry*, 1 (1961) 1.
8 T. Geissman and H. Neukom, *Helv. Chim. Acta*, 54 (1971) 1108.
9 H. U. Markwalder and H. Neukom, *Phytochemistry*, 15 (1976) 836.
10 H. Neukom, in M. G. Simic and M. Karel (Editors), *Antioxidation in Food and Biological Systems*, Plenum Press, New York, London, 1980, p. 249.
11 W. R. Gray and B. S. Hartley, *Biochem. J.*, 89 (1963) 379.
12 K. R. Woods and K. T. Wang, *Biochim. Biophys. Acta*, 133 (1967) 369.
13 M. N. Reddy, G. Ramagopal and A. S. Rao, *Plant and Soil*, 46 (1977) 655.
14 H. Fausch, W. Kuendig and H. Neukom, *Nature*, 199 (1963) 287.
15 R. D. Hartley and E. C. Jones, *J. Chromatogr.*, 107 (1975) 213.
16 S. G. Ring and R. R. Selvendran, *Phytochemistry*, 19 (1980) 1723.
17 A. A. El-Dash and J. A. Johnson, *Cereal Chem.*, 47 (1970) 247.

Journal of Chromatography, 362 (1986) 263–273
Elsevier Science Publishers B.V., Amsterdam — Printed in The Netherlands

CHROM. 18 648

DETERMINATION OF Ro 14-1761, A NEW THIRD-GENERATION CEPHALOSPORIN, IN THE PLASMA AND MILK OF CATTLE BY COLUMN SWITCHING HIGH-PERFORMANCE LIQUID CHROMATOGRAPHY

JEAN-CLAUDE JORDAN and BERNARD M. LUDWIG*
Biopharmaceutical Research Department, F. Hoffmann-La Roche & Co. Ltd., 4002 Basle (Switzerland)
(Received March 12th, 1986)

SUMMARY

A sensitive and specific high-performance liquid chromatographic procedure was developed for the determination of the third-generation cephalosporin Ro 14-1761 in cow plasma and milk. The molecular structure of the new antimicrobial was very close to that of ceftriaxone, but the high-performance liquid chromatographic methods available for the latter could not be used as Ro 14-1761 adsorbed and/or degraded during the chromatographic process. Furthermore, the high-performance liquid chromatographic technique derived for ceftriaxone was not sensitive enough for our purposes. In the new assay, the plasma (milk) protein was precipitated with acetonitrile after dilution of the sample with water. For low concentrations ($\leqslant 10$ μg/ml), the supernatant obtained after centrifugation was concentrated by extracting acetonitrile with methylene chloride. Quantification was performed by column switching high-performance liquid chromatography with UV detection (274 nm) using ion-pair reversed-phase chromatography. Ethylenediaminotetraacetic sodium salt had to be added to the mobile phase (1.2 m*M*) to prevent adsorption and/or degradation of the cephalosporin on the analytical column. The selectivity of the chromatographic separation was enhanced by heating the column to *ca.* 50°C.

The drug recovery was better than 85%. The limit for quantitative determination in both milk and plasma was 0.1 μg of Ro 14-1761 per millilitre with an accuracy of 1% (coefficient of variation 10%). The overall accuracy and precision were 1–10% in the 0.1–100 μg/ml concentration range.

INTRODUCTION

Ro 14-1761, whose systematic name is (6*R*,7*R*)-7-[(*Z*)-2-(2-amino-4-thiazolyl)-acetamido]-3-{[(2,5-dihydro-6-hydroxy-2-methyl-5-oxo-*as*-triazin-3-yl)thio]-methyl}-8-oxo-5-thia-1-azabicyclo[4.2.0]oct-2-ene -2-carboxylic acid, is a member of the "third-generation" cephalosporin antimicrobials. It is characterized by a relatively broad antibacterial spectrum, including good activity against streptococci, staphylococci and escherichiae strains, together with high resistance to beta-lactamase-producing organisms. These characteristics offer potential clinical advantages,

0021-9673/86/$03.50

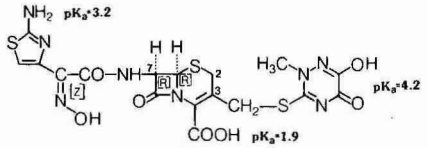

Ro 14-1761 **Ceftriaxone**

Fig. 1. Molecular structures of Ro 14-1761 and ceftriaxone.

which may lead to the use of this drug in treating mastitis infections in cattle. The molecular structure of Ro 14-1761 is very close to that of ceftriaxone: the oxime in the side-chain at the C-7 position of the beta-lactam moiety bears a methyl group in ceftriaxone, whereas it is free in Ro 14-1761 (Fig. 1). Currently published methods for the determination of ceftriaxone and other cephalosporins in biological fluids include bioassay[1–4] and high-performance liquid chromatography (HPLC)[1,5,6]. The bioassay tends to be cumbersome and is susceptible to interference from drug metabolites and currently administered antimicrobial drugs. HPLC appears to be more specific. Two of the HPLC methods utilized the technique of ion-pair reversed-phase chromatography[1,5], whereas the third used a normal phase column[6]. Unfortunately, these methods appeared to be inadequate to quantify Ro 14-1761 in cow plasma and milk. When using reversed-phase methods, strongly distorted peaks or split peaks were observed; likewise, Ro 14-1761 could not be eluted using a normal phase system such as the one described by Ascalone and Dal Bò[6].

In this report we describe a reversed-phase HPLC method using ion-pair chromatography with column switching for the quantification of Ro 14-1761 in cow plasma and milk.

EXPERIMENTAL

Reagents, solvents and materials

Ro 14-1761 was kindly supplied by Dr. F. Furlenmeier (Hoffman-La Roche) as its disodium (Ro 14-1761/001) or N,N′-dibenzylethylenediamine (Ro 14-1761/003) salts. Acetonitrile was HPLC grade from Rathburn (U.K.); methylene chloride, ethanol, and ethylenediaminetetraacetic disodium salts (Titriplex® III) were all p.a. grade from E. Merck (Darmstadt, F.R.G.). *Trans*-1,2-Diamino-cyclohexane-N,N,N′,N′-tetraacetic acid and tetraoctylammonium bromide were p.a. grade from Fluka (Buchs, Switzerland). The buffer solution was the ready-to-use titrisol from Merck. Water was distilled twice in an all-glass apparatus.

Standard solutions; plasma and milk solutions

Typically, a stock solution of 4.831 mg of Ro 14-1761/001 or /003 in 10 ml of water buffered to pH 8 was prepared. This solution was then used to prepare plasma or milk standards by adding known volumes to blank milk or blank plasma obtained from oxalated cow blood. Control plasma and milk solutions were prepared by successive dilutions of a 96.62 μg/ml standard solution of the drug in plasma (milk). Both the stock solution and the control plasma/milk were kept at +4°C and prepared again after one week. All the calculations were carried out using the free acid Ro

14-1761 concentration after a correction factor was applied to the weighed sodium or N,N′-dibenzylethylenediamine salt.

Sample preparation procedure

Doubly distilled water (2 ml and 6 ml for plasma and milk, respectively) was added to 1 ml of plasma (or 3 ml of milk), followed by 6 ml of acetonitrile (or 18 ml for milk). After vortex mixing, the plasma (milk)–acetonitrile mixture was shaken for 5 min using a rotating shaker (Heidolph, F.R.G.) and then centrifuged for 5 min at 3000 rpm (1800 *g*, 10°C). The supernatant (20 μl) was injected for HPLC analysis.

When the plasma or milk concentration of Ro 14-1761 was lower than 10 μg/ml, the procedure was the same as above and was followed by a concentration step: after centrifugation, 6 ml of the supernatant were transferred to a clean tube and 6 ml of methylene chloride were added. The mixture was shaken for 5 min using a rotating shaker. After centrifugation (5 min, 1200 *g*), the aqueous phase was separated, and the remaining trace of solvent was removed under vacuum (200 Torr, 5 min, 30°C). Then 20–40 μl was injected onto the HPLC column.

Chromatographic procedure

Apparatus design and operating conditions. The HPLC apparatus consisted of a Kontron LC 414 pump (Kontron, Zurich, Switzerland), an autoinjector (Kontron, Model ASI 45), a 125 × 4 mm I.D. stainless-steel column filled with MOS Hypersil C_8 5 μm (Shandon, Frankfurt (M), F.R.G.), and a Spectroflow 773 LC-UV detector (Kratos, Riehen, Switzerland) connected to a Spectra Physics SP 4100 computing integrator (Spectra Physics, Basle, Switzerland). The columns were packed according to the method of Halàsz *et al.*[7,8]. When in operation, the column was heated by means of a column block heater (Ercatech, Berne, Switzerland). The mobile phase was a mixture of 300 ml of acetonitrile containing 1 g of tetraoctylammonium bromide ("TOAB", Merck), 10 ml of ethanol, 12 ml of buffer solution of ethylenediaminetetraacetic disodium salt (EDTA 0.1 *M*, pH 8), made up to 1 l with doubly distilled water.

Because concentrated biological samples were injected, the analytical column was protected from highly retained endogenous products by means of a 4 × 4 mm I.D. Hibar LiChrocart (LiChrosorb RP-18) pre-column[9] filled with RP-18 LiChrosorb (Merck). A short time after the injection (less than 1 min), the retained plasma products were washed from the pre-column by backflushing. The additional apparatus for column switching consisted of a second pump (414T, Kontron), and an electronic interface (designed and prepared in the PF/BP electronic workshop, Hoffmann-La Roche, Basle, Switzerland) for actuating the automatic switching valve (Rheodyne, Coteti, CA, U.S.A. Model 7000 HPLC switching valve; Model 7001 pneumatic actuator, Model 7163 solenoid valve) which directed the flow from the pre-column either to the analytical column or to waste. The interface was controlled by the integrator. Fig. 2 is a schematic of the complete HPLC system.

The operating conditions were as follows: flow-rate, 1.5 ml/min; column temperature, 50°C; detection wavelength, 274 nm; volume injected (fixed loop), 20 μl for concentrations higher than 10 μg of Ro 14-1761 per millilitre, and 40 μl for lower concentrations. Under these conditions, the retention time of Ro 14-1761 was *ca.* 8 min.

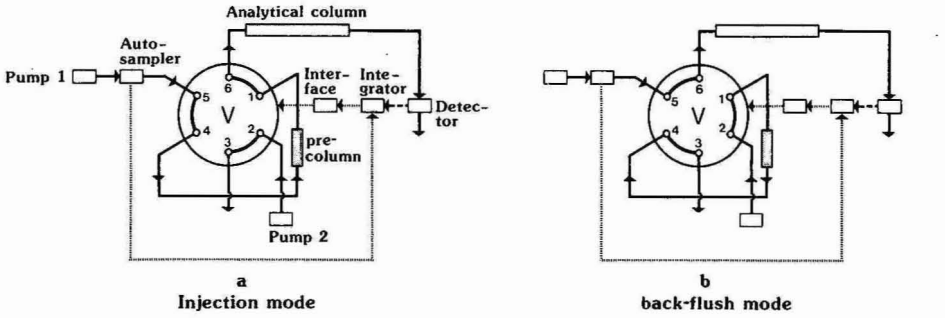

Fig. 2. Design of the column switching HPLC apparatus in (a) injection mode and (b) back-flush mode. The solid lines show the solvent flow, the dashed line shows the analogue signal from the detector, and the dotted line the electronic control of switching valve.

Chromatographic process description (Fig. 2a and b). The supernatant obtained after plasma (milk) protein precipitation, or the aqueous phase remaining after the extraction of the supernatant with methylene chloride, was injected by the autosampler onto the pre-column (Fig. 2a). Immediately after the elution of Ro 14-1761 from the pre-column (0.80 min), the HPLC valve (V) was switched to the second position (Fig. 2b) by means of the computing integrator, and the cephalosporin was then chromatographed in the usual manner on the analytical column, while longer-retained endogenous products were removed from the system by back-flushing the pre-column. When chromatography was complete, the valve (V) was switched back to the initial position (Fig. 2a). After a 2-min equilibration time, the system was ready for the next run. A complete cycle lasted *ca.* 13 min.

Calibration and calculation

The calibration samples, each consisting of nine plasma standards containing the appropriate concentration of Ro 14-1761, were processed as described above. The calibration curves were obtained by least-squares regression of the peak height of Ro 14-1761 against the respective concentrations. These curves were then used to interpolate the concentrations of the cephalosporin from the respective peak height of quality control or unknown samples. All data processing and calculations were carried out by the Spectra Physics computing integrator and the minifile 4100D.

RESULTS AND DISCUSSION

Chromatographic system

Initial evaluation indicated that simple reversed-phase HPLC techniques employed for other cephalosporins did not provide acceptable chromatographic peak shape or retention of Ro 14-1761. The single ion-pairing HPLC procedures reported for ceftriaxone[1,5,6,10] resulted in either no retention or strong peak assymetry. Various alkyl ammonium and sulphonate salts with C_4–C_{18} alkyl chain, as well as different reversed-phase materials, were tested at various pH values (pH 4 to 8) without any success. With the ammonium salts, distorted peaks and even peak splitting (depending on the Ro 14-1761 concentration) were sometimes observed. This was at-

tributed to the involvement of two discrete chromatographic mechanisms operating simultaneously in the column[11–13].

Mobile phase composition and working temperature. A combination of tetraoctylammonium bromide and methylamine reagent in acetonitrile–water (1:1) at pH 8 gave some retention of the cephalosporin, with acceptable peak shape after the mobile phase was recycled overnight on the column. Other amines such as mono-, di-, triethanolamines, and mono-, di-, triethylamines gave poor peak shapes. Increasing the column temperature did not improve these results.

Such distorted chromatographic peaks could result from irreversible or slowly reversible adsorption and/or degradation on the surface of the reversed-phase material. These phenomena could be catalysed by metal ions. Surprisingly, ceftriaxone was eluted with good peak shape in almost all of the investigated chromatographic systems. The difference in molecular structure between ceftriaxone and Ro 14-1761 is the oxime function in the C-7 side-chain of the beta-lactam moiety, which bears a methyl group in ceftriaxone, whereas it is free in Ro 14-1761. Such a free oxime group could react with metal cations, *e.g.* aluminium, which may be present on the surface of the solid support. EDTA was then tried as a complexing agent.

Changing from the phosphate buffer solution (pH 8) to a buffer prepared with EDTA disodium salt and potassium hydroxide (pH 8) resulted in a good peak shape (see Fig. 3). The chromatographic improvement was observed within a few minutes following the addition of the EDTA solution to the mobile phase. Such an effect had

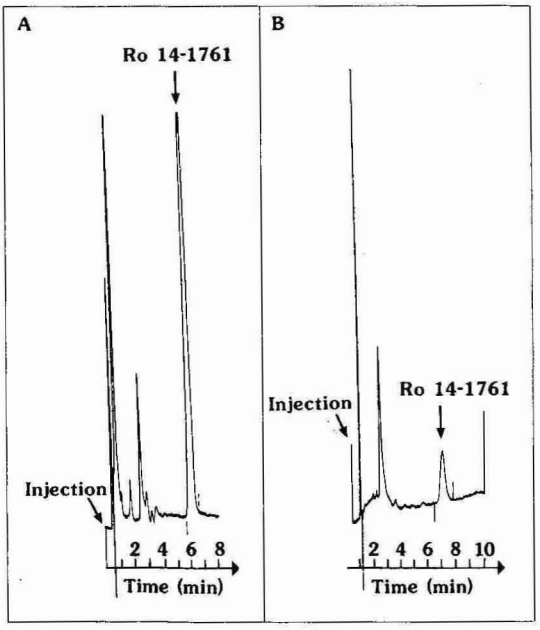

Fig. 3. Influence of EDTA on the peak shape and height of Ro 14-1761. Column, 125 × 4 mm I.D. MOS Hypersil (5 μm); mobile phase, 300 ml of acetonitrile, 1 g of TOAB, 10 ml of ethanol, buffer solution, and water to 1000 ml; flow-rate 1.5 ml/min. (A) Buffer solution, 12 ml of 0.1 *M* EDTA (pH 8); (B) buffer solution, 0.6 ml of phosphate buffer titrisol (pH 8). The injected solution contained 10 μg Ro 14-1761 per millilitre of water.

already been observed with cefpimizole by Lakings and Wozniak[14]. As ceftriaxone and Ro 14-1761 have the same UV spectrum (Fig. 4), the chromatographic peak heights of both substances should be the same at the same free acid concentration. As the two cephalosporins were separated in this system, this mixture could be used as an index to establish whether Ro 14-1761 was quantitatively eluted from the analytical column. Thus, it was observed that Ro 14-1761 could not be eluted quantitatively, although increasing the EDTA concentration did improve the results. Using *trans*-1,2-diaminocyclohexane-N,N,N′,N′-tetraacetic acid instead of EDTA led to similar observations.

Increasing the salt concentration decreased the selectivity of the separation with respect to the plasma (milk) endogenous compounds. Changes in retention time and a clear improvement of the selectivity were observed with the addition of 10 ml of ethanol to the mobile phase and when working at higher temperatures[15,16]. Fig. 5 shows how the chromatographic profile changed with the column temperature.

Influence of the reversed-phase material. Several reversed-phase materials, and various batch numbers within the same material were tested. The best chromatographic results were achieved with MOS Hypersil (5 μm). Nucleosil C_{18} or C_8 (5 μm), and ODS Hypersil C_{18} (5 μm) also gave good results, whereas other stationary phases such as μBondapak, LiChrosorb RP-18 or RP-8, Partisil 5, ODS-3 from Whatmann, Ultrasphere IP (Altex), were not adequate for Ro 14-1761 analysis.

Moreover, when the column was changed, it was necessary to tune the column temperature and the mobile phase composition to achieve the best chromatographic separation.

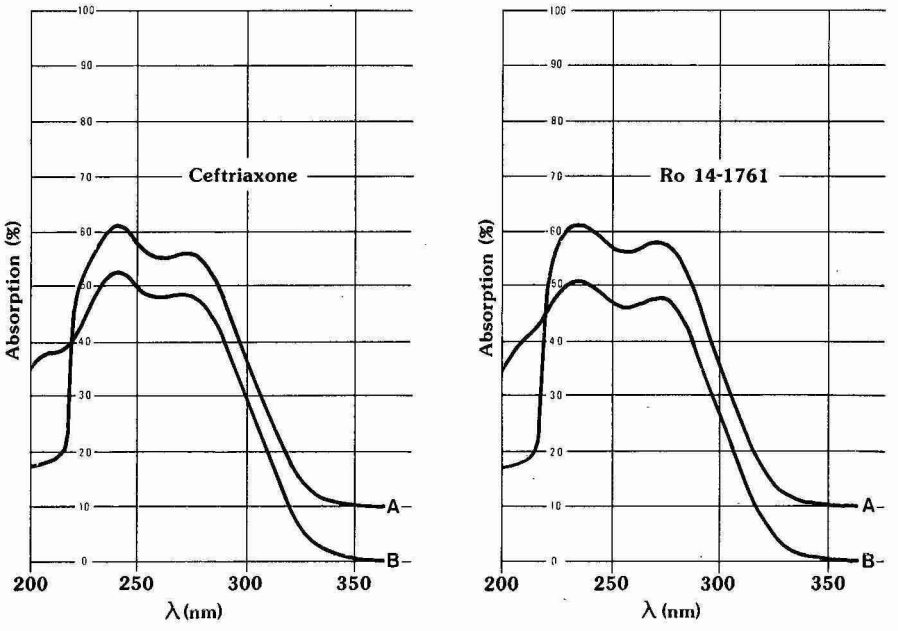

Fig. 4. UV spectra of ceftriaxone and Ro 14-1761. The compounds were dissolved in the mobile phase used for the HPLC analysis of Ro 14-1761, (A) with and (B) without tetraoctylammonium bromide. Cephalosporin concentration, 0.08 mol/l.

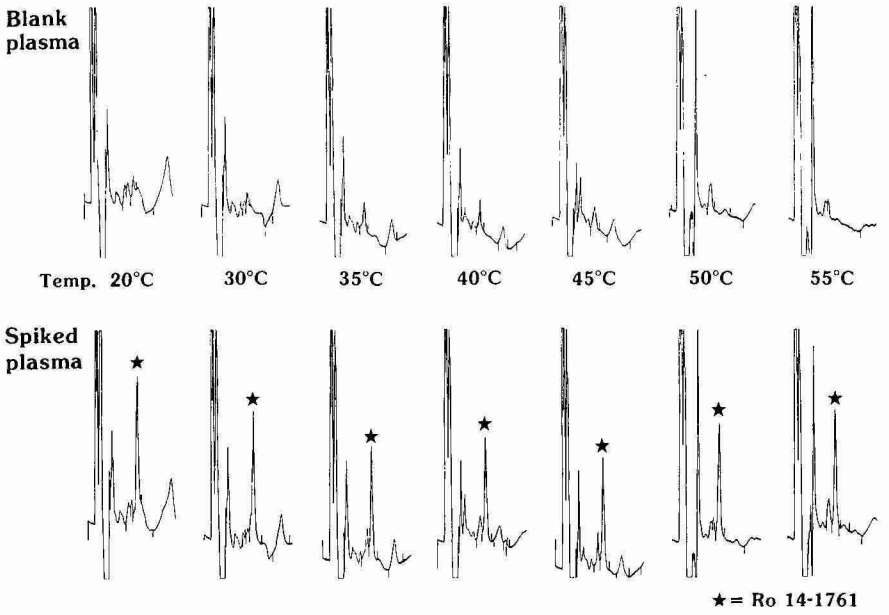

Fig. 5. Influence of the column temperature on the separation of Ro 14-1761 and endogenous compounds from plasma. The plasma samples were spiked with 10 μg/ml (20, 30 and 40°C) and 5 μg/ml (45, 50 and 55°C) of cephalosporin. Column: 125 × 4 mm I.D. MOS Hypersil (5 μm); mobile phase, 300 ml of acetonitrile, 1 g of TOAB, 10 ml of ethanol, 12 ml of 0.1 *M* EDTA (pH 8), and water to 1000 ml; flow-rate, 1.5 ml/min.

Sample preparation and recovery

The recovery of the drug was estimated from the change in the peak height when Ro 14-1761 was added to plasma or milk before protein precipitation, compared with the peak height when the drug was added to the final extract of a blank plasma (milk). During this study, it was observed that Ro 14-1761 was adsorbed onto glass to some extent when an aqueous solution of the cephalosporin was used.

The recovery of Ro 14-1761 in plasma and milk was 85–90% and 93–98%, respectively (Table I).

Selectivity

Ro 14-1761 has a high polarity which makes it impossible to extract the drug into an organic solvent. Therefore, sample preparation must involve protein precipitation and direct injection of "dirty" biological samples containing large amounts of endogenous products, which may interfere with the assay. Several blank plasma and milk samples from cow were analysed as described in the previous section. The assay is specific for Ro 14-1761 down to 10 μg of Ro 14-1761 per millilitre without heating the analytical column. Below this limit, the plasma (milk) endogenous products, which eluted together with the cephalosporin, disturbed the assay. This was overcome by heating the analytical column to *ca.* 50°C (see Fig. 5). The temperature had to be adapted from column to column, even when the reversed-phase material was from the same batch. Small changes in the temperature (± 5°C) strongly influenced the quality of separation.

TABLE I

RECOVERY OF Ro 14-1761 FROM PLASMA AND MILK

$n = 5$.

Medium	*Conc. added (μg/ml)*	*Recovery (%)*
Plasma	25	89.7
	100	86.1
	150	89.4
Milk	25	98.1
	100	92.9
	150	96.3

When the system was optimized, the assay was specific in the 0.1–100 μg/ml concentration range.

Linearity and limit of quantitation

According to the expected concentration in the unknown or quality control samples, two calibration ranges were used, either 0.1–1 μg/ml of Ro 14-1761 or 10–150 μg/ml. A linear relationship between the peak height and the concentration was obtained within both these ranges. The values of the slope, the intercept, and the coefficient of determination calculated from the calibration curves of Ro 14-1761 are listed in the Tables II and III. They were obtained on several consecutive days with plasma and milk, respectively. The limit for quantitative determination, defined as the concentration of Ro 14-1761 in plasma (milk) which can be measured with a precision and an accuracy better than 10%[17–19], was 0.1 ± 0.01 μg/ml ($n = 6$).

Precision and accuracy

The precision[20] of this method was evaluated over the concentration range 0.1–100 μg/ml plasma (milk). The overall intra-assay precision, determined by analysing each concentration at least five times on the same day, was found to be 1–10% in plasma (Table IV). The overall inter-assay precision determined over 5–7 consecutive days was better than 1–5% (Table V). The accuracy[20] was better than 5%

TABLE II

MEAN VALUE OF THE INTERCEPT (A), THE SLOPE (B), THE COEFFICIENT OF DETERMINATION (r^2), AND THE MEAN DEVIATION AROUND THE CURVE, CALCULATED FROM THE CALIBRATION LINES OF Ro 14-1761 OBTAINED ON FIVE CONSECUTIVE DAYS IN PLASMA

Coefficient	*Mean ± S.D.*	*Median*	*95% conf. limits*
A (μg/ml)	−69.2 ± 136.5	−113.8	−238.6/100.2
B	136.9 ± 9.1	133.9	125.6/148.1
r^2	0.9996 ± 0.0002	0.9997	0.9994/0.9999
Mean dev. (%)	1.6 ± 0.9	1.1	0.5/2.7

TABLE III

MEAN VALUE OF THE INTERCEPT (A), THE SLOPE (B), THE COEFFICIENT OF DETERMINATION (r^2), AND THE MEAN DEVIATION AROUND THE CURVE, CALCULATED FROM THE CALIBRATION LINES OF Ro 14-1761 OBTAINED ON SEVEN CONSECUTIVE DAYS IN MILK

Coefficient	*Mean ± S.D.*	*Median*	*95% conf. limits*
A (μg/ml)	−84.2 ± 114.5	−33.8	−190.1/21.8
B	187.01 ± 22.79	195	165.93/208.10
r^2	0.9997 ± 0.0003	0.9997	0.9994/1.0000
Mean dev. (%)	1.1 ± 0.4	1.1	0.7/1.4

in both cases. It was observed that the measured concentrations were always under the concentrations calculated from the weighted Ro 14-1761 added to the standard (*i.e.* the accuracy was always negative). This could originate from (i) an adsorption of the cephalosporin on the glass tube used during the sample preparation and/or (ii) a non-quantitative elution of the drug from the analytical column.

Stability of the new cephalosporin in milk

Solutions of Ro 14-1761 were processed in control plasma at concentrations

TABLE IV

Ro 14-1761: INTRA-ASSAY PRECISION AND ACCURACY IN PLASMA

Conc. added (μg/ml)	*Conc. found ± S.D. (μg/ml)*	*Accuracy: found − added (%)*	*95% conf. limits (μg/ml)*	*n*
0.1	0.100 ± 0.01	⩽1	0.093/0.196	6
1.0	0.985 ± 0.032	−1.5	0.962/1.007	10
24.15	24.10 ± 0.26	⩽1	23.8/24.4	5
96.62	96.54 ± 1.5	⩽1	94.7/98.4	5

TABLE V

Ro 14-1761: INTER-ASSAY PRECISION AND ACCURACY IN PLASMA

Conc. added (μg/ml)	*Conc. found ± S.D. (μg/ml)*	*Accuracy: found − added (%)*	*95% conf. limits (μg/ml)*	*n*
21.43	20.5 ± 0.4	−4.3	20.0/21.0	5
24.15	22.9 ± 0.9	−5.2	22.1/23.7	7
85.72	84.6 ± 0.8	−1.3	83.6/85.6	5
96.62	94.2 ± 1.0	−2.5	93.3/95.1	7

TABLE VI

Ro 14-1761: STABILITY IN MILK AT ROOM TEMPERATURE OVER 24 h

Determined according to the method of Timm *et al.*[21]. LL = lower limit; UL = upper limit; *D* = percentage difference in response after storage.

Conc. added (μg/ml)	*Peak height ref. 21*	*Peak height 24 h*	*D (%)*	*LL (%)*	*UL (%)*
10	1653	1436	−13	−16.2	−9.9
125	20 843	19 122	−8	−10.7	−5.6
250	41 056	37 176	−9	−11.7	−7.2

of 10, 125 and 250 μg/ml. They were stored at room temperature for 24 h under normal laboratory lighting conditions and analysed. Together with each set of stored samples, an equal number of freshly spiked samples were analysed to provide the 100% values. The procedure and subsequent statistical calculations were carried out according to the method of Timm *et al.*[21]. The data from these stability determinations are presented in Table VI. The results showed that Ro 14-1761 was not stable in milk at room temperature as a decrease of the peak height of *ca.* 10–16% was observed. Therefore, the plasma and milk samples containing the cephalosporin Ro 14-1761 should not be stored at room temperature for 24 h but should be deep frozen soon after collection (biological samples) or preparation (standard). Nevertheless, the assay may be regarded as suitable for pharmacokinetics in cow and residue evaluation in the milk following Ro 14-1761 administration.

ACKNOWLEDGEMENTS

The authors thank Dr. H. Eggers (F. Hoffmann-La Roche & Co. Ltd., Grenzach, F.R.G.) for stimulating discussion and Dr. D. Dell for correcting the manuscript.

REFERENCES

1 R. E. Bawdon, D. L. Hemsell and P. L. Hemsell, *J. Liq. Chromatogr.*, 1 (1985) 2011.
2 R. S. Griffith, H. R. Black, G. L. Brier and J. D. Wolny, *Antimicrob. Agents Chemother.*, 10 (1976) 814.
3 T. Bergan, *Chemotherapy*, 23 (1977) 389.
4 R. D. Foord, *Antimicrob. Agents Chemother.*, 9 (1976) 741.
5 K. H. Trautmann and P. Haefelfinger, *J. High Resolut. Chromatogr. Chromatogr. Commun.*, 4 (1981) 54.
6 V. Ascalone and L. Dal Bo, *J. Chromatogr.*, 273 (1983) 357.
7 I. Halàsz and J. Asshauer, *J. Chromatogr. Sci.*, 12 (1974) 139.
8 I. Halàsz, H. Schmidt and P. Vogtel, *J. Chromatogr.*, 126 (1976) 19.
9 C. E. Goewie, M. W. F. Nielen, R. W. Frei and U. A. Th. Brinkman, *J. Chromatogr.*, 301 (1984) 325.
10 D. B. Bowman, M. K. Aravind, J. N. Miceli and R. E. Kauffman, *J. Chromatogr.*, 309 (1984) 209.
11 G. K. C. Low, A. M. Duffield and P. R. Haddad, *Chromatographia*, 15 (1982) 289.
12 T.-L. Ng and S. Ng., *J. Chromatogr.*, 329 (1985) 13.
13 G. K. C. Low, P. R. Haddad and A. M. Duffield, *J. Chromatogr.*, 336 (1984) 15.
14 D. B. Lakings and J. M. Wozniak, *J. Chromatogr.*, 308 (1984) 261.

15 R. J. Perchalski and B. J. Wilder, *Anal. Chem.*, 91 (1979) 774.
16 L. R. Snyder, *J. Chromatogr.*, 179 (1979) 167.
17 L. A. Currie, *Anal. Chem.*, 40 (1968) 586.
18 J. P. Foley and J. G. Dorsey, *Chromatographia*, 18 (1984) 503.
19 S. M. Kalman, D. R. Clark and L. E. Moses, *Clin. Chem.*, 30 (1984) 515.
20 G. H. Morrison, *Anal. Chem.*, 52 (1980) 2241A.
21 U. Timm, M. Wall and D. Dell, *J. Pharm. Sci.*, 74 (1985) 972.

Journal of Chromatography, 362 (1986) 274–277
Elsevier Science Publishers B.V., Amsterdam — Printed in The Netherlands

CHROM. 18 694

Note

Gas chromatographic–mass spectrometric analysis of monodemethylated metabolites of 6,7- and 7,8-dimethoxycoumarin isomers

KENJI YAMAMOTO*, SACHIKO KATO and HITOMI SHIMOMURA
School of Pharmacy, Hokuriku University, Kanazawa 920-11 (Japan)
(Received March 24th, 1986)

6,7-Dimethoxycoumarin is the main factor in the cholekinetic activity of *Artemisiae capillaris* Flos, which is the most representative crude drug for jaundice in Chinese medicine[1,2]. A study of the *in vivo* metabolism of 6,7-dimethoxycoumarin in rabbits by paper chromatographic analysis has shown that this compound is mainly monodemethylated to 6-hydroxy-7-methoxycoumarin (6-OH-7-OCH_3) and 7-hydroxy-6-methoxycoumarin (7-OH-6-OCH_3)[3]. In a previous paper[4] we described the gas chromatographic (GC) separation of monodemethylated derivatives of dimethoxycoumarin isomers, in their free forms, using a column packed with a phthalate–alkylene glycol polyester phase.

The present study was undertaken to develop a gas chromatography–mass spectrometry–selected-ion monitoring (GC–MS–SIM) procedure with deuterated internal standards capable of measuring accurately micro-amounts of the monodemethylated metabolites of 6,7-dimethoxycoumarin, which would be applicable to the determination of metabolites in tissue incubations. For purposes of comparison, the monodemethylated metabolites of 7,8-dimethoxycoumarin were also analyzed.

EXPERIMENTAL

Standards

6-OH-7-OCH_3, 7-OH-6-OCH_3, 7-hydroxy-8-methoxycoumarin (7-OH-8-OCH_3) and 8-hydroxy-7-methoxycoumarin (8-OH-7-OCH_3) were synthesized according to the described methods[5]. The deuterated analogues were similarly synthesized by methylation with [$^2H_6$]dimethyl sulphate (E. Merck, Darmstadt, F.R.G.).

GC–MS–SIM

GC–MS–SIM was performed on a JEOL Model JMS DX-300 gas chromatograph–mass spectrometer system equipped with a data processing system. Chromatographic separation was performed on a 1 m × 2 mm I.D. glass column packed with 5% Thermon 3000 on Chromosorb W AW DMCS (80–100 mesh), supplied by Shimadzu (Kyoto, Japan). The column temperature was maintained at 250°C. The injector port, separator and transfer line were operated at 270°C. Helium was used as the carrier gas at a flow-rate of 40 ml/min. The electron-impact energy was set at 70 eV. The selected-ion monitor was focused on the molecular ions at m/z

0021-9673/86/$03.50

192 for the monodemethylated derivatives of dimethoxycoumarin isomers and at *m/z* 195 for the corresponding deuterated internal standards.

Sample preparation

To 2.5 ml of an incubation mixture were added 750 ng each of deuterated 6-OH-7-OCH_3 and 7-OH-6-OCH_3 or 750 ng each of deuterated 7-OH-8-OCH_3 and 8-OH-7-OCH_3 dissolved in 20 μl of acetone, and the pH was adjusted to 2.0 with 10% hydrochloric acid. The mixture was extracted three times with 3 ml of diethyl ether by mechanical shaking for 5 min, followed by centrifugation at 1000 *g*. The organic phase was dried over anhydrous sodium sulphate and then evaporated to dryness under a stream of nitrogen. The residue was dissolved in 50 μl of acetone, and a 1.0-μl aliquot was subjected to GC–MS–SIM.

Calibration graphs

Calibration graphs for 6-OH-7-OCH_3 and 7-OH-6-OCH_3 were constructed by analyzing a series of 2.5-ml samples of the incubation mixtures (minus cofactors) to which 150–3000 ng of each of the unlabelled standards and 750 ng of each of the deuterated internal standards had been added. These standards were then subjected to the same extraction procedure as used for unknown samples.

Calibration graphs for 7-OH-8-OCH_3 and 8-OH-7-OCH_3 were constructed as described above.

RESULTS AND DISCUSSION

Table I shows a comparison of the electron-impact mass spectral data for 6-OH-7-OCH_3, 7-OH-6-OCH_3, 7-OH-8-OCH_3 and 8-OH-7-OCH_3 with those for 6,7-dimethoxycoumarin[6]. The four monodemethylated metabolites of dimethoxycoumarin isomers present in incubation mixtures containing the supernatant obtained by centrifugation of rat liver at 9000 *g* were identified by GC–MS and comparison with authentic samples.

Figs. 1 and 2 show the GC–MS–SIM traces of 6-OH-7-OCH_3 and 7-OH-6-OCH_3 and of 7-OH-8-OCH_3 and 8-OH-7-OCH_3, respectively, and the corresponding deuterated internal standards. Using the described sample preparation, no interfering substances were present in the analyzed samples from tissue incubations. The detec-

TABLE I

ELECTRON-IMPACT MASS SPECTRAL DATA FOR MONODEMETHYLATED DERIVATIVES OF DIMETHOXYCOUMARIN ISOMERS

Compound	*Relative intensity (%)*				
	m/z 192 $[M]^{+\cdot}$	*177* $[M-CH_3]^+$	*164* $[M-CO]^{+\cdot}$	*149* $[M-CH_3-CO]^+$	*121* $[M-CH_3-2CO]^+$
6-OH-7-OCH_3	100	11	35	48	11
7-OH-6-OCH_3	100	55	21	33	11
7-OH-8-OCH_3	100	21	16	19	14
8-OH-7-OCH_3	100	10	14	28	12

Fig. 1. Selected-ion monitoring of 6-OH-7-OCH_3 (1) and 7-OH-6-OCH_3 (2) and the deuterated internal standards.

Fig. 2. Selected-ion monitoring of 7-OH-8-OCH_3 (1) and 8-OH-7-OCH_3 (2) and the deuterated internal standards.

tion limits of these analyses were *ca.* 40 ng/ml of an incubation mixture, and the detection limits for the pure substances were *ca.* 2 ng per injection.

Calibration graphs for these four monodemethylated metabolites were constructed in the range of 60–1200 ng/ml of incubate as shown in Fig. 3. Least-squares analysis of the peak area ratio *versus* weight ratio of the unlabelled and labelled standards gave a linear relationship with a correlation coefficient of greater than 0.99 for each metabolite. The average recovery for each metabolite at a concentration of 300 ng/ml was found to be 96.2–99.9%, with a coefficient of variation of $\leqslant 5.1\%$ ($n = 4$).

The proposed method has been used successfully to monitor the *in vitro* metabolism of 6,7- and 7,8-dimethoxycoumarin isomers by the rat liver supernatant obtained by centrifugation at 9000 *g* (Table II). Metabolite levels in the incubation mixtures ranged from *ca.* 100 to *ca.* 1000 ng/ml, values which are within the dynamic range of the assay described.

From the data shown, the proposed method for the determination of mono-

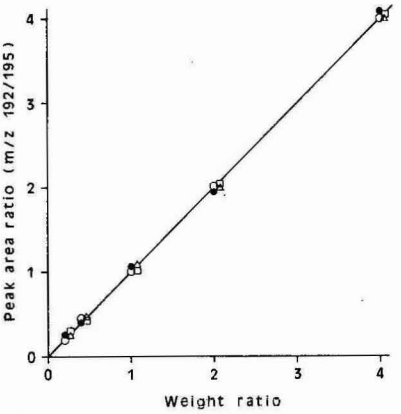

Fig. 3. Calibration graphs for 6-OH-7-OCH_3 (●), 7-OH-6-OCH_3 (○), 7-OH-8-OCH_3 (□) and 8-OH-7-OCH_3 (△). The amount of unlabelled standard was varied between 60 and 1200 ng/ml; the amount of deuterated internal standard was fixed at 300 ng/ml.

TABLE II

IN VITRO FORMATION OF MONODEMETHYLATED METABOLITES FROM DIMETHOXYCOUMARIN ISOMERS BY RAT LIVER SUPERNATANT

Incubation was carried out at 37°C for 20 min with 0.5 m*M* dimethoxycoumarin, 0.5 m*M* NADP, 5 m*M* glucose-6-phosphate, 5 m*M* magnesium chloride, the supernatant obtained by centrifugation of rat liver at 9000 *g* (1 ml/0.25 g of liver) and 0.1 *M* phosphate buffer (pH 7.4) in a total volume of 2.5 ml.

Substrate	*Metabolite*	*(nmol/g liver · min)**
6,7-Dimethoxycoumarin	6-OH-7-OCH_3	2.62 ± 0.12
	7-OH-6-OCH_3	0.86 ± 0.01
7,8-Dimethoxycoumarin	7-OH-8-OCH_3	1.37 ± 0.08
	8-OH-7-OCH_3	0.32 ± 0.01

* Values are the means ± S.E. for $n = 4$.

demethylated metabolites of dimethoxycoumarin isomers is specific, accurate, precise and easy to use. Since 7-ethoxycoumarin was introduced by Ullrich and Weber[7] as an interesting substrate for measuring mixed-function monooxygenase activity, the O-dealkylation activities of several 7-alkoxycoumarins have been measured to characterize the different species of cytochrome P-450[8,9]. Further studies are planned for the analysis of the regioselective monodemethylation of dimethoxycoumarin isomers by microsomal preparations.

REFERENCES

1 M. Aburada, H. Sasaki and M. Harada, *Yakugaku Zasshi*, 96 (1976) 147.
2 M. Kimura, *Proc. 10th Symposium on WAKAN-YAKU, Toyama, August 28-29, 1976*, Research Institute for WAKAN-YAKU, Toyama, 1977, pp. 121–126.
3 T. Furuya, *Chem. Pharm. Bull.*, 6 (1958) 696.
4 S. Kato and K. Yamamoto, *J. Chromatogr.*, 333 (1985) 175.
5 R. D. H. Murray, J. Méndez and S. A. Brown, *The Natural Coumarins*, Wiley, Chichester, 1982.
6 R. H. Shapiro and C. Djerassi, *J. Org. Chem.*, 30 (1965) 955.
7 V. Ullrich and P. Weber, *Hoppe-Seyler's Z. Physiol. Chem.*, 353 (1972) 1171.
8 T. Kamataki, M. Ando, Y. Yamazoe, K. Ishii and R. Kato, *Biochem. Pharmacol.*, 29 (1980) 1015.
9 M. Komori, Y. Imai and R. Sato, *J. Biochem (Tokyo)*, 95 (1984) 1379.

Journal of Chromatography, 362 (1986) 278–280
Elsevier Science Publishers B.V., Amsterdam — Printed in The Netherlands

CHROM. 18 716

Note

Separation of nitromusks by capillary gas chromatography

LORENZO SPANEDDA*, MARINELLA MELIS and CLARA RONI
Faculty of Pharmacy, Institute of Pharmaceutical, Toxicological and Applied Chemistry, Via Ospedale 72, 09100 Cagliari (Italy)
(Received April 8th, 1986)

Musk ambrette [1-(1,1-dimethylethyl)-2-methoxy-4-methyl-3,5-dinitrobenzene] and musk xylene [1-(1,1-dimethylethyl)-3,5-dimethyl-2,4,6-trinitrobenzene] belong to the class of benzenoid synthetic nitromusks. They are widely used in manufacturing of cosmetics and toiletries[1,2] instead of natural musks, which are much more expensive and insufficiently available to satisfy the commercial demand.

The widespread use of nitromusks is not yet free from risks to humans: some authors have pointed out the occurrence of photoallergic reactions[3–5] caused by musk ambrette; and moreover peroxides produced by the photodecomposition of nitromusks may be involved in skin cancer promotion[6].

It is therefore necessary to develop a simple and reliable method for the identification of nitromusks. Betts *et al.*[7] have suggested the use of electron-capture gas chromatography (GC), but they found some difficulties in resolving musk ambrette from musk xylene, owing to the closely similar retention times of these two compounds on both polar and non-polar stationary phases.

A sharp distinction between these two nitromusks is of a great importance for the verification of the presence of musk ambrette, which is so far the only nitromusk that has been shown to be responsible for photoallergic contact dermatitis.

In order to achieve a clear resolution of musk ambrette from musk xylene, we decided to use capillary GC.

EXPERIMENTAL

Apparatus and material

A Carlo Erba Model 4200 gas chromatograph was used, fitted with a ^{63}Ni electron-capture detector and a split-splitless injector. A fused-silica column (30 m × 0.32 mm I.D.) was employed, with OV-17 liquid phase (film thickness 0.3 μm). The chromatograph was connected to a recorder-integrator (Hewlett-Packard 3390 A).

The nitromusks were kindly donated by Esperis (Milan, Italy).

Procedure

A stock solution of each nitromusk was prepared, containing *ca.* 1000 mg/l each of musk ambrette and musk xylene in absolute ethanol. Working solutions

0021-9673/86/$03.50

were then prepared with a constant concentration of musk ambrette (100 ng/ml) and concentrations of musk xylene ranging from 1 to 100 ng/ml; analogous working solutions were prepared with the same concentration of musk xylene (100 ng/ml) and concentrations of musk ambrette ranging from 1 to 100 ng/ml. The two series of solutions were then tested according to the operating conditions listed in Table I.

RESULTS AND DISCUSSION

A sharp resolution of musk ambrette from musk xylene was always achieved, in both mode A (Fig. 1) and mode B. In mode A the interferences of extraneous peaks were minimized, and in mode B the analysis time was shorter, with a sharper resolution between the two peaks of interest. In the first case the minimum detectable

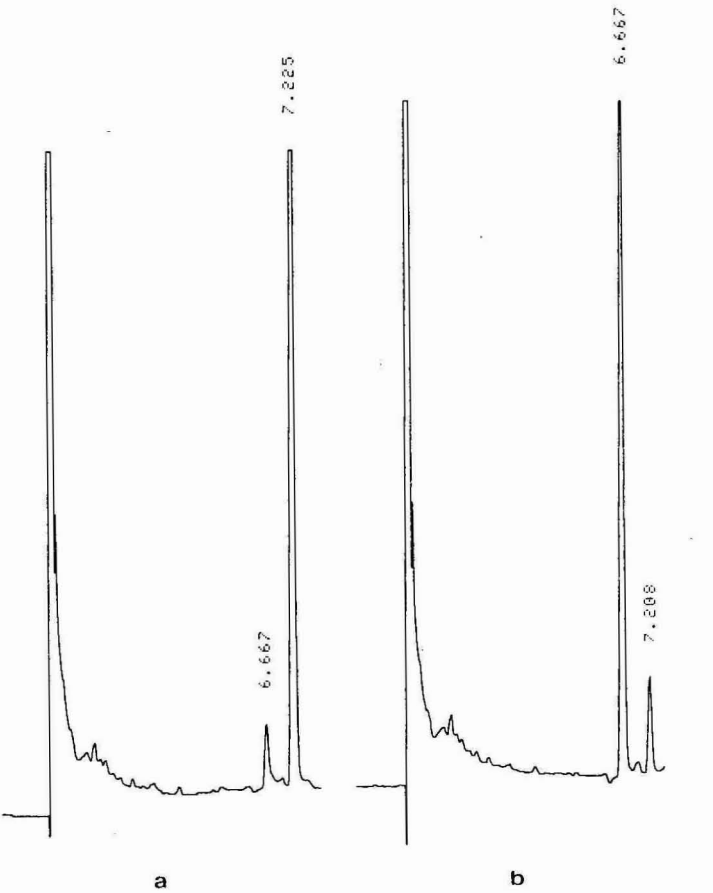

Fig. 1. Chromatograms of working solutions: (a) musk ambrette, 10 ng/ml; musk xylene, 100 ng/ml; (b) musk ambrette, 100 ng/ml; musk xylene, 10 ng/ml. Operating conditions as listed in Table I, mode A. Musk ambrette is the peak with a retention time of 6.667; musk xylene is the peak with a retention time of 7.225 (a) or 7.208 (b). In mode B (not shown in this figure) retention times were *ca.* 5.035 and 5.650 for musk ambrette and musk xylene, respectively.

TABLE I

OPERATING CONDITIONS

The detector was always operated in the constant current mode: pulse width, 1 μs; voltage, 45 V.

	Mode A	*Mode B*
Injection mode	Split	Splitless
Split ratio	1:30	–
Carrier	Nitrogen	Nitrogen
Carrier flow-rate	1.5 ml/min	2.5 ml/min
Scavenger flow-rate	20 ml/min	20 ml/min
Injector temp. (°C)	230	200
Detector temp. (°C)	250	225
Oven temp. (°C)	210	180
Injected volume	1 μl	0.5 μl

concentration was 2 ng/ml for musk ambrette and musk xylene; in the second it was 5 ng/ml for both nitromusks.

Numerous toiletries were tested in accordance with the operating conditions proposed. This confirmed that the use of open tubular columns, as used for this work, overcomes the obstacle of the separation of musk ambrette from xylene, which is not otherwise obtainable with packed columns.

The method proposed here can be helpful for the rapid and reliable detection of musk ambrette in commercial supplies that have caused photoallergy or could cause it. It could also be used to verify the purity of raw materials used by manufacturers, by detecting any adulteration of musk ambrette with musk xylene.

REFERENCES

1 Maison G. de Navarre, *The Chemistry and Manufacture of Cosmetics*, Van Nostrand, New York, 2nd ed., 1962.
2 P. Z. Bedoukian, *Perfumery and Flavouring Synthetics*, Elsevier, New York, 2nd ed., 1967.
3 G. J. Raugi, F. J. Storrs and W. G. Larsen, *Contact Dermatitis*, 5 (1979) 251.
4 G. J. Raugi and F. J. Storrs, *Arch. Dermatol.*, 115 (1979) 106.
5 V. J. Giovinazzo, H. Ichikawa, I. E. Kochevar, R. B. Armstrong and L. C. Harber, *Photochem. Photobiol.*, 33 (1981) 773.
6 I. Emerit and P. A. Cerutti, *Nature (London)*, 293 (1981) 144.
7 T. J. Betts, G. M. Tai and R. A. Turner, *J. Chromatogr.*, 244 (1982) 381.

Journal of Chromatography, 362 (1986) 281–285
Elsevier Science Publishers B.V., Amsterdam — Printed in The Netherlands

CHROM. 18 686

Note

Kinetic studies of epimerization of cobalt(III) complexes by means of high-performance liquid chromatography on a cation exchanger derived from TSKgel G3000PW

KIYOHIKO NAKAJIMA, MASAAKI KOJIMA and JUNNOSUKE FUJITA*
Department of Chemistry, Faculty of Science, Nagoya University, Chikusa-ku, Nagoya 464 (Japan)
(Received March 24th, 1986)

When kinetically unstable species are subjected to column chromatographic separation, they are transformed gradually into other species in the column, and thus the patterns of chromatograms depend on the relative rates of separation and transformation[1]. In order to study kinetics of reactions in solution by high-performance liquid chromatography (HPLC), the separation should be performed much faster than the transformation occurs, so that transformation during chromatography can be negligible. In a previous paper[2], we reported that a cation-exchanger, sulphoethyl (SE)-Toyopearl is suitable for use in HPLC under a reasonable pressure, and this method was successfully applied to kinetic studies of the inversion at the selenium atom of $[Co(acac)_2(CH_3SeCH_2CH_2NH_2)]^+$ (acac = 2,4-pentanedionate ion).

An HPLC column packed with a strong cation-exchanger with sulphopropyl groups derived from TSKgel G3000PW was found to be more effective than an SE-Toyopearl column for separation of the isomers of metal complexes. In this paper, we describe the application of HPLC on this exchanger to kinetic studies of inversion at the selenium atom of $[Co(Clacac \text{ or } Meacac)_2(CH_3SeCH_2CH_2NH_2)]^+$ (Clacac = 3-chloro-2,4-pentanedionate ion, Meacac = 3-methyl-2,4-pentanedionate ion) and that at the secondary amine nitrogen atom of $[Co(acac)_2(C_6H_5NHCH_2CH_2NH_2)]^+$.

EXPERIMENTAL

The cation-exchanger (exchange capacity, $0.14 \cdot 10^{-3}$ equiv. cm^{-3}) used in this study was a gift from Toyo Soda (Tokyo, Japan). According to the manufacturer, this exchanger was developed by introducing sulphopropyl groups into TSKgel G3000PW[3], which is a hydrophilic-polymer-based gel carrying aliphatic hydroxyl groups. The allyl groups introduced into the hydroxyl groups of the gel were transformed into sulphopropyl groups by the oxygen-induced, anti-Markownikoff addition of sodium hydrogen sulphite to the C=C double bonds[4]. A similar cation-exchanger derived from TSKgel G5000PW is commercially available under the tradename of TSKgel SP-5PW.

0021-9673/86/$03.50

Kinetics

A racemic pair of diastereomers, $\Delta(S)\Lambda(R)$-[Co(Clacac or Meacac)$_2$-($CH_3SeCH_2CH_2NH_2$)]ClO_4[5] (*ca.* 10^{-4} mol dm^{-3}) in 0.05 mol dm^{-3} sodium sulphate was epimerized at 40°C. Portions of the reaction mixture were withdrawn at intervals and then chromatographed (sample volume, $4 \cdot 10^{-3}$–$6 \cdot 10^{-3}$ cm^3) with a column (7.5 × 0.75 cm I.D.) of the cation-exchanger and 0.05 mol dm^{-3} (Clacac complex) or 0.025 mol dm^{-3} sodium sulphate (Meacac complex) as the eluent. Chromatography was carried out with a JASCO Tri Rotar V system at a flow-rate of 2.0 cm^3 min^{-1} (Clacac complex) or 1.0 cm^3 min^{-1} (Meacac complex) and the complexes were detected with a JASCO UVIDEC 100IV spectrophotometric detector at 312 nm (Clacac complex) or 307 nm (Meacac complex) where the two isomers [$\Delta(R)\Lambda(S)$ and $\Delta(S)\Lambda(R)$] give the same molar absorption coefficient. No detectable change in absorbance was observed during the epimerization reactions. The $\Delta(R)\Lambda(S)$ isomer was eluted faster in either complex. The areas of two bands on the chromatograms were determined by paper cut-outs matching the bands.

The kinetics of epimerization of [Co(acac)$_2$($C_6H_5NHCH_2CH_2NH_2$)]$^+$ (ref. 6) was studied by a similar way. A solution of $\Delta(R)\Lambda(S)$-[Co(acac)$_2$-($C_6H_5NHCH_2CH_2NH_2$)]Cl (*ca.* 10^{-3} mol dm^{-3}) in a phthalate buffer (pH 4.07, 4.77, and 5.22) was epimerized at 34°C. Portions of the reaction mixture were withdrawn at intervals and mixed with a small amount of dilute nitric acid, which served to stop effectively the epimerization reaction. The mixture was then chromatographed (column, 25 × 0.46 cm I.D.; eluent, 0.1 mol dm^{-3} sodium nitrate–0.03 mol dm^{-3} nitric acid; flow-rate, 2.0 cm^3 min^{-1}; sample volume, *ca.* 4 × 10^{-3} cm^3; detection wavelength, 340 nm).

RESULTS AND DISCUSSION

The selenium atom of free 2-(methylseleno)ethylamine ligand becomes chiral on coordination to a cobalt(III) ion. For [Co(Clacac or Meacac)$_2$-($CH_3SeCH_2CH_2NH_2$)]$^+$, two isomers (racemic pairs of the diastereomers) $\Delta(R)\Lambda(S)$ and $\Delta(S)\Lambda(R)$ are possible (Fig. 1). Such isomers are also possible for [Co(acac)$_2$($C_6H_5NHCH_2CH_2NH_2$)]$^+$. Each complex has been separated into its iso-

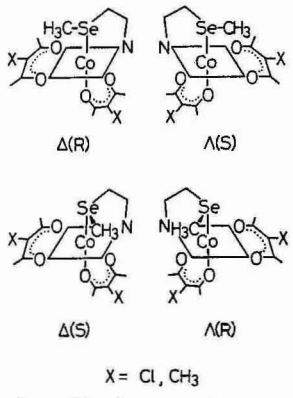

Fig. 1. The four stereoisomers of [Co(Clacac or Meacac)$_2$($CH_3SeCH_2CH_2NH_2$)]$^+$.

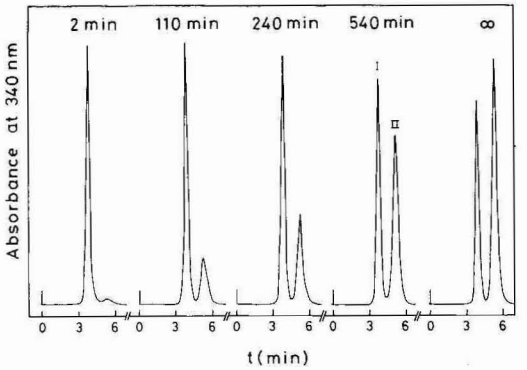

Fig. 2. Change in elution curve during the epimerization of $\Delta(R)\Lambda(S)$-$[Co(acac)_2(C_6H_5NHCH_2CH_2NH_2)]^+$ at pH 4.07 and 34°C. Chromatographic conditions: column, 25 × 0.46 cm I.D.; eluent, 0.1 mol dm^{-3} sodium nitrate–0.03 mol dm^{-3} nitric acid; flow-rate, 2.0 cm^3 min^{-1}; UV detection, 340 nm.

mers by ordinary column chromatography and characterized by spectroscopy[5,6]. The selenide complexes isomerize in solution to give an equilibrium mixture of the isomers, and the isomerizations proceed by inversion at the selenium centres[5]. The isomerization of the diamine complex has been shown to take place by inversion at the secondary amine nitrogen atom, the reaction being catalysed by OH^-[6,7].

Kinetic studies of reversible isomerization (epimerization) between the two isomers of the present complexes were carried out by observing the change in chromatograms with reaction time. This method has the great advantages of a short elution time and micro amounts of samples[2,8]. Fig. 2 shows a typical set of elution curves obtained at intervals after $\Delta(R)\Lambda(S)$-$[Co(acac)_2(C_6H_5NHCH_2CH_2NH_2)]^+$ had been dissolved in water at pH 4.07 and 34°C. The pseudo first-order rate con-

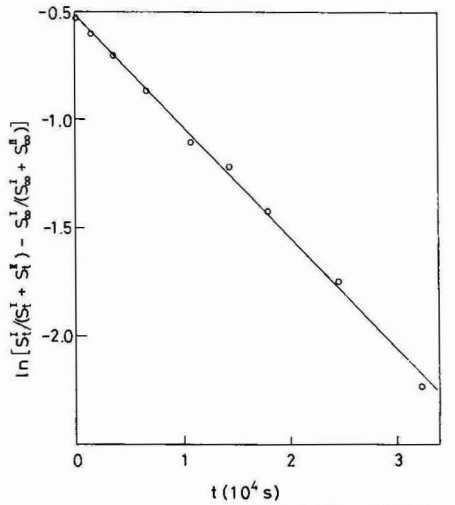

Fig. 3. The plots of $\ln[S_t^{\mathrm{I}}/(S_t^{\mathrm{I}} + S_t^{\mathrm{II}}) - S_\infty^{\mathrm{I}}/(S_\infty^{\mathrm{I}} + S_\infty^{\mathrm{II}})]$ *vs.* time for the epimerization of $\Delta(R)\Lambda(S)$-$[Co(acac)_2(C_6H_5NHCH_2CH_2NH_2)]^+$ at pH 4.07 and 34°C (S_t^{I}, S_t^{II}, S_∞^{I}, and S_∞^{II} denote the areas of bands I and II at time t and at infinite time).

TABLE I

RATE CONSTANTS (k_{obsd} AND k_{ep}) FOR RACEMIZATION OF $[Co(acac)_2(C_6H_5NHCH_2CH_2NH_2)]^+$ AT 34°C

pH	k_{obsd} (s^{-1})	k_{ep} ($mol^{-1}\ dm^3\ s^{-1}$)
5.22	$(7.49 \pm 0.07) \cdot 10^{-4}$	$(2.31 \pm 0.08) \cdot 10^5$
4.77	$(2.67 \pm 0.02) \cdot 10^{-4}$	$(2.35 \pm 0.07) \cdot 10^5$
4.07	$(5.14 \pm 0.03) \cdot 10^{-5}$	$(2.25 \pm 0.07) \cdot 10^5$

stant, k_{obsd}, was obtained by the method described previously (Fig. 3, Table I)[2]. The $k_{obsd}/[OH^-]$ ($= k_{ep}$) values are constant at 34°C in the pH range 4.07–5.22, indicating that the reaction is first order in $[OH^-]$ (Table I). Thus, the rate law was the same as that obtained for racemization (epimerization) of other amine complexes such as $[Co(NH_3)_4(CH_3NHCH_2CH_2NH_2)]^{3+}$, $R = k_{ep}[complex][OH^-]$ (ref. 9). The runs starting from either of the isomers gave the same result within experimental error. From these observations, the reaction can be expressed as

$$\Delta(R)\Lambda(S) \underset{k_{-1}}{\overset{k_1}{\rightleftharpoons}} \Delta(S)\Lambda(R)$$

The forward and reverse second-order rate constants, k_1 and k_{-1}, were obtained from $k_{ep}(k_{ep} = k_1 + k_{-1})$ and the equilibrium constant, K_{eq} ($K_{eq} = k_1/k_{-1} = 1.68$). The average values of k_1 and k_{-1} are $(1.44 \pm 0.04) \cdot 10^5$ and $(0.86 \pm 0.03) \cdot 10^5$ $mol^{-1}\ dm^3\ s^{-1}$, respectively. These values are *ca.* 10^6 times as large as those obtained for $[Co(acac)_2(CH_3NHCH_2CH_2NH_2)]^+$ at the same temperature[7].

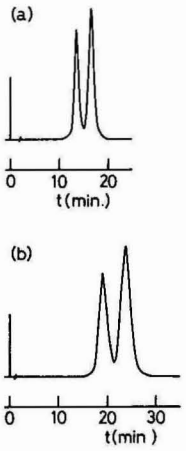

Fig. 4. The elution curves of $[Co(Meacac)_2(CH_3SeCH_2CH_2NH_2)]^+$ (a) and $[Co(Clacac)_2(CH_3SeCH_2CH_2NH_2)]^+$ (b) equilibrated in 0.05 mol dm^{-3} sodium sulphate at 40°C. Chromatographic conditions: column, 7.5 × 0.75 cm I.D.; eluent, 0.025 mol dm^{-3} (Meacac complex) or 0.05 mol dm^{-3} sodium sulphate (Clacac complex); flow-rate, 1.0 $cm^3\ min^{-1}$ (Meacac complex) or 2.0 $cm^3\ min^{-1}$ (Clacac complex); UV detection, 307 nm (Meacac complex) or 312 nm (Clacac complex).

TABLE II

RATE CONSTANTS, k_{obsd}, k_1, AND k_{-1}, FOR EPIMERIZATION OF [Co(β-DIKETONATE)$_2$-($CH_3SeCH_2CH_2NH_2$)]$^+$ (β-DIKETONATE = Clacac, Meacac, acac) IN 0.05 mol dm^{-3} SODIUM SULPHATE AT 40°C

$$\Delta(R)\Lambda(S) \underset{k_{-1}}{\overset{k_1}{\rightleftharpoons}} \Delta(S)\Lambda(R), \qquad k_{obsd} = k_1 + k_{-1}$$

β-Diketonate	k_{obsd} (10^{-5} s^{-1})	k_1 (10^{-5} s^{-1})	k_{-1} (10^{-5} s^{-1})
Clacac	1.29 ± 0.05	0.80 ± 0.03	0.50 ± 0.03
Meacac	20.0 ± 0.3	12.1 ± 0.2	7.9 ± 0.2
acac*	3.39 ± 0.09	1.78 ± 0.06	1.61 ± 0.06

* From ref. 2.

The rates of epimerization for [Co(Clacac or Meacac)$_2$-($CH_3SeCH_2CH_2NH_2$)]$^+$ were studied in the same way (Fig. 4). The K_{eq} values are 1.6 for the Clacac complex and 1.5 for the Meacac complex, and the values of k_1 and k_{-1} at 40°C are listed in Table II, together with those for [Co(acac)$_2$-($CH_3SeCH_2CH_2NH_2$)]$^+$ at the same temperature[2]. The kinetics of the acac complex was studied by HPLC on SE-Toyopearl[2], however, relatively long elution time (90 min) was required. A column packed with a cation-exchanger derived from TSKgel G3000PW used in the present study seems to be superior to an SE-Toyopearl column. Two related complexes, the Clacac and Meacac complexes were separated into the isomers within 30 min (Fig. 4). Inversion at selenium of [Co(β-diketonate)$_2$($CH_3SeCH_2CH_2NH_2$)]$^+$ at 40°C becomes faster in the order Clacac < acac < Meacac; an electronic effect induced by replacing the 3-hydrogen atom of acac with an electron-withdrawing chlorine atom or with an electron-releasing methyl group seems to affect the rate.

REFERENCES

1 M. Moriyasu, Y. Hashimoto and M. Endo, *Bull. Chem. Soc. Jpn.*, 56 (1983) 1972.
2 K. Nakajima, M. Kojima, M. Fujita and J. Fujita, *J. Chromatogr.*, 301 (1984) 241.
3 T. Hashimoto, H. Sasaki, M. Aiura and Y. Kato, *J. Polym. Sci., Polym. Phys. Ed.*, 16 (1978) 1789.
4 I. D. Roberts and M. C. Caserio, *Basic Principles of Organic Chemistry*, W. A. Benjamin, New York, 1964, p. 762.
5 K. Nakajima, M. Kojima and J. Fujita, in preparation.
6 Y. Ouyang, M. Kojima and J. Fujita, *Inorg. Chim. Acta*, 114 (1986) 197.
7 M. Kojima, T. Hibino, Y. Ouyang and J. Fujita, *Inorg. Chim. Acta*, 116 (1986) in press.
8 Y. Yoshikawa, M. Kojima, M. Fujita, M. Iida and H. Yamatera, *Chem. Lett.*, (1974) 1163.
9 W. G. Jackson and A. M. Sargeson, in P. de Mayo (Editor), *Rearrangements in Ground and Excited States*, Vol. 2, Academic Press, New York, 1980, p. 273, and refs. cited therein.

Journal of Chromatography, 362 (1986) 286–290
Elsevier Science Publishers B.V., Amsterdam — Printed in The Netherlands

CHROM. 18 687

Note

Quantitative analysis of 2-acetyl-4(5)-tetrahydroxybutylimidazole

U. KRÖPLIEN
Coca-Cola GmbH, Max-Keith-Strasse 66, D-4300 Essen 1 (F.R.G.)
(Received March 26th, 1986)

Of the four classes of caramel colours[1], some caramel colours III (also known as ammonia caramels and often called "beer caramels") have been found to be capable of decreasing the number of circulating lymphocytes in rats fed on a diet deficient in vitamin B_6. None of the other caramel classes provoked such a response. The substance responsible for this effect could be identified as 2-acetyl-4(5)-tetrahydroxybutylimidazole (THI)[2].

Separation of THI from other caramel constituents of similar basicity and polarity is achieved by a two-step procedure. Sequential treatment of caramel colours III (AC) with weakly and strongly acidic cation-exchange resins removes neutral, acidic and more basic substances. Weak bases, among them THI, are recovered with hydrochloric acid from the strong cation-exchanger. Reaction with the carbonyl reagent 2,4-dinitrophenylhydrazine converts THI into a coloured derivative. The latter is separated from excess reagent and interfering substances on a reversed-phase high-performance liquid chromatography (HPLC) column, and quantified spectrophotometrically.

EXPERIMENTAL

Solvents and other chemicals

These were of reagent-grade quality from Merck (Darmstadt, F.R.G.), Baker (Gross-Gerau, F.R.G.) and Fluka (Buchs, Switzerland).

Purification of dimethoxyethane

Dimethoxyethane was distilled from dinitrophenylhydrazine (DNPH), then from sodium hydroxide, stored over sodium sulphate, and percolated through alkaline alumina immediately prior to use.

2,4-DNPH · HCl

Reagent-grade 2,4-DNPH (Fluka)*, recrystallized from ethyl acetate, was suspended in water, and hydrochloric acid (32%) was added until the yellow hydro-

* Use of Fluka DNPH is recommended because DNPH from several other manufacturers remained impure even after recrystallization, leading to spurious peaks in HPLC.

0021-9673/86/$03.50

chloride was formed completely and the reddish-orange free base was no longer detectable. The crystals were dried under suction, washed repeatedly with dimethoxyethane, then with diethyl ether, and carefully dried.

Strong cation-exchanger

Dowex 50 AG × 8, 100–200 mesh, H^+ (Bio-Rad, Munich, F.R.G.) was used.

Weak cation-exchanger

Amberlite CG AG 50 I, 100–200 mesh, H^+ (Serva, Heidelberg, F.R.G.) was used. The resin must be sedimented repeatedly to remove fines.

Methanol, carbonyl-free

This was prepared[3] by treatment with Girard P reagent.

THI–2,4-DNPH

THI–HCl (133 mg) was dissolved in 95% ethanol (10 ml) and 32% hydrochloric acid (0.2 ml) was added, followed by 10 ml of a saturated solution of 2,4-dinitrophenylhydrazine hydrochloride in dimethoxyethane. After standing for 1 h, the solution was taken to dryness under vacuum. The residue was treated with 95% ethanol (2 ml), then dimethoxyethane (5 ml) was added. The yellow crystals were dried under suction, washed with dimethoxyethane, then with diethyl ether, and dried. Yield, 205 mg (88%); m.p., 151°C. Calculated for $C_{15}H_{18}N_6O_9 \cdot H_2O \cdot HCl$: C = 38.75%; H = 4.52%; N = 18.08%; Cl = 7.64%. Found: C = 38.71%; H = 4.59%; N = 16.97%; Cl = 7.33%.

Combination columns (clean-up device)

A lower column (175 mm × 10 mm I.D., with a PTFE stopcock and capillary outlet), an upper column (150 mm × 12.5 mm I.D., with a capillary outlet of 1 mm I.D.) and a 100-ml dropping funnel with a PTFE stopcock[4] were used. All parts were linked by standard ground-glass joints (14.5 mm).

High-performance liquid chromatographic equipment

A double-piston pump 6000 A (Waters, Eschborn, F.R.G.), an injector U6K (Waters, Eschborn, F.R.G.), a variable-wavelength detector 87.00 (Knauer, Bad Homburg, F.R.G.) and a recording integrator HP 3390 (Hewlett-Packard, Düsseldorf, F.R.G.) were used. Commercial* LiChrosorb RP-8, 10 μm, 250 × 4 mm I.D. "Vertex" columns (Knauer) were used. The HPLC mobile phase was methanol–0.02–0.05 *M* phosphoric acid (50:50, v/v); the concentration of phosphoric acid depended on the column performance.

Reacti-Vials

These were of 1-ml volume from Pierce/Karl (Geisenheim-Johannisberg, F.R.G.) with Tuf-Bond Teflon-Silicone septa.

---

* Other RP-8 materials such as "LiChrosorb" manufactured in America or "Nucleosil" were unsuitable. They were found not to retain THI–DNPH, which is eluted in the void volume together with non-carbonylic contaminants.

Caramel colours III and IV

These were provided by the International Technical Caramel Association (Washington D.C., U.S.A.).

Sample clean-up

The lower part of the combination column was filled with strong cation-exchanger to a bed-height of 60 mm. Then the upper column was connected and filled with weak cation-exchanger to a bed-height of 80–90 mm. After passage of *ca.* 20 ml of water through the columns, the device was operational. Caramel (200–250 mg, weighed accurately) was dissolved in water (*ca.* 3 ml) and the solution was transferred quantitatively to the combination column (preferably with a Pasteur pipet). The dropping funnel was adjusted and the column system eluted exhaustively with water (80–100 ml). The upper column was then disconnected and the lower column eluted with 0.5 *M* hydrochloric acid (45 ml). The first 10.0 ml were discarded, and the remaining 35 ml were collected.

Preparation of derivative

The solution was evaporated to dryness under vacuum at 40–45°C. The glassy or syrupy yellow or light brown residue is dissolved in carbonyl-free methanol (250 µl), and a saturated solution of 2,4-DNPH · HCl in dimethoxyethane (250 µl)[5] is added by syringe. The reaction mixture is transferred rapidly, to avoid solvent losses, to a septum-capped vial.

High-performance liquid chromatography

The derivative solution was kept for 5 h at room temperature. Volumes between 1 and 25 µl (usually 5 or 10 µl) were injected onto the HPLC column, which was eluted isocratically with the mobile phase at a flow-rate of 2.0 ml/min. THI–2,4-DNPH was detected and measured at 385 nm and 0.16 a.u.f.s., using peak-height determination because of the occasional occurrence of a slightly later eluting, scarcely resolved peak.

For calibration, THI dinitrophenylhydrazone (*ca.* 100 mg) was dissolved in absolute, carbonyl-free methanol. Stored in a refrigerator, the solution is stable for at least twelve months if kept in alkali-free glassware.

RESULTS

A typical chromatogram is shown in Fig. 1. The largest peak represents excess reagent.

Calibration

THI–DNPH was dissolved in methanol. Volumes from 1 to 25 µl were injected onto the HPLC column. A linear response was found for the whole range of 5–1200 ng of THI. Above 25 ng, relative standard deviations (R.S.D.) of 3.65% (peak area mode) and 2.25% (peak height mode) were found. R.S.D. values increased to 13% with 10 ng, and to 23% with 5 ng of THI, with corresponding averages of 106% and 146% of theoretical amounts being measured.

Responses and errors did not vary significantly with time. However, for peak

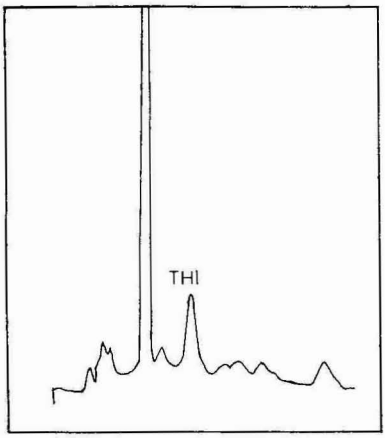

Fig. 1. Chromatographic separation of THI–DNPH on LiChrosorb RP-8 (10 μ). Mobile phase, methanol–0.02 *M* phosphoric acid (50:50, v/v); detector wavelength, 385 nm.

height mode determinations, one or two injections for recalibration are indispensable owing to slight changes of column efficiencies with time.

Limit of detection

A signal with less than 2000 peak height impulses cannot be distinguished clearly from noise, corresponding to a detection limit of *ca.* 5 ng of THI. This value corresponds to 1 mg/kg (1 ppm) in caramels under standard conditions (sample weight, 250 mg; derivative volume, 500 μl, injection volume, 10 μl). Matrix effects may raise this limit to up to 5 ppm, depending on the nature of the caramel sample.

Recovery

THI was processed through the clean-up and derivatization steps, or was previously added to caramel colours IV, also known as sulphite–ammonia caramels (THI-free) or caramel colours III (ammonia caramels). The amounts corresponded to 45–1130 ppm in the caramels. Recoveries ranged from 95.7% to 103.4%, averaging 98.6%. They were not matrix- or concentration-dependent.

THI concentrations determined in a number of commercial caramel colours III (AC) are listed in Table I.

TABLE I

CONCENTRATIONS OF THI DETERMINED IN COMMERCIAL CARAMEL COLORS III (AC)

AC	*THI (ppm)*	*AC*	*THI (ppm)*
1	41	7	61
2	373	8	173
3	68	9	8
4	196	10	44
5	162	11	2
6	11	12	3

CONCLUSIONS

The recently detected constituent of some caramel colours III, 2-acetyl-4(5)-tetrahydroxybutylimidazole (THI), can be determined by HPLC with high accuracy. THI contents of caramel colours III manufactured between 1979 and 1983 cover a range from virtually nil to 400 ppm. Further work will show how these levels are affected by manufacturing conditions.

ACKNOWLEDGEMENTS

The author is grateful to The Coca-Cola Company for permission to publish his results. Thanks are due to Mr. J. Rosdorfer for his skillful technical assistance, and to Drs. D. V. Myers and T. Radford for their help in preparing the manuscript.

REFERENCES

1 *Specifications for Caramel Color*, International Technical Caramel Association, Washington, DC, Dec. 1984, amended May 1985.
2 U. Kröplien, J. Rosdorfer, J. van der Greef, R. C. Long, Jr. and J. H. Goldstein, *J. Org. Chem.*, 50 (1985) 1131.
3 Y. Peleg and C. H. Mannheim, *J. Agric. Food Chem.*, 18 (1970) 176.
4 U. Kröplien, *J. Agric. Food Chem.*, 22 (1974) 110.
5 S. Honda and H. Kakehi, *J. Chromatogr.*, 152 (1978) 405.

Journal of Chromatography, 362 (1986) 291–297
Elsevier Science Publishers B.V., Amsterdam — Printed in The Netherlands

CHROM. 18 688

Note

Hydrolysis of ginsenosides in artificial gastric fluid monitored by high-performance liquid chromatography

PIERGIORGIO PIETTA* and PIERLUIGI MAURI
Dipartimento di Scienze e Tecnologie Biomediche, Sezione di Chimica Organica, Via Celoria 2, 20133 Milan (Italy)
and
ANGELO RAVA
Istituto Biochimico Pavese, Viale Certosa 10, 27100 Pavia (Italy)
(Received March 27th, 1986)

Ginseng saponins, isolated from the root of Panax Ginseng C. A. Meyer (Araliaceae), can be classified into two groups, namely the 20(*S*)-protopanaxatriol group (I) and the 20(*S*)-protopanaxadiol group (II) (Fig. 1).

In spite of the many pharmacological[1] and biochemical studies[2], there is only one report[3] on the degradation of ginsenosides under mild acidic conditions. According to this work, R_{g_1} and R_e ginsenosides were hydrolyzed with 0.1 *M* hydrochloric acid at 37°C for 2 h and the structures of the resulting prosapogenins assigned by ^{13}C NMR spectroscopy. Ginsenoside R_{b_1} representative of group II, was similarly treated, but evidence of the structure of its prosapogenins was not produced.

Recently, the stability of the same saponins at pH 1.81 and 37°C was examined using isocratic high-performance liquid chromatography (HPLC), although the chromatographic data refer only to R_{g_1}[4].

Owing to this lack of information, we applied a previously described[5] HPLC procedure to the kinetics of the hydrolysis of ginsenosides of groups I, II and of Ginseng extracts in artificial gastric fluid at 37°C. The results of this investigation are now reported.

EXPERIMENTAL

Materials and reagents

Ginsenosides R_{b_1}, R_{b_2}, R_c, R_d, R_{g_1} and R_e were obtained from Pharmaton (Lugano-Bioggio, Switzerland). Ginseng extracts were from different commerical sources. Acetonitrile and water were of HPLC grade (Chromasolv, Riedel-de Haën, Hannover, F.R.G.).

Standard stock solutions were prepared by dissolving each ginsenoside (1 mg/ml) and Ginseng extracts (45 mg/ml) in 1 m*M* phosphate (NaH_2PO_4) adjusted to pH 1.2 with 5 *M* hydrochloric acid and to a constant ionic strength of 0.15 with potassium chloride.

0021-9673/86/$03.50

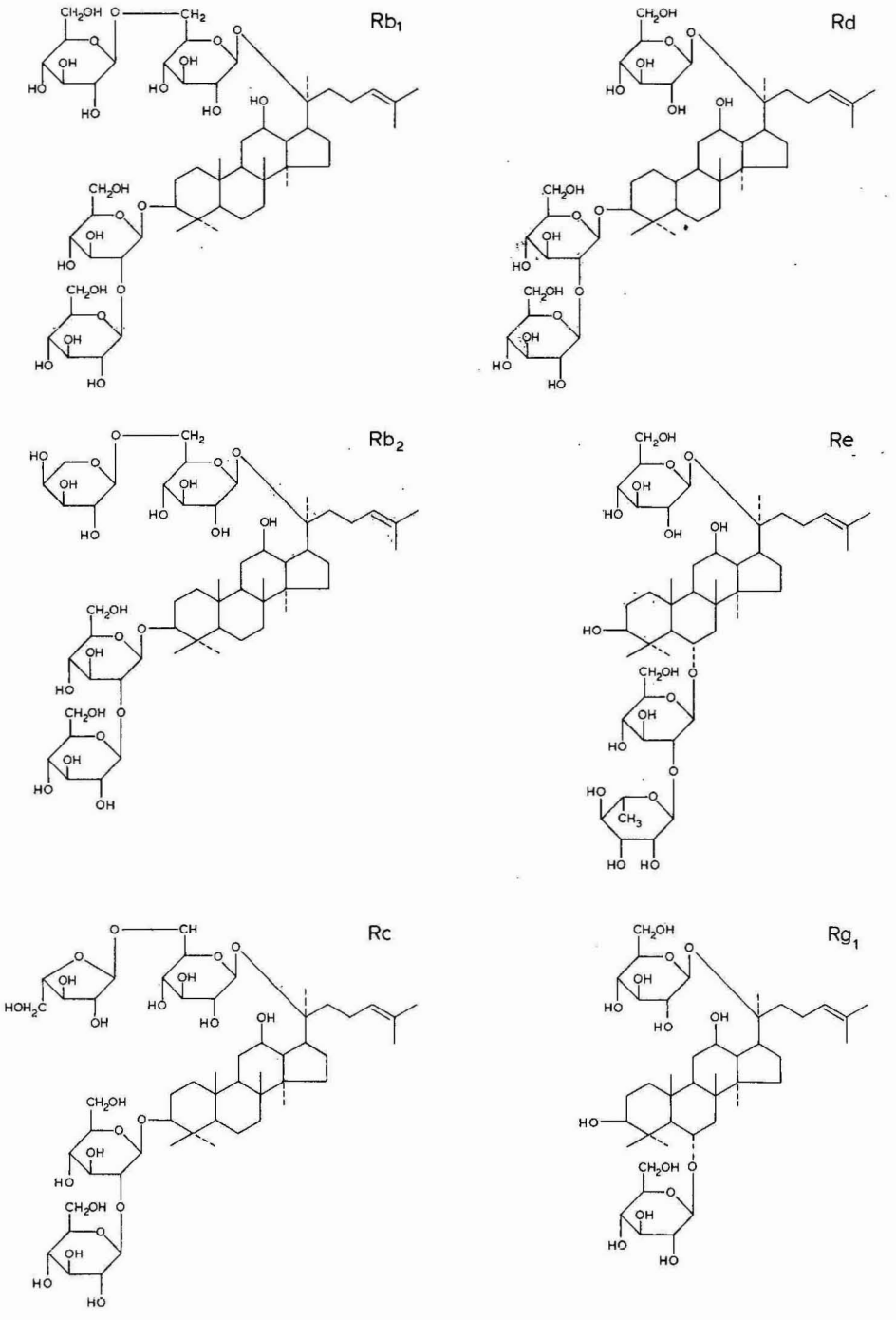

Fig. 1. Chemical structures of the ginsenosides.

Ginsenosides hydrolysis

Aliquots (50 μl) of each stock solution were incubated at 37°C for different times. Every 30 min the appropriate aliquot was cooled, neutralized by addition of 50 μl of 0.1 *M* phosphate (NaH_2PO_4–Na_2HPO_4) buffer, pH 6.8, and then analyzed. Control blanks were performed by analyzing each sample at zero time. The pH of the reaction mixture remained unchanged during the hydrolysis.

Chromatographic conditions

HPLC was performed on a Waters Assoc. liquid chromatograph equipped with a M-590 pump, a M-510 pump, a M-680 gradient controller, a M-U6K universal injector and a M-lambda max 480 ultraviolet detector. The column was a RP-18 Spheri 5 cartridge (100 mm × 4.6 mm, 10 μm) from Kontron (Milan, Italy). The separations were obtained isocratically with acetonitrile–water (28.5:71.5; 20:80, v/v) or by gradient elution, using the eluents 15% acetonitrile (A) and 80% acetonitrile (B) according to the following profile: 0–12 min, 93% A, 7% B; 12–30 min, 72% A, 28% B (curve 5); 30–45 min, 72% A, 28% B (curve 6). The flow-rate was 3 ml/min and the peaks were monitored at 203 nm (0.05 a.u.f.s.).

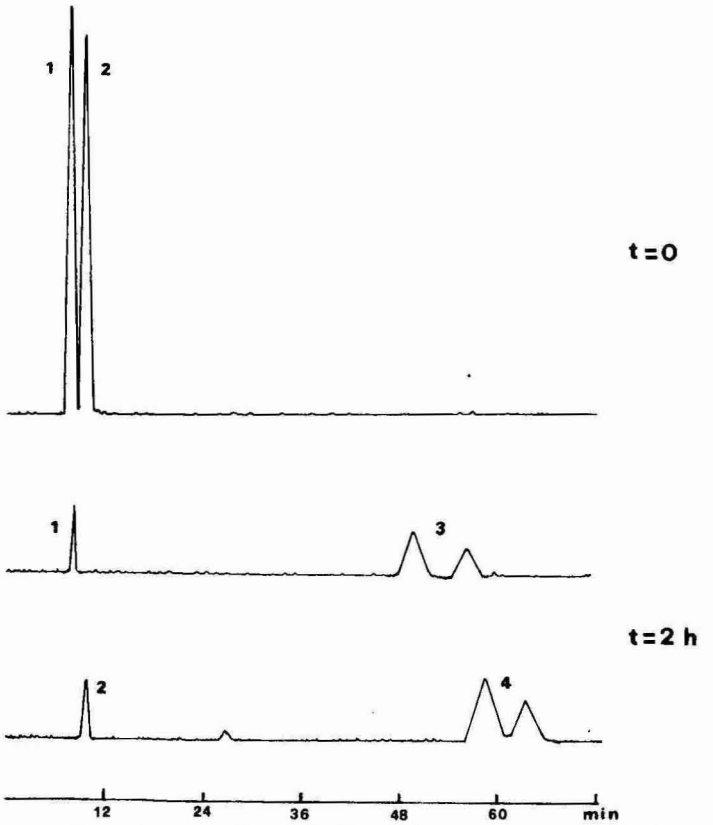

Fig. 2. Chromatograms of R_{g1}(1), R_e (2) and their prosapogenins (3, 4) at zero time and after hydrolysis for 2 h. Eluent: 20% acetonitrile.

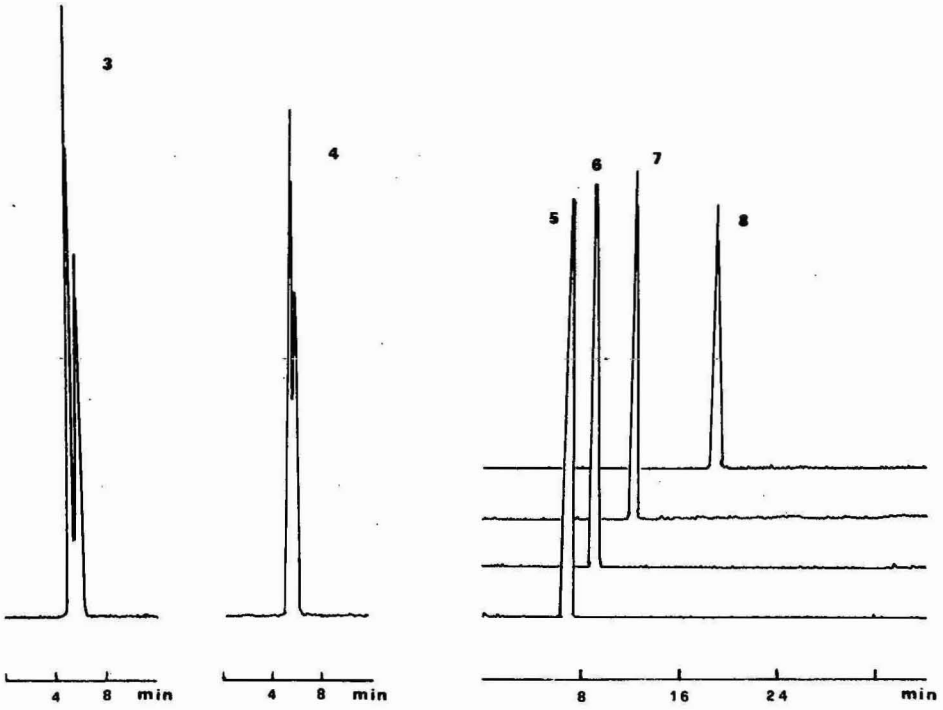

Fig. 3. Chromatograms of R_{g1} (1) and R_e (2) after hydrolysis for 2 h. Eluent: 28.5% acetonitrile.

Fig. 4. Chromatograms of R_{b1} (5), R_e (6), R_{b2} (7) and R_d (8) after hydrolysis for 2 h. Eluent: 28.5% acetonitrile.

RESULTS AND DISCUSSION

Fig. 2 shows typical chromatograms obtained from ginsenosides R_{g_1} and R_e at the initial time and after 2 h at pH 1.2 and 37°C. The R_{g_1} and R_e prosapogenins produced by the cleavage of the C-20 glucosidic bond are eluted after 50 min using 20% acetonitrile, which is the customary solvent for these saponins. 28.5% Acetonitrile elutes intact R_{g_1} and R_e with the "solvent front", while the related prosapogenins yield peaks with retention times of 4.8–5.6 min (Fig. 3). Under these chromatographic conditions, the ginsenosides of group II are eluted within 20 min, but their common prosapogenin is retained on the column, as shown in Fig. 4. To elute this less polar derivative, it has been necessary to apply a gradient (Fig. 5). A chromatogram obtained from ginsenosides R_{g_1} and R_e, and their prosapogenins, using the same gradient is also shown (Fig. 6).

The hydrolysis of Ginseng extracts at pH 1.2 and 37°C has been followed similarly. The peaks of the ginsenosides of group II decrease as the reaction proceeds and a new peak due to R_{g_1} and R_e prosapogenins appears (Fig. 7). To extend these results, the Ginseng extracts have also been monitored using the gradient approach. As Fig. 8 shows, the R_{g_1} and R_e prosapogenins are eluted at 21 min, while the common derivative from the ginsenosides of group II is clearly identifiable at 48 min.

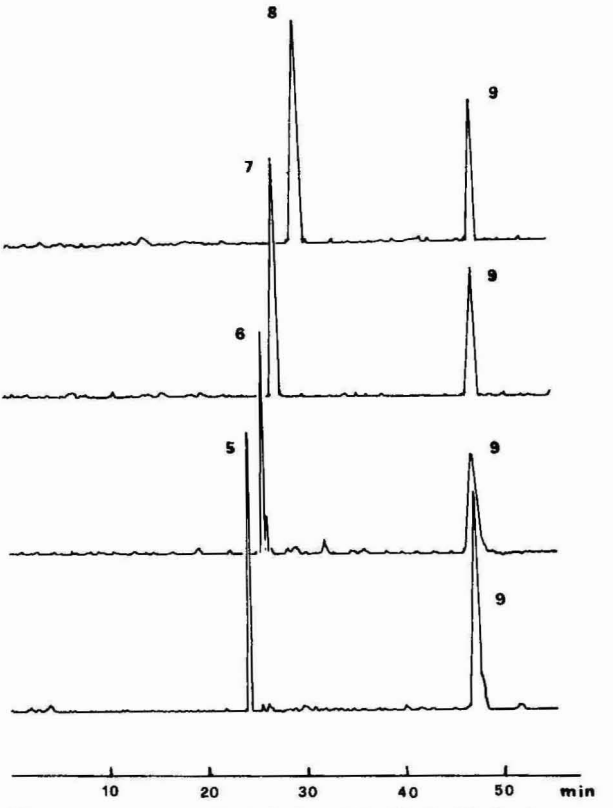

Fig. 5. HPLC with gradient elution of R_{b_1}(5), R_e (6), R_{b_2}(7), R_d (8) and their common prosapogenin (9) after hydrolysis for 2 h. See text for eluents and profiles.

The hydrolysis of each ginsenoside has been followed up to 70% degradation, and a linear relationship between the reaction time, x (h), and the residual amount of intact ginsenoside (peak area, y) has been found:

Relationship	*R*	*Half-time (h)*	
$y = -3.44x + 6.38$	0.999	0.928	(R_{g_1})
$y = -7.92x + 5.18$	0.997	0.896	(R_e)
$y = -1.13x + 7.52$	0.996	3.31	(R_{b_1})
$y = -1.12x + 7.45$	0.995	3.32	(R_c)
$y = -0.764x + 3.89$	0.995	3.77	(R_{b_2})
$y = -0.584x + 3.89$	0.997	3.33	(R_d)

As is seen, the half-times for the ginsenosides of group II are similar and nearly three times higher than those of R_{g_1} and R_e.

In conclusion, the described procedure allows the kinetics of hydrolysis in artificial gastric fluid of each ginsenoside in Ginseng extracts to be followed by monitoring both intact and degradation products.

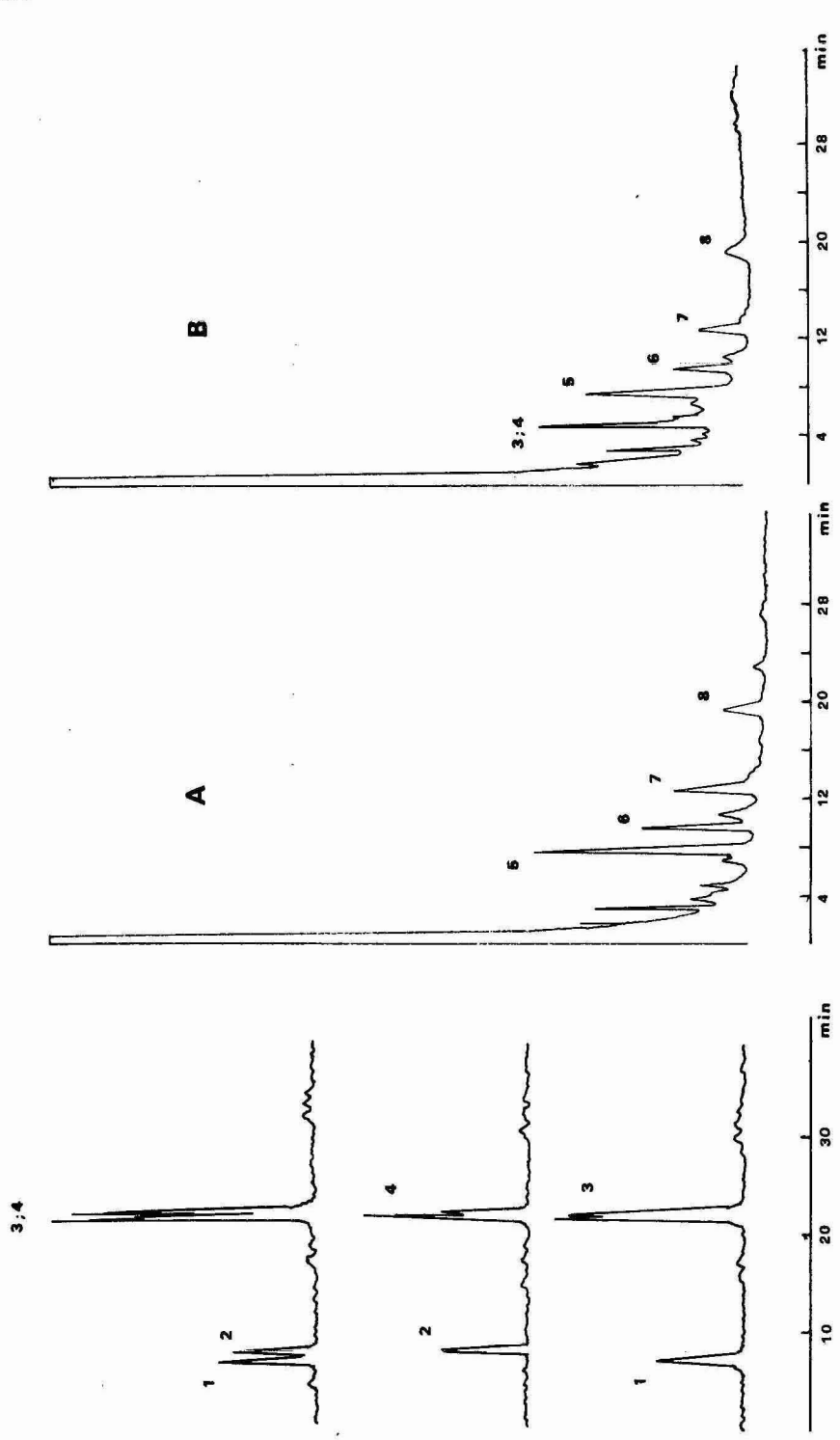

Fig. 6. HPLC with gradient elution of R_{g1} (1), R_e (2) and their prosapogenins (3, 4) after hydrolysis for 2 h. See text for eluents and profiles.

Fig. 7. HPLC with isocratic elution of a Ginseng extract at zero time (A) and after hydrolysis for 2 h (B). Peaks as in Figs. 2 and 4. Eluent: 28.5% acetonitrile.

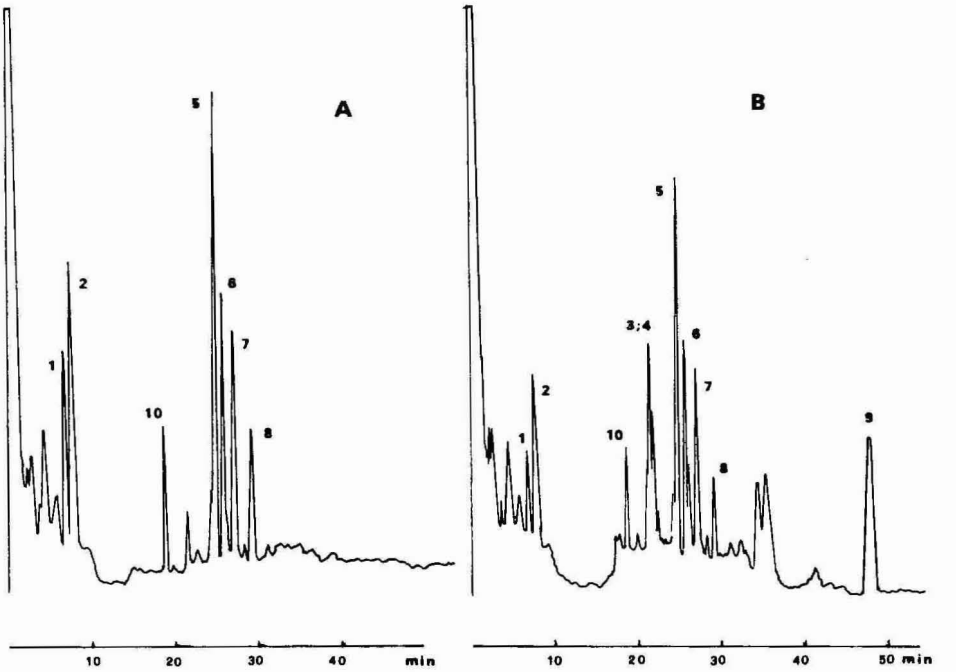

Fig. 8. HPLC with gradient elution of a Ginseng extract at zero time (A) and after 2 h (B). Peaks as in Figs. 2 and 5, except for 10 = R_f. See text for eluents and profiles.

ACKNOWLEDGEMENT

The authors wish to acknowledge the expert technical assistance of S. De Alberti.

REFERENCES

1 S. Sanada, N. Kondo, J. Shoji, O. Tanaka and S. Shibata, *Chem. Pharm. Bull.*, 22 (1974) 2407.
2 T. D. Lin, N. Kondo and J. Shoji, *Chem. Pharm. Bull.*, 24 (1976) 253.
3 B. H. Han, H. M. Park, Y. N. Han, L. K. Woo, S. Yahara and O. Tanaka, *Planta Med.*, 44 (1982) 146.
4 E. Miyamoto, S. Odashima, I. Kitogawa and A. Tsuji, *J. Pharm. Sci.*, 73 (1984) 409.
5 P. Pietta, P. Mauri and A. Rava, *J. Chromatogr.*, 356 (1986) 212.

Journal of Chromatography, 362 (1986) 298–302
Elsevier Science Publishers B.V., Amsterdam — Printed in The Netherlands

CHROM. 18 699

Note

High-performance liquid chromatographic analysis of hydroxyurea in pharmaceutical formulations and in the bulk

JOSIP PLUSCEC* and YA-CHI YUAN
E. R. Squibb and Sons, Inc., P.O. Box 191, New Brunswick, NJ 08903 (U.S.A.)
(Received April 3rd, 1986)

Hydroxyurea is structurally a simple compound that was first synthesized more than one hundred years ago[1]. However, its palliative role in the treatment of leukemia and in malignant melanoma was first recognized in 1963[2]. Hydrea (distributed in Germany as Litalir capsules) is the only commercially available pharmaceutical preparation of hydroxyurea.

The current analysis of hydroxyurea, as given in the United States Pharmacopoeia (U.S.P.), is an iodometric titration. Although an accurate method, it still lacks the simplicity of the high-performance liquid chromatography (HPLC) method. A number of HPLC methods have been described, however, they deal with the analysis of drugs and drug-related compounds that are derivatives of hydroxyurea[3–5]. Some of them require prior or post-column derivatization[6–8]. This paper describes a simple HPLC method for the determination of hydroxyurea and potential impurities which may be present in Hydrea or bulk.

EXPERIMENTAL

Apparatus

A Waters 6000 A pump and a Perkin-Elmer LC-55 variable-wavelength UV detector were used to perform the analyses. The UV detector was set at 214 nm with a range of 0.02 a.u.f.s. A supelco LC-18 Column (250 × 4.6 mm I.D.; particle size, 5 μm) was used for chromatographic separation with a Rheodyne 7010 injection valve fitted with a 20-μl sample loop for sample introduction and degassed distilled water as the mobile phase. A flow-rate of 0.5 ml/min was found to give acceptable retention times for hydroxyurea, possible impurities (hydroxylamine, urea) and the components present in the Hydrea formulation (citric acid, magnesium stearate, milk sugar). Chromatographic peaks were recorded on a Pharmacia recorder (chart speed 150 mm/h) and integrated by analog-to-digital converters in a Hewlett-Packard 3357 laboratory automatin system.

Reagents

The following reagents were used: hydroxyurea (reference standard or equivalent); Hydrea capsule (500 mg; E.R. Squibb and Sons); uracil (Eastman Kodak, Rochester, NY, U.S.A.); hydroxylamine hydrochloride (Fisher Scientific, Fairlawn, NJ, U.S.A.); and urea (J. T. Baker, Phillipsburg, NJ, U.S.A.).

0021-9673/86/$03.50

Internal standard solution

An accurately weighed amount of uracil (24–26 mg) was transferred into a 200-ml volumetric flask. About 150 ml of distilled water were added. The flask was placed in an ultrasonic bath (Sonicor Instrument Corporation, Copiague, NY, U.S.A.) until solution was complete. The solution was then diluted to volume and mixed.

Standard solution

Hydroxyurea reference standard (48–52 mg) was accurately weighed into a 50-ml volumetric flask. To the flask, 10 ml of the internal standard solution were added, and the resulting solution was diluted to volume with water.

Sample preparation of capsule

The average weight of the content of Hydrea capsules was determined from the difference in weights of 20 filled and empty capsules. The contents of 20 capsules was placed in a glass mortar and ground quickly to a fine, smooth powder. In duplicate, accurately weighed amounts (3.1–3.3 g) of powder were transferred quantitatively into 1000-ml volumetric flasks. To each of the flasks, 900 ml of distilled water were added and the contents were sonicated for 5 min. The solutions were then stirred on a magnetic stirrer for an additional 30 min at room temperature, diluted to volume with distilled water, mixed and sonicated for an additional 5 min. An aliquot of 75 ml from each solution was filtered through a membrane filter (Versapor 1200, supported membrane filter, 12 μm, Gelman Science, Ann Arbor, MI, U.S.A.) discarding the first 10–15 ml from each solution. Aliquots of 25 ml of the clear filtrate were transferred to 50-ml volumetric flasks. To each flask, 10 ml of the internal standard solution were added before the solutions were diluted to volume with distilled water and mixed.

Raw material sample preparation

It was carried out as described under *Standard solution.*

System suitability test

Resolution. The hydroxylamine peak is closest to the peak of hydroxyurea. These peaks were resolved completely (resolution > 1.0).

Precision. The standard solution was chromatographed repeatedly and the coefficient of variation (C.V.) calculated for the response ratios of hydroxyurea *versus* uracil. A precision with a C.V. of $\pm$ 0.6% was observed for five consecutive chromatographic runs.

Calibration. The linearity of response with respect to concentration was tested with standard concentrations from 20 to 140% of the labeled potency. The correlation coefficient was found to be 0.9999 with a slope of 1.255 and a Y-intercept of -0.01.

Sample resolution

Baseline resolution was achieved between the citric acid used in the formulation of Hydrea and the hydroxyurea (resolution = 1.8).

Recovery study

Placebos used in the formulation of Hydrea, and samples of Hydrea were spiked with hydroxyurea equivalent to 100% and 30% of label respectively. The average recovery was 100.5% (C.V. = 0.4%) for the placebos and 99.2% (C.V. = 2.6%) for samples. The average material balance of spiked samples was 99.8% (C.V. = 0.6%).

Assay

Aliquots (20 μl) of the standard and sample preparation of Hydrea and raw material were injected into the chromatograph. Chromatograms were recorded and the peak heights of hydroxyurea and uracil were measured. The concentration of the active ingredient, in mg per capsule, was calculated as follows:

$$\text{mg/caps} = \frac{R_u\ W_s\ C\ P\ 10}{R_s\ W_u\ 25}$$

where R_u = response ratio (hydroxyurea to uracil) of active ingredient in the sample preparation; R_s = response ratio (hydroxyurea to uracil) of active ingredient in the standard preparation; W_u = weight of the sample in mg; W_s = weight of the standard in mg; C = average capsule net content in mg/caps; P = purity of the standard.

RESULTS AND DISCUSSION

During the course of the study, a number of chromatographic columns was tested (PRP-1, Partisil ODS-2, cyano phases, ion-exchange materials etc); however, only the one described in this work gave a satisfactory separation of hydroxyurea from potential impurities resulting from decomposition. An infrequent impurity originating from the synthesis of hydroxyurea, misnamed isohydroxyurea (O-carbamoylhydroxylamine) is also well separated from hydroxyurea.

Complete baseline separation was achieved between hydroxyurea and hydroxylamine, the most frequently observed impurity, as noted in Fig. 1.

Analyses of a series of formulations are summarized in Table I with a typical chromatogram depicted in Fig. 2. All results are within regulatory limits (±3% of labeled) with an average of 99.1%. The analyses of five batches of hydroxyurea raw

TABLE I

RESULTS OF ANALYSIS OF HYDREA 500 mg

Each sample represents an average of 15 different weights and chromatographic runs.

Sample	*Hydroxyurea found*		*C.V. (%)*
	mg/caps	*% label*	
1	486	97.2	1.3
2	495	99.0	1.2
3	509	101.8	0.9
Mean	497	99.1	1.1

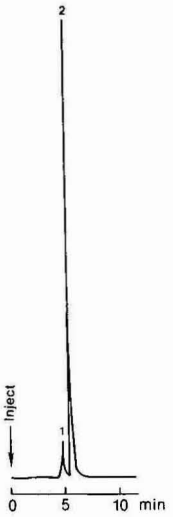

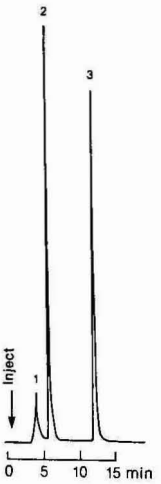

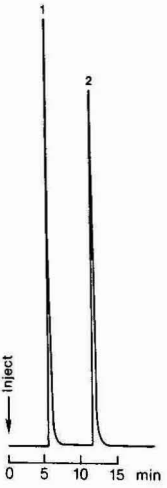

Fig. 1. Resolution of hydroxylamine (1) and hydroxyurea (2).

Fig. 2. Typical HPLC analysis of hydroxyurea in Hydrea capsule 500 mg. Peaks: 1 = citric acid present in the formulation of Hydrea; 2 = hydroxyurea; 3 = uracil (internal standard).

Fig. 3. HPLC analysis of hydroxyurea raw material. Peaks: 1 = hydroxyurea; 2 = uracil (internal standard).

TABLE II

RESULTS OF ANALYSIS OF HYDROXYUREA RAW MATERIAL

Each sample represents an average of four different weights and seven chromatographic runs.

Sample	*Found (%)*	*C.V. (%)*	*U.S.P. method (iodometric) (%)*
1	99.7	0.3	–
2	99.7	0.9	99.3
3	99.9	0.4	99.1
4	99.7	0.6	99.4
Mean	99.8	0.6	99.3

TABLE III

RECOVERY STUDY OF HYDROXYUREA

Data are average of six determinations.

Determined in sample (mg)*	*Added (mg)*	*Found (mg)*	*Material balance** (%)*	*C.V. (%)*	*Recovery**** (%)	C.V. (%)
2037	604.3	2636	99.8	0.6	99.1	2.6

* 3.1–3.3 g powder (corresponding to four capsules) obtained by grinding 20 capsules, was used for each determination.

** $\text{Material balance} = \dfrac{\text{found}}{\text{added} + \text{determined in sample}}$

*** $\text{Recovery} = \dfrac{\text{found} - \text{determined in sample}}{\text{added}}$

material were compared with data obtained by the iodometric analyses given in the U.S.P. (Table II). Although the results are comparable, the HPLC method described in this paper is faster, simpler and more reliable than the currently used U.S.P. method. A typical chromatographic run of the raw material is seen in Fig. 3. The recovery study is presented in Table III.

In summary, a fast, simple and accurate method for hydroxyurea in a pharmaceutical preparation and in a raw material is presented.

REFERENCES

1 W. F. C. Dresler and R. Stein, *Ann. Chem. Pharm.*, 150 (1869) 242.
2 G. A. Nagel, M. Regnotto and J. Sartorius, *Schweiz. Apoth.-Ztg.*, 112 (1963) 201.
3 T. Daldrup, F. Susanto and P. Michalke, *Fresenius Z. Anal. Chem.*, 308 (1981) 413.
4 J. Pribyl and F. Herzel, *J. Chromatogr.*, 125 (1976) 487.
5 B. Makuch, B. Sledzinska and W. Sokolowska, *Fresenius Z. Anal. Chem.*, 287 (1977) 316.
6 J. Kawase, H. Ueno, A. Nakae and K. Tsuji, *J. Chromatogr.*, 252 (1982) 209.
7 K. R. Beck, B. J. Leibowitz and M. R. Ladisch, *J. Chromatogr.*, 190 (1980) 226.
8 M. Jaworski, *Chromatographia*, 13 (1980) 101.

Journal of Chromatography, 362 (1986) 303–307
Elsevier Science Publishers B.V., Amsterdam — Printed in The Netherlands

CHROM. 18 692

Note

Visualization of sulphonamide drugs on thin-layer plates using π-acceptors as spray reagents

SURAJ P. AGARWAL
Faculty of Pharmaceutical Sciences, University of Nigeria, Nsukka (Nigeria)
(First received February 3rd, 1986; revised manuscript received April 2nd, 1986)

Antibacterial sulphonamides, alone or in combination with trimethoprim, are still widely used in the treatment of infection[1]. Methods for the visualization of these drugs on thin-layer plates have been reviewed[2,3]. The use of fluorescamine, either as a spray reagent[4] or by dipping the developed plate quickly in a solution of reagent in acetone, has found application both in qualitative detection and in quantitative determination of these drugs when present in low concentration, *e.g.* in animal tissues[5–9]. Fluorescamine derivatization is slow (15–30 min)[7,10] and the fluorescent product has limited stability (2–3 h)[5]. Touchstone *et al.*[10] recommend the use of dimethyl sulphoxide (DMSO) or dimethylformamide (DMF) as solvent for fluorescamine in order to improve the stability of fluorescence.

The use of π-acceptors as spray reagents for the detection of alkaloids, triterpenoids, steroids, penicillins, diuretics and hypoglycemic drugs on thin-layer plates has been reported[11–14]. The use of several π-acceptors in the visualization of eighteen sulphonamides and a related drug (trimethoprim) on thin-layer plates is reported here.

EXPERIMENTAL

Materials

Acetylsulphisoxazole, phthalylsulphathiazole, succinylsulphathiazole monohydrate, sulphacetamide, sulphadiazine, sulphadimethoxine, sulphadoxine, sulphaethidole, sulphaguanidine, sulphamerazine, sulphamethazine, sulphamethizole, sulphamethoxazole, sulphanilamide, sulphapyridine, sulphathiazole, sulphisomidine, sulphisoxazole, and trimethoprim were either reference standards or pure samples supplied by the manufacturer and used as such. *o*-Chloranil, *p*-chloranil, *p*-fluoranil and 2,5-dichloro--*p*-benzoquinone were from Pflätz and Baüer and were used as received. Solvents and other chemicals were of reagent grade.

Spray reagents

The following spray reagents were freshly prepared: (I) 0.5% *o*-chloranil in dioxane; (II) 0.5% *p*-chloranil in dioxane; (III) 0.5% *p*-fluoranil in dioxane; (IV)–(VI) 0.5% 2,5-dichloro-*p*-benzoquinone in dioxane, DMSO or DMF, respectively.

0021-9673/86/$03.50

TABLE I

REACTIONS OF SULPHONAMIDE DRUGS WITH SPRAY REAGENTS

Order of increasing response: ±, +, ++, +++.

Drug	*I, o-Chloranil**		*II, p-Chloranil***		*III, p-Fluoranil****		*V, 2,5-Dichloro-p-benzoquinone (in DMSO)§*	
	Colour (response)	*Detection limit (μg)*	*Colour (response)*	*Detection limit (μg)*	*Colour (response)*	*Detection limit (μg)*	*Colour (response)*	*Detection limit (μg)*
Acetylsulphisoxazole	Purple (+)	2.0	Green (±)	4.0	Yellow (±)	4.0	Yellowish green (+)	2.0
Phthalylsulphathiazole	Purple (+)	2.0	Green (±)	4.0	–		Pink (+)	2.0
Succinylsulphathiazole	Purple (+)	2.0	Green (±)	4.0	–		Pink (+)	2.0
Sulphacetamide	Purple (++)	1.5	Green (+)	2.0	Yellow (+)	2.0	Yellowish green (+)	2.0
Sulphadiazine	Purple (+)	2.0	Green (++)	1.5	Yellow (+)	2.0	Orange (+)	2.0
Sulphadimethoxine	Purple (+)	2.0	Green (+)	2.0	Yellow (±)	4.0	Orange (+)	2.0
Sulphadoxine	Purple (+)	2.0	Green (±)	4.0	Yellowish green (±)	4.0	Yellowish green (+)	2.0
Sulphaethidole	Purple (+)	2.0	Green (+)	2.0	Yellow (±)	2.0	Pink (+)	2.0
Sulphaguanidine	Purple (+)	2.0	Green (++)	1.5	Yellow (+)	2.0	Yellowish green (±)	4.0

Sulphamerazine	Purple (+)	2.0	Green (+)	2.0	Yellow (+)	2.0	Orange (++)	1.5
Sulphamethazine	Purple (+)	2.0	Grey (++)	1.5	Yellow (+)	2.0	Grey (+)	2.0
Sulphamethizole	Purple (+)	2.0	Green (+)	2.0	Yellow (+)	2.0	Pink (+)	2.0
Sulphamethoxazole	Purple (+)	2.0	Green (+)	2.0	Yellow (+)	2.0	Orange (++)	1.5
Sulphanilamide	Purple (+)	2.0	Green (+)	2.0	Yellow (+)	2.0	Grey (+)	2.0
Sulphapyridine	Purple (+)	2.0	Green (++)	1.5	Yellow (+)	2.0	Orange (+++)	1.0
Sulphathiazole	Purple (+)	2.0	Green (++)	1.5	Yellow (+)	2.0	Orange (++)	1.5
Sulphisomidine	Purple (+)	2.0	Green (+)	2.0	Yellow (+)	2.0	Grey (+)	2.0
Sulphisoxazole	Purple (+)	2.0	Green (+)	2.0	Grey (+)	2.0	Grey (+)	2.0
Trimethoprim	Purple (++)	1.5	Purple (+)	2.0	Brown (+)	2.0	Purple (+++)	1.0

* Initial purple colour changes to grey (rapid) and then to yellowish green (slow).
** No immediate visualization. Colours develop slowly after several hours.
*** Colours develop in *ca.* 2 min.
§ Full colour development takes 2–5 min.

Thin-layer chromatography

The drugs were dissolved in either acetone or methanol. The sample was applied to silica gel G (0.2 mm) thin-layer plates and, after development in ethyl acetate–methanol (90:10), the plates were air-dried and sprayed. Where necessary the plates were oversprayed with DMSO or DMF.

RESULTS

Table I gives the results of colour reactions of sulphonamide drugs with various spray reagents. *o*-Chloranil in dioxane (I) produced an immediate visualization of all drugs as purple spots against an orange (the same as colour of reagent) background. The initial intense purple colour, however, fades rapidly to grey while the background becomes purple. The spots, which later turn into yellowish green (against a white background), are clearly visible even after several weeks. Spraying of the plate with DMSO either prior to or after spraying with *o*-chloranil did not improve the visualization. The use of *p*-chloranil in dioxane (II) was unsatisfactory as none of the drugs could be seen immediately after spraying with this reagent. After the sprayed plates have been stored overnight the drugs appears as green spots (grey for sulphamethazine and purple for trimethoprim). The use of DMSO did not accelerate the reaction, except that the drugs appeared as yellow or yellowish green when the plate was sprayed with DMSO either before or after spraying with *p*-chloranil.

The use of fluoranil in dioxane (III) resulted in prompt visualization of all drugs as yellow spots, except for sulphisoxazole which appeared as grey. Phthalylsulphathiazole and succinylsulphathiazole could not be visualized by this reagent. The use of DMSO was found to have no effect. 2,5-Dichloro-*p*-benzoquinone in dioxane (IV) gave a light grey colour with all the drugs, except sulphisomidine and sulphisoxazole which appeared as purple. The reaction was very slow as the colours developed only after overnight storage of the sprayed plate. The use of either DMSO (V) or DMF (VI) as solvent for 2,5-dichloro-*p*-benzoquinone resulted in the immediate visualization of sulphoamide drugs as given in Table I. The use of 2,5-dichloro-*p*-benzoquinone in DMSO (V) as spray reagent is to be preferred as the colours produced are sharper and more stable. Other reagents tried included 0.5% chloranilic acid in dioxane, and 2,3-dichloro-5,6-dicyanobenzoquinone in dioxane, but these did not give any noticeable colour reaction immediately.

In conclusion, the use of 2,5-dichloro-*p*-benzoquinone in DMSO (V) is recommended as a spray reagent for the prompt visualization of sulphonamide drugs on silica gel G thin-layer. The reaction between the reagent and drugs is rapid and produces sharp colours, which are highly stable.

ACKNOWLEDGEMENTS

The author is grateful to various pharmaceutical companies for the generous supply of authentic samples of drugs and in particular to Roche (Nigeria) Ltd. for the supply of sulphadoxine, trimethoprim and dosage forms containing these drugs. This work was supported by Senate Research Grant Committee, University of Nigeria (Grant No. 00354/79).

REFERENCES

1 E. F. Reynolds, *Martindale, the Extra Pharmacopoeia*, Pharmaceutical Press, London, 28th edn., 1982, p. 1457.
2 M. I. Walash and S. P. Agarwal, *J. Pharm. Sci.*, 61 (1972) 277.
3 W. Horowitz, *J. Assoc. Off. Anal. Chem.*, 64 (1981) 104.
4 N. Haagsma, B. Dielman and B. G. Gortemaker, *Vet. Q.*, 6 (1984) 8.
5 M. H. Thomas, R. L. Epstein, R. B. Ashworth and H. Marks, *J. Assoc. Off. Anal. Chem.*, 66 (1983) 884.
6 M. H. Thomas, K. E. Soroka and S. H. Thomas, *J. Assoc. Off. Anal. Chem.*, 66 (1983) 881.
7 M. H. Thomas, K. E. Soroka, R. M. Simpson and R. L. Epstein, *J. Agric. Food Chem.*, 29 (1981) 621.
8 J. L. Woolley Jr., O. Murch and C. W. Sigel, *J. Assoc. Off. Anal. Chem.*, 61 (1978) 545.
9 C. W. Siegel, J. L. Wooley Jr. and C. A. Nichol, *J. Pharm. Sci.*, 64 (1975) 973.
10 J. C. Touchstone, J. Sherma, M. F. Dobbins and G. R. Hansen, *J. Chromatogr.*, 124 (1976) 111.
11 S. P. Agarwal and M. A. Elsayed, *Planta Med.*, 45 (1982) 40.
12 S. P. Agarwal and J. Nwaiwu, *J. Chromatogr.*, 295 (1984) 537.
13 S. P. Agarwal and J. Nwaiwu, *J. Chromatogr.*, 323 (1985) 424.
14 S. P. Agarwal and J. Nwaiwu, *J. Chromatogr.*, 351 (1986) 383.

PUBLICATION SCHEDULE FOR 1986

Journal of Chromatography (incorporating *Chromatographic Reviews*) and *Journal of Chromatography, Biomedical Applications*

MONTH	D 1985	J 1986	F	M	A	M	J	J	A	S	O	N	D
Journal of Chromatography	346–350	351/1 351/2 351/3	352 353 354	355/1 355/2 356/1	356/2 356/3 357/1	357/2 357/3 358/1 358/2 359	360/1 360/2 361	362/1 362/2 362/3	363/1 363/2	364 365 366	The publication schedule for further issues will be published later		
Chromatographic Reviews						373/1							
Bibliography Section			372/1		372/2		372/3		372/4		372/5		372/6
Biomedical Applications		374/1 374/2	375/1	375/2	376 377	378/1	378/2 379	380/1	380/2 381/1	381/2	382	383/1	383/2

INFORMATION FOR AUTHORS

(Detailed *Instructions to Authors* were published in Vol. 329, No. 3, pp. 449–452. A free reprint can be obtained by application to the publisher.)

Types of Contributions. The following types of papers are published in the *Journal of Chromatography* and the section on *Biomedical Applications:* Regular research papers (Full-length papers), Short communications and Notes. Short communications are preliminary announcements of important new developments and will, whenever possible, be published with maximum speed. Notes are usually descriptions of short investigations and reflect the same quality of research as Full-length papers, but should preferably not exceed four printed pages. For review articles, see page 2 of cover under Submission of Papers.

Submission. Every paper must be accompanied by a letter from the senior author, stating that he is submitting the paper for publication in the *Journal of Chromatography.* Please do not send a letter signed by the director of the institute or the professor unless he is one of the authors.

Manuscripts. Manuscripts should be typed in double spacing on consecutively numbered pages of uniform size. The manuscript should be preceded by a sheet of manuscript paper carrying the title of the paper and the name and full postal address of the person to whom the proofs are to be sent. Authors of papers in French or German are requested to supply an English translation of the title of the paper. As a rule, papers should be divided into sections, headed by a caption (*e.g.*, Summary, Introduction, Experimental, Results, Discussion, etc.). All illustrations, photographs, tables, etc., should be on separate sheets.

Introduction. Every paper must have a concise introduction mentioning what has been done before on the topic described, and stating clearly what is new in the paper now submitted.

Summary. Full-length papers and Review articles should have a summary of 50–100 words which clearly and briefly indicates what is new, different and significant. In the case of French or German articles an additional summary in English, headed by an English translation of the title, should also be provided. (Short communications and Notes are published without a summary.)

Illustrations. The figures should be submitted in a form suitable for reproduction, drawn in Indian ink on drawing or tracing paper. Each illustration should have a legend, all the *legends* being typed (with double spacing) together on a *separate sheet.* If structures are given in the text, the original drawings should be supplied. Coloured illustrations are reproduced at the author's expense, the cost being determined by the number of pages and by the number of colours needed. The written permission of the author and publisher must be obtained for the use of any figure already published. Its source must be indicated in the legend.

References. References should be numbered in the order in which they are cited in the text, and listed in numerical sequence on a separate sheet at the end of the article. Please check a recent issue for the layout of the reference list. Abbreviations for the titles of journals should follow the system used by *Chemical Abstracts.* Articles not yet published should be given as "in press", "submitted for publication", "in preparation" or "personal communication".

Dispatch. Before sending the manuscript to the Editor please check that the envelope contains three copies of the paper complete with references, legends and figures. One of the sets of figures must be the originals suitable for direct reproduction. Please also ensure that permission to publish has been obtained from your institute.

Proofs. One set of proofs will be sent to the author to be carefully checked for printer's errors. Corrections must be restricted to instances in which the proof is at variance with the manuscript. "Extra corrections" will be inserted at the author's expense.

Reprints. Fifty reprints of Full-length papers, Short communications and Notes will be supplied free of charge. Additional reprints can be ordered by the authors. An order form containing price quotations will be sent to the authors together with the proofs of their article.

Advertisements. Advertisement rates are available from the publisher on request. The Editors of the journal accept no responsibility for the contents of the advertisements.

THE WORLD IS AT YOUR FINGERTIP!

If chemical analysis is your world, explore it in ways never before possible with the BAS 200 PROBLEM SOLVER™. One finger on our System Director™ will take you to places you've never been. Built-in methods files help you down the road. Direct changes in a multi-electrode electrochemical detector of 4-channel variable wavelength UV/VIS detector up to 8 times during a single run. Let your column, cell and valve bask in controlled temperatures up to 80°C. Discover the advantages of the first complete LC deoxygenation system. Cruise through ternary gradient analysis with a solvent delivery system so smooth that it requires NO pulse damping.

Take the BAS 200 for a test drive and let us expand your horizons.

BAS

2701 Kent Ave
West Lafayette
Indiana 47906

Telex 276141
(317) 463-4527